

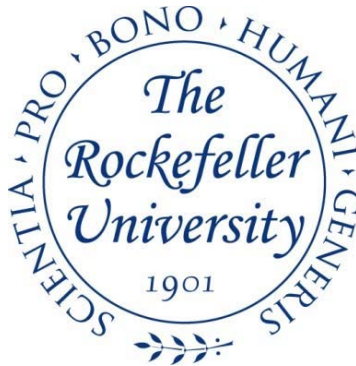
2018

Biological Consequences of Atypical Phage Conversion in Gram-Positive Pathogens

Douglas R. Deutsch

Follow this and additional works at: https://digitalcommons.rockefeller.edu/student_theses_and_dissertations

 Part of the [Life Sciences Commons](#)



**BIOLOGICAL CONSEQUENCES OF ATYPICAL PHAGE CONVERSION IN
GRAM-POSITIVE PATHOGENS**

A Thesis Presented to the Faculty of
The Rockefeller University
in Partial Fulfillment of the Requirements for
the degree of Doctor of Philosophy

by

Douglas R. Deutsch

June 2018

BIOLOGICAL CONSEQUENCES OF ATYPICAL PHAGE CONVERSION IN GRAM-POSITIVE PATHOGENS

Douglas R. Deutsch, Ph.D.

The Rockefeller University 2018

Temperate bacteriophage have a complex, dynamic relationship with bacteria: parasitizing in the lytic cycle, but often increasing bacteria's fitness as lysogens. The phage-bacteria relationship is vast and has evolved over more than an estimated three billion years, and there are likely many uncharacterized, intricate events between host and phage with important impacts on bacterial pathogenesis. This Thesis explores some of these lesser-studied phage-bacteria interactions, describing atypical mechanisms ("conversion events") by which phage shape the populations of *Bacillus anthracis* and *Staphylococcus aureus*, driving their increased diversity and likely impacting their natural behaviors.

In *B. anthracis*, phage contributions to virulence are largely unknown. The first part of this Thesis describes how an induced phage from a highly virulent, *B. anthracis*-like isolate affects the well-characterized strain Sterne and selects for a phage-resistant variant with a markedly altered phenotype, but with no apparent difference in virulence potential. In this work, we characterize this variant strain by a variety of techniques, including whole-genome DNA and RNA-sequencing. In addition, we connect the Sterne variant phenotype to that of the phage's parent strain, *B. cereus* Biovar *anthracis* CA, uncovering lytic phage-bacteria interactions

(i.e., selection by lysis) that may act to promote phenotypic diversity and shape populations of *B. anthracis* and *B. anthracis*-like pathogenic species in the wild.

Unlike *B. anthracis*, *S. aureus* has well-characterized bacteriophage contributions to its virulence potential, with known lysogens carrying virulence factors stably integrated into the host chromosome. The second part of this Thesis describes an extra-chromosomal DNA sequencing screening that uncovers the presence of episomal prophages in a number of *S. aureus* clinical isolates. QPCR characterization of one of these strains, MSSA476, reveals that the episomal nature of one of its prophages, ϕ Sa4ms, would have been missed if sequencing whole-genomic and not specifically extra-chromosomal DNA. In addition, we find that ϕ Sa4ms excision into the cytoplasm is a temporal event, and that the prophage does not appear to undergo lytic cycle replication after excision—suggesting that its excision is part of a lysogenic switch. Follow-up experiments show that ϕ Sa4ms excision can alter expression of *htrA₂* and promote increased heat-stress tolerance. This work suggests that for *S. aureus*, in addition to carrying important virulence determinants, phage may also play a rather widespread role as DNA-level switches to control virulence factor expression and/or generate distinct subpopulations. While this Thesis discusses atypical phage conversion events, it also illustrates perhaps the most important, universal role of phage in bacterial pathogens: tools to create diversity and allow for bacteria's increased infection and success under different evolutionary selections and environmental conditions.

For my Parents, thank you for making everything else so easy
For Genny, thank you for always making me question everything

ACKNOWLEDGEMENTS

I have been privileged to call The Rockefeller University my home institution (and home) for the past six years.

Foremost, I would like to thank my Advisor, Dr. Vincent A. Fischetti, for allowing me to conduct my Thesis research in his laboratory. Vince's Lab is a warm, supportive, and relaxed environment, making it always enjoyable to come into the lab, even when experiments and progress moved slowly. As an advisor, Vince was always keen on letting me pursue my own research interests and tackle the questions that I felt were most interesting. As a result, I feel much more confident in my ability to formulate my own questions as well as execute the research necessary to answer them. One thing I will always take with me beyond Rockefeller is Vince's mindset and ability to always think about experiments and questions in a larger biological context, which helps drive at the answers for even some of the most specific, detailed problems. Indeed, this has helped shape the way I think about bacteria and phage, especially within this Thesis. As a result of my time in the Fischetti Laboratory, I know my abilities as a scientist have greatly improved, and I am forever grateful.

I would also like to thank my Committee Members, Drs. Seth Darst and Sean Brady for their time and years of advice and direction. They offered key experimental suggestions that significantly shaped and strengthened both of my research projects. I would also like to thank my External Examiner, Dr. Jonathan Dworkin for serving on my Defense Committee, as well as for organizing the New York Bacillus Interest Group Meetings, where I had the pleasure of giving my first public research talk in 2015.

Other members of the Fischetti Laboratory I would like to specifically thank include Drs. Chad Euler, Rolf Lood, and Bryan Utter. Chad has been an amazing lab mate, knowledgeable resource, and friend. I am thankful to him for always indulging me whenever I would cross the hall to talk about experiments or anything else, despite his constantly busy schedule. Chad was instrumental in both projects, helping me carry out and design experiments, as well as analyze data. Much of the work I did my first two years in the Fischetti Laboratory was also under the guidance of Rolf Lood, a smart, kind, and generous Postdoctoral Fellow who always went out of his way to help. Bryan Utter did the initial study of *S. aureus* extra-chromosomal sequencing, setting the basis for future work I carried out, and we began both of the projects detailed in this Thesis together. I would also like to thank the other members of the Fischetti Laboratory for their discussions, help, kindness, and for making the Lab such a welcoming place.

I am also grateful to the Marraffini Lab for helpful discussions, especially Drs. Gregory Goldberg and Wenyan Jiang for their insightful comments as well as reagents (ϕ NM4 γ 4) which significantly helped my work with *S. aureus*.

I am especially grateful and indebted to The Rockefeller University Dean's Office. To Dr. Sidney Strickland, Dr. Emily Harms, Kristen Cullen, Marta Delgado, Cristian Rosario, Stephanie Fernandez, and everyone involved in The David Rockefeller Graduate Program: Thank You. The levels of support, and the structure and quality of the Graduate Program are beyond measure. It was an absolute pleasure and privilege to be a Graduate Fellow at Rockefeller—and I know it is due to your hard work and tireless commitment to the students.

I would additionally like to thank the Rockefeller University Genomics Resource Center for help, advice, and carrying out part of the sequencing work detailed in this Thesis. I would also like to thank everyone else at Rockefeller for the day-to-day interactions that make the campus such a special place.

Outside of Rockefeller, I would like to thank the following collaborators for their work and advice: Kathleen Verratti (Johns Hopkins University), Kim Bishop-Lilly, Ph.D. and Shanmuga Sozhamannan, Ph.D (Naval Medical Research Center), Heike Sichtig (FDA), Luke Tallon (University of Maryland, IGS), Konstantinos Krampis (CUNY Hunter), Wolfgang Beyer (University of Hohenheim), and Alexandra Gruss (L'Institut Micalis).

I would like to give a special thank you to my high-school chemistry teacher, Dr. Lillian Rankel for inspiring my interest in the boundless possibilities in science, as well as to Dr. Eloy Rodriguez at Cornell for the introduction to laboratory research. I would also like to thank my undergraduate thesis advisor, Dr. Manuel Aregullin at Cornell for helping me develop as a young scientist and inspiring me to further pursue research at Rockefeller.

I would also like to thank some of my friends (Jason, Alex, Josh, Greg, Chase, and Jeff) for great conversations (science, food, drink, and life), romps throughout NYC, and all the fun times that helped me keep my sanity. I'd especially like to thank Benjamin Preston who has been a constant source of laughter, fun, deep and shallow conversation, as well as a *co-bon vivant* for the past 10+ years, from Cornell to New York and now to when and wherever we may meet.

I would like to thank my family—especially my parents—for their constant support and encouragement over the last 28 years. Their hard work and dedication has allowed me to spend my time focusing on my interests and education. I would not be here today without them.

Lastly, I would like to thank my partner, Genevieve, for her constant love, support, and encouragement all these years. I am grateful for her patience, particularly when a quick trip to the lab turns into an hour-long spell. I am especially grateful for her always pushing to me to question my assumptions, even though I don't show it in the moment. Thank you for being my travel, climbing and eating partner, and best friend. I can't wait for what's next.

TABLE OF CONTENTS

ACKNOWLEDGEMENTS	iv
TABLE OF CONTENTS	vii
LIST OF FIGURES	xi
LIST OF TABLES	xiv
CHAPTER 1. INTRODUCTION.....	1
1.1 A brief history and classification of virulent and temperate bacteriophage .	2
1.2 Temperate phage biology	4
1.2.1 The lytic/lysogenic switch	8
1.2.2 Prophage replication.....	9
1.3 Temperate phage as agents of diversity and benefactors of bacteria.....	13
1.3.1 Positive (lysogenic) conversion	14
1.3.2 Negative conversion	17
1.3.3 Phage as drivers of DNA sequence diversity in bacteria	18
1.3.4 Lytic induction of temperate prophage.....	20
1.3.5 Transduction and other gene transfer events.....	23
1.4 Exploring phage contributions to the lifestyles of <i>B. anthracis</i> and <i>S. aureus</i>	24
CHAPTER 2. SELECTION BY PHAGE LYSIS AMPLIFIES A PHAGE- RESISTANT <i>BACILLUS ANTHRACIS</i> VARIANT SUBPOPULATION WITH UNUSUAL AND DYNAMIC PHENOTYPES	26
INTRODUCTION	26
2.1 A brief overview of <i>B. anthracis</i> biology, the <i>B. cereus sensu lato</i> group, and the discovery of <i>B. anthracis</i> -like <i>B. cereus</i> isolates.....	26
2.2 Role of phage in <i>B. anthracis</i>	35
2.3 How do phage from anthrax-endemic areas affect <i>B. anthracis</i> ?	40
RESULTS.....	42
2.4 Exposure of <i>B. anthracis</i> Sterne to an anthrax-derived phage identifies a Sterne variant with distinct phenotypes.....	42
2.5 Sterne:: ϕ BACA1 is not lysogenized by ϕ BACA1	50

2.6 DNA sequencing reveals a single-nucleotide insertion responsible for Sterne:: ϕ BACA1 phenotypes and ϕ BACA1-resistance	51
2.7 Sterne <i>dcsaB</i> does not show altered virulence potential in a mouse model, and exhibits an altered phenotype in the infection environment.....	57
2.8 Sterne <i>dcsaB</i> grown in fetal bovine serum displays a similar phenotype as observed in mouse tissues	59
2.9 RNA-seq reveals global gene expression differences between Sterne and Sterne <i>dcsaB</i> in BHI and FBS growth environments	64
2.10 Western blot of protective antigen correlates with RNA-seq data.....	68
2.11 Deep-sequencing reveals unstable carriage of ϕ BACA1 and that <i>csaB</i> mutation does not readily revert.....	71
DISCUSSION	77
2.12 Selection by lysis drives unique phenotypes in CA and Sterne <i>dcsaB</i>	77
2.13 <i>csaB</i> mutation in <i>B. anthracis</i> may not negatively impact fitness.....	81
2.14 How does <i>csaB</i> mutation and the external environment affect <i>B. anthracis</i> ?	83
2.15 What accounts for <i>dcsaB</i> 's Sterne-like phenotype in FBS?.....	85
2.16 How does phage-resistance affect <i>B. anthracis</i> ?	90
SUMMARY	98
MATERIALS AND METHODS.....	99
2.18 Bacterial strains and growth conditions.....	99
2.19 Exposure and lysogeny of <i>B. anthracis</i> Sterne with ϕ BACA1.....	102
2.20 Phenotypic analysis of <i>B. anthracis</i> strains	103
2.21 Next-generation sequencing of phage DNA, PCR and Southern blot screening for ϕ BACA1	105
2.22 Genomic DNA preparation and sequencing of <i>B. anthracis</i> strains.....	106
2.23 Molecular cloning and complementation of <i>B. anthracis dcsaB</i>	107
2.24 <i>In vivo</i> virulence mouse models.....	109
2.25 RNA-seq of <i>B. anthracis</i> Sterne and Sterne <i>dcsaB</i> in BHI and FBS cultures	110
2.26 Western Blot of protective antigen from <i>B. anthracis</i> culture supernatants	112

2.27 Determination of <i>B. anthracis</i> Sterne spontaneous resistance rate to ϕ BACA1	113
2.28 Determination of <i>B. anthracis</i> Sterne <i>dcaB</i> genomic reversion	114
2.29 PCR amplicon preparation and deep-sequencing of <i>csaB</i>	114
CHAPTER 3. EXTRA-CHROMOSOMAL DNA SEQUENCING REVEALS EPISOMAL PROPHAGE CAPABLE OF IMPACTING VIRULENCE FACTOR EXPRESSION IN <i>STAPHYLOCOCCUS AUREUS</i>.....	
INTRODUCTION	116
3.1 Impacts of prophage on the biology and virulence of <i>S. aureus</i>	116
3.2 The importance of phage-mobilization for bacterial pathogens	120
3.3 Uncovering extra-chromosomally localized prophage in <i>S. aureus</i>	125
RESULTS	127
3.4 Extra-chromosomal sequencing reveals the presence of episomal prophage elements within <i>S. aureus</i> clinical isolates	127
3.5 QPCR characterization of MSSA476 validates extra-chromosomal sequencing data, but also reveals episomal prophage are detectable only in extra-chromosomal DNA samples.....	133
3.6 Extra-chromosomal DNA isolation enriches circular prophage elements	138
3.7 Extra-chromosomal localization of ϕ Sa4ms circular prophage is a temporal and rare event	147
3.8 Promoter alteration by ϕ Sa4ms excision/integration affects <i>htrA₂</i> transcription and heat-stress survival in <i>S. aureus</i>	151
DISCUSSION	156
3.9 Strains and phages possess different mobilization capacities.....	156
3.10 Episomal prophage are detected only in extra-chromosomally enriched DNA samples, and are circular DNA elements that appear to be active lysogenic prophages	159
3.11 What is the biological significance of episomal phage?.....	165
SUMMARY	173
MATERIALS AND METHODS.....	174
3.12 Bacterial strains and growth conditions.....	174

3.13 Whole-genome and extra-chromosomal DNA isolation and manipulation	177
3.14 DNA sequencing of extra-chromosomal <i>S. aureus</i> samples	178
3.15 Bioinformatic sequence analysis of extra-chromosomal DNA samples .	179
3.16 QPCR analysis of <i>S. aureus</i> strains.....	179
3.17 Linear DNase and restriction endonuclease treatment of extra-chromosomal DNA samples and end-point PCR of DNA targets	180
3.18 Construction and testing of <i>PhtrA₂</i> -GFP reporter system and <i>htrA₂</i> -complemented knockouts.....	185
CHAPTER 4. CONCLUSIONS AND OUTLOOK	188
APPENDIX 1. RAW SEQUENCES OF ϕBACA1 CONTIGS	195
APPENDIX 2. PRELIMINARY DATA AND SUGGESTED FUTURE EXPERIMENTS	222
A2.1 Determination of fetal bovine serum (FBS) component(s) responsible for <i>dcsaB</i> 's phenotypic switch	222
A2.2 Uncovering ϕ BACA1-pXO1 crosstalk in <i>B. anthracis</i>	230
APPENDIX 3. RNA-SEQUENCING DIFFERENTIAL EXPRESSION DATA	233
REFERENCES	252

LIST OF FIGURES

Figure 1-1. The lytic, lysogenic, and pseudolysogenic cycles of bacteriophage	7
Figure 1-2. Overview of the λ (and λ -like) phage lysis/lysogeny switch and replication in the bacterial host.....	12
Figure 2-1. <i>B. anthracis</i> SCWP and S-layer structures	29
Figure 2-2. The plasmids and outer cell structures of <i>B. anthracis</i> , <i>B. cereus</i> G9241 and <i>B. cereus</i> BV <i>anthracis</i> CI	34
Figure 2-3. Atypical cellular morphologies of <i>B. cereus</i> Biovar <i>anthracis</i> CA	35
Figure 2-4. Phage-mediated lifestyle changes of <i>B. anthracis</i>	39
Figure 2-5. <i>B. anthracis</i> Sterne exposed to ϕ BACA1 displays atypical <i>B. anthracis</i> phenotypes.....	45
Figure 2-6. <i>B. anthracis</i> Sterne:: ϕ BACA1 harbors phenotypes similar to <i>B. cereus</i> Biovar <i>anthracis</i> CA and grows in unique, rope-like multi-chain structures.....	47
Figure 2-7. <i>B. anthracis</i> Sterne:: ϕ BACA1 displays unique growth characteristics	48
Figure 2-8. <i>B. anthracis</i> comp- <i>csaB</i> displays Sterne-like phenotypes.....	56
Figure 2-9. Survival curves of Sterne and Sterne <i>dcsaB</i> from mouse infection model.....	57
Figure 2-10. <i>B. anthracis</i> Sterne <i>dcsaB</i> displays a unique and reversible phenotype in the infection environment.....	59
Figure 2-11. Sterne <i>dcsaB</i> in FBS harbors Sterne-like and similar phenotypes to those seen in mouse infection.....	60
Figure 2-12. <i>B. anthracis</i> Sterne <i>dcsaB</i> displays different growth characteristics in BHI liquid culture at 30°C versus 37°C	61
Figure 2-13. FBS induces phenotypic changes in <i>B. anthracis</i> Sterne <i>dcsaB</i> in a dose-response-like manner	62
Figure 2-14. <i>B. anthracis</i> Sterne <i>dcsaB</i> grows in turbid culture in heat-treated FBS.....	63

Figure 2-15. Principal component analysis (PCA) plot of samples from RNA-seq	66
Figure 2-16. Western blot of protective antigen in culture supernatants validates RNA-seq data.....	70
Figure 2-17. A new, potential model of the <i>B. anthracis</i> lifecycle	97
Figure 3-1. Illustration of phage localization in <i>S. aureus</i> cystic fibrosis and bacteremic isolates	119
Figure 3-2. Illustration of SpyCIM1 genome and integration dynamics....	121
Figure 3-3. Forms of lysogeny and mechanisms for expression of virulence or fitness factors.....	124
Figure 3-4. Read-mapping and coverage analysis of MSSA476 extra-chromosomal DNA sequencing	129
Figure 3-5. QPCR characterization of MSSA476 prophage copy numbers and excision rates	137
Figure 3-6. Schematic of endonuclease and/or exonuclease treatment of MSSA476 exDNA	139
Figure 3-7. Agarose gel of PCR reactions from ϕ Sa4ms selective-depletion experiment.....	142
Figure 3-8. QPCR characterization of <i>hly</i> -converting prophages.....	146
Figure 3-9. QPCR characterization of MSSA476 prophage excision rates and copy numbers from logarithmic and overnight cultures	150
Figure 3-10. ϕ Sa4ms excision/integration alters the promoter and transcription of <i>htrA</i> ₂	155
Figure 3-11. Qualitative model of MSSA476 early logarithmic culture.....	162
Figure 3-12. Mobilizing phage can generate diverse subpopulations of <i>S. aureus</i>	169
Figure 4-1. Illustration of “conversion” and phage effects on bacterial hosts	193
Figure A2-1. <i>dcsaB</i> displays different phenotypes in fractionated FBS....	224
Figure A2-2. Sterne <i>dcsaB</i> growth in reconstituted BHI and reconstituted FBS.....	225

Figure A2-3. Sterne *dcsaB* growth in BHI-FBS and FBS-BHI mixed fraction cultures.....227

Figure A2-4. ϕ BACA1 plaquing efficiency on *B. anthracis* Δ Sterne versus Sterne strains.....230

LIST OF TABLES

Table 2-1. Phenotypes of <i>B. cereus</i> bv <i>anthracis</i> CA, <i>B. anthracis</i> , and <i>B. cereus</i>	33
Table 2-2. Phenotypic comparisons of <i>B. anthracis</i> Sterne and Sterne:: ϕ BACA1	43
Table 2-3. <i>B. anthracis</i> biofilm formation capacities.....	50
Table 2-4. Genomic alterations uncovered in Sterne:: ϕ BACA1 by whole-genome DNA sequencing.....	53
Table 2-5a. <i>B. anthracis</i> Sterne and Sterne <i>dcsaB</i> whole-genome differential expression (DE) summary.....	65
Table 2-5b. <i>B. anthracis</i> Sterne and Sterne <i>dcsaB</i> pXO1-only differential expression (DE) summary	65
Table 2-6. <i>csaB</i> variant frequencies of selected <i>Bacillus anthracis</i> strains.....	72
Table 2-7. Individual variants uncovered by deep-sequencing of <i>csaB</i> PCR amplicons	74
Table 2-8. Strains, plasmids, and primers used in this study	100
Table 3-1. Important phage-encoded virulence factors of <i>S. aureus</i>	117
Table 3-2. Detection of episomal prophage in strains from extra-chromosomal DNA isolation and sequencing.....	131
Table 3-3. Copy numbers and excision rates of MSSA476 prophages from exDNA sequencing conditions	135
Table 3-4. Copy numbers and excision rates of selected <i>hly</i> -converting prophages.....	144
Table 3-5. Copy numbers and excision rates of MSSA476 prophages at selected optical densities	148
Table 3-6. Bacterial strains and constructs used in this study	175
Table 3-7. Primers and probes used in this study.....	181
Table A3-1. Differential expression (DE) of pXO1-encoded genes comparing <i>dcsaB</i> and Sterne in FBS.....	233

CHAPTER 1. INTRODUCTION

Bacteriophage, or phage for short, are viruses that infect bacteria. They are the most abundant “organisms” on earth, have co-evolved with their hosts, and unsurprisingly, exert significant influence over the bacterial domain, in pathogenic and non-pathogenic species alike. Estimates of the total phage population in the biosphere are 10^{31} , an order of magnitude greater than their hosts (Wommack and Colwell, 2000), and in addition, the scale of bacteria-phage infections is also exceedingly large. There are an estimated 10^{24} infections per second, and as well-discussed by (Hendrix, 2005), biological interactions on this scale offer nearly unlimited opportunities for genetic exchange, horizontal gene-transfer (HGT), and evolution among phages and their bacterial hosts (Bertozzi Silva et al., 2016; Samson et al., 2013). Research in phage biology has uncovered the numerous roles the viruses play, of course as bacterial predators, but also as genetic elements imparting hosts with virulence factors (Beres and Musser, 2007; Coleman et al., 1989), promoting the bacterial colonization of animals (Schuch and Fischetti, 2009), and even driving global nutrient cycling (Wilhelm and Suttle, 1999). While bacteria are natural human pathogens, they and the microbiome are also positively implicated in human health, impacting immune system development and inflammation (Cho and Blaser, 2012), shaping the gut-brain axis (Yano et al., 2015), and preventing the development of cancer (Zitvogel et al., 2017), and phage have been shown to play a clear role in shaping microbiome composition and its associated effects (Mirzaei and Maurice, 2017). With many reports suggesting that

bacteria may be “controlling” us and research describing phage control over bacteria, it is intriguing to think that perhaps our ultimate “masters” are actually bacteria’s predators—the bacteriophage—and research efforts focused on uncovering new phage-bacteria interactions should no doubt lead to greater insights on human health. This Thesis aims to better understand the interactions between phage and bacteria, and explores some of the atypical ways in which phage influence their bacterial hosts, focusing on their roles in the Gram-positive pathogens *Bacillus anthracis* and *Staphylococcus aureus*.

1.1 A brief history and classification of virulent and temperate bacteriophage

Bacteriophage first appeared in the literature just over a century ago, with their independent discovery by Twort in 1915 and d’Herelle in 1917. In his seminal work, Twort discovered that some colonies of micrococci would turn “glassy” in cultures, that non-glassy micrococci could transform to this phenotype upon exposure to glassy colonies, and suggested that this transformation was propagated by ultra-microscopic viruses of a lower order than bacteria (Twort, 1915). Shortly after, d’Herelle uncovered microbes that would lyse “Shiga-bacilli”, terming the microbes “bacteriophage” for “bacteria eaters” (D’Herelle, 2007). Earlier reports of likely phage discovery exist in the literature as well, with one report from 1898 uncovering the phage-mediated lysis of *B. anthracis* (Gamaleya, 1898). The discovery of bacteriophage however is generally credited to Twort and d’Herelle.

The one-hundred years since these initial discoveries have found phage to exist and exert their influence over almost all corners of the biosphere, but in addition to their biological roles, bacteriophage were (and still are) indispensable tools in molecular biology (well-reviewed in (Summers, 2005)), are used directly as or provide the basis for novel antibiotics (Fischetti, 2005; O'Flaherty et al., 2009), and have numerous other biotechnological applications. This Thesis however, focuses on the natural, biological roles of phage.

The phages uncovered by Twort, d'Herelle, and other early researchers were likely virulent rather than temperate phage, and a broad distinction can be made between the two. Virulent phage are obligate predators of bacteria (existing in a lytic cycle), while temperate phage, in addition to predating bacteria via the lytic cycle, can associate with a bacterial host in a more “quiescent” state known as lysogeny. (Examples challenging the notion of lysogeny as truly “quiescent” though, will be discussed later in the text.) Virulent and temperate phage are selfish elements, focusing on their own survival and replication, and using bacterial hosts to accomplish these goals. Outside of their own propagation however, both also engage in activities that serve to generate diversity in bacterial pathogens and non-pathogens alike. Though when considering the mechanisms by which phages shape bacterial diversity, temperate phages outshine virulent phages because of their capacity to exist in the lysogenic state. This Thesis, and the remainder of the introduction, focus on temperate phage and discuss some of the known ways in

which they generate diversity among their bacterial hosts. Chapters 2 and 3 highlight research uncovering more atypical and subtle impacts of temperate phage on Gram-positive pathogens. A brief section detailing temperate phage biology is below, followed by a discussion of how such phage impact their bacterial hosts.

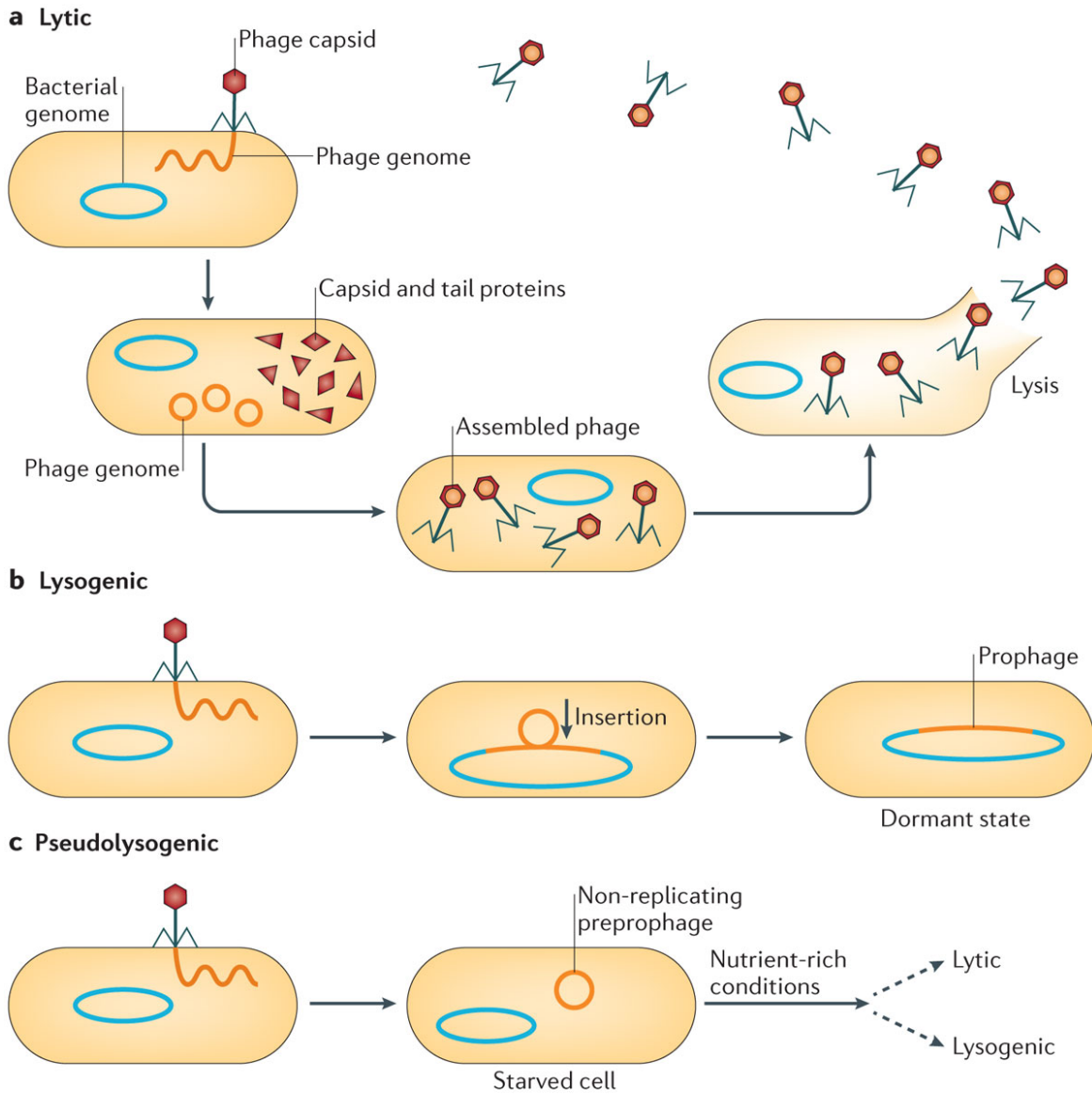
1.2 Temperate phage biology

Temperate phage were first described by Bordet in 1919, who showed that bacteria isolated from infected mice could be induced to produce phage particles in the laboratory, though he incorrectly predicted that such particles were a product of the bacteria itself rather than a separate biological entity (Summers, 2005). Esther Lederberg later uncovered phage λ (Lederberg and Lederberg, 1953), a lysogenic phage of *Escherichia coli*, setting the stage for fundamental discoveries in phage biology, particularly in the factors that govern maintenance of lysogeny and the switch to the lytic state. (Early bacteriophage work and a history of lambda are reviewed in (Summers, 2005; Casjens and Hendrix, 2015; Ptashne, 2004).

Unlike virulent phages, temperate phages are capable of a multitude of lifestyles, including the lysogenic and lytic cycles, as well as pseudolysogeny and chronic infection. Briefly, they are described and distinguished. Phage replication via the lytic cycle consists of: 1) viral adherence to a bacterial cell, 2) injection of genetic material (typically double-stranded DNA), 3) replication of DNA and synthesis of viral building blocks, 4) phage structural assembly and packaging of DNA into

heads, and 5) lytic burst from the host cell and release into the surrounding environment (Figure 1-1a). In the lysogenic cycle, phage co-exist with the bacterial host. Like the lytic cycle, phage 1) adhere to the bacterial cell and 2) inject genetic material, however following this step, phage genomes integrate within the bacterial chromosome or get maintained as cytoplasmic plasmids, but do not undergo replication and production of progeny viral particles. These phage DNA elements, termed prophage, divide with the host cell (Figure 1-1b). They can exit the lysogenic cycle however, and be induced into the lytic cycle (often in times of bacterial stress or DNA damage), executing steps 3-5 and killing the host cell. (Factors governing the lytic/lysogenic switch in phage λ will be briefly discussed in the following paragraph.) Pseudolysogeny is an intermediate state where phage 1) adsorb to the bacterial cell and 2) inject genetic material, however are held in a purgatory-like state, putting off the decision to enter the lysogenic or lytic cycle until a change in the external environment (Figure 1-1c). Lastly, chronic phage infection (not pictured), is a state where phage stably infect the bacterial cell, but continuously release progeny into the external environment without host cell death. Such a phage state occurs in the filamentous phage of *E. coli* for example, but does not occur in lambdoid (lambda-like) phages (Rakonjac et al., 2011).

Figure 1-1. The lytic, lysogenic, and pseudolysogenic cycles of bacteriophage. A) In the lytic cycle, phage recognize a specific cellular receptor and adsorb to the outside of the bacterium before injecting genetic material, then begin genome replication and synthesis of viral proteins. Packaging of genetic material into viral proteins forms functional virions, which burst from the cell in controlled host lysis. B) In the lysogenic cycle, phage recognize specific bacteria and inject their DNA as in A), however do not undergo a viral particle replication program. Instead, the prophage genome either integrates into the host chromosome or is maintained as a plasmidial element, and replicates in tune with host cellular division. C) In the pseudolysogenic state, phage follows the first steps in A) and B), however the prophage element is maintained in a non-replicative state, unlike the lytic and lysogenic cycles, which remains until changes in the external environment prompt a lysis/lysogeny decision. Reprinted from (Feiner et al., 2015) with permission.



1.2.1 The lytic/lysogenic switch

The molecular processes governing the lytic/lysogenic switch in λ are well studied (Casjens and Hendrix, 2015; Ptashne, 2004) (Figure 1-2). Briefly, the decision hinges on successful repression of the lytic state by the CI repressor protein. CI repressor protein has two core activities: 1) repression of Cro (an activator of the lytic cycle), and 2) autoregulation of CI production. Cro and CI have opposite-facing genes (5' ends closest) and share operator regions in their promoters, producing the following functional switch. CI protein binds upstream of its encoding gene, promoting its own production while simultaneously blocking the promoter for Cro. As long as CI is stably produced and maintained, the phage remains in the lysogenic state. When cellular DNA damage occurs, RecA (a bacterially-encoded protein) becomes activated and promotes the cleavage of CI, preventing CI positive autoregulation and the repression of Cro. With CI no longer repressing Cro, the lytic cycle activator is now produced and accumulates, binding CI operators, repressing CI production, allowing its own production, and activating the prophage's lytic cycle program (Calendar and Inman, 2005). The lytic/lysogenic decision for newly infecting phage depends upon levels of another protein, CII, which promotes the initial production of CI (Echols, 1986; Ptashne, 2004).

1.2.2 Prophage replication

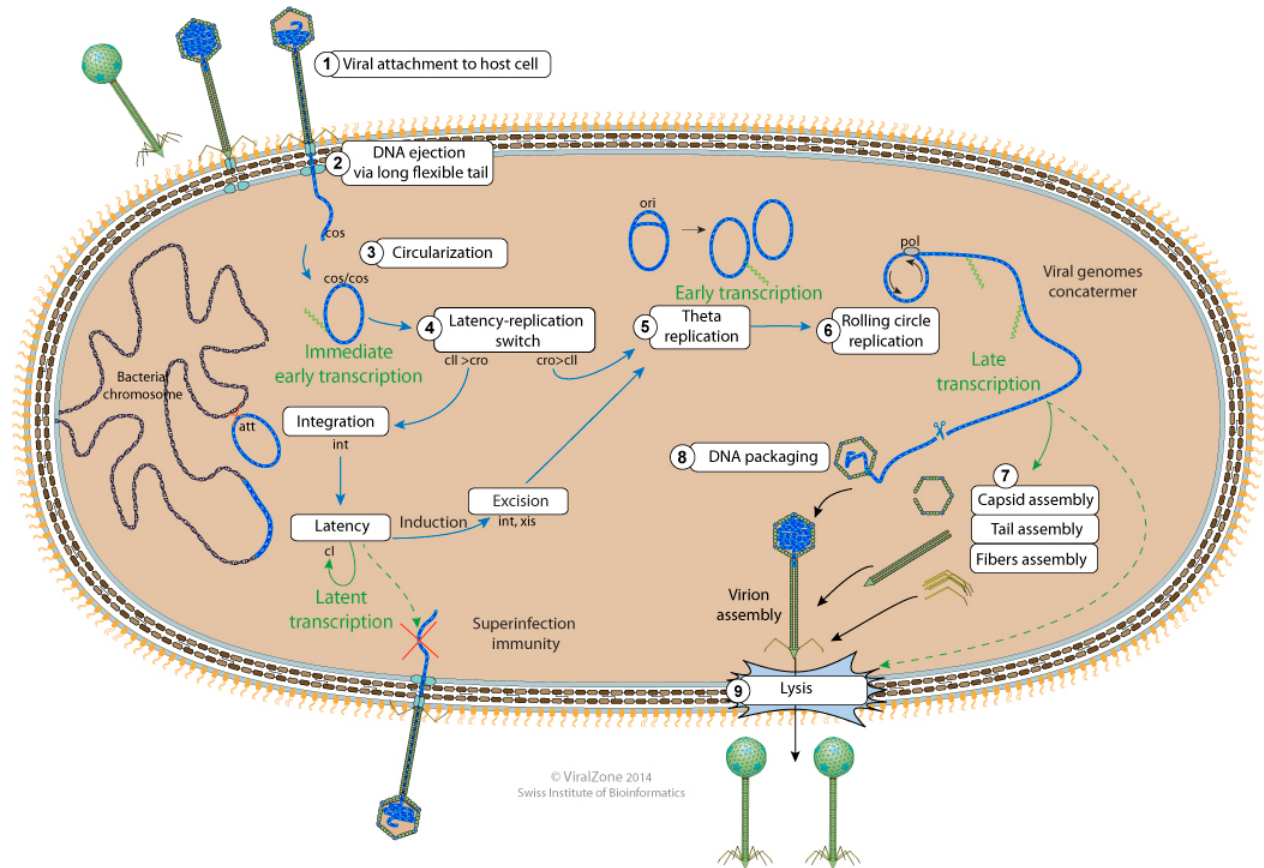
Replication of prophage is necessary to ensure its survival. In the lysogenic cycle, replication allows for phage dissemination to the host's daughter cells, and for lytic phages, the spread to new, uninfected hosts. For integrated lysogenic prophage, this is accomplished during host chromosomal replication, with chromosomes containing the prophage genome segregating to each daughter cell. Lysogenic plasmidial phages must ensure their own dissemination, and encode genes for their replication, equal segregation to daughter cells, and often, anti-curing, plasmid-addiction systems (Abeles et al., 1984; Łobocka et al., 2004).

Replication of λ (and λ -like) phage in the lytic cycle is well-studied and will be briefly summarized (Enquist and Skalka, 1978) (Figure 1-2). Following induction into the lytic cycle, the prophage excises from the chromosome into the cytoplasm as a circular DNA element and begins bi-directional, θ -replication, creating multiple circular copies of its genome. Following θ -replication, unidirectional rolling-circle replication generates long, linear prophage concatemers, containing multiple copies of prophage genome per DNA molecule. For λ , these concatemers are cut at specific sites, creating individual phage genomes with single-stranded cohesive ends of DNA (cos sites). Genomes are then packaged into phage particles. Other lambda-like phages can contain either cos sites or are packaged through an alternative mechanism known as headful packaging. Here, a linear concatemer is recognized at a "pac"-site, cut, and DNA injected into a phage head until it can no longer contain

any more DNA. This is typically about 105% of the phage genome. After the second cut, the next phage genome in the molecule is packaged in the same manner until the phage head is full, however the resulting phage contains different DNA ends than the first phage. This process continues until the rest of the DNA molecule is packaged, and results in a phage population that contains terminally redundant and circularly permuted genomes.

The discussion of phage biology thus far has not addressed host impacts of phage carriage. Clearly, phage infection (lytic or lysogenic) does not exist in a vacuum, and the bacterial cell should not be thought of as merely a factory for phage propagation, but rather a dynamic organism that is drastically changed by carriage of viruses. The following section discusses a number of the known mechanisms by which temperate phage impact and influence their bacterial hosts.

Figure 1-2. Overview of the λ (and λ -like) phage lysis/lysogeny switch and replication in the bacterial host. 1), 2) and 3) The lytic and lysogenic cycles begin with the same series of steps: phage adsorption to the cell surface, DNA ejection from the phage head, and circularization of the genome (for λ this is achieved through annealing of single-stranded, complementary cos ends). 4) A decision is made to enter the lytic or lysogenic cycle, dependent upon levels of CII protein. If levels of CII are relatively high, the phage enters the lysogenic cycle, typically integrating within the host chromosome via recombination between *attB* and *attP* sites, and the state stabilized by CI production, also providing superinfection immunity. Under inducing conditions, CI is cleaved, allowing Cro production, phage excision and exit from the lysogenic cycle. Alternatively, phage can enter the lytic cycle immediately following injection of DNA (2). 5) In the lytic cycle, phage replicate their genome, first undergoing θ -replication resulting in multiple circular genome copies, followed by 6) rolling circle replication where long linear concatemers containing multiple phage genomes are generated. Then, 7) transcription and production of phage structural proteins occurs. Lastly, 8) single phage genomes are cut from concatemers, packaged into phage particles, and 9) virions released by endolysin-induced cell lysis. Figure reprinted with permission from ViralZone and SIB Swiss Institute of Bioinformatics. © 2014 ViralZone and SIB Swiss Institute of Bioinformatics.



1.3 Temperate phage as agents of diversity and benefactors of bacteria

Temperate phage, especially within the lysogenic cycle, impart important advantages to their bacterial hosts. This positive feature of phage infection for the bacteria is an evolutionary trade-off: bacteria house elements that can and will likely kill them at signs of damage or stress, but they allow better survival and adaptation to the external environment than in their absence. The benefits of this tradeoff are no doubt why we see so many diverse bacterial species harboring lysogenic prophage today. Besides, it is possible that if a bacterium harbors no phage, it will be outcompeted by related phage-harboring strains and fail to survive regardless. This section outlines some of the ways phage impart benefits to their hosts as “benefactors of bacteria”. While the following mechanisms discussed are diverse, they all result in the same end goal: generating diversity within bacterial species. Phage can drive the diversity of and benefit bacteria through a number of mechanisms including: 1) positive (lysogenic) conversion, 2) negative conversion, 3) genome diversity and chromosomal rearrangements, 4) lytic induction, and 5) transduction and other DNA transfer events. Phage-driven diversity, coupled with evolutionary selection, likely accounts for the excellent pathogens many bacterial species are today. A discussion of each diversity mechanism follows, however the contributions of phage to bacteria are also well reviewed in (Brussow et al., 2004; Canchaya et al., 2004; Feiner et al., 2015; Nanda et al., 2015).

1.3.1 Positive (lysogenic) conversion

Perhaps the most impactful role of temperate phage in bacteria is through positive (lysogenic) conversion, or the introduction and expression of foreign genes in a bacterial host. The genes implicated in lysogenic conversion are often termed “morons”, for **more** DNA **on** the prophage genome than necessary for survival, replication, or establishment of the lysogenic state (Brussow et al., 2004). Any connotation of these genes being useless or “moronic” should however be quickly dispensed of; as a consequence of selection, morons typically encode important virulence determinants or other bacterial fitness factors responsible for survival or severe invasive disease (e.g. streptococcal toxins and superantigens) (Beres and Musser, 2007)). The term positive conversion itself denotes the bacterial phenotype being converted by harboring prophage (i.e. non-lysogenized bacterium: phenotype⁻ → lysogenized bacterium: phenotype⁺). A few important examples of lysogenic conversion are discussed below.

The pathogenicity of *S. aureus* depends on an arsenal of virulence factors, many of which are encoded on temperate prophage genomes (Thammavongsa et al., 2015; Thomer et al., 2016). In *S. aureus* Newman, for example, the strain displays severely reduced virulence in a mouse model when cured of its four resident prophages (Bae et al., 2006). One of its prophages, ϕ NM3, encodes virulence factors including staphylokinase (SAK), staphylococcal enterotoxin A (SEA), chemotaxis inhibitory protein of *S. aureus* (CHIPS), and staphylococcal complement inhibitor

(SCIN), and its curing significantly reduces abscess formation. Importantly, ϕ NM3 is a β -hemolysin (*hly*)-converting phage, indicating that while it positively converts cells for SEA, SAK, CHIPS and SCIN, it integrates within the gene for another virulence factor, *hly*, disrupting its transcription, and negatively converting cells (i.e., Newman: $hly^-/sea^+/sak^+/scin^+/chips^+$; Newman $\Delta\phi$ NM3: $hly^+/sea^-/sak^-/scin^-/chips^-$). Negative conversion will be discussed further in the next section.

In *Streptococcus pyogenes*, prophages carry DNases, hyaluronidases, as well as a number of superantigens called SPEs (streptococcal pyrogenic exotoxins), which are non-specific T-cell activators that contribute to the symptoms of “Scarlet Fever” (Beres and Musser, 2007). Their direct contributions to disease however, have not been fully elucidated. Notably, The Rockefeller University was founded following the death of John D. Rockefeller Sr.’s grandson from streptococcal disease. Whether or not lysogenic conversion is responsible for the foundation of other universities is unclear, but it appears we owe it to phage for the development of our home institution.

In a distinct manner from strict virulence factor carriage, morons can also encode fitness factors (Brussow et al., 2004), including transcription and sigma factors that alter the activities of the cell. Lysogeny of *B. anthracis* by *Bacillus spp.*-infecting phages was shown to alter the pathogen’s biofilm formation capacity, promote

earthworm colonization, promote or block sporulation, and induce exopolysaccharide coatings on vegetative cells and spore structural changes (Schuch and Fischetti, 2009). These phenotypes were found to be mediated by phage-encoded sigma factors. Whether or not these factors are truly morons with no role in the phage lifecycle however, is unclear. Also notable for *B. anthracis* and the related species *Bacillus cereus* and *Bacillus thuringiensis* are the findings that while these three species have highly related chromosomes, they exhibit markedly different phenotypes (Kolstø et al., 2009). In addition, these strains have been shown to harbor an array of inducible prophage, suggesting that positive conversion may play a role in generating the unique phenotypes among the three species (BUCK et al., 1963; Kiel et al., 2008).

While not encoded by morons per se, superinfection immunity (blocking of infection by similar phage) may also be considered a feature of lysogenic conversion.

Typically, superinfection immunity occurs through the production of compatible CI repressor, preventing infecting phage from executing a lytic cycle. In some cases, however, prophage will encode specialized immunity genes to prevent superinfection. *E. coli* ϕ V10, for example, encodes an O157 antigen-modifying enzyme (*oac*) that alters the ϕ V10 receptor, preventing superinfection (Perry et al., 2009).

1.3.2 Negative conversion

Negative conversion is not quite the direct opposite of positive conversion, but rather is a potential consequence of carrying integrated prophage. Prophage integration occurs in various parts of the chromosome (or on resident plasmids) and depending upon where prophage integrate, the transcription of genes may be interrupted and cells converted to a negative phenotype. As previously mentioned, the *hly*-converting phages of *S. aureus* integrate within the β -hemolysin gene, and disrupt transcription of the full-length gene product. For *S. aureus*, the trade-off appears evolutionarily favorable, as the phage carries multiple virulence factors, and strains containing *hly*-converting phages are most commonly associated with infection (Coleman et al., 1989; 1991; Goerke et al., 2006). In a similar manner, ϕ L54a and related phage of *S. aureus* integrate within the lipase (*geh*) gene, shutting down its functional production. These phage however, do not appear to code for known virulence determinants, morons, or other fitness factors (Lee and Iandolo, 1986; Lee et al., 1985). Lipase is a known virulence factor, making the evolutionary appeal for phage carriage and associated negative conversion as of yet, unclear (Hu et al., 2012).

In *S. pyogenes*, a different type of “negative conversion” occurs with the phage-like chromosomal island SpyCIM1 (formerly termed ϕ 370.4). This prophage-like element integrates within the mismatch-repair (MMR) operon on the chromosome, negatively converting cells for the loss of MMR activity, resulting in an increase of

the cellular mutation rate approximately 200-fold (Scott et al., 2008; 2012).

Interestingly, this element displays a unique excision/integration pattern dependent on cell density, allowing the cell to regain MMR activity while still retaining the phage-like element. A more detailed discussion of SpyCIM1 and similarly related events in other bacterial species is located in Chapter 3.

1.3.3 Phage as drivers of DNA sequence diversity in bacteria

Lysogeny is also a key driver of sequence diversity among strains within a given bacterial species. Bacterial pathogens carry essential and non-essential genes, with the latter typically involved in virulence and other fitness-associated activities.

These non-essential genes are typically different among strains, and often are the key differences allowing strain differentiation. Fitzgerald *et al.* report that nearly a quarter of the *S. aureus* genome (22%) encodes such non-essential genes, and it is in fact prophage sequences that comprise the majority of these regions. Similar patterns are also present in other pathogenic species such as *E. coli* and *Helicobacter pylori* (Fitzgerald et al., 2001). Such differences in prophage content may drive the pathogenicity of select strains and differences in clinical manifestations of disease (Goerke et al., 2004; 2006). In *S. pyogenes*, the majority of sequence-level differences among strains and M-types are prophage related (Beres and Musser, 2007). M1 and M18 strains differ primarily in prophage sequences (Smoot et al., 2002), and the enhanced virulence of the M3 strain MGAS315 is speculated to arise from a diverse array of phage-encoded morons that all appear in

the poly-lysogenized strain (Beres et al., 2002). The M3 strain in particular is an example of an additional method by which prophages can introduce diversity: serving as anchor points for chromosomal rearrangements. In the SSI-1 M3 strain of *S. pyogenes*, the presence of two integrated prophage allowed a 1 Mbp chromosomal inversion and the generation of this unique strain. The inversion itself also resulted in a swap of phage virulence genes, and as a consequence, the strain contains novel prophage genomes in addition to altered M3 chromosomal synteny (Nakagawa et al., 2003).

Prophage genomes are arranged in modules, or groups of genes with specific functions. Typically these are: lysogeny, DNA replication, transcriptional control, DNA packaging, head/tail morphogenesis, lysis, and in some cases, accessory genes. This structure allows the rapid swapping of modules between prophage genomes in multiply phage-infected cells and the fast evolution of prophage genomes. Such exchanges occur because the DNA sequences on module borders tend to be highly homologous among phages, while the genes of the modules themselves can be vastly different. Thus, phage can easily exchange modules via homologous recombination and markedly change their genomes, potentially affecting both their host-range and the virulence or fitness of their hosts. For example, if phage “A” with a broad host range swaps accessory gene modules with a co-infecting narrow-range phage “B” (which encodes potent virulence factors), phage B’s original morons can now rapidly disseminate to new strains, or even species. The γ -phage of *B. anthracis* is believed

to have undergone such a homologous recombination, exchanging a spore-antigen moron for a fosfomycin resistance-encoding gene from ϕ 4066 (Schuch and Fischetti, 2006). A particularly interesting case is seen in the phages SpaA1 and BceA1. These phages are nearly identical by sequence, are a chimera of different prophage regions from *B. thuringiensis* and *B. cereus*, and remarkably, also contain an additional complete prophage (MZTP02) in their genomes, in what is termed a “Russian Doll” arrangement. BceA1 has a broad host range, capable of infecting *Staphylococcus pasteurii* and *B. cereus/B. thuringiensis*, however it is unclear if the phage carries lysogenic conversion genes that can affect both hosts (Swanson et al., 2012). Regardless, these phages represent the extent to which module exchange produces novel prophage genomes, generating new elements to affect bacterial hosts.

1.3.4 Lytic induction of temperate prophage

The methods by which temperate phage drive diversity and impact hosts discussed so far have mainly dealt with phage in the lysogenic cycle. The induction of temperate phage into the lytic cycle however, also has a number of consequences both on the individual cell and population levels. For individual bacterial cells, induction into the lytic cycle likely leads to cell death, and cannot be seen as beneficial. On the population level however, limited induction of lysogenic phage can be beneficial, especially when the induced phage carry important lysogenic conversion genes. Quite often, morons are carried in the late lytic region of the prophage genome, such that when phage induction occurs, these genes are

significantly upregulated. In *S. aureus* MSSA476, the *hly*-converting phage ϕ Sa3ms carries *sak*, *sea*, and *scin*, located adjacent to the host lysis cassette. Induction of phage by mitomycin C increases transcription of *sak* and *sea*, from both native and phage lytic cycle promoters (Sumbly and Waldor, 2003). In an infection environment, ϕ Sa3ms induction in a small proportion of the MSSA476 population could provide the whole population with increased levels of SEA and SAK, and allow more successful infection of hosts.

In a similar manner, pathogenic *E. coli* harboring Shiga-toxin converting phage (*stx* phage, encoding the Shiga toxin) are found to be induced in mammalian hosts and low-iron conditions. The location of the *stx* gene (controlled by lytic cycle promoters) allows its increased expression during phage induction, and phage-mediated lysis of *E. coli* cells allows the release of toxin into the external environment. Shiga toxin itself liberates iron from mammalian host cells, and in this case, the sacrifice of a few *E. coli* cells improves conditions for the remainder of the pathogenic bacterial population (Nanda et al., 2015). For *S. aureus* and *E. coli*, phage induction allows clonal populations to diversify into “toxin producing factories” and their beneficiaries who will go on to survive. Separate from the increased transcription of virulence genes, the controlled induction of temperate phage in *Pseudomonas aeruginosa* allows for the release of DNA and other cellular debris to seed biofilms, benefiting the rest of the population (Webb et al., 2003).

In a distinct manner, induction of temperate phage can also alter populations for the selection of phage-resistant variants. While not benefitting the bacteria directly, selection for phage resistance can impart protection against other phages present in the environment if they use similar mechanisms for adsorption, entry, or replication. In clonal populations, phage reinfection of cells is generally blocked by superinfection immunity, however there are reports of successful superinfection by *Bacillus*-infecting phage (BUCK et al., 1963). In these cases, development of phage-resistance (or keeping a small phage-resistant subpopulation) may benefit the whole population, serving as insurance in case of exposure to superinfecting phages. In general however, the selection of phage-resistant variants is typically associated with negative fitness, and phage-resistant strains often show decreased virulence (Filippov et al., 2011; León and Bastías, 2015). In *S. aureus*, phage-resistant strains were found to be attenuated for virulence, and even used for successful vaccine development (Capparelli et al., 2010). In *E. coli*, phage-resistant mutants can lack antigenic capsular polysaccharides (Stirm, 1968). Some reports, mainly outside of pathogenesis, have shown phage resistance as a potential benefit, with *Streptococcus thermophilus* resistant variants showing equivalent levels of acidifying activity in milk cultures (Binetti et al., 2007). This benefit, however, is likely directed toward humans using the strain in industrial fermentations, and not bestowed upon the bacteria themselves. Chapter Two details the discovery of a phage-resistant mutant in *B. anthracis* that harbors a unique phenotype without

apparent attenuation of virulence potential, challenging the notion that development of phage-resistance by genomic alteration results in negative fitness.

1.3.5 Transduction and other gene transfer events

Also occurring outside of the lysogenic cycle is transduction, or the transfer of non-phage DNA by phage. (Virulent phage are also capable of transduction.)

Generalized or specialized transduction (movement of any DNA versus typically phage genome-adjacent or -associated DNA) by phage allows the rapid spread of genes that may encode virulence determinants or other fitness factors (e.g. antibiotic resistance). In *S. aureus*, for example, bacteriophage transduction was shown to transfer *mecA*, encoding methicillin resistance (Chlebowicz et al., 2014). Such activity becomes increasingly important given the present-day relative ease of phage (and pathogenic bacteria as well) to travel to far reaches of the globe. For bacteria, phage can serve as an easy delivery system to acquire new sequence diversity and functional genes from related strains or species to increase survival, fitness, or virulence.

In addition to these forms of transduction, phages can also serve as helpers for the dissemination of other non-self, phage-like elements. One key example is found in the phage-like chromosomal islands of *S. aureus*. *S. aureus* pathogenicity islands (SaPIs) can fill phage heads of a “helper” phage with their own genetic material, akin to a hijacker stealing a car. Here, the hijacker (SaPI) gets to its desired

destination (uninfected surrounding bacteria), but the owner (the helper phage genome) is left behind (Novick et al., 2010). SaPIs have been found to encode for virulence factors, including those responsible for toxic-shock syndrome, and phages allow their dissemination and generate increased diversity among *S. aureus* isolates (Lindsay et al., 1998). SpyCIM1, the phage-related chromosomal island of *S. pyogenes* is thought to require helper phages as well, but such potential phage vehicles have not yet been uncovered (Nguyen and McShan, 2014).

1.4 Exploring phage contributions to the lifestyles of *B. anthracis* and *S. aureus*

Classifications of phage and bacteria-phage interactions are often thought of in broad strokes: virulent versus temperate, lytic versus lysogenic, and concepts of positive and negative conversion as 100% absolute. Indeed, this introduction has presented some major concepts in this way. Thinking in this manner is useful for initially understanding phage biology, however it oversimplifies the vast nature of phage and their interactions with bacterial hosts. Recent reports have illustrated that a more complex and dynamic relationship exists between bacteria and their phages as well as between phages themselves (Goerke et al., 2004; 2006; Swanson et al., 2012). The phage-bacteria relationship is estimated to be greater than three billion years old (Hatfull and Hendrix, 2011), and no doubt intricacies exist between bacteria and phage beyond these broad strokes. The following chapters explore a couple of these more atypical, intricate phage-bacteria interactions: the selection

and expansion of phage-resistant subpopulations in *B. anthracis*, and the excision/integration dynamics of episomal lysogenic prophage in *S. aureus*.

Both projects were initially undertaken to explore potential lysogenic conversion in each Gram-positive pathogen. In *S. aureus*, extra-chromosomal DNA isolation and next generation sequencing screened clinical isolates for the presence of rare, lysogenic plasmidial phages that could be “hidden in plain sight”. Such work aimed to uncover novel phages encoding virulence determinants and lend greater understanding into the virulence potential of clinical strains. For *B. anthracis*, the impacts of phage from non-pathogenic environmental sources are well-described (Schuch and Fischetti, 2009), however this project sought to help understand how lysogenic conversion of *B. anthracis* by phage from anthrax-endemic environments could affect the bacteria, and whether such phage played any role in pathogenesis. In both projects, we did not identify novel phage capable of lysogenic conversion, but rather, uncovered more subtle, intricate mechanisms by which phage influence bacterial hosts. In *S. aureus*, we find that episomal lysogenic prophage are fairly widespread among clinical isolates, and that their excision/integration dynamics have important impacts on the host. In *B. anthracis*, we discover that phage-resistant subpopulations may play a role in the lifestyle of the pathogen, and uncover a phage-resistant variant with a unique and highly unusual phenotype. The following Chapters describe these projects, and begin with introductions detailing relevant project- and species-specific background information.

CHAPTER 2. SELECTION BY PHAGE LYSIS AMPLIFIES A PHAGE-RESISTANT *BACILLUS ANTHRACIS* VARIANT SUBPOPULATION WITH UNUSUAL AND DYNAMIC PHENOTYPES

INTRODUCTION

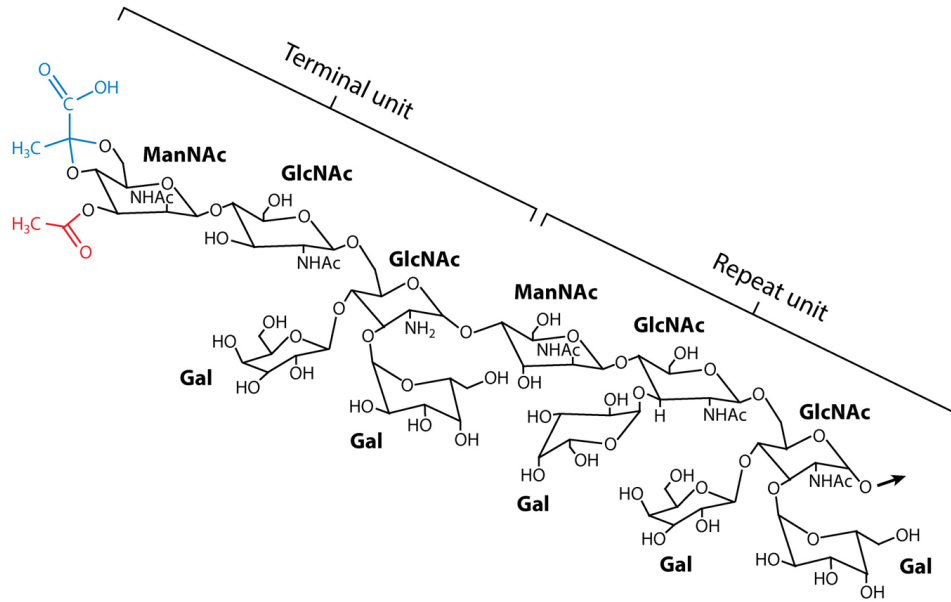
2.1 A brief overview of *B. anthracis* biology, the *B. cereus* sensu lato group, and the discovery of *B. anthracis*-like *B. cereus* isolates

Bacillus anthracis is a Gram-positive, spore-forming pathogen that exists as a monomorphic species within the *Bacillus cereus* sensu lato (s.l.) group. This group contains six species in total, including *B. cereus* and *B. thuringiensis* which are highly related to *B. anthracis*. The three species share a conserved chromosome, core set of genes, and an array of chromosomally-encoded virulence factors (Kolstø et al., 2009; Radnedge et al., 2003; Zwick et al., 2012). Genomically, *B. anthracis* is distinguished in the group by the presence of four chromosomally-integrated prophages (Sozhamannan et al., 2006) and a specific nonsense mutation in the *plcR* (phospholipase C regulator) gene, which encodes a transcriptional activator of virulence factors such as enterotoxins, hemolysins, phospholipases, proteases, and other extracellular protein-encoding genes (Kolstø et al., 2009). Phenotypically, *B. anthracis* is a non-hemolytic, non-motile, penicillin-sensitive and γ -phage sensitive species with some of these phenotypes linked to PlcR transcriptional activation. *B. cereus* on the other hand is typically hemolytic, motile, penicillin-resistant, γ -phage resistant, and encodes a functional PlcR protein. Despite clear phenotypic

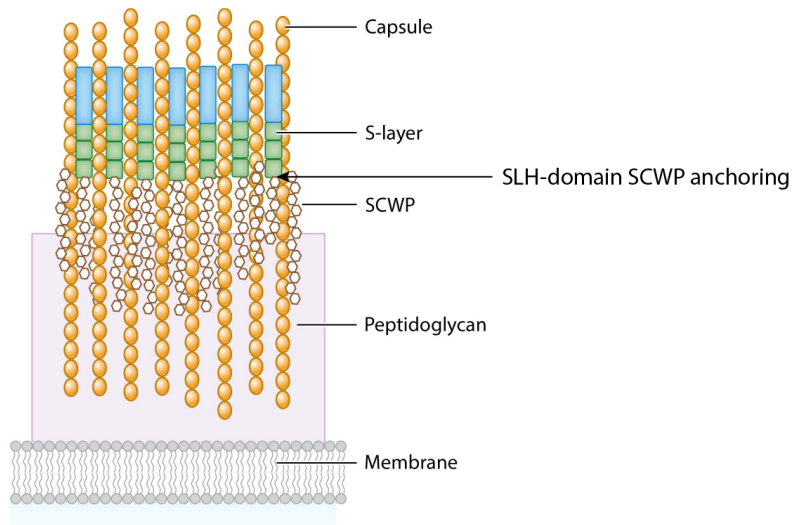
differences, differentiation between *B. anthracis* and some *B. cereus* strains has become increasingly difficult with the emergence of pathogenic *B. cereus* strains presenting anthrax-like disease (Brézillon et al., 2015; Hoffmaster et al., 2004; Wang et al., 2013). One report however, distinguished *B. anthracis*, *B. cereus*, and *B. thuringiensis* on the basis of *csaB* (cell surface anchoring) gene nucleotide sequence analysis, finding the three *B. cereus* sensu lato species clustered into two groups, with all *B. anthracis* and the majority of mammalian-isolated pathogenic *B. cereus* in one cluster, and *B. thuringiensis* insect-infecting strains clustered in the other (Zheng et al., 2013). The *csaB* gene itself encodes a pyruvyl-transferase essential for Surface-layer (S-layer) and S-layer-associated protein (BSL) anchoring to the *B. anthracis* secondary cell wall polysaccharide (SCWP) (Mesnage et al., 2000). Specifically, CsaB catalyzes the addition of a ketal pyruvyl group onto the terminal N-acetylmannosamine (ManNAc) of the SCWP, allowing the non-covalent anchoring of S-layer proteins and BSLs via a surface layer homology (SLH) domain (Figure 2-1a) (Anderson et al., 2011; Missiakas and Schneewind, 2017; Soufiane et al., 2011).

Figure 2-1. *B. anthracis* SCWP and S-layer structures. A) Molecular structure of *B. anthracis* SCWP. The *B. anthracis* SCWP contains a repeating backbone of N-acetylglucosamine-N-acetylmannosamine (GlcNAc-ManNAc) linkages, with β - and α -galactose (Gal) substitutions on GlcNAc as shown (Choudhury et al., 2006). The terminal unit of the SCWP contains acetylated and ketal-pyruvylated ManNAc, with the pyruvyl group serving as an anchor for non-covalent bonding of the S-layer proteins Sap and EA1, and in addition, BSLs. B) Diagram of the *B. anthracis* cell envelope. *B. anthracis* contains a single plasma membrane and peptidoglycan to which the SCWP and poly- γ -D-glutamic acid capsule are attached. The S-layer proteins are attached to the SCWP by non-covalent anchoring of SLH-domains (green) to pyruvylated terminal ManNAc (arrow). Figure adapted from (Missiakas and Schneewind, 2017) with permission.

A



B



The *B. anthracis* S-layer itself has been well-characterized (Etienne-Toumelin et al., 1995; Mesnage et al., 1997; Missiakas and Schneewind, 2017) and is an important, distinguishing feature for *B. anthracis* and *B. anthracis*-like pathogenic strains of *B. cereus* (Figure 2-1b). Fagan and Fairweather describe the S-layer as a modulating, functional structure allowing the cell to carry out specific activities and interactions with its external environment (Fagan and Fairweather, 2014). For *B. anthracis*, the S-layer is chiefly comprised of two proteins, Sap and EA1, which cover the cell in a para-crystalline lattice and have demonstrated murein-hydrolase activity (Ahn et al., 2006). Twenty-two other BSLs have been confirmed or predicted with roles in cell-separation (Anderson et al., 2011), virulence (Kern and Schneewind, 2008), and nutrient acquisition (Tarlovsky et al., 2010). These include: adhesins (BslA) (Kern and Schneewind, 2008), N-acetylglucosaminidases (BslO) (Anderson et al., 2011), amidases (BslS, BslT, BslU, AmiA) (Fagan and Fairweather, 2014), β -lactamases (BslM) (Fagan and Fairweather, 2014), and heme-scavenging proteins (BslK) (Tarlovsky et al., 2010). Clearly, the S-layer is an important structure for *B. anthracis* to execute activities important to its survival and pathogenesis (Nguyen-Mau et al., 2012; Oh et al., 2017; Schneewind and Missiakas, 2012). Perhaps unsurprisingly, given the number of proteins that comprise the S-layer and their total reliance on CsaB-mediated SCWP pyruvylation for anchoring (Kern et al., 2010), mutation in *csaB* carries multiple downstream effects on the cell. (Mesnage et al., 2000) describe a *B. anthracis csaB* knockout harboring a phenotype of small convex colonies, clusters of cells that fall to the

bottom of tubes in liquid culture, and long chains of twisted cells. This *csaB* knockout was also unable to deposit Sap and EA1 on the cell wall (Mesnage et al., 2000). Similarly, (Wang et al., 2013) show that BslO is not deposited on the cell walls of a *B. cereus* G9241 *csaB* mutant. In addition, phage-resistance has also been linked to *csaB* mutation (Bishop-Lilly et al., 2012; van Zyl et al., 2015), with CsaB-deficient mutants selected for by infection with AP50c phage.

In addition to the S-layer, the well-described virulence plasmids pXO1 and pXO2 are key components of pathogenic *B. anthracis* (Figure 2-2a). The pXO1 plasmid encodes for the three anthrax-toxin components: protective antigen (*pag*), lethal factor (*lef*), and edema factor (*cya*), as well as the regulator genes *atxA* and *pagR*, while pXO2 encodes for the poly- γ -D-glutamic acid (PDGA) capsule important for host immune system evasion (Moayeri et al., 2015; Mock and Fouet, 2001; Young and Collier, 2007). Previously, the presence of pXO1 and pXO2 was used to differentiate *B. anthracis* from *B. cereus* and *B. thuringiensis*. It is now recognized however, that the presence of these plasmids is not solely *B. anthracis*-specific (Kolstø et al., 2009). A number of *B. cereus* disease-causing isolates with anthrax-like pathogenesis have been found to carry the highly homologous virulence plasmids, pBCXO1 and pBCXO2. G9241 is one such isolate, harboring pBCXO1 with 99.6% sequence similarity over homologous regions to pXO1, and encodes *pag*, *lef*, *cya*, *atxA* and *pagR* (Figure 2-2b) (Hoffmaster et al., 2004; 2006; Oh et al., 2011). Other *B. cereus* isolates harbor both pBCXO1 and pBCXO2 (Leendertz et al., 2006).

B. cereus Biovar *anthracis* CA harbors both plasmids and is a *B. anthracis*-like strain isolated from the carcass of an ape believed to have died of anthrax infection in Cameroon (Brézillon et al., 2015). *B. cereus* bv *anthracis* CA, herein referred to as “CA”, straddles the classic boundaries of *B. anthracis* and *B. cereus* (Klee et al., 2010). The strain encodes both the *B. anthracis*-associated PDGA capsule on pBCXO2 as well as a hyaluronic acid capsule on pBCXO1 via functional *hasA*, which is typically mutated in *B. anthracis* (Figure 2-2c).

(Klee et al., 2006) describe unusual phenotypes in the initial report of the CA strain, where colonies at 24 hours growth displayed typical *B. anthracis* phenotypes including: non-hemolytic, rough-edged colonies with grey-green coloring and “Medusa heads” (curled projections at the colony edge), but after 48 hours growth, the same colonies were found to have transitioned and displayed a smooth, shiny phenotype with a yellow-green center, and in addition were smaller than that of classic *B. anthracis*. Subclones of single CA colonies were found to repeatedly display a mix of phenotypes, including some small, smooth colonies with β -hemolytic activity (a hallmark of *B. cereus*) and sensitivity to γ -phage (a hallmark of *B. anthracis*) (Klee et al., 2006). In addition, CA cells contained twisted, corkscrew-like morphologies, atypical of *B. anthracis* (Figure 2-3). A summary of CA’s characteristics is presented in Table 2-1. The CA strain represents an unusual hybrid of *B. anthracis* and *B. cereus*, possessing phenotypic hallmarks of both species (Kamal et al., 2017; Klee et al., 2006; 2010), while also displaying unusual

behavior where subclones of the same colony possess different phenotypes. CA represents a unique, disease-causing, anthrax-presenting isolate; research described later in this Chapter details efforts to uncover the role and contributions of phage to its unusual characteristics and lifestyle.

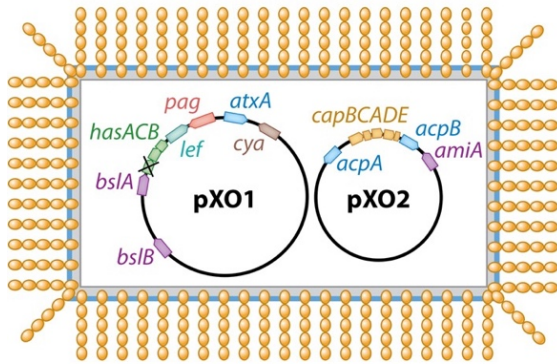
Table 2-1. Phenotypes of *B. cereus* bv *anthracis* CA, *B. anthracis*, and *B. cereus*.

Microbiological characteristic	Result			
	<i>B. cereus</i> bv <i>anthracis</i> CA		<i>B. anthracis</i>	<i>B. cereus</i>
	Primary culture	Subculture		
Hemolysis	–	+/-	–	+
Motility	+	+	–	+
Susceptibility to γ-phage	–	+/-	+	–
Penicillin G	R	R	S	R
Capsule	+	+/-	+	Absent <i>in vitro</i>

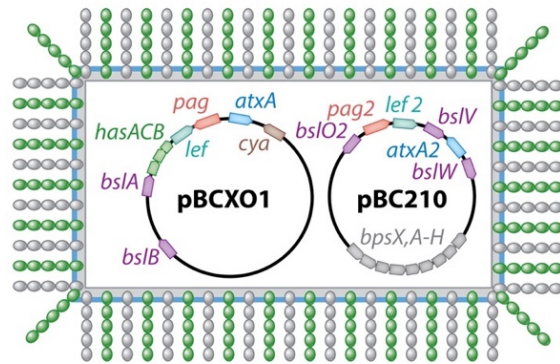
S, sensitive; R, resistant; –, negative; +, positive; +/-, some subclones positive, others negative.

Table adapted and reprinted with permission from (Klee et al., 2006).

a *Bacillus anthracis*



b *Bacillus cereus* G9241



c *Bacillus cereus* biovar anthracis CI

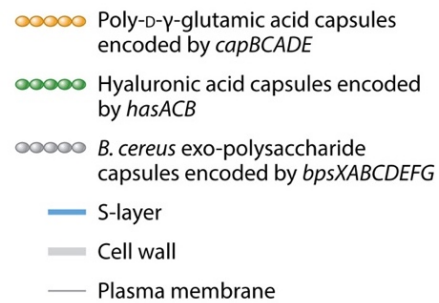
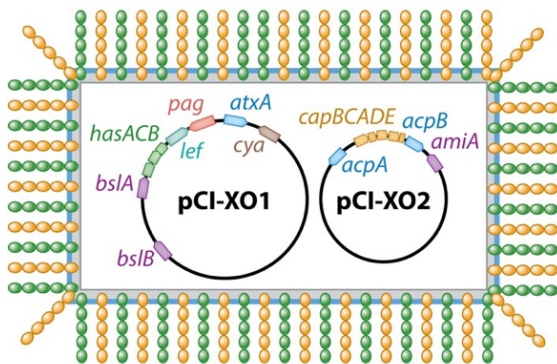


Figure 2-2. The plasmids and outer cell structures of *B. anthracis*, *B. cereus* G9241 and *B. cereus* BV *anthracis* CI. A) *B. anthracis* harbors virulence plasmids pXO1 and pXO2, encoding the anthrax toxin genes *pag*, *lef*, *cya* as well as the regulator *atxA*. It contains a poly-γ-D-glutamic acid capsule and functional S-layer. B) *B. cereus* G9241 harbors pBCXO1, highly homologous to pXO1, however it encodes functional *hasA*. It does not encode for a pXO2-like plasmid. Consequently, it produces anthrax toxin, as well as a hyaluronic acid and *B. cereus*-specific capsule, but not PDGA. C) *B. cereus* Biovar *anthracis* CI is a unique African isolate highly homologous to CA, which encodes pXO1- and pXO2-like virulence plasmids. It produces anthrax toxin, poly-γ-D-glutamic acid capsule, and via functional *hasA*, hyaluronic acid capsule. Figure used with permission from (Missiakas and Schneewind, 2017).

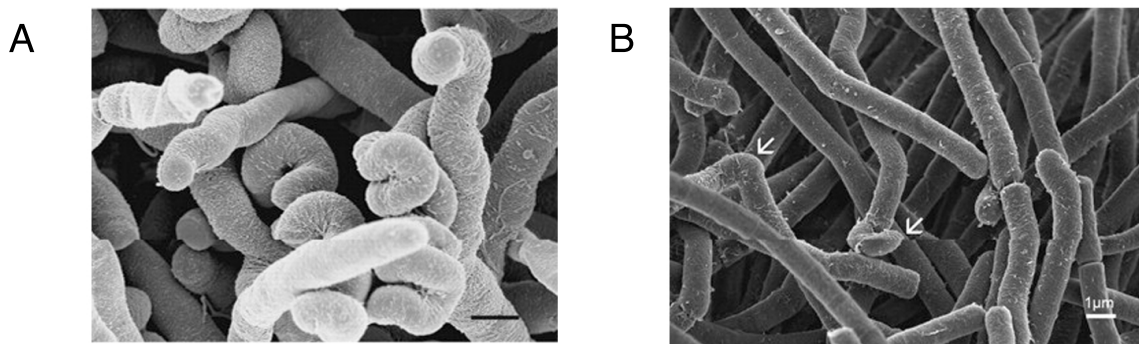


Figure 2-3. Atypical cellular morphologies of *B. cereus* Biovar *anthracis* CA. CA has unique cellular morphologies with twisted, corkscrew-like cells seen in (A). In addition, clear cell division septa are not apparent. Typical *B. anthracis* (B) contains straight, rod-like cells with clear division septa. The unique structures seen in (A) are rarely found (arrows) on *B. anthracis* cells. Figures reprinted with permission from (Klee et al., 2006).

2.2 Role of phage in *B. anthracis*

The roles of phage in *B. anthracis* are unique from those of other Gram-positive pathogens, in that they are traditionally not associated with virulence. In *S. aureus*, lysogenic conversion imparts the bacteria with factors important for pathogenicity (Bae et al., 2006), while in *S. pyogenes*, prophage also encode factors thought to be crucial to virulence (Beres and Musser, 2007), however a direct link *in vivo* has not yet been made. Why a similar role for phage in the Gram-positive pathogen *B. anthracis* is not seen is unclear. However, the difference could be perhaps attributed to *B. anthracis*'s virulence plasmids, which may supply sufficient virulence determinants for successful infection, rendering such a phage role unnecessary.

Despite seemingly no role in virulence, phage have been well-studied in the *B. cereus* sensu lato group (reviewed in (Gillis and Mahillon, 2014)). Such research however, has typically focused on their host-range and structural characteristics. A brief review of the phages of the *B. cereus* s.l. group (and in particular, *B. anthracis*) follows.

The phages of the *B. cereus* s.l. group belong to the *Myoviridae* (large phage with contractile tails), *Siphoviridae* (phage with non-contractile tails), *Podoviridae* (phage containing short non-contractile tails), and *Tectiviridae* (tailless phage containing spikes) families. Many phages in the group have broad host ranges and can infect *B. anthracis*, *B. cereus*, and *B. thuringiensis*, and also serve as transducing agents for HGT (Gillis and Mahillon, 2014). Other phages however, are specific to *B. anthracis*. Foremost are the chromosomally-integrated prophages (λ Ba01- λ Ba04) that distinguish *B. anthracis* from *B. cereus* and *B. thuringiensis*. Interestingly however, these phages cannot form viable virions and lyse cells. Their effects on the host are to date, unclear (Sozhamannan et al., 2006). A well-studied non-integrating *B. anthracis*-infecting phage is the gamma (γ) phage. The γ -phage, and related phages (known as γ -like phages) are virulent phages highly-specific for *B. anthracis* (but also a few *B. cereus* strains) that are believed to have originated from the temperate phage W β and are used for strain typing (Schuch and Fischetti, 2006). ϕ 20 is a plasmidial temperate phage isolated from *B. anthracis* Sterne (containing the pXO1, but not pXO2 virulence plasmid), however

its sequence is unknown as are any of its effects on the bacteria (Inal and Karunakaran, 1996).

Some studies have examined lysogens for phenotypic changes associated with phage carriage, however are limited in scope. One early study found capsule-producing *B. anthracis* displayed no difference in a mouse model of virulence between strains lysogenized or not lysogenized with phage β . The same strain lysogenized with the close relative phage α however, showed decreased virulence, and the phage was found to induce into the lytic cycle and lyse cells when exposed to sodium bicarbonate and high CO₂ levels. It was believed that the decreased virulence of α -infected cells was due to phage induction occurring *in vivo* (Iyanovics, 1962). Regardless in either case, lysogeny was associated with either no change or decreased virulence of *B. anthracis*, effects typically not associated with phage carriage. In another report, the *B. anthracis*-infecting phage AP50 was found to convert colonies to a flat, wrinkled phenotype (Sozhamannan et al., 2008). Recently, a lytic variant of the phage, AP50c, was found to select for resistant mutants in a *B. anthracis* population. Resistant mutants all contained inactivating mutations in *csaB*, the pyruvyl-transferase encoding gene, and displayed a mucoid phenotype associated with *csaB* mutation (Bishop-Lilly et al., 2012). While AP50, α , β , ϕ 20 and lambdaBa01-04 can lysogenize *B. anthracis*, detailed study of their potential impacts on the bacteria's lifestyle has not been carried out.

In general, the effects of phage carriage on *B. anthracis* are not well-described. One recent report from the Fischetti Laboratory has however, provided examples of phage-mediated contributions to the *B. anthracis* lifestyle (Schuch and Fischetti, 2009). In this report, phages isolated from soil environments were found to stably lysogenize *B. anthracis*, and resulting lysogens harbored new phenotypes promoting long-term vegetative survival. Phage promoted biofilm formation, earthworm colonization, vegetative cell changes, and also blocked sporulation, enabling long-term vegetative cell survival outside of an animal host (an environment where cells typically sporulate). Some phages, surprisingly however, increased sporulation. Regardless, in both cases, phenotypes were found to be driven by phage-encoded sigma factors (Schuch and Fischetti, 2009). For *B. anthracis*, lysogenic conversion appears to be crucial in controlling outside-host vegetative cell survival, and stands in contrast to typical virulence-associated lysogenic conversion in other pathogens (Figure 2-4).

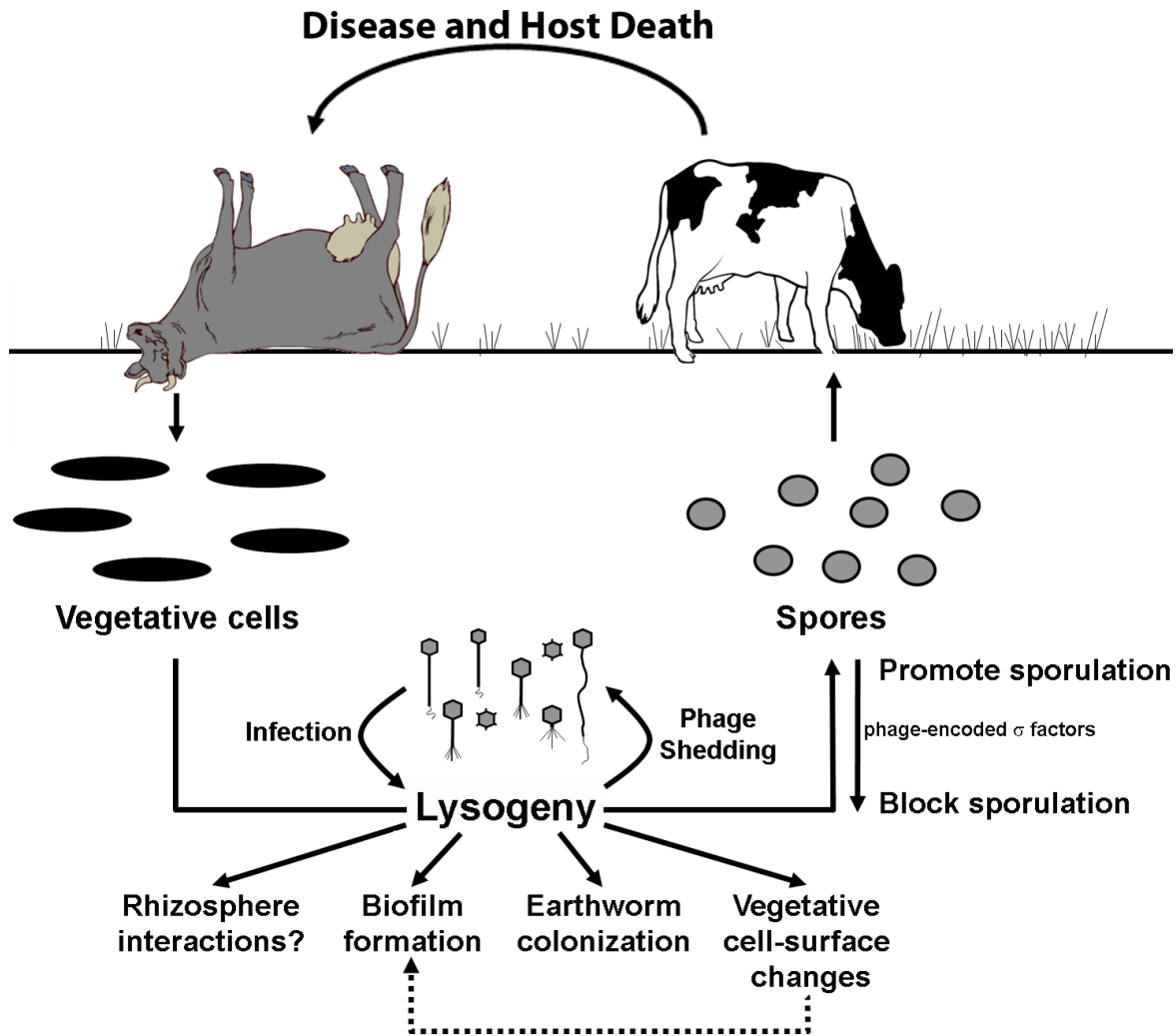


Figure 2-4. Phage-mediated lifestyle changes of *B. anthracis*. Lysogeny of *B. anthracis* by phage from soil-environments can control vegetative cell survival after mammalian host death. Phage can promote long-term soil survival by enabling biofilm formation, earthworm colonization, cell-surface changes, and by blocking sporulation. Other phages however, can promote sporulation in typically aspooreagenous conditions. Both changes are driven by phage-encoded sigma factors. Reprinted with permission from (Schuch and Fischetti, 2009).

2.3 How do phage from anthrax-endemic areas affect *B. anthracis*?

While the report by Schuch and Fischetti lent critical insights into the roles of phage for *B. anthracis*, it also reinforced the notion that phage do not play a major role in the pathogen's virulence, with phages promoting post-disease vegetative soil survival, and the phages used in the study themselves isolated from non-anthrax endemic areas (potting soil, earthworm guts, and fern root systems) (Schuch and Fischetti, 2009). No studies thus far have examined how phage from anthrax contamination zones in particular may affect the Gram-positive pathogen, and if they play any role in the virulence of the organism. The following research explores this question and describes how a phage induced from the unusual disease-causing isolate *B. cereus* Biovar *anthracis* CA alters the well-characterized Sterne strain of *B. anthracis*.

For this study we induced a novel phage (ϕ BACA1) from the pathogenic strain *B. cereus* Biovar *anthracis* CA, and exposed Sterne to the phage, finding that ϕ BACA1 could infect *B. anthracis* Sterne, and that phage exposure selected for a resistant variant which displayed unusual and distinct phenotypes surprisingly similar to those of the phage's parent strain, CA. In the following sections, we show that infection with ϕ BACA1 selects for a *B. anthracis* *csaB* mutant, a gene target with high homology between *B. anthracis* and *B. anthracis*-like *B. cereus* pathogenic strains (Zheng et al., 2013), with the mutant harboring the phenotype previously reported including: long chains of twisted cells, small convex colonies, and clump-

like growth in liquid culture (Bishop-Lilly et al., 2012). We also describe however, novel *csaB* mutant characteristics in Sterne, including hemolytic activity, small colonies without rough edges or “Medusa heads”, the appearance of multi chain rope-like bacilli, and altered biofilm formation capacity. In addition, we examine the virulence of the *csaB* mutant and describe a growth media-induced phenotypic switch where the *csaB* mutant displays markedly altered phenotypes in rich media versus animal host or serum growth environments, and characterize these transcriptional changes via RNA-seq. Lastly, we link the observed *csaB* mutant phenotype in Sterne to that reported for *B. cereus* by *anthracis* CA, uncovering by deep-sequencing a subpopulation of *csaB* mutants in a CA genomic sample. Taken together, this research suggests that lytic phage-bacteria interactions (in addition to lysogeny) may be an important factor shaping populations of *Bacillus anthracis* and *B. anthracis*-like pathogenic species in the wild.

RESULTS

2.4 Exposure of *B. anthracis* Sterne to an anthrax-derived phage identifies a Sterne variant with distinct phenotypes

This study aimed to understand the effects of induced phage from disease-causing isolates of *B. anthracis* and *B. anthracis*-like species on the well-characterized strain *B. anthracis* Sterne. *B. cereus* Biovar *anthracis* CA, a unique anthrax-like strain isolated from an infected ape carcass in Cameroon (Klee et al., 2006), was cultured with mitomycin C to induce potential prophage. We incubated Sterne with an induced and purified phage from CA, termed ϕ BACA1, and found the resulting colonies to harbor a markedly different phenotype after phage exposure. We then purified this variant strain, termed Sterne:: ϕ BACA1, for further phenotypic analysis.

On BHI plates, Sterne:: ϕ BACA1 colonies were smooth, mucoid, and smaller than Sterne, did not contain rough edges or “Medusa heads”, and were not easily removable with pipet tips or loops; they would stick to plates before being pulled off whole (Figures 2-5a and 2-5b). On Columbia blood agar, Sterne:: ϕ BACA1 culture spots contained a yellow-green center, maintained their smaller size as compared to Sterne, and after >24 hrs growth at 37°C, displayed β -hemolytic activity in the center of the culture spots (Figure 2-5c) (Table 2-2).

In liquid BHI culture, *Sterne::ϕBACA1* settled to the bottom of tubes resulting in clear supernatants, while *Sterne* displayed a uniform turbid culture (Figure 2-5d). By microscopy, *Sterne::ϕBACA1* displayed its most remarkable characteristics, including increased chain length, a lack of clear division septa, and twisted corkscrew-like cellular morphologies similar to structures described for CA (Klee et al., 2006) (Figure 2-6). In addition, we observed the appearance of highly organized, multi-chain rope-like structures. These structures were observed in static and shaken liquid cultures. Staining with acridine orange and DAPI revealed both the organized nature of these structures and that cellular division and partitioning of DNA was occurring despite no visible division septa (Figure 2-6). The rope like structures would often converge at nodes connecting the culture as one contiguous mass (Figure 2-7).

Table 2-2. Phenotypic comparisons of *B. anthracis* *Sterne* and *Sterne::ϕBACA1*.

Strain	Rough-edged colonies	Hemolysis	DNase activity	γ-phage susceptibility	Penicillin sensitivity	Motility	Sporulation
<i>Sterne</i>	+	–	+	+	S	–	+
<i>Sterne::ϕBACA1</i>	–	+	+	+	S	–	+

- (+) Positive for trait
- (–) Negative for trait
- (S) Penicillin sensitive

Figure 2-5. *B. anthracis* Sterne exposed to ϕ BACA1 displays atypical *B. anthracis* phenotypes. A) Comparison of Sterne (left) and phage-exposed Sterne (right) on BHI agar plates. Sterne colonies display rough edges with larger colony size. Phage-exposed Sterne colonies display more compact and smaller colonies with smooth edges. B) Photograph of individual Sterne (left) or phage-exposed Sterne (right) colonies. Sterne colony contains weak borders with a dense colony center; phage-exposed Sterne displays a tight colony border and is of uniform density throughout. C) Culture spots of Sterne (left) and phage-exposed Sterne (right) grown on 5% sheep blood agar at 37°C. Sterne does not display hemolytic activity, while phage-exposed Sterne displays hemolytic activity in the middle of the colony and yellow-green color; D) Sterne (left) and phage-exposed Sterne (right) grown in liquid BHI culture at 30°C. Sterne culture is uniformly turbid, while phage-exposed Sterne culture grows as one bacterial mass settled at the bottom of the culture tube, with the surrounding media clear.

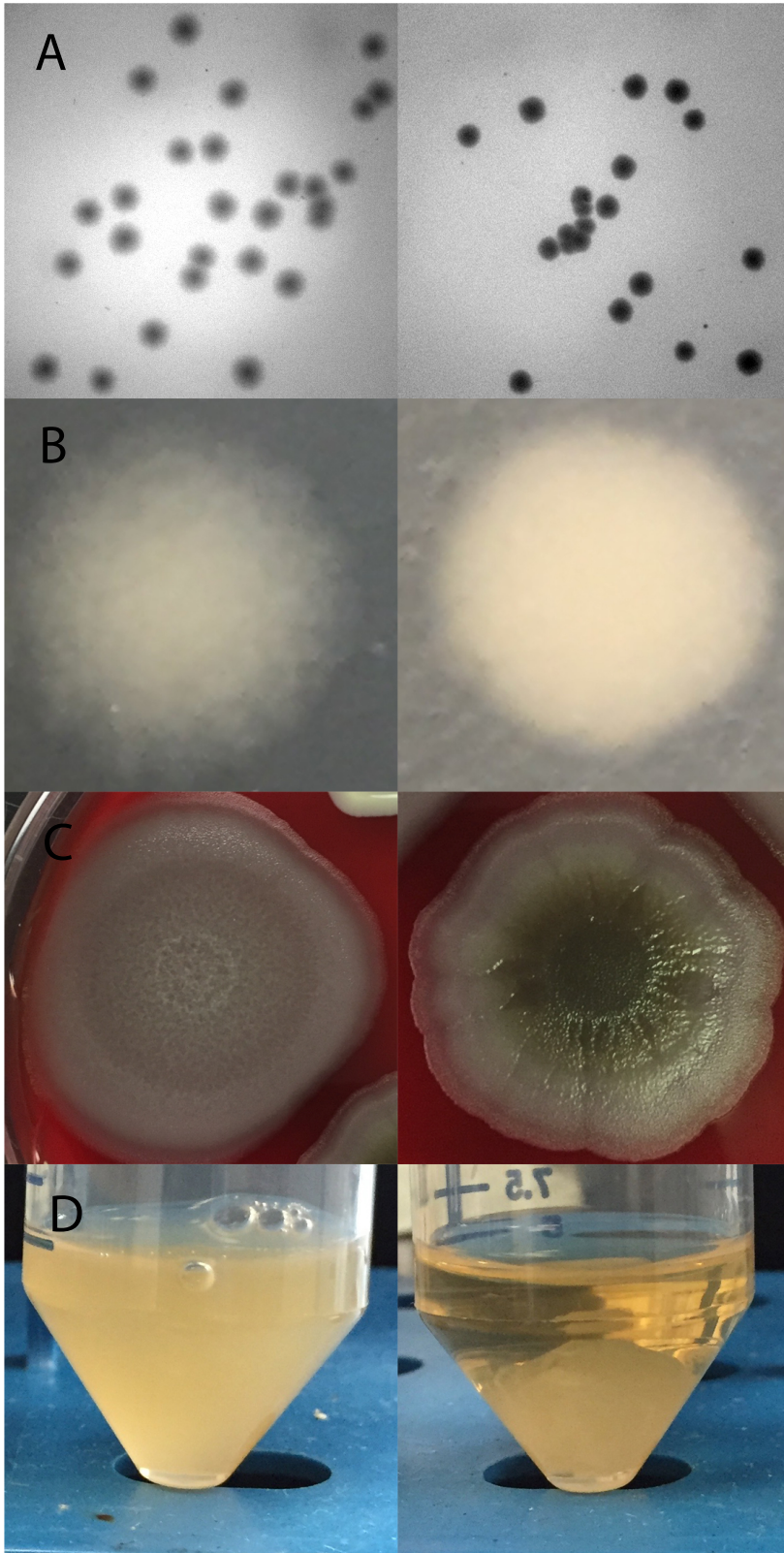
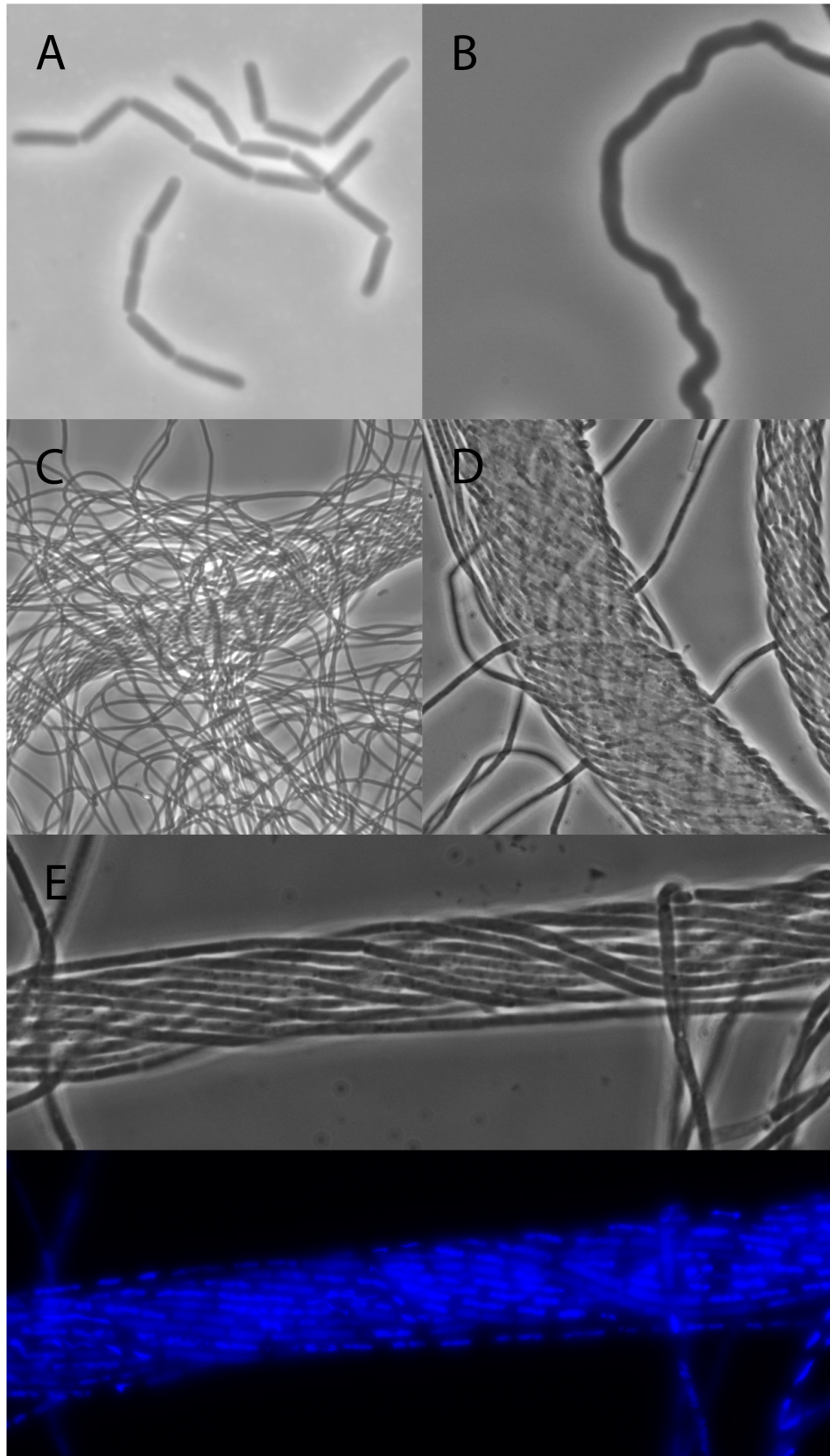


Figure 2-6. *B. anthracis* Sterne:: ϕ BACA1 harbors phenotypes similar to *B. cereus* Biovar *anthracis* CA and grows in unique, rope-like multi-chain structures. A) *B. anthracis* Sterne grown in liquid culture displays chains with clear division septa. B) *B. anthracis* Sterne:: ϕ BACA1 grows with an abnormal twisted morphology. C) *B. anthracis* Sterne:: ϕ BACA1 grows in longer multi-cell chains without clear division septa as compared to Sterne. D) *B. anthracis* Sterne:: ϕ BACA1 grows in organized, rope-like, multi-chain structures. E) (top) phase-contrast image of Sterne:: ϕ BACA1 rope-like structure does not show clear division septa; (bottom) Sterne:: ϕ BACA1 stained with DAPI shows DNA-partitioning and cellular division within multi-cell chains. All images captured at 1000X magnification, except C at 400X.



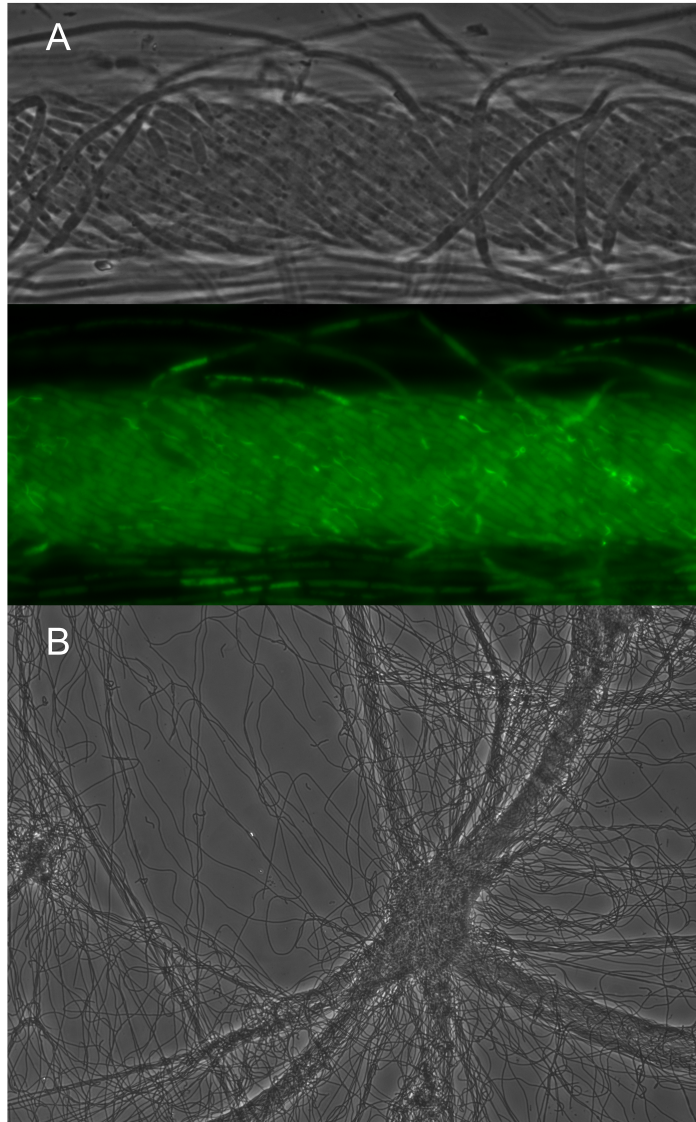


Figure 2-7. *B. anthracis* Sterne:: ϕ BACA1 displays unique growth characteristics. A) (top) Sterne:: ϕ BACA1 robust rope-like structure with phase-contrast microscopy; (bottom) Sterne:: ϕ BACA1 stained with acridine orange reveals clear division septa and organization of the rope-like structure (captured at 1000X magnification). B) Representative example of a Sterne:: ϕ BACA1 “node” in liquid culture, where multiple rope-like structures converge (captured at 100X magnification).

We also tested Sterne:: ϕ BACA1 for DNase activity, susceptibility to γ -phage, penicillin resistance, motility, sporulation, and biofilm formation. Sterne:: ϕ BACA1 and Sterne did not show penicillin resistance or motility as compared to the positive control *B. cereus* T. Sterne and Sterne:: ϕ BACA1 were also sensitive to γ -phage and did not show qualitative differences in DNase activity nor significant differences in sporulation (Table 2-2). Sterne:: ϕ BACA1 differed in biofilm formation capacity compared to Sterne, with the variant strain displaying no biofilm formation at room-temperature (RT) or 30°C until 10 weeks, whereas Sterne was capable of forming biofilms at earlier time points. However, both Sterne and Sterne:: ϕ BACA1 formed equivalent biofilms at similar time points at 37°C with or without glucose (Table 2-3). Sterne:: ϕ BACA1's inability to form a biofilm at RT and 30°C may arise from its sticky and clump-like growth, preventing sufficient cellular seeding at the liquid-air interface.

Table 2-3. *B. anthracis* biofilm formation capacities.

3 weeks	RT	RT + glucose	30°C	30°C + glucose	37°C	37°C + glucose
Sterne	–	–	+	++	+++	+++
Sterne:: ϕ BACA1	–	–	–	–	++	+++
6 weeks						
Sterne	–	+++	++	++	–	+++
Sterne:: ϕ BACA1	–	–	–	+	–	+++
10 weeks						
Sterne	+	+++	++	+	–	++
Sterne:: ϕ BACA1	+	–	–	+++	+	+++

Biofilms were scored weekly for strength/robustness. Scoring key: (-) no biofilm; (+) weak growth; (++) medium growth; (+++) strong growth.

2.5 Sterne:: ϕ BACA1 is not lysogenized by ϕ BACA1

Sterne:: ϕ BACA1 had a unique phenotype, and we were curious to understand the genomic changes, if any, responsible for its novel characteristics. Re-exposure of Sterne:: ϕ BACA1 to ϕ BACA1 stocks did not result in cell lysis on plates or in liquid cultures, indicating that the variant strain was resistant to infection. Phage-resistance can occur, in part, due to lysogeny, receptor modification, or other genomic changes in the organism. To test if Sterne:: ϕ BACA1 was indeed lysogenized with ϕ BACA1, we first sequenced the genomic DNA of ϕ BACA1 to allow for construction of PCR screening primers. *De novo* assembly of phage DNA reads resulted in two contigs that had a 16 base-pair overlap. RAST and PHASTER

analysis of joined contigs predicted an intact prophage element, with *Siphoviridae*-like genome organization, and gene sequences commonly resembling those of other *Siphoviridae* phages by BLAST analysis. We did not complete the ϕ BACA1 genome, however the *de novo* assembled contigs of the prophage element are available in Appendix 1. We used this contig sequence to design PCR primers (ϕ BACA1_F, ϕ BACA1_R) to probe for phage-specific sequence in Sterne and Sterne:: ϕ BACA1 by PCR. Surprisingly, no ϕ BACA1-product was detected in Sterne or Sterne:: ϕ BACA1, while the phage stock as positive control produced the predicted product. Southern blots of whole genome DNA preparations from Sterne and Sterne:: ϕ BACA1 were also negative for ϕ BACA1 DNA (data not shown).

2.6 DNA sequencing reveals a single-nucleotide insertion responsible for Sterne:: ϕ BACA1 phenotypes and ϕ BACA1-resistance

Results from the PCR and Southern blot experiments indicated Sterne:: ϕ BACA1 is not lysogenized with ϕ BACA1 and that Sterne likely undergoes selection for phage-resistant variants upon ϕ BACA1 exposure. Separately, we were able to transiently lysogenize Sterne with ϕ BACA1 after repeated attempts, but the lysogens grew very weakly on plates and in liquid culture. Restreaking these lysogenic colonies on BHI agar often resulted in no growth or colonies that had Sterne:: ϕ BACA1-like phenotypes. Therefore Sterne can carry ϕ BACA1, however unstably under our conditions, with ultimate selection for ϕ BACA1-resistant Sterne variants.

To understand the genomic background of Sterne:: ϕ BACA1's phage-resistance and its associated phenotypes, we sequenced Sterne and Sterne:: ϕ BACA1 for direct comparison. *De novo* assembly of reads from Sterne:: ϕ BACA1 did not reveal any novel elements nor reads corresponding to ϕ BACA1, supporting PCR and Southern blot data that the variant strain is not lysogenized with the phage. However, two single nucleotide insertions in Sterne:: ϕ BACA1 were uncovered by comparing read alignments of the chromosome: a (G)₄→(G)₅ insertion at position 1,730,529, and an (A)₇→(A)₈ insertion in position 1,710,151 of the chromosome (Table 2-4). Both insertions were confirmed by Sanger sequencing. The A(7)→A(8) insertion is in the 3' end of a tRNA methyltransferase, and is predicted to change the amino acid sequence of the protein product from ...KGSFSRQILVCE* to ...KRIIF*. It is unclear if or how truncation and alteration of the gene product may affect its activity. The (G)₄→(G)₅ insertion lies in the 5' region of the *csaB* gene, a pyruvyltransferase that acts on the SCWP. The specific (G)₄→(G)₅ insertion that Sterne:: ϕ BACA1 harbors appears to be a "hotspot" of mutation in *csaB* as it has previously been implicated in *B. anthracis* AP50c phage resistance (Bishop-Lilly et al., 2012), with AP50c phage unable to adsorb to the *csaB* mutant's cell surface. Both the AP50c-resistant variant and the ϕ BACA1-resistant variant from this current study appear to encode a truncated, inactive CsaB protein (Table 2-4).

Table 2-4. Genomic alterations uncovered in *Sterne::ϕBACA1* by whole-genome DNA sequencing.

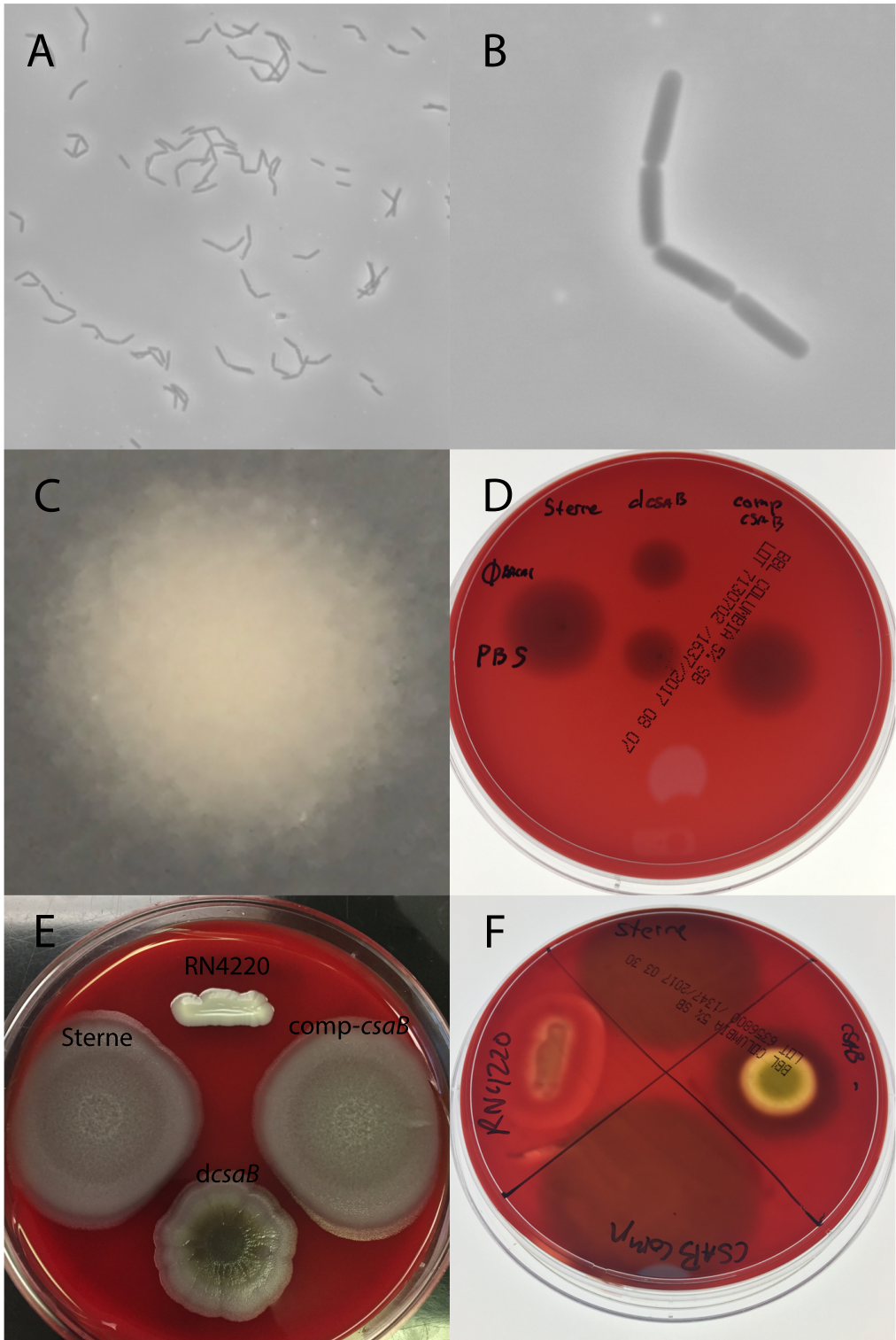
Position	Change	Type	Frequency	Coverage	P-Value	Result
1730529	(G)4 → (G)5	Insertion	98.2%	338	0	Frameshift mutation (truncation of CsaB protein)
1710151	(A)7 → (A)8	Insertion	97.1%	383	0	Frameshift mutation (7 AA truncation of tRNA methyltransferase protein)

From our sequencing, *Sterne::ϕBACA1* appears to be a *csaB* mutant that harbors a number of reported phenotypes linked to CsaB deficiency, including long bacterial chains, twisted cells, and clumping in liquid culture. However, we also report additional phenotypes for the *ϕBACA1*-selected *csaB* mutant, including: rope-like multi-chain structures, hemolytic activity with small, yellow-green culture spots on SBA plates, and resistance to the phage *ϕBACA1*. Since no lysogeny was proven to exist, we will refer to *Sterne::ϕBACA1* as *Sterne dcsaB* for the remainder of this Thesis. To definitively link *ϕBACA1* resistance and the observed *Sterne dcsaB* phenotypes to *csaB* and not the single-nucleotide insertion in the tRNA-methyltransferase, we reverted the (G)4→(G)5 mutation, while leaving intact the

(A)7→(A)8 insertion. Successful construction of the strain was confirmed by Sanger sequencing and the strain termed Sterne comp-*csaB*.

Comp-*csaB* phenotypes were Sterne-like and reversed those from *dcsaB*. By microscopy, comp-*csaB* cells had short chain lengths, clear division septa, and the absence of any twisted cells or rope-like multi-chain structures. Sterne comp-*csaB* had larger colonies with rough edges and “Medusa heads” on BHI agar, and culture spots did not display hemolytic activity (Figure 2-8). BHI liquid cultures of Sterne comp-*csaB* were turbid and similar to Sterne. Biofilm and sporulation analysis of the revertant strain did not show qualitative differences in biofilm formation capacity, nor significant differences in sporulation (data not shown). In addition, sensitivity to ϕ BACA1 was regained in comp-*csaB* (Figure 2-8). The reversion of distinct *dcsaB* phenotypes observed in comp-*csaB* therefore links a number of reported (Mesnage et al., 2000) and newly discovered pleiotropic effects to the *csaB* gene. The single-nucleotide insertion in the tRNA-methyltransferase does not result in observable phenotypes different from Sterne, however we cannot rule out their existence. Notably, *B. anthracis* strains resistant to AP50c phage via *csaB* mutation were also shown to harbor additional SNPs in their genomes (Bishop-Lilly et al., 2012); the roles and genes of these mutations are unclear.

Figure 2-8. *B. anthracis* comp-*csaB* displays Sterne-like phenotypes. A) Sterne comp-*csaB* visualized under phase-contrast microscopy displays short chains and the absence of multi-chain structures (captured at 100X magnification). B) Sterne comp-*csaB* shows clear division septa (captured at 1000X magnification). C) A single Sterne comp-*csaB* colony on BHI agar displays a Sterne-like rough edge. D) Sterne and Sterne comp-*csaB* are sensitive to infection by ϕ BACA1; Sterne *dcsaB* is resistant. All strains grow with PBS spotted as a negative control. E) Sterne, Sterne *dcsaB*, and Sterne comp-*csaB* grown on Columbia 5% sheep blood agar display different growth phenotypes. F) Sterne and Sterne comp-*csaB* culture spots do not display hemolytic activity, whereas Sterne *dcsaB* displays hemolytic activity in the center of growth. RN4220 is included as a positive control for hemolysis.



2.7 Sterne *dcsaB* does not show altered virulence potential in a mouse model, and exhibits an altered phenotype in the infection environment

As the mutant Sterne *dcsaB* exhibited a distinct phenotype, we tested whether a *csaB* mutation event would affect the virulence potential of Sterne. We compared the virulence of Sterne and Sterne *dcsaB* in a mouse bacteremia model. Since Sterne *dcsaB* had longer chain lengths than Sterne, we normalized the two strains to ensure equivalent bacterial dosing. We determined that Sterne *dcsaB* chain length was on average 5-6-fold longer than Sterne under the conditions used for this experiment, and therefore Sterne *dcsaB* was injected at a 5-6-fold lower CFU/mL dose. Normalized Sterne and Sterne *dcsaB* did not show a significant virulence difference between survival curves in survival percentage or median time to death ($P = 0.3450$, Figure 2-9).

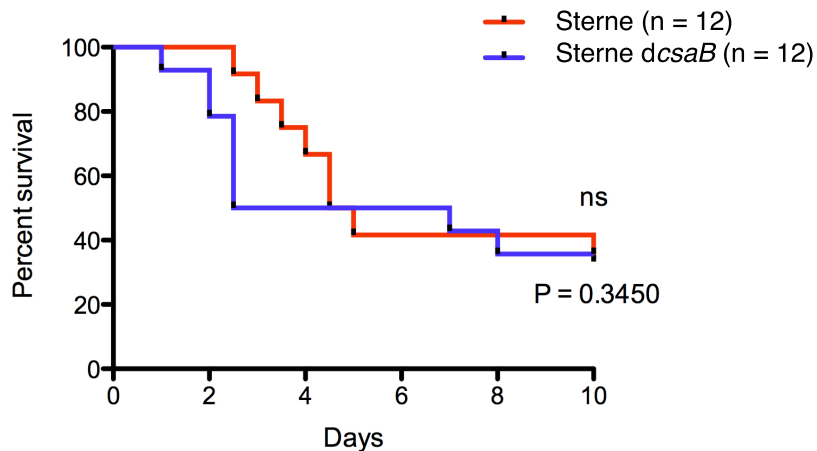


Figure 2-9. Survival curves of Sterne and Sterne *dcsaB* from mouse infection model.

While Sterne *dcsaB* did not show altered virulence potential in our animal model, we were curious if or how the rope-like structures might contribute to disease, and examined various mouse organs 48 hours after initial infection. GFP-PlyG^{BD} visualization of bacilli by microscopy surprisingly did not reveal the long chain, rope-like structures typical of the variant grown in BHI, but rather shorter chains and dispersed bacteria resembling Sterne (Figure 2-10a). Occasionally we observed longer-chain rope-like structures and cells with corkscrew-like twisted morphologies, however they did not comprise the majority of visualized Sterne *dcsaB* cells (data not shown). We also passaged Sterne *dcsaB* directly from infected tissues into liquid BHI culture for growth at 37°C overnight. Remarkably, these cultures harbored the phenotype initially observed with long chains of cells, rope-like multi-chain structures, cells with a lack of clear division septa and corkscrew/twisted morphologies (Figure 2-10b). The distinct change in growth characteristics of Sterne *dcsaB* in mouse tissues as compared to BHI suggested a phenotypic switch dependent upon the bacteria's external environment.

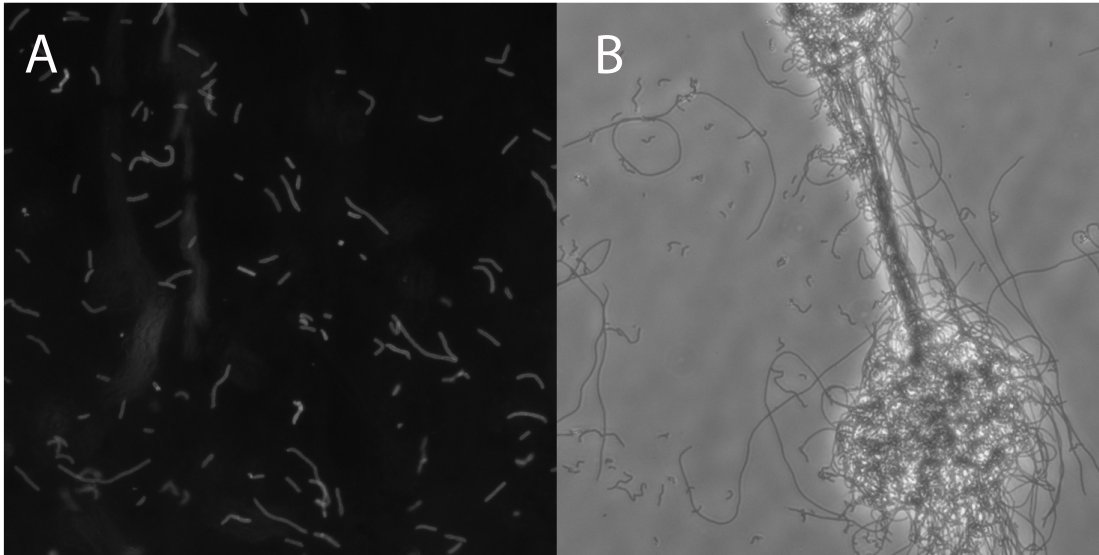


Figure 2-10. *B. anthracis* Sterne *dcsaB* displays a unique and reversible phenotype in the infection environment. A) Sterne *dcsaB* extracted from mouse kidney, labeled with GFP-PlyG^{BD} displays Sterne-like morphology and chain lengths (captured at 200X magnification). B) Reculturing Sterne *dcsaB* from the mouse into liquid BHI reveals long-chain, rope-like bacterial structures and twisted morphologies (captured at 100X magnification).

2.8 Sterne *dcsaB* grown in fetal bovine serum displays a similar phenotype as observed in mouse tissues

Results from mouse infection experiments suggested that the animal host environment induces a switch that alters the phenotype of the variant Sterne *dcsaB* strain. To mimic this growth outside the mouse, we cultured Sterne *dcsaB* in fetal bovine serum (FBS). Sterne *dcsaB* in FBS displayed turbidity similar to that of Sterne, without the appearance of any bacterial clumping or masses. By microscopy,

cells resembled Sterne: short chains with clear division septa, and the total absence of any multi-chain or rope-like structures (Figure 2-11). While we observed occasional disorganized clusters of cells in the Sterne *dcsaB* FBS culture, we observed similar structures to the same degree with the Sterne FBS culture.

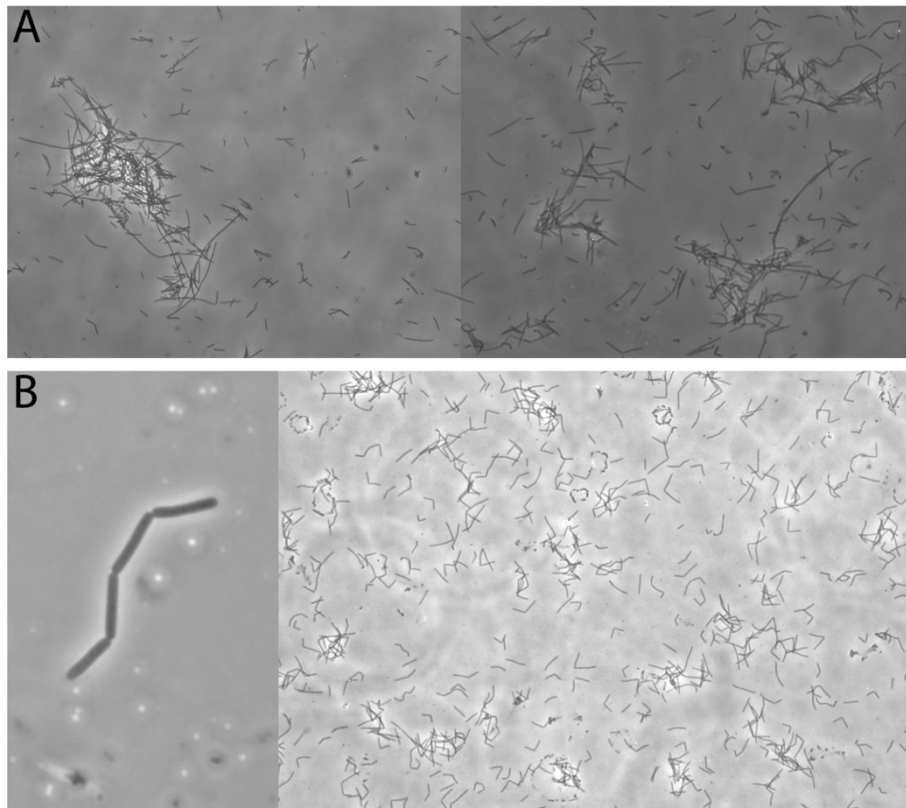


Figure 2-11. Sterne *dcsaB* in FBS harbors Sterne-like and similar phenotypes to those seen in mouse infection. A) *B. anthracis* Sterne (left) and Sterne *dcsaB* (right) grown in FBS at 37°C display similar phenotypes (captured at 100X magnification). B) (left and right) Sterne *dcsaB* displays clear division septa in FBS culture and a distinct phenotype as compared to BHI growth (images captured at 1000X (left) and 100X (right) magnifications).

Sterne *dcsaB* in Figure 2-11 was grown in FBS at 37°C to mimic temperatures in the mouse. Interestingly, when we cultured *dcsaB* in liquid BHI at 37°C, we normally observed growth of the strain as a single mass, but occasionally, the bacteria would disperse and grow as a turbid culture. When grown in BHI at 30°C however, we did not observe this behavior; Sterne *dcsaB* cultures always remained as one mass at the bottom of tubes with a non-turbid, clear supernatant (Figure 2-12). Growth in FBS at 30°C did not alter the observed serum phenotypes of Sterne *dcsaB*, however 36 hours of growth was required for the entire culture to be devoid of any bacterial clumps or masses.

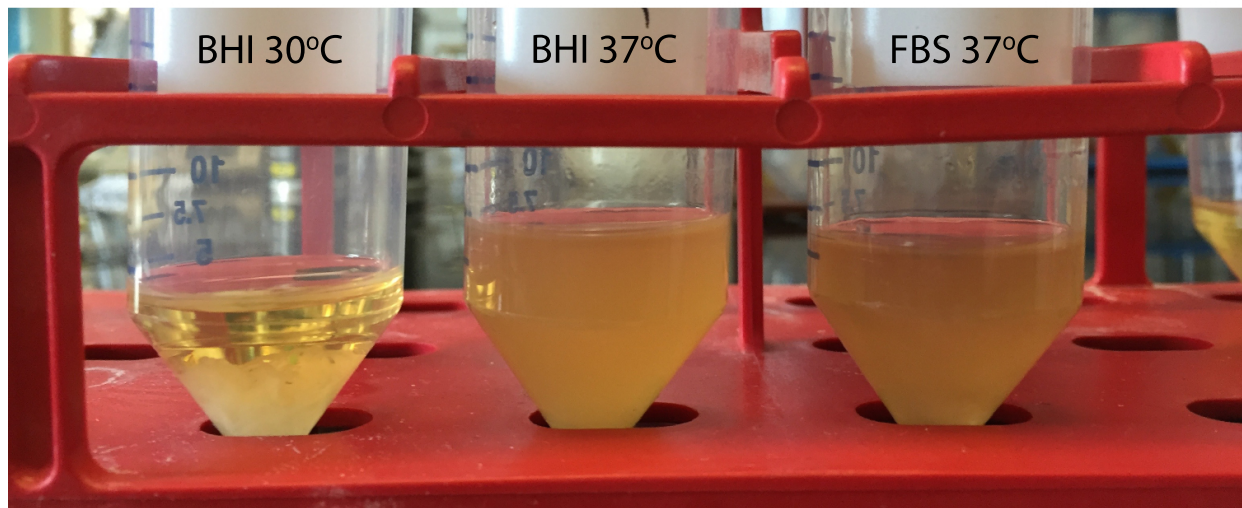


Figure 2-12. *B. anthracis* Sterne *dcsaB* displays different growth characteristics in BHI liquid culture at 30°C versus 37°C. Labeled liquid culture tubes of Sterne *dcsaB* show characteristic “clumped” growth in BHI at 30°C, and occasionally observed turbid growth in BHI at 37°C. Sterne *dcsaB* grown in FBS at 37°C, in which turbidity was always observed, is shown for reference.

Using this temperature-based growth characteristic of *dcsaB*, we examined the minimum FBS dose necessary to observe the growth media-induced phenotypic switch by culturing Sterne *dcsaB* in increasing ratios of BHI:FBS at 30°C. Cultures showed higher turbidity with increased concentrations of FBS, with a complete loss of the BHI-associated phenotype at a 90:10 BHI:FBS ratio, suggesting that serum-derived factors are too dilute to elicit a phenotypic switch below a 10-fold dilution (Figure 2-13).

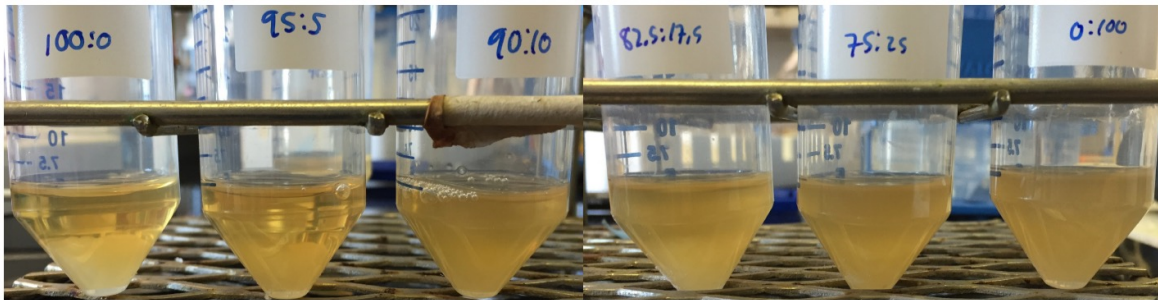


Figure 2-13. FBS induces phenotypic changes in *B. anthracis* Sterne *dcsaB* in a dose-response-like manner. BHI:FBS mixed media cultures of Sterne *dcsaB* ranging from 100:0 BHI:FBS to 0:100 BHI:FBS. Cultures display little to no turbidity from 100% to 90% BHI by volume, but become increasingly turbid and uniform as % FBS increases.

In addition, growth of *Sterne dcsaB* in 85°C heat-treated FBS displayed similar phenotypes and morphologies to growth in non-heat-treated FBS, suggesting that heat labile factors are not responsible for the observed switch (Figure 2-14).

Preliminary fractionation experiments to uncover the serum factor(s) responsible suggested multiple components may be at play for the phenotypic switch, but we did not characterize these factors for this study; experiments are ongoing for their future discovery and purification (Appendix 2).

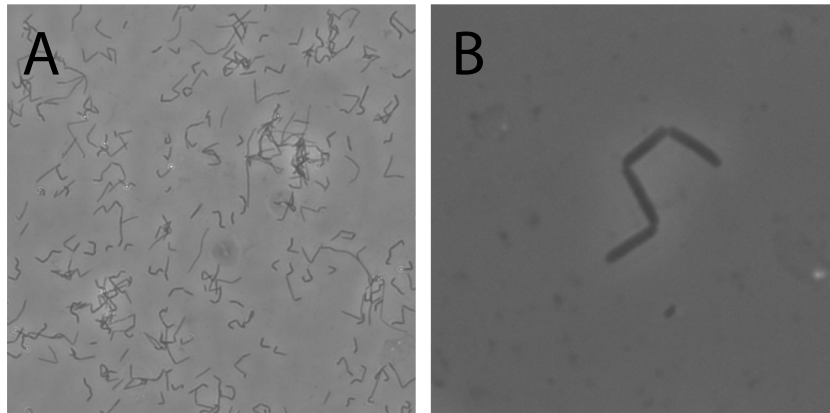


Figure 2-14. *B. anthracis* Sterne *dcsaB* grows in turbid culture in heat-treated FBS. *Sterne dcsaB* was grown in heat-treated FBS and observed for growth phenotypes and morphologies. A) *Sterne dcsaB* grown in heat-treated FBS at 37°C displays short chains and the absence of multi-chain structures, with similar growth to that of FBS culture (captured at 100X magnification). B) *Sterne dcsaB* grown in heat-treated FBS shows clear division septa and short chains (captured at 1000X magnification).

2.9 RNA-seq reveals global gene expression differences between Sterne and Sterne *dcsaB* in BHI and FBS growth environments

The distinct phenotypes of Sterne *dcsaB* suggested there may be large-scale gene expression changes due to *csaB* mutation and the bacteria's external environment. In addition, we hypothesized that differential expression (DE) between Sterne and Sterne *dcsaB* may be occurring to a greater degree in BHI than FBS due to the disparate BHI-associated phenotypes observed. We designed an RNA-seq experiment to test these hypotheses and compare gene expression patterns between and within Sterne and Sterne *dcsaB* grown in BHI or FBS media, resulting in four group comparisons: 2 of genotype (Sterne against *dcsaB* in BHI and FBS), and 2 of growth condition (Sterne or *dcsaB* BHI against FBS). RNA-seq was carried out as described in *Materials and Methods*, and a summary of the differential expression data is presented in Tables 2-5a and 2-5b; the full data set is given in Appendix 3.

Our RNA-seq experiment revealed several changes associated with both genotype and growth condition. Despite imparting strict limits on calling DE due to the number of sample replicates, our 4 group comparisons yielded a percentage range of called DE genes from 10.94 - 56.56% of the genome. *CsaB* mutation has a noted pleiotropic effect on the bacterial cell (Mesnage et al., 2000); by RNA-seq, it also appears to fundamentally alter its transcriptome.

Table 2-5a. *B. anthracis* Sterne and Sterne *dcsaB* whole-genome differential expression (DE) summary.

Group Comparison (A vs. B)	# downregulated DE genes (in A)	# upregulated DE genes (in A)	% downregulated / % upregulated genes	% DE genes of all <i>B. anthracis</i> Sterne genes
<i>dcsaB</i> BHI vs. <i>dcsaB</i> FBS	1620	1606	50.2/49.8	56.6
Sterne BHI vs. Sterne FBS	828	849	49.4/50.6	29.4
<i>dcsaB</i> BHI vs. Sterne BHI	1194	1106	51.9/48.1	40.3
<i>dcsaB</i> FBS vs. Sterne FBS	237	387	48/62	10.9

Table 2-5b. *B. anthracis* Sterne and Sterne *dcsaB* pXO1-only differential expression (DE) summary.

Group Comparison (A vs. B)	# downregulated DE genes (in A)	# upregulated DE genes (in A)	% downregulated / % upregulated genes	% DE genes of all pXO1-encoded genes
<i>dcsaB</i> BHI vs. <i>dcsaB</i> FBS	56	11	83.7/16.4	39.9
Sterne BHI vs. Sterne FBS	67	2	97.1/2.9	41.07
<i>dcsaB</i> BHI vs. Sterne BHI	30	9	76.9/23.1	23.2
<i>dcsaB</i> FBS vs. Sterne FBS	23	4	85.2/14.8	16.1

For Sterne *dcsaB*, phenotypic differences are markedly pronounced between BHI and FBS growth, and a similar gene expression pattern is reflected in the RNA-seq data. 56.56% of Sterne *dcsaB* genes were DE comparing growth in BHI versus FBS. For Sterne, this value was 29.4%. Sterne and Sterne *dcsaB* showed a number of different phenotypes in BHI, but less so in FBS. This is also reflected in the differential expression data. 40.3% of genes were DE between the two strains grown in BHI, but this value was reduced to 10.9% for FBS. Principal component analysis (PCA) of the RNA-seq samples shows a similar result (Figure 2-15). Sterne and Sterne *dcsaB* BHI samples are distinctly clustered from each other, as are intra-strain BHI and FBS samples. Sterne and Sterne *dcsaB* samples grown in FBS however, cluster closer together in the plot.

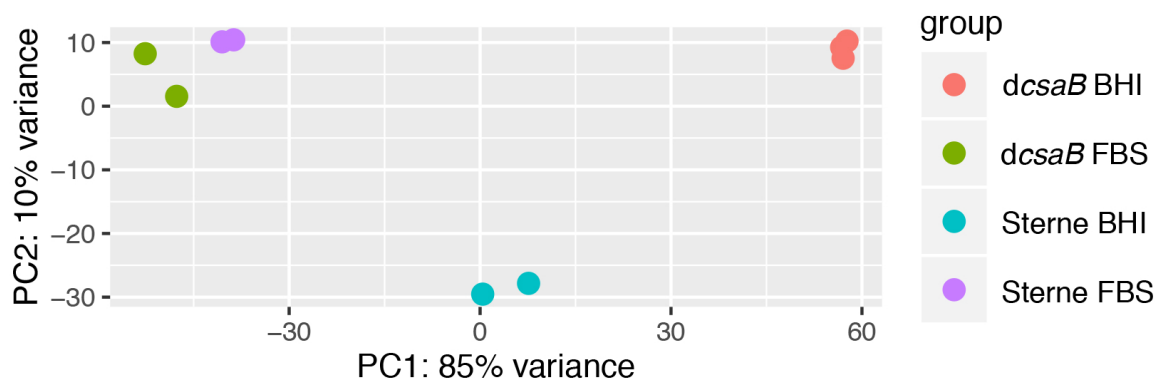


Figure 2-15. Principal component analysis (PCA) plot of samples from RNA-seq. Sterne and Sterne *dcsaB* RNA-seq sample distances visualized using PCA. Sterne BHI and Sterne *dcsaB* BHI biological groups form distinct clusters with their respective replicates clustered together. Sterne and Sterne *dcsaB* FBS groups cluster both near each other and with their respective replicates clustered together, indicating smaller sample distance between the two biological groups than between Sterne and Sterne *dcsaB* BHI groups.

For Sterne and Sterne *dcsaB* whole genomes, DE in BHI versus FBS environments is equally split between upregulated and downregulated genes. Examining pXO1-encoded genes only however, reveals that most of its DE genes are upregulated in FBS (Table 2-5b, Appendix 3). In Sterne *dcsaB*, 67 pXO1 genes were differentially expressed in total, with 56 upregulated in FBS growth. For Sterne, of 69 DE genes, 67 are upregulated in FBS growth. The upregulation of pXO1 virulence-associated genes we observe is similar to reports of pXO1 upregulation in CO₂/bicarbonate atmospheres (McKenzie et al., 2014; Passalacqua et al., 2009a). Therefore, we believe upregulation of pXO1-encoded genes in FBS suggests the media may be a partial mimic of the infection environment. The RNA-seq data we present shows global transcriptional changes in Sterne and Sterne *dcsaB*, revealing a growth-media induced switch of the transcriptome and the dynamic nature of *B. anthracis* Sterne, wild-type and *dcsaB*. In addition, our data highlights the pleiotropic effects of *csaB* mutation and correlates the disparate phenotypes of Sterne and Sterne *dcsaB* with differential expression. At this time however, we cannot describe specific transcriptional changes that may account for the two strains' similarities in FBS and distinct differences in BHI growth media. Experiments to uncover key genes involved in this event are ongoing.

2.10 Western blot of protective antigen correlates with RNA-seq data

To validate data generated from our RNA-seq experiment, we took an orthogonal approach, measuring levels of protective antigen (PA) in culture supernatants by Western blot. Growth condition comparisons revealed that in Sterne, *pag* is upregulated 4-fold in FBS as compared to BHI culture, while in *dcsaB* this upregulation is 50-fold. Genotype comparison data showed Sterne expresses *pag* 10-fold higher than *dcsaB* in BHI, while in FBS there is no significant difference in *pag* expression between the two strains. Results from Western blots corroborated these data (Figure 2-16). A combined blot (Figure 2-16a) displays normalized samples from Sterne, Sterne *dcsaB*, and Sterne *comp-csaB* grown in BHI or FBS, as well as negative controls of Δ Sterne (lacking pXO1 and pXO1-encoded *pag*), and BHI or FBS growth media alone. The combined blot shows equivalent detection of protective antigen at the expected molecular mass among Sterne, Sterne *dcsaB*, and Sterne *comp-csaB* in FBS-growth environments in agreement with our RNA-seq data, and the absence of PA in Δ Sterne and FBS-only samples. As FBS contains a high level of endogenous proteins, to obtain distinct bands on a gel, dilution of samples 1:100 in 1X PBS was required. PA protein levels were below the limit of detection for all BHI samples at this dilution, suggesting lower levels of PA expression in BHI culture. Therefore, an additional blot was generated using concentrated BHI supernatants. This blot (Figure 2-16b) shows normalized, concentrated supernatants from Sterne, Sterne *dcsaB*, and Sterne *comp-csaB* BHI

samples, as well as Δ Sterne and BHI-only controls. Sterne and Sterne comp-*csaB* display equivalent band intensities for PA, while Sterne *dcsaB* displays a fainter band. No PA is detected in Δ Sterne and BHI-only controls. This blot indicates that *pag* expression for Sterne *dcsaB* is downregulated compared to Sterne, and reversal of the single nucleotide insertion in *csaB* (and not within in the 3' tRNA-methyltransferase) restores *pag* expression to that of wild-type Sterne. Our Western blot is in accordance with data generated from our RNA-seq, and validates its results in an orthogonal manner.

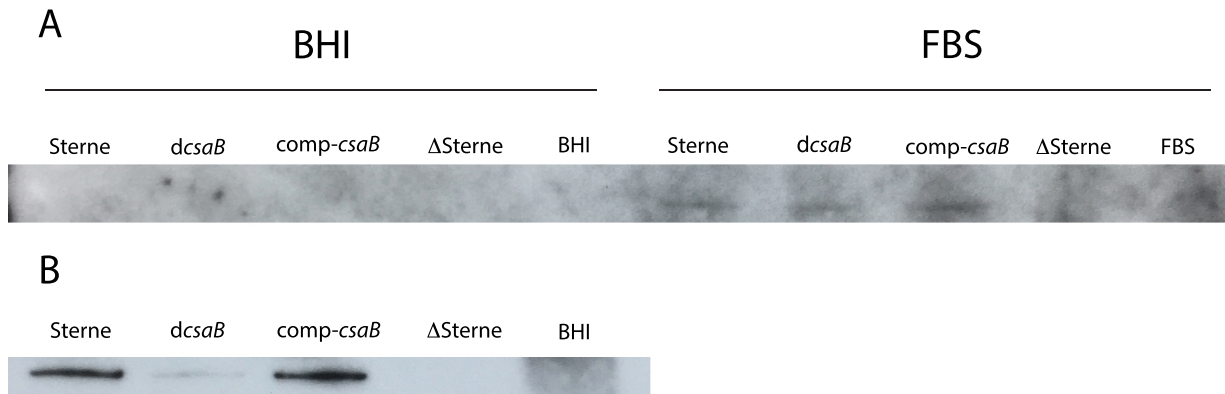


Figure 2-16. Western blot of protective antigen in culture supernatants validates RNA-seq data. Western blot of culture supernatants from Sterne, Sterne *dcsaB*, and Sterne *comp-csaB* grown as described for RNA-seq are probed for protective antigen. Selected area of blots between 75-100 kD are shown for clarity. A) 1:100 diluted and normalized samples in 1X PBS from strains grown in BHI or FBS are shown. Normalized BHI samples are below the limit of detection. For FBS samples, Sterne, *dcsaB*, and *comp-csaB* show approximately equivalent bands for protective antigen. Negative controls Δ Sterne and FBS-only do not show bands corresponding to protective antigen. B) Western blot of concentrated, normalized BHI supernatant samples shows approximately equal band intensity for Sterne and Sterne *comp-csaB*, but decreased band intensity for Sterne *dcsaB*. Δ Sterne and BHI negative control samples do not show protective antigen-specific bands.

2.11 Deep-sequencing reveals unstable carriage of ϕ BACA1 and that *csaB* mutation does not readily revert

Given the phenotypic similarities between Sterne *dcsaB* and *B. cereus* by *anthracis* CA, we were curious if a proportion of the CA population may harbor mutations in *csaB*, potentially uncovering a genomic basis for the previous phenotypic observations of CA (Klee et al., 2006). We used a deep-sequencing approach to examine *csaB* variants in CA as well as several Sterne strains. Prior to carrying out deep-sequencing of *csaB* amplicons however, we determined the spontaneous resistance rate of Sterne to ϕ BACA1 and examined Sterne *dcsaB* for potential reversion to wild-type. Sterne ϕ BACA1-resistant colonies were found to appear at an average rate of 4.8×10^{-7} resistant colonies/CFU. We also examined if Sterne *dcsaB* would revert its *csaB* mutation in the absence of phage selection. Potential *csaB* reversion was not observed in cultures, suggesting that under our conditions and in the absence of phage, there is not a high selective pressure for revertant cells.

The spontaneous ϕ BACA1 resistance rate and lack of *csaB* reversion suggested that uncovering *csaB* variants in Sterne or Sterne *dcsaB* by deep-sequencing was unlikely unless sequencing was carried out with a very high read depth and coverage of the *csaB* amplicon was in excess of 2,000,000x. For CA, phenotypes suggestive of CsaB deficiency were readily seen (Klee et al., 2006), and given that this strain harbors ϕ BACA1, we hypothesized that selection for *csaB* mutation

might occur at a higher rate and be uncovered by deep-sequencing. We carried out deep-sequencing of *csaB* amplicons from CA, Sterne and the Sterne-derived strains *dcsaB* and *comp-csaB*. Summarized results are in Table 2-6, including percentage variant type classified as harboring nonsense, nonsynonymous, or silent mutations. Individual variants uncovered by deep-sequencing are listed in Tables 2-7a-d.

Table 2-6. *csaB* variant frequencies of selected *Bacillus anthracis* strains.

Strain	% Frequency of mutation type in population		
	Nonsense	Nonsynonymous	Silent
Sterne	0	0	0.3
Sterne <i>dcsaB</i>	0	0	0
Sterne <i>comp-csaB</i>	0	0.2	0.1
CA	1.9	6.7	0.2

We found Sterne did not contain any variants with nonsense or nonsynonymous mutations, but 0.3% of the population carried silent mutations in three distinct loci. Sterne *dcsaB* did not contain any mutations in its population, excluding the (G)4→(G)5 insertion. Sterne *comp-csaB* did not contain any nonsense mutations, however 0.2% of the population did contain a nonsynonymous A→G transition resulting in a serine to glycine substitution. It is not clear the downstream effect of this substitution on CsaB activity. Sterne *comp-csaB* also harbored silent mutations in 0.1% of its population. While Sterne and Sterne-derived strains did not harbor any nonsense mutations, sequencing of CA revealed nonsense, single-nucleotide

substitutions in 1.9% of the population and nonsynonymous, single-nucleotide substitutions in 6.7% of the population. Silent mutations were present in 0.2% of the CA population.

We have not verified that the nonsense mutations disrupt CsaB activity, however of the 5 nonsense mutations found, 4 (1.7% of the CA population) occur upstream of a mutation in *csaB* as reported by (Bishop-Lilly et al., 2012) to inactivate the CsaB protein. It is unclear if the C878A variant also encodes for inactive CsaB.

Nonsynonymous mutations have been reported to inactivate CsaB in addition to truncations of the protein. The nonsynonymous mutations we uncovered were not the same nucleotide changes as previously reported (Bishop-Lilly et al., 2012), however they are predicted to result in similar amino acid substitutions (charged (+/-) to noncharged, noncharged to charged (+/-)). It is possible that a number of these nonsynonymous mutations may reduce or disrupt CsaB activity. Results from this deep-sequencing experiment show that *B. cereus* bv *anthracis* CA has an increased level of variation and mutation in the *csaB* gene as compared to Sterne and other Sterne-derived strains. We believe this variation is likely driven by interaction of CA with ϕ BACA1. From PCR screening, CA appears to carry ϕ BACA1, however variation in *csaB* suggests this lysogeny is not entirely stable, and ϕ BACA1 may drive the selection of CsaB-deficient mutants through lytic interactions, giving rise to CA's unique and atypical phenotypes.

Table 2-7. Individual variants uncovered by deep-sequencing of *csaB* PCR amplicons.

Sequence	Position	Change	Coverage	Variant Frequency	Variant P-Value	Result (amino acid change)	Mutation	Quality score	Strand bias %
A. Sterne									
T	123	T → C	237,223	0.10%	3.80E-26	N → N	silent	34	59.4
A	144	A → G	240,118	0.10%	1.60E-26	K → K	silent	32	94.6
T	1,059	T → C	175,980	0.10%	1.70E-18	S → S	silent	33	97.3
B. Sterne <i>dcsaB</i>									
No variants passing cut-off filter requirements									
C. Sterne <i>comp-csaB</i>									
A	144	A → G	214,453	0.10%	7.90E-10	K → K	silent	30	90.6
A	223	A → G	266,763	0.20%	8.40E-22	S → G	nonsynonymous	31	61.8

D. CA									
C	48	C → A	155,561	0.30%	3.20E-191	D → E	nonsynonymous	34	71.5
C	94	C → G	218,255	0.20%	1.80E-100	P → A	nonsynonymous	34	57
C	119	C → T	200,206	0.10%	1.30E-15	S → S	silent	31	89.2
A	122	A → G	203,609	0.30%	1.80E-56	N → S	nonsynonymous	30	96.7
G	124	G → T	205,618	0.10%	2.80E-10	D → Y	nonsynonymous	31	57.8
C	127	C → A	219,922	0.20%	1.50E-76	P → T	nonsynonymous	32	65
A	144	A → G	209,668	0.10%	1.20E-15	K → K	silent	32	94.6
G	293	G → T	220,697	0.10%	8.30E-22	R → I	nonsynonymous	31	76.3
C	301	C → A	212,536	0.20%	8.70E-46	R → S	nonsynonymous	32	55
C	332	C → A	233,478	0.10%	3.10E-07	A → E	nonsynonymous	30	69.7
C	346	C → A	300,363	0.70%	0.00E+00	P → T	nonsynonymous	35	51.1
C	367	C → A	197,735	0.20%	1.90E-11	R → S	nonsynonymous	31	63.8
C	392	C → A	188,342	0.50%	0.00E+00	S → *	nonsense	32	61.2
G	400	G → T	182,960	0.90%	0.00E+00	E → *	nonsense	36	53.8
C	485	C → A	176,215	0.50%	0.00E+00	P → Q	nonsynonymous	32	56.7
C	499	C → A	204,695	0.20%	6.90E-24	Q → K	nonsynonymous	31	58.5
G	559	G → T	211,738	0.40%	0.00E+00	A → S	nonsynonymous	34	59.3
C	560	C → A	221,461	0.20%	1.10E-32	A → E	nonsynonymous	30	62.1
G	562	G → T	199,746	0.40%	0.00E+00	V → F	nonsynonymous	35	58.3
G	613	G → T	270,400	0.40%	0.00E+00	D → Y	nonsynonymous	35	57.7
C	725	C → G	236,197	0.10%	2.10E-87	A → G	nonsynonymous	36	51.5
C	776	C → A	232,652	0.10%	1.10E-09	S → *	nonsense	30	75.8

C	785	C → A	250,178	0.20%	2.80E-23	S → *	nonsense	30	74.2
G	846	G → T	223,686	0.50%	0.00E+00	M → I	nonsynonymous	35	53.7
G	862	G → T	204,780	0.20%	1.20E-102	D → Y	nonsynonymous	32	68.3
G	874	G → T	186,993	0.10%	8.40E-08	D → Y	nonsynonymous	31	55.8
C	878	C → A	203,659	0.20%	7.20E-13	S → *	nonsense	30	73.2
C	973	C → A	161,633	0.60%	0.00E+00	Q → K	nonsynonymous	34	86.1
G	999	G → T	199,199	0.40%	0.00E+00	L → F	nonsynonymous	33	82
G	1,060	G → T	126,765	0.20%	6.00E-07	D → Y	nonsynonymous	30	72.9
A	1,072	A → G	110,304	0.20%	7.50E-17	K → E	nonsynonymous	30	93.8

* = stop codon; quality scores shown as Phred values

DISCUSSION

Previous work in the Fischetti Lab uncovered the influence of bacteriophage on the environmental lifecycle of *B. anthracis*, finding that phage-bacteria interactions—and in particular lysogeny—control and can enable phenotypes that promote long-term vegetative survival (Schuch and Fischetti, 2009). These changes were driven by sigma factors, encoded by phage isolated from diverse land and marine environments. For this current study, we aimed to uncover how phage induced from disease-causing isolates may shape *B. anthracis*. We found that exposure of Sterne to ϕ BACA1, a novel *Siphoviridae*-like phage induced from *B. cereus* bv *anthracis* CA (itself a strain recovered from an ape presumed to have died of anthrax in Cameroon (Klee et al., 2006)), selects for a phage-resistant variant with a unique phenotype.

2.12 Selection by lysis drives unique phenotypes in CA and Sterne *dcsaB*

Whole-genome DNA sequencing revealed that exposure of Sterne to ϕ BACA1 selected for and expanded a *csaB* variant population. This variant displayed a unique phenotype atypical of classic *B. anthracis*, and remarkably, a number of its observed traits were also reported for CA (Klee et al., 2006). These included colonies lacking “Medusa heads” that were smaller, mucoid and smooth, and in addition, the variant also displayed hemolytic activity on blood-agar plates. Under the microscope, we observed increased chain lengths of bacilli without clear division

septa, and like CA, the appearance of twisted and corkscrew-like cells. The number of characteristics shared between *dcsaB* and CA suggests that the same factor(s) (likely ϕ BACA1) drives the appearance of atypical *B. anthracis* traits in both strains. In *dcsaB*, we also observed a novel characteristic of multi-chain and organized rope-like growth. It is presently unclear how these structures form, as they were observed in both shaken and static cultures, and if the individual twisted cellular morphologies observed translate into the genesis of these macromolecular structures.

Strain *dcsaB* shared a number of characteristics with CA, but also harbored classical *B. anthracis* traits different from the African strain, including penicillin sensitivity, a lack of motility, and sensitivity to γ -phage. CA is penicillin resistant and motile, however as previously reported (Klee et al., 2006), some subcultures of the strain display inconsistent hemolytic activity, γ -phage sensitivity, and capsule production. Why the two strains differ is likely due to the evolutionary lineage and associated genomic background of each strain. *B. anthracis* is a monomorphic lineage within *B. cereus* sensu lato, while CA lies at the frontier between *Bacillus anthracis* and *Bacillus cereus* sensu stricto (Antonation et al., 2016; Brézillon et al., 2015). Thus, it is not surprising that CA possesses a mixture of typical *B. anthracis* and *B. cereus* phenotypes. While the exact regulation mechanism behind CA's dynamic phenotypes is unclear, our data suggests that for CA, hemolytic activity, twisted cellular forms, atypical growth and the appearance of small, smooth, shiny

and mucoid colonies could in part, arise from selection for CsaB-deficient subpopulations. We show that the phage ϕ BACA1, isolated from CA itself, selects for a phage-resistant *csaB* Sterne mutant that harbors CA-like phenotypes. Deep-sequencing revealed that selection for *csaB* mutation occurred at a higher rate in CA than for other *B. anthracis* strains tested. Whether ϕ BACA1 is the agent responsible for the selection of these mutants in CA is presently unclear and should be studied further, but is a likely candidate. The previous reports of CA colonies transitioning from a classic *B. anthracis* phenotype at 24 hours growth to colonies with a CsaB-deficient phenotype at 48 hours growth (Klee et al., 2006), coupled with our deep sequencing data and Sterne *dcsaB*'s phenotype suggest that lytic interactions may indeed be occurring between CA and ϕ BACA1 selecting for *csaB* mutants in the CA population. We cannot yet state if such phage-bacteria interactions are happening out of the laboratory setting and in native infection environments such as the primate, but such future study will be crucial to better understand the influence of phage on pathogenic *Bacillus spp.*

A simple approach to drive at this unresolved question is through deep-sequencing of the *csaB* gene region from PCR of environmental samples, i.e., PCR using a DNA template from direct swabs of ape carcasses without any exposure to the laboratory or other artificial environments. Amplification and sequencing of the *csaB* region should reveal if a subpopulation of cells harbor *csaB* mutation at a frequency greater than that of spontaneous mutation. If from these samples, mutation in *csaB*

is found in a significantly higher proportion of the population than suggested by a random mutation rate, then phage-resistance and subpopulations of phage-resistant cells would be suggested as an important component of the *B. anthracis* lifecycle, in addition to lysogeny. It is also possible however, that *csaB* mutation is selected for after initial strain isolation, and laboratory culturing may actually select for *csaB* mutation instead. This would suggest however the presence of a phage-stabilizing factor for ϕ BACA1, specific to CA's native environment that keeps the phage in the lysogenic cycle. Such a factor could come from the animal host, the surrounding soil environment, or potentially even the bacteria itself. If this were the case, then it would be in contrast to typical events reported in other bacterial pathogens, where phage tend to induce in infection conditions. In *S. pyogenes* for example, a soluble factor from human pharyngeal cells was found to induce its phage and allow the increased expression of phage-encoded superantigens and DNase which presumably increase bacterial fitness (Broudy and Fischetti, 2003; Broudy et al., 2001; 2002). ϕ BACA1 does not encode any obvious virulence factors, and any potential benefits from its induction are unclear. Thus, it may make sense for *B. anthracis* to prevent phage induction when in an animal host, and for other pathogens to induce phage which carry virulence factors located adjacent to or within lytic cycle operons. Indeed, CO₂/bicarbonate has been shown to cause the induction of *B. anthracis* phage α , and α lysogens were found less virulent than non-lysogenized strains, presumably due to indiscriminate lytic cycle induction and *B. anthracis* cell death in the animal host (Iyanovics, 1962). For CA, preventing ϕ BACA1 phage induction

may maximize its virulence potential in the host. Given recent reports of other lysogenized *B. anthracis* derivatives and their effects on vegetative cells (Schuch and Fischetti, 2009), it may also be worthwhile to study the virulence potential of these lysogens and examine if/how they maintain phage in infection environments. Such work will better illustrate the roles of phage (if any) in the virulence program of *B. anthracis*. If phage are lost in these lysogens as well, or there is selection for resistant subpopulations, then lytic phage-bacteria interactions will appear to have a broader role in *B. anthracis* infection and its further study will be warranted.

2.13 *csaB* mutation in *B. anthracis* may not negatively impact fitness

As *B. cereus* bv *anthracis* CA was isolated from the carcass of an infected ape, we were curious of *dcsaB*'s virulence potential as compared to wild-type Sterne in an animal model, and found that Sterne and *dcsaB* did not show a significant difference in virulence potential. To our knowledge, this is the first virulence comparison of a *csaB* mutant in *B. anthracis*, however comparison in a mouse model between *B. cereus* G9241 and its *csaB* knockout was performed in Wang et al., where the *csaB* mutant displayed a significantly lower virulence potential (Wang et al., 2013). The strains and methods used in our model versus Wang et al. vary considerably and therefore cannot be meaningfully compared. It is noteworthy however, that while *B. cereus* G9241 and its *csaB* knockout differed in virulence potential, a larger difference was seen in time to death rather than percentage of

animal death. Our animal model work showed no significant difference in either comparison, but surprisingly, we found that *dcsaB*'s distinct BHI-associated phenotype was largely absent in mouse tissues. Cells from the mouse examined by fluorescence microscopy had Sterne-like morphologies, while reculturing the same cells in BHI regenerated the long-chain, rope-like forms. This result suggested an environmental dependent switch that alters the *dcsaB* phenotype. As *B. anthracis* pathogenesis involves multiple organ systems (Moayeri et al., 2015), it is likely that the bacteria would evolve strategies to ensure its dispersal throughout an animal host and the presence of such a phenotypic switch makes evolutionary sense. If *dcsaB* were to maintain its long chain, rope-like growth, it is unclear if the bacteria would be able to disseminate effectively throughout the host and successfully infect (Guichard et al., 2012). That *dcsaB* can effectively disseminate in this context suggests *csaB* mutation may not be evolutionarily disadvantageous (at least in Sterne) as the strain can apparently overcome the downstream effects of the genomic alteration as needed.

We successfully mimicked the phenotypic changes seen in the animal environment by growing *dcsaB* in fetal bovine serum, but it is presently unclear how FBS (or the animal environment) precipitates this switch. Sterne *dcsaB* grown in heat-treated serum also displays Sterne-like characteristics, suggesting that its serum-phenotype is not due to direct action by FBS but likely changes from within the bacteria itself, and preliminary fractionation experiments suggested there may be

multiple components of serum that induce specific phenotypic changes. In addition, a seemingly stochastic event was observed with turbid *dcsaB* growth in BHI at 37°C, suggesting that temperature can induce phenotypic changes in the *csaB* mutant as well. Regardless, our data suggests that *B. anthracis* Sterne *dcsaB* can respond to different growth environments, alter its phenotype accordingly and overcome some of the effects of *csaB* mutation.

2.14 How does *csaB* mutation and the external environment affect *B. anthracis*?

Given the phenotypic differences between Sterne and *dcsaB* as well as the mutant's multiple phenotypes, we designed an RNA-seq experiment to examine the transcriptional changes occurring in Sterne and *dcsaB* during BHI and FBS growth. RNA-seq revealed large scale, whole-genome expression differences between Sterne and *dcsaB* as well as within each strain in BHI versus FBS environments. Within-strain comparisons of Sterne and Sterne *dcsaB* showed large differential expression in BHI versus FBS growth environments, though the changes for *dcsaB* were greater than those of Sterne. Between-strain DE observed in our RNA-seq appears to correlate with phenotypic comparisons of the strains; Sterne and *dcsaB* displayed stark differences in BHI media and more similar phenotypes in FBS, and this trend is reflected in the transcriptome data. The close transcriptional profile of the two strains in FBS may explain why Sterne and Sterne *dcsaB* exhibit similar virulence potentials in our animal model. While *csaB* mutation should prevent S-layer

associated virulence factors such as BslA, an adhesin (Kern and Schneewind, 2008), from attaching to the cell wall, the virulence contribution of these gene products does not appear large enough to significantly alter virulence in our model. Other genes associated with virulence such as lethal factor and protective antigen did not meet the criteria for calling differential expression in comparing Sterne and *dcsaB* in FBS, but were called in BHI, highlighting 1) that Sterne and Sterne *dcsaB* have vastly different profiles in a “non-infection” environment but are far more similar in an “infection” context, and 2) the dynamic nature and phenotypic switch of *dcsaB*. We showed an orthogonal example of this in a Western blot of protective antigen.

We found that many of the transcriptional changes associated with a CO₂-bicarbonate environment (upregulation of pXO1 and other virulence-associated genes) (McKenzie et al., 2014; Passalacqua et al., 2009a) also appear to occur in FBS growth, suggesting that FBS carries chemical queues that *B. anthracis* responds to. Indeed FBS does contain bicarbonate, but there are likely other components in the media as well that serve as queues for *B. anthracis* transcriptional modulation. *Eag* expression is reported to increase with CO₂-bicarbonate exposure, and we note similar expression changes in FBS-cultured Sterne and Sterne *dcsaB*. To our knowledge, our study is the first to examine via RNA-seq the transcriptional changes of *B. anthracis* in serum versus rich-growth media, though a previous report did study the transcriptional profile of *B. anthracis* in bovine blood by microarray (Carlson et al., 2015). We link FBS growth, like that

of CO₂-bicarbonate enriched environments, to upregulation of genes important in virulence, and give a global view of gene expression changes associated with BHI and FBS growth for *B. anthracis* Sterne. We believe these two growth environments may be good proxies for “infection” and “non-infection” environments, giving researchers a useful resource to study gene regulation associated with growth within and outside animal hosts. In addition, our RNA-seq data show the stark differences in transcription arising from *csaB* mutation, again highlighting the pleiotropic effects of this gene. CsaB-mediated pyruvylation of the SCWP enables anchoring of Sap, EA1, and other Bacillus S-layer associated proteins with demonstrated roles in virulence (Wang et al., 2013), cell-wall maintenance (Ahn et al., 2006; Anderson et al., 2011), and nutrient acquisition (Tarlovsky et al., 2010). In addition, CsaB may be acting in an, as of yet, uncharacterized manner on the transcriptional level, similar to Sap and EA1 (Mignot et al., 2002). We believe *csaB* mutation likely leads to a cascade of downstream effects, driving the large-scale differential expression observed.

2.15 What accounts for *dcsaB*'s Sterne-like phenotype in FBS?

While our RNA-seq generated global transcriptional data, we cannot yet highlight specific mechanisms behind the FBS-induced phenotypic switch for Sterne *dcsaB*. Mesnage *et al.* reported the presence of *csaB*-independent pyruvylation pathways in *B. anthracis*, detecting a pyruvylated fraction of SCWP in a *B. anthracis csaB* knockout (Mesnage et al., 2000). It is unclear if SCWP pyruvylation is occurring in

Sterne *dcsaB* in FBS growth environments, which would allow anchoring of SLH-domain proteins. Interestingly, expression of *csaA-csaB* is downregulated roughly 7-fold in the *csaB* mutant grown in FBS compared to BHI. In Sterne, the operon does not show differential expression between FBS and BHI culture, and comparison of Sterne and *dcsaB* in FBS does not reveal differential expression of the genes, while in BHI, *dcsaB* has increased *csaA-csaB* expression. This indicates that *dcsaB* expression of the *csaAB* operon is increased in BHI culture. It is unclear why the operon is more highly expressed in the mutant than in wild-type in BHI. It is possible that CsaB protein might also act to control the expression of the *csaAB* operon, in a similar manner to that of Sap and EA1, and that the truncated CsaB product cannot exert such activity, offering a potential mechanism behind *csaAB* upregulation. Alternatively, for the mutant in serum environments, CsaB protein may play a diminished role.

We examined Sterne and Sterne *dcsaB* sensitivity to ϕ BACA1 in FBS, finding that Sterne—but not *dcsaB*—cultures were lysed by the phage (data not shown).

ϕ BACA1 resistance is not reversed by FBS growth, and we believe it is likely the ϕ BACA1 receptor is not anchored to the cell wall in BHI or FBS cultures. This result also suggests that an alternate pyruvylation pathway is likely not “picking up the slack” for inactive CsaB. If pyruvylation is not occurring on the SCWP in FBS, how does *dcsaB* grow in short chains with clear division septa? Mesnage *et al.* also showed that CsaB-pyruvylated SCWP is not absolutely necessary for all autolysin

activity, and Anderson *et al.* reported that in *B. anthracis* $\Delta csaB$, the addition of recombinant BslO to cultures reduced average chain length of the knockout strain, despite no apparent SLH-domain anchoring (Anderson *et al.*, 2011; Mesnage *et al.*, 2000). So, it is possible that BslO or other peptidoglycan hydrolases could allow cell wall division in the absence of CsaB activity. Our RNA-seq data shows that BslO expression is higher in BHI than FBS, making it unlikely that increased BslO concentration is directly contributing to the observed FBS phenotype. We cannot rule out however that BslO or other peptidoglycan-modifying enzymes may possess the ability to bind *dcsaB* SCWP in FBS and not in BHI by an unknown mechanism.

Interestingly, the genes encoding PatA1/B1 and PatA2/B2 (involved in peptidoglycan and SCWP O-acetylation (Lunderberg *et al.*, 2013)) also show downregulation in *dcsaB* FBS growth as compared to BHI culture, suggesting a possible reduction of peptidoglycan and SCWP O-acetylation in FBS cultured cells. For Sterne, there is no DE for *patA1/B1* or *patA2/B2* between BHI and FBS cultures, similar to the pattern seen for *csaB*. How this is directly related to *csaB* mutation remains to be clarified. While a lack of O-acetylation has been linked to limiting azide-induced autolysis in *B. anthracis* (Laaberki *et al.*, 2011), the presence of O-acetylation may contribute to the blocking of autolysin activity via steric hindrance (Blackburn and Clarke, 2002). Therefore one possibility is that for *dcsaB* grown in FBS, decreased O-acetylation may lead to increased autolysin activity and peptidoglycan processing, allowing cell septation/separation even in the absence of

CsaB-mediated SCWP pyruvylation. Given the number of genes involved in peptidoglycan synthesis and remodeling, identifying specific gene products involved in generating the *dcsaB*, FBS-associated morphologies may prove to be a difficult and exhaustive task. However, focusing on those genes significantly upregulated or downregulated in CO₂/bicarbonate or FBS environments (Passalacqua et al., 2009a; 2009b; Rollins et al., 2008) may cull the list and offer potential candidate genes.

One possible candidate enzyme that may account for the serum-associated morphology is EA1. In serum and bicarbonate environments, *eag* is expressed higher than *sap*, and cells produce the *eag*-encoded enzyme EA1. In BHI culture, the reverse is true, with Sap production dominating. This regulation by *B. anthracis* is previously reported in the literature (Mignot et al., 2002; 2004; Missiakas and Schneewind, 2017) and observed in our RNA-seq data set. Both Sap and EA1 proteins are capable of murein hydrolase activity (Ahn et al., 2006), and it is possible that EA1 possesses the ability to septate cell walls in a manner similar to BsIO, while Sap may not have this activity. Experiments adding recombinant EA1 and Sap could examine both enzymes' ability to cut cell walls in the absence of CsaB-mediated SCWP pyruvylation and may indicate whether the expression of *eag* relative to *sap* plays any role in the *dcsaB* serum phenotype.

If EA1 does not appear to alter the cell wall of *dcsaB*, an additional approach to uncover factors important to *dcsaB* serum-associated morphology would be to add

the supernatant from a *dcsaB* FBS culture to *dcsaB* cells grown in BHI. In the absence of SCWP pyruvylation, autolysins and other associated peptidoglycan-sculpting proteins are likely secreted into surrounding media and FBS culture supernatant could contain a variety of murein hydrolases that may have activity against *dcsaB* cells. Addition of filtered supernatant to *dcsaB* cells in grown in BHI could result in their decreased chain length and the loss of the *csaB* knockout-associated morphologies. However, peptidoglycan and other SCWP modifications present in BHI but not FBS culture may block their activity. If added FBS supernatant does however shorten chain length and promote cell septation, then these FBS-upregulated enzymes would be implicated in the phenotypic switch. An additional experiment comparing added supernatant versus “heat-killed” supernatant could show if the factors responsible are proteins susceptible to heat degradation. Previous experiments comparing growth of *dcsaB* in FBS versus “heat-killed” FBS revealed that serum factors causing *dcsaB*'s phenotypic switch are not heat labile, however the factors produced by the bacteria in response to serum may be subject to such degradation. Mass spectrometry and/or fractionation could elucidate specific factors.

Perhaps the most direct method to uncover factors critical to the *dcsaB* phenotypic switch is through transposon mutagenesis or a similar gene inactivation approach. Here, functional knockouts could be generated in *dcsaB*; screening libraries of *dcsaB* variants on FBS-agar for clones lacking rough-edges or “Medusa heads” with convex

colony morphology (i.e., the *dcsaB*-associated phenotype) could identify genes important to the *dcsaB* serum switch. Alternatively, single colonies could be grown in FBS liquid culture, with candidate clones as those failing to display the expected culture turbidity. Either method could highlight gene products important to *dcsaB*'s serum-associated morphological changes, however it is possible that multiple genes are involved in this event, which could prevent identification of candidate clones, or clones with intermediate phenotypes may appear as well. Regardless of these potential shortcomings, this approach may help elucidate how Sterne *dcsaB* harbors phenotypes atypical of *csaB* mutation when grown in FBS culture and should be pursued. Identification of genes crucial to the phenotypic switch would also confirm that the *dcsaB* morphologies associated with FBS culture are caused by *B. anthracis* sensing its environment and adjusting accordingly via transcriptional modulation, and not through direct serum activity.

2.16 How does phage-resistance affect *B. anthracis*?

The ability of Sterne *dcsaB* to alter its phenotypes dependent upon growth environment suggests that *csaB* mutation may not have a negative fitness cost, at least under our conditions. In our case, *csaB* mutation was selected for by exposure to ϕ BACA1, and serves a mechanism for the organism to acquire phage resistance. Mutation in *csaB* was also found to impart resistance to AP50c phage, with multiple distinct phage-resistant variants all showing different mutations within the *csaB* gene. Why *csaB* is selected for by both ϕ BACA1 and AP50c is likely because of its

role in anchoring numerous S-layer and S-layer associated proteins which may serve as cell-receptors for the phage. Indeed for AP50c, Sap is believed to be the phage's receptor (Bishop-Lilly et al., 2012; Plaut et al., 2014). ϕ BACA1's receptor has not yet been uncovered, but is most likely an S-layer or BSL protein, potentially even Sap. It is not clear however why *csaB* and not *sap* is selected for mutation as knockouts of *sap* are viable (Plaut et al., 2014). It is also noteworthy that in the *csaB* mutants uncovered in (Bishop-Lilly et al., 2012) as well as our *dcsaB* strain, mutation in *csaB* always occurred with other secondary SNPs in seemingly unrelated genomic loci. It is unclear why this is the case, but *csaB* appears to be a hotspot for mutation in *B. anthracis*, comparative to other potential genes which could also confer phage-resistance. Regardless, for *B. anthracis* we find that a CsaB-deficient, phage-resistant variant is selected for by exposure to ϕ BACA1, but interestingly and in contrast to what is typically seen with other pathogens (Capparelli et al., 2010; Filippov et al., 2011), phage-resistance is not associated with decreased virulence and fitness in our experiments.

Why might this be the case for *B. anthracis*? From our RNA-seq data, *csaB* mutation does not appear to affect the expression of pXO1-encoded genes important to virulence in FBS culture. In BHI culture however, the same genes were significantly downregulated in the mutant. In other species, phage-resistance is often associated with decreased expression of important virulence factors (León and Bastías, 2015). While this is true for *dcsaB* in BHI, *B. anthracis* appears to encode

mechanisms to minimize the virulence-reducing effects of phage-resistance when in an “infection environment”. If the expression profile of *dcsaB* in BHI held firm within the animal host, it is likely the variant would show decreased virulence as compared to wild-type Sterne. Why *B. anthracis* appears to get around this phage resistance-associated issue may have to do with the fact that it has multiple lifestyles and is successful in both soil/earthworm environments as well as mammalian hosts. That the pathogen encodes mechanisms to control expression of its virulence factors in each environment may allow the success of phage-resistant variants. Other bacterial pathogens such as *S. aureus* or *S. pyogenes* have more limited lifestyles, typically existing solely as colonizers or invasive species of humans. Therefore the effects of phage-resistance may be more impactful on their virulence potential. It is also possible that the factors affected by *csaB* mutation in *B. anthracis* (S-layer proteins) happen to not play large a role in virulence. If such proteins were critical to virulence, then clearly phage-resistance would decrease bacterial pathogenicity. It is unclear if this lack of virulence decrease in our phage-resistant *B. anthracis* variant is pure coincidence or was selected for in some manner.

While not related to phage-resistance, it is also interesting to note the general role of phages and virulence in *B. anthracis* compared to pathogens such as *S. aureus* and *S. pyogenes*. Phages are not obviously associated with the pathogenicity of *B. anthracis*, and are not major carriers of virulence determinants, whereas the phages

of *S. aureus* and *S. pyogenes* are well known to encode important virulence genes (Bae et al., 2006; Beres and Musser, 2007). For *B. anthracis*, plasmids seem to take up the virulence role, with pXO1 and pXO2 encoding toxins and capsule, respectively, making the bacteria a dangerous pathogen. For *S. aureus* and *S. pyogenes*, plasmids often encode antibiotic resistance genes, but are not the main determinants of virulence potential. In comparing *B. anthracis* to other Gram-positive pathogens, there appear to be important differences in the roles of phage for the species. Further research may illustrate explanatory mechanisms behind these differences.

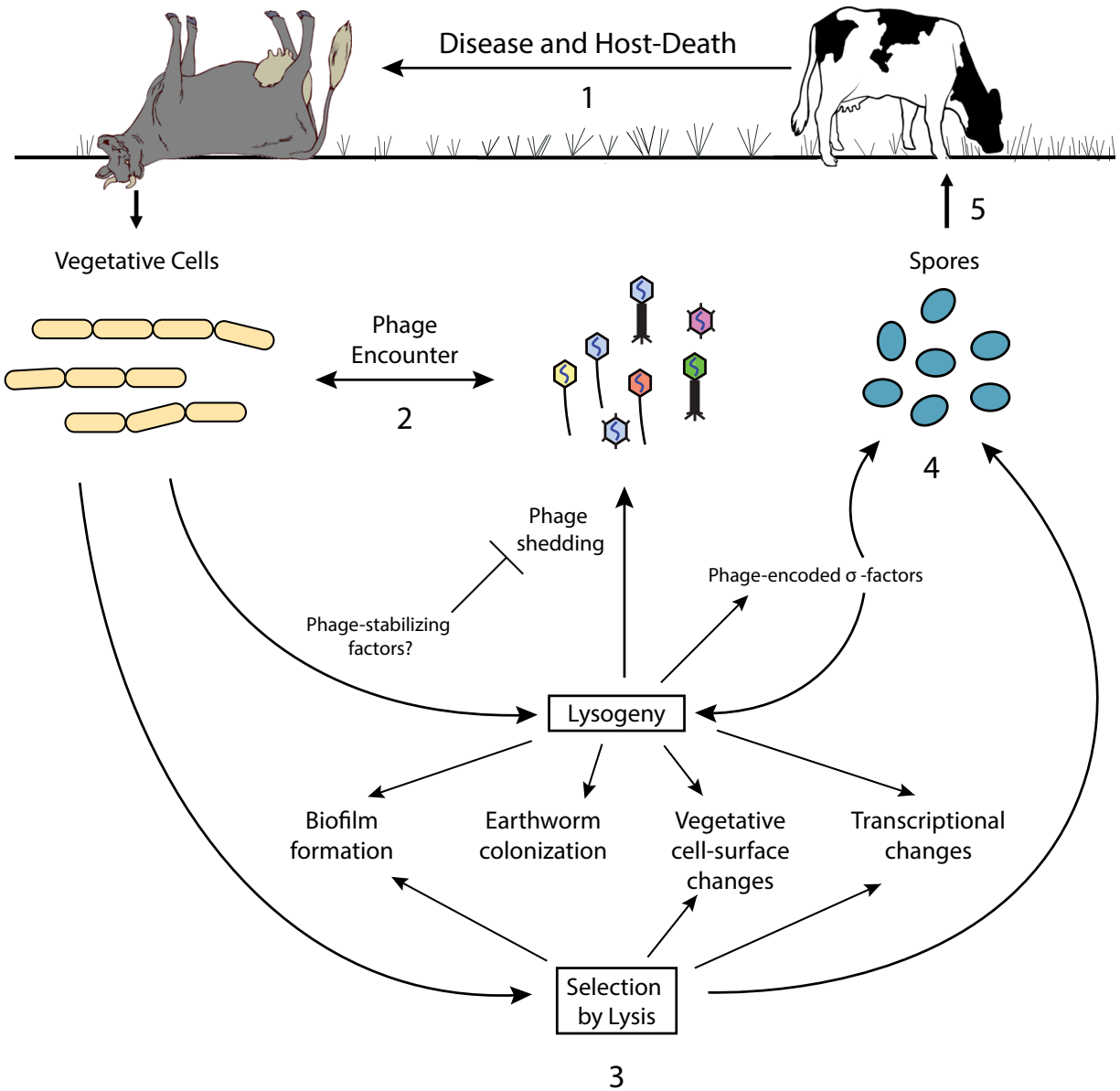
Given that our experiments did not show a fitness decrease for *dcsaB*, we were curious if reversion would occur in the absence of phage or without environmental selection. We examined *dcsaB* for reversion of the *csaB* mutation via deep-sequencing and in culture-based experiments, but did not detect any reversion to wild-type. We did successfully revert our *csaB* mutant to form the viable Sterne strain comp-*csaB* (still containing the tRNA-methyltransferase mutation), suggesting reversion to wild-type should be possible as well as the selection of *csaB* mutants without secondary genomic alterations. If *csaB* mutation was associated with negative fitness, then reversion to wild-type would be expected, however it is possible that we are not growing the variant in the appropriate environment for such selection. We also found that temporal lysogeny of Sterne with ϕ BACA1 was possible, but the lysogen grew poorly and would often generate colonies with *dcsaB*-

like phenotypes after multiple passages. In Sterne, ϕ BACA1 appears to be carried unstably and selects for a CsaB-deficient, phage-resistant population. For CA, our deep-sequencing data suggests a comparable event occurs, though only in a portion of the population. More stable carriage of ϕ BACA1 in CA could explain why only some of the population is CsaB-deficient: the rest may be lysogenized.

For CA, a subpopulation of CsaB-deficient variants may be advantageous, or at the very least, not associated with a decrease in overall fitness. Sterne *dcsaB* has increased hemolytic activity, altered cellular and colony morphologies, as well as different biofilm formation capacity as compared to Sterne. Such phenotypes could alter behaviors such as vegetative survival outside the host, while not impeding the population's virulence potential. Surprisingly, this may be similar to some of the effects of phage carriage in *B. anthracis* (Schuch and Fischetti, 2009), however the virulence potential of these reported lysogens has not been studied. *CsaB* mutation however, also likely confers on CA resistance to other phages that also rely upon a SLH-domain containing receptor for infection (e.g. AP50). This could protect a CA population from complete lysis if encountering a novel phage. (Lysogeny will also however typically provide superinfection immunity to compatible phages). It is possible that CA may be "using" ϕ BACA1, or at least benefiting from its somewhat unstable carriage to drive the expansion of a CsaB-deficient subpopulation, giving the bacteria a new tool for survival. Thus, both lysogeny *and* lysis may play significant roles in the *B. anthracis* lifecycle. The research presented in this

Chapter examines this lesser studied aspect of phage conversion—selection by lysis—which may serve to enable *B. anthracis* to maintain a subpopulation with different phenotypes “at the ready” for certain environmental conditions. Given the insights from this work, a new, hypothetical model for the *B. anthracis* lifecycle including selection by lysis is shown in Figure 2-17. The magnitude and importance of this aspect of phage conversion for *B. anthracis* in the wild however, remains to be clarified through future research.

Figure 2-17. A new, potential model of the *B. anthracis* lifecycle. After anthrax disease and host death (1), vegetative *B. anthracis* cells enter the soil environment where phage encounter (2) can drive lysogeny or potentially, selection by lysis for phage-resistant variants. Both lysogenized cells and resistant variants harbor different characteristics from non-lysogenized or wild-type cells, including altered biofilm formation, vegetative cell-surface changes, and transcriptional modulation (3). Lysogeny can also promote earthworm colonization, and lysogenized cells occasionally shed phages into the environment by limited lytic induction. For CA, further research is needed to understand the prevalence of phage-resistance in its native environment. If a significant proportion of wild, uncultured *B. anthracis* cells harbor resistance-causing mutations, then selection by lysis will appear to play an important role in the natural *B. anthracis* lifecycle, and an updated model is warranted. Alternatively, there may exist environmental phage-stabilizing factors that prevent phage-shedding and expansion of phage-resistant subpopulations. Both phage-resistant and lysogenized cells can sporulate (4), however phage-encoded sigma factors can promote or block this event. In CsaB-deficient phage-resistant cells, no effect on sporulation was observed. Spores taken up by an animal host (5) can germinate, cause anthrax (1), and restart the *B. anthracis* lifecycle. Figure adapted and modified with permission from (Schuch and Fischetti, 2009).



SUMMARY

In this Chapter, we characterized a Sterne variant, *dcsaB*, that is resistant to infection by ϕ BACA1, a bacteriophage isolated from *B. cereus* Biovar *anthracis* CA. Phage-resistance was the result of selection for a frameshift mutation in *csaB*, a SCWP pyruvyl-transferase, with the mutation and resistance reversible by genomic manipulation. We show that *dcsaB* harbors distinct phenotypes similar to CA and a growth media-induced switch, where *dcsaB* displays Sterne-like phenotypes in FBS or an animal host, and in addition, the variant does not show an altered virulence potential. We examined the global transcriptional profiles of Sterne and Sterne *dcsaB* in BHI and FBS by RNA-seq, highlighting the gene expression changes associated with both FBS growth and *csaB* mutation. Lastly, we showed the prevalence of *csaB* variants within a CA population, suggesting that phage-resistance and selection by lysis may be occurring in the wild, and along with lysogeny, is a potential factor shaping pathogenic *B. anthracis* populations.

MATERIALS AND METHODS

2.18 Bacterial strains and growth conditions

All strains used in this study are listed in Table 2-8. *Bacillus* strains were grown at 30°C in brain-heart infusion broth (BHI) with shaking at 150 RPM and aeration except as otherwise noted. *E. coli* was grown at 37°C, 200 RPM in Luria-Bertani (LB) liquid media or on LB-agar plates with ampicillin selection or without selection as required. *S. aureus* RN4220 and *S. pyogenes* SF370 were grown at 200 RPM in BHI media. Antibiotics were used at the following concentrations: ampicillin, 100 µg/mL; kanamycin, 50 µg/mL.

Induction of phage from *B. cereus* Biovar *anthracis* CA was performed as follows: an overnight culture grown in BHI was back-diluted 1:100 in fresh BHI containing 5 µg/mL mitomycin C and grown overnight. Cells were pelleted and the clarified supernatant filtered with 0.22 µm filters to remove debris. To prepare high-titer phage stocks, induced phage supernatants were amplified using *B. anthracis* Sterne cultures. Overnight cultures of Sterne were back-diluted 1:100 in BHI and grown at 200 RPM, to an OD₆₀₀ = 0.1 - 0.2. An equivalent volume of phage supernatant was added to the bacterial culture and grown at 150 RPM until visible lysis occurred, typically 3-4 hrs. Cultures were then spun down at 4000 RPM and filtered with 0.22 µm filters to remove bacterial debris. This procedure was repeated as necessary to

generate large volume phage stocks. All serum growth media used in this study was heat-inactivated fetal bovine serum (Sigma) unless otherwise noted.

To determine the minimum serum dilution required to observe *B. anthracis* Sterne *dcsaB* phenotypes associated with serum (FBS) growth, BHI:FBS (v/v) mixtures were prepared ranging from 100:0 to 0:100. Bacteria from an overnight culture were vortexed to homogeneity, back-diluted 1:100, grown 36 hours at 30°C in BHI, FBS or BHI:FBS mixtures, and observed. For experiments using heat-treated FBS, the media was prepared by placing 30 mL FBS in a Falcon tube in a room temperature water bath, and slowly increasing the bath temperature to 85°C to prevent serum aggregation. The FBS was heated at 85°C for 60 mins. For all experiments, negative, non-inoculated controls were included. Bacteria used in heat-treated serum experiments were established from overnight BHI cultures, back-diluted 1:100 into media and grown at both 30°C and 37°C.

Table 2-8. Strains, plasmids, and primers used in this study.

Strains	Description	Notes
<i>E. coli</i> TOP10	Cloning host	Invitrogen
<i>E. coli</i> SCS100	dam ⁻ /dcm ⁻ cloning host	NEB
<i>B. anthracis</i> Sterne	Sterne strain Pasteur 7702, pXO1 ⁺ , pXO2 ⁻	
<i>B. anthracis</i> ΔSterne	ΔSterne strain pXO1 ⁻ , pXO2 ⁻	
<i>B. anthracis dcsaB</i>	Sterne strain Pasteur 7702 with 2 single nucleotide insertions, inactivating <i>csaB</i> insertion, insertion in tRNA-methyltransferase	
<i>B. anthracis</i> comp- <i>csaB</i>	Sterne strain Pasteur 7702 with 1 single nucleotide	

	insertion, in tRNA-methyltransferase	
<i>B. cereus</i> Biovar <i>anthracis</i> CA	Transition <i>B. cereus</i> strain containing pXO1 and pXO2-like plasmids pBCXO1, pBCXO2	(Klee et al., 2006.)
<i>S. aureus</i> RN4220	Lab strain	Hemolysis positive
<i>S. pyogenes</i> SF370	Lab strain	DNase positive
<i>B. cereus</i> T	Lab strain	Motility positive, Penicillin resistant
Plasmids		
pASD2	<i>E. coli</i> - <i>B. anthracis</i> shuttle vector for generating genetic knockouts and complements	(Day et al., 2007)
pDD1001	pASD2 with wild-type <i>csaB</i> sequence insert for generating Sterne comp- <i>csaB</i>	this work
Primers	Sequence	
<i>csaB</i> _deep_seq_F	CCAACATTCCTTATATATTAATGTTAGG	for deep-sequencing experiments
<i>csaB</i> _deep_seq_R	CGCATTAAAGTTGAACTGGATATC	for deep-sequencing experiments
<i>csaB</i> _comp_F	TCGATCGGTACCAAATGTTGGAGGAGATTAAGAGTGCGGTTAG	for comp- <i>csaB</i> construction
<i>csaB</i> _comp_R	TCGATCGGTACCTTAAGATCCCATTCCTCTTTTTT TGA ACTC	for comp- <i>csaB</i> construction
pASD2_F	CAATCAATCACCGGATCCCC	for Sanger sequencing
pASD2_R	TAACCCTCACTAAAGGGAACAAA	for Sanger sequencing
<i>csaB</i> _check_seq_2	GGTGT CACAAGTAATTGAGC	for Sanger sequencing

B_anthraxis_16S_rRNA_ F	TGAAAACTGAACGAAACAAAC	for PCR of <i>B. anthracis</i> gDNA
B_anthraxis_16S_rRNA_ R	CTCTCAAACTGAACAAAACGAAA	for PCR of <i>B. anthracis</i> gDNA
phiBACA1_F	AAAATGAACACTTTGAAAGGTCGAATTGA	for screening of ϕ BACA1
phiBACA1_R	CTTCTGTATTAGTAGCAAAGCGATCCACTG	for screening of ϕ BACA1
tRNA_methyltransferase _check_F	TACGGAGAACTACGACGTTGCAATTATTG	for Sanger sequencing
tRNA_methyltransferase _check_R	CGACGATTCGACATGGAATATCGAC	for Sanger sequencing

2.19 Exposure and lysogeny of *B. anthracis* Sterne with ϕ BACA1

Exposure and lysogeny of *B. anthracis* Sterne with ϕ BACA1 was achieved following a modified protocol (Schuch and Fischetti, 2009). Briefly, 10 mL cultures of *B. anthracis* Sterne were grown overnight in BHI and back-diluted 1:100 in 10 mL fresh BHI and grown to $OD_{600} = 0.6$. 1 mL of phage stock was added to 4 mL bacterial culture and incubated with shaking for 30 min. Bacteria-phage mixtures were spun down (4000 RPM, 4°C, 20 min), washed 1X in cold phosphate-buffered saline (PBS), resuspended in 5 mL BHI, serially diluted and plated on BHI agar. Plates were grown overnight at 30°C, and the resulting individual colonies were patched onto new BHI plates, and grown overnight. Potential lysogens were screened when applicable via colony PCR using the ϕ BACA1-specific primers phiBACA1_F and phiBACA1_R (Table 2-8).

2.20 Phenotypic analysis of *B. anthracis* strains

Colonies were imaged using the Cell Biosciences AlphaImager HP instrument with AlphaImager HP software or an iPhone 6 camera. For microscopy studies, strains from overnight cultures were washed 1X with PBS and examined using the Nikon Eclipse E400 Phase Contrast Microscope and images captured with QCapture Pro 5.1 software. Magnification and exposures were adjusted manually as necessary. Strains were stained using acridine orange or 4',6-diamidino-2-phenylindole (DAPI) following standard protocols. To visualize *B. anthracis* extracted from animal tissues, manually homogenized tissue samples were incubated with GFP-PlyG^{BD}, a *B. anthracis*-specific protein fusion containing the binding domain of the phage lysin PlyG and GFP for visualization (Raz et al., 2017; Schuch and Fischetti, 2009). Samples and GFP-PlyG^{BD} were incubated for 10 minutes at room temperature, washed 1X in PBS, and visualized using standard protocols.

To test for DNase and hemolytic activity, strains were grown overnight and spotted onto BD Difco DNase Test Agar with Methyl Green for DNase testing, or BBL Columbia Agar with 5% Sheep Blood for hemolytic activity tests. Plates were grown at 24°C, 30°C, or 37°C overnight. For DNase testing, *Streptococcus pyogenes* SF370 was used as a positive control, and strains producing clear halos in the agar were recorded as DNase positive. For hemolysis studies, *Staphylococcus aureus* RN4220 was used as a positive control, and strains producing clearing zones were recorded as hemolysis positive.

Penicillin resistance was tested following a protocol outlined in the WHO Manual for Laboratory Diagnosis of Anthrax (World Health Organization, 2003). *B. cereus* T was used as a positive control for penicillin resistance, and *B. anthracis* Sterne as a negative control. BD BBL Sensi-Disc Susceptibility Test Discs: Penicillin (10U) were used for assays. For motility assays, 10 μ L of overnight cultures were spotted on 0.3% BHI soft-agar and allowed to grow at 37°C overnight. Motility was measured by outward growth from the initial bacterial spot. *B. cereus* T was used as a positive control and *B. anthracis* Sterne a negative control for motility. For sporulation studies, strains were grown overnight at 30°C on BHI plates from freezer stocks, and the following day, single colonies selected and struck out on LD sporulation agar plates sealed with parafilm and grown at 30°C for 7 days. After 7 days growth, plates were scraped into 0.5 mL BHI, the wet pellets weighed and vortexed to homogeneity, and 0.25 mL aliquots removed, heated at 65°C for 30 mins, placed on ice for 5 mins, diluted and plated for enumeration of spores on BHI plates. Viable colonies were counted the following day after overnight growth at 30°C. Non-heat-treated aliquots were plated and enumerated for viable vegetative CFU counts on BHI plates. Sporulation significance testing was performed using the Student's t-test with GraphPad Prism software. Phage susceptibility was tested by co-spotting 10 μ L mid-logarithmic phase cultures with 5 μ L high-titer phage stock (or 1X PBS) on Columbia agar plates and growing at 37°C or 30°C overnight.

For biofilm formation and analysis, a protocol adapted from (Schuch and Fischetti, 2009) was used. Overnight 5 mL cultures grown in BHI at 30°C with or without 0.2% glucose were washed 2X in PBS, resuspended in PBS and diluted 1:1000 into 10 mL BHI with or without 0.2% glucose. Cultures were grown at 24°C, 30°C, or 37°C. Biofilm formation capacity was measured visually weekly for 10 weeks and assigned values of: no growth, weak, medium, or strong growth.

2.21 Next-generation sequencing of phage DNA, PCR and Southern blot screening for ϕ BACA1

To prepare phage genomic DNA for NGS, high-titer phage supernatants were polyethylene glycol (PEG)-precipitated with 10% PEG 8K and 1 M NaCl added to 200 mL phage supernatant and shaken overnight (4°C, 80 RPM). The precipitated solution was pelleted at 8000 RPM, 4°C for 1 hr, and the pellet resuspended in PBS. Phage genomic DNA was extracted and purified using the Norgen Biotek Corp. Phage DNA Isolation Kit following manufacture's protocol. A phage DNA library was generated using the Illumina Nextera XT kit, quantitated with the Agilent Technologies High Sensitivity DNA kit and paired-end sequenced on an Illumina MiSeq using the Illumina MiSeq Reagent Kit v2 (500 cycle). FASTQ files were saved and downstream bioinformatic analysis done using CLC Genomics Workbench software. Reads were *de novo* assembled using default parameters. The resulting contigs were annotated using RAST (Rapid Annotation using Subsystem

Technology) (Aziz et al., 2008) and PHASTER (PHAge Search Tool Enhanced Release) (Arndt et al., 2016) online tools.

PCR screening of Sterne and Sterne:: ϕ BACA1 gDNA (prepared as described in Section 2.22) was performed using phiBACA1_F and phiBACA1_R primers and the KAPA2G Robust Hotstart DNA Polymerase following manufacture's protocol.

Purified ϕ BACA1 DNA or ϕ BACA1 stock was used as a positive control. Southern blotting was carried out using the same DNA samples. Briefly, gDNA was run out on a 0.7% TAE agarose gel, transferred onto Hybond-N+ membrane (GE) using a standard capillary action protocol, and UV fixed the following day. ϕ BACA1 DNA was used as a positive control. Detection was carried out using the Amersham ECL Direct Labeling and Detection System. Probe was generated from a gel-purified ϕ BACA1-specific PCR product created using phiBACA1_F and phiBACA1_R primers, ϕ BACA1 DNA, and the KAPA2G Robust Hotstart DNA Polymerase.

2.22 Genomic DNA preparation and sequencing of *B. anthracis* strains

Genomic DNA for sequencing was prepared from an overnight culture using the QIAGEN Genomic-Tip 100/G kit. PlyG (Schuch et al., 2002) and lysozyme were added to Buffer B1 and allowed to incubate with resuspended bacteria at 37°C for 30 minutes before addition of proteinase K and further incubation at 37°C as per manufacturer's directions. Genomic DNA was dissolved in QIAGEN elution buffer (Buffer EB). DNA concentration was measured using Qubit Fluorometric

Quantitation and diluted to 0.2 ng/μL. DNA libraries for sequencing were prepared using the Illumina Nextera XT DNA Library Preparation and Index Kit following manufacturer's directions. Libraries were quality and size checked with the Agilent 2100 Bioanalyzer with a High Sensitivity DNA chip, manually normalized and pooled together with a 5% PhiX control spike-in. Libraries were paired-end sequenced using an Illumina MiSeq with the MiSeq Reagent Kit v3 (150 cycle). FASTQ files were saved for each sample and downstream bioinformatic analysis was performed using Geneious software. Reads were aligned to the *B. anthracis* chromosome (NZ_CP009541.1) and pXO1 (NZ_CP009540.1) and examined for regions of variation and/or SNPs. Unaligned reads were *de novo* assembled.

2.23 Molecular cloning and complementation of *B. anthracis* *dcsaB*

The *csaB* gene and 500 bp upstream and downstream of the gene was amplified using *B. anthracis* Sterne gDNA as template with primers *csaB_comp_F* and *csaB_comp_R* and Q5 Polymerase (NEB). The PCR product was gel-purified, cut with Kpn1-HF restriction endonuclease (NEB) and further purified with QIAquick PCR Purification Kit. Plasmid pASD2 (Schuch and Fischetti, 2009) was mini-prepped from an overnight culture with QIAprep Spin Miniprep Kit, cut with Kpn1-HF, dephosphorylated with Antarctic Phosphatase (NEB) and ligated with the *csaB* DNA fragment using T4 DNA Ligase (NEB) to form pDRD1001. 2 μL of ligation mixture was used to transform One Shot TOP10 Chemically Competent *E. coli* (Thermo Fisher) according to manufacturer's directions. Colonies were screened via

PCR using primers pASD2_F and pASD2_R, and PCR products Sanger sequenced with GENEWIZ (South Plainfield, NJ). A single colony harboring the desired *csaB* sequence was grown overnight, miniprepped, and pDRD1001 shuttled into the dam⁻/dcm⁻ Competent *E. coli* SCS100 (NEB) following manufacturer's transformation protocol. Miniprepped pDRD1001 from SCS100 cells was electroporated into 400 μ L electrocompetent Sterne *dcsaB* prepared as described in (Koehler et al., 1994) using a Bio-Rad Gene Pulser and a 0.4 cm electrode gap Gene Pulser Cuvette with the following conditions: 2.5 kV, 400 Ω , 25 μ F.

B. anthracis Sterne *dcsaB* harboring pDRD1001 was then subjected to the following growth protocol to promote plasmid integration followed by excision and curing to generate a *csaB* revertant strain. A single colony from BHI-kanamycin agar was grown for 5 hours in 10 mL BHI-kan at 30°C, then grown for an additional 5 hours at 39.5°C (non-permissive temperature for plasmid replication), before plating at 10^{-1} - 10^{-4} dilutions on BHI-kan agar and overnight growth at 39.5°C. Single colonies the following day were struck on BHI-kanamycin agar and grown overnight at 38°C. Colonies were screened via PCR using primers pASD2_F and *csaB_check_seq_2* for plasmid integration. A single colony with integrated pDRD1001 was then grown in 10 mL BHI at 30°C the following day for 8 hours, back-diluted 1:100 and grown in 10 mL BHI at 39.5°C overnight. Following overnight growth, the culture was plated on BHI agar at 10^{-3} - 10^{-6} dilutions and grown at 39.5°C. Resulting single colonies were restruck on BHI and grown at

39.5°C, then replica plated on BHI-kan agar plates and grown at the non-permissive temperature to screen for plasmid loss. Colonies that grew on BHI but not BHI-kan plates were restreaked on BHI agar, grown at 30°C, and the *csaB* gene region amplified via PCR and DNA sequenced via Sanger sequencing (GENEWIZ) to check for the wild-type *csaB* DNA sequence, using primers *csaB_check_seq_2* and *csaB_deep_seq_R*. The resulting revertant strain was termed *B. anthracis* Sterne comp-*csaB*.

2.24 *In vivo* virulence mouse models

The Rockefeller University institutional animal care and use committee approved all *in vivo* protocols. Overnight cultures of *B. anthracis* Sterne and Sterne *dcsaB* grown at 37°C, 200 RPM in BHI, were back-diluted 1:100 into pre-warmed BHI and grown 2.25 hrs at 37°C, 200 RPM. Cultures were spun down at 4000 RPM, 4°C for 10 min and washed in ice-cold 1X PBS and resuspended in PBS and diluted to the following concentrations for chain length normalization: for *B. anthracis* Sterne, 1.0×10^7 CFUs/mL; for Sterne *dcsaB* $1.5 - 2.0 \times 10^6$ CFUs/mL. To calculate the normalization factor, Sterne and Sterne *dcsaB* were prepared as described and images taken of individual chains on a phase-contrast microscope. Chain lengths for each strain were measured for over 100 individual chains using ImageJ and the average chain length determined. For mouse experiments, 4-6 week old C57BL/6 female mice from Charles River Laboratories were injected intraperitoneally with 0.5 mL bacterial suspensions. Survival was observed and recorded for 10 days

following injection after which all animals were sacrificed. Survival and virulence comparisons were calculated using the Gehan-Breslow-Wilcoxon Test and curves generated using GraphPad Prism software. For experiments examining infected tissues, a protocol was followed as described above, except animals with established infection were sacrificed 48 hours after injection, with organs removed and manually ground to homogeneity in 1X PBS. The cellular suspension was incubated with GFP-PlyG^{BD} and bacterial cells imaged as described previously by microscopy.

2.25 RNA-seq of *B. anthracis* Sterne and Sterne *dcsaB* in BHI and FBS cultures

For RNA-seq studies, all growth conditions were 37°C, 150 RPM. Sterne and Sterne *dcsaB* were established from overnight cultures in BHI, then passaged 1:1000 into BHI or FBS and grown overnight. The following morning, cultures were back-diluted 1:100 into the same pre-warmed media, grown to late-log phase (an OD₆₀₀ approximately 2/3 of the maximal logarithmic growth OD₆₀₀), and 1 mL culture removed for preparation of RNA. Sterne *dcsaB* grown in BHI was removed at comparable time point as it was not amenable to OD₆₀₀ readings. Four groups of samples were generated: Sterne-BHI; Sterne-FBS; Sterne-*dcsaB*-BHI; Sterne-*dcsaB*-FBS. Samples were washed 2X in PBS, cells lysed using PlyG and suspended in 600 µL TRI Reagent (Zymo Research). Samples were frozen at -80°C, until RNA was purified. RNA was prepared using the Zymo Research Direct-zol RNA Mini-Prep Plus Kit, following manufacturer's directions including an in-column DNase

digestion. Additional DNase digestion was performed with DNase I, Amplification grade (Thermo Fisher) as needed until RNA samples showed no DNA contamination measured by 40-cycle PCR with *B. anthracis*-specific 16S rRNA primers. RNA samples were quality checked after DNase digestion using an Agilent RNA Nano Kit on an Agilent 2100 Bioanalyzer. RNA samples were then rRNA depleted using the Illumina Ribo-Zero rRNA Removal Kit for Gram-positive Bacteria. All samples were in prepared and sequenced in duplicate, except for Sterne *dcsaB*, which was in triplicate.

rRNA depleted samples were submitted to The Rockefeller University Genomics Resource Center for library construction and sequencing. Libraries were constructed using the Illumina TruSeq stranded mRNA LT kit starting at the RNA fragmentation step to prepare libraries. Libraries were prepared with unique barcodes and pooled at equal molar ratios. The pool was denatured and sequenced on an Illumina NextSeq 500 Sequencer, generating 75 bp single reads, following the manufacturer's protocol. Reads for each sample were generated as FASTQ files and downstream analysis done offline.

Reads generated for each sample were first aligned to the Sterne Genome (Accessions: NZ_CP009541, NZ_CP009540) using Bowtie2 (Langmead and Salzberg, 2012) and BAM files sorted, indexed, and converted to SAM files using samtools (Li et al., 2009). Files were processed using RStudio and Bioconductor. Count and

differential expression (DE) data was processed using a protocol adapted from (Love et al., 2016). Read counts were generated using *GenomicAlignments* package (Lawrence et al., 2013) to create a *SummarizedExperiment* (Morgan et al.) and *DESeq2* (Love et al., 2014) was used to generate graphical visualizations and differential expression analysis. The following four DE comparisons were generated: 1) Sterne-BHI against Sterne-*dcsaB*-BHI; 2) Sterne-BHI against Sterne-FBS; 3) Sterne-FBS against Sterne-*dcsaB*-FBS; 4) Sterne-*dcsaB*-BHI against Sterne-*dcsaB*-FBS. DE was called using a minimum fold-change cut-off of 2, and an adjusted p-value of < 0.01. DE comparison tables were saved as CSV files.

2.26 Western Blot of protective antigen from *B. anthracis* culture supernatants

Supernatants for Western blot were prepared as follows: Sterne, Sterne *dcsaB*, or Sterne *comp-csaB* strains were grown as described for RNA-seq sample preparation, but upon reaching late-log phase, cultures were spun down, resuspended in fresh pre-warmed media and allowed to continue growth for 1 hr. After 1 hr growth, cultures were spun down and the supernatant sterile filtered through 0.22 μm filters. Δ Sterne supernatant was used as a negative control for protective antigen. Supernatants were normalized for OD₆₀₀ values/cell number and were run on Thermo Fisher NuPAGE 4-12% Bis-Tris Protein Gels, with MOPS running buffer at 200 V for 1 hr. FBS supernatants, and BHI supernatants compared to FBS supernatants were diluted 1:100 in PBS to allow for distinct FBS protein bands on

the gel. For blots containing only BHI samples, BHI supernatants were concentrated 5x using Vivaspin 500 3 kDa MWCO filters (GE). Gels were stained with the Colloidal Blue Staining Kit (Thermo Fisher) as per manufacturer's directions. Protein gels for Western blots were transferred onto Immobilon-P PVDF membrane (Millipore) following standard protocols, blocked and probed with Anthrax protective antigen antibody (Invitrogen Cat. # PA1-41695) as primary and Peroxidase AffiniPure Donkey anti-rabbit IgG (Jackson Cat. # 711-035-152) as secondary. Blots containing FBS and BHI supernatants were developed using SuperSignal West Femto Maximum Sensitivity Substrate (Thermo Fisher). Blots containing only BHI supernatant samples were developed using SuperSignal West Pico Chemiluminescent Substrate (Thermo Fisher). Developed film was photographed using an iPhone 6 camera.

2.27 Determination of *B. anthracis* Sterne spontaneous resistance rate to ϕ BACA1

To determine the spontaneous resistance rate of Sterne to ϕ BACA1, an overnight culture of Sterne was back-diluted 1:100 in 5 mL BHI and grown at 30°C, 150 RPM to an $OD_{600} = 0.1 - 0.2$. The culture was then split and infected with $MOI = 10$ of ϕ BACA1 or mock-infected with an equal volume BHI. Cultures were then grown for an additional 30 mins, before plating both untreated and treated cultures for CFU counts. Resistance rate was determined by comparison of treated to untreated CFU counts. Experiments were performed in triplicate.

2.28 Determination of *B. anthracis* Sterne *dcsaB* genomic reversion

To observe potential reversion of *dcsaB*, an overnight culture of Sterne *dcsaB* was back-diluted 1:100 and grown in 5 mL BHI or FBS at 37°C, 150 RPM. Following overnight growth, each culture was examined under a microscope for Sterne-like morphologies and phenotypes. 10 µL of each culture was then passaged into the same media (BHI or FBS) and allowed to grow overnight in the same conditions. In addition, 10 µL of each culture was also used to inoculate 10 mL of BHI, grown at 30°C overnight. 30°C BHI cultures (inoculated from 37°C BHI or FBS cultures) were examined the following day for turbidity and visualized for Sterne-like morphologies and phenotypes. This protocol was repeated for seven consecutive passages.

2.29 PCR amplicon preparation and deep-sequencing of *csaB*

Genomic DNA for use as template in PCR reactions amplifying the *csaB* gene region were prepared as follows: colonies from a BHI plate grown overnight at 30°C were scraped and resuspended into 25 µL 0.5 M NaOH, before adding 25 µL of 1 M Tris pH 7.0 and 450 µL nuclease-free water. PCR reactions used the Q5 High-Fidelity DNA Polymerase (NEB), *csaB_deep_seq_F* and *csaB_deep_seq_R* primers, and 0.5 µL of previously prepared template DNA in a 50 µL reaction. PCR amplicons were gel-purified using the QIAquick Gel Extraction Kit, quantified with Qubit, and diluted to 0.2 ng/µL in QIAGEN EB. DNA libraries and sequencing was carried out

as described previously in Section 2.22, with the exception that library quantitation was performed using the Agilent High Sensitivity D1000 ScreenTape Assay on an Agilent TapeStation. FASTQ files were saved for each sample, and bioinformatic analysis done using Geneious software. Variants with strand biases $> 98\%$ or Phred quality scores < 30 were filtered out from results.

CHAPTER 3. EXTRA-CHROMOSOMAL DNA SEQUENCING REVEALS EPISOMAL PROPHAGE CAPABLE OF IMPACTING VIRULENCE FACTOR EXPRESSION IN *STAPHYLOCOCCUS AUREUS*

INTRODUCTION

3.1 Impacts of prophage on the biology and virulence of *S. aureus*

As discussed in Chapter 1, *S. aureus* is a major human pathogen which employs an array of virulence factors to execute a highly successful infection program (Thammavongsa et al., 2015; Thomer et al., 2016). Many of these determinants are encoded by prophage elements (Novick and Matthews, 2005). In addition to the *hly*-converting phages previously discussed, other phages of *S. aureus* carry virulence factors important for pathogenesis. These include the pore-forming Pantone-Valentine leukotoxin (PVL), and exfoliative toxin A (ETA), the causative agent of staphylococcal scaled skin syndrome (SSSS) (Kaneko et al., 1998; Yamaguchi et al., 2000). Important phage-encoded virulence factors of *S. aureus* are listed in Table 3.1.

The dependence of *S. aureus* on its resident prophage is clear, as phage-cured strains show markedly reduced virulence (Bae et al., 2006). In addition, the coordination of chromosomally-encoded regulators (e.g. Agr) with phage-encoded virulence determinants suggests a long co-evolution and dependence on phage by the bacterial host (Fischetti, 2006). As such, the importance of positive conversion

for *S. aureus*'s virulence cannot be overstated, however, recent reports have revealed that other processes such as phage excision/integration and atypical genome localization play roles in the virulence potential of the organism in addition to the “traditional roles” of positive and negative conversion (Goerke et al., 2004; 2006; Utter et al., 2014).

Table 3-1. Important phage-encoded virulence factors of *S. aureus*.

Virulence factor (gene)	Encoding Phage
Leukocidin (<i>lukS</i> , <i>-F</i> , <i>-M</i>)	φPVL, φPV83
Enterotoxin P (<i>sep</i>)	φN315
Enterotoxin A (<i>entA</i> , <i>sea</i>)	φMRSA252*, φMu50A*
Exfoliative toxin A (<i>eta</i>)	φETA, φSTL
Toxic shock syndrome toxin (<i>tst</i>)	SaPI-1**
Staphylokinase (<i>sak</i>)	φ13*
Chemotaxis inhibitory protein of <i>S. aureus</i> (<i>chips</i>)	φ13*
Staphylococcal complement inhibitor (<i>scin</i>)	φ13*

*φ13 and other *hly*-converting phages can encode *sak*, *sea*, *scin*, or *chips*

**SaPI-1 is a mobile pathogenicity island transduced by helper phage

Adapted from (Boyd and Brüssow, 2002) with permission.

For example, in *S. aureus* isolates from cystic fibrosis and bacteremic patients, genomic alterations driven by *hly*-converting phages were found to occur in the transition from nasal colonization to invasive infection. Specifically, in infection isolates, *hly*-converting phages (Figure 3-1a) were found integrated at atypical chromosomal locations, resulting in Hly⁺/*sak*⁺ phenotypes (cells with an intact *hly*

gene, but also positively converted by prophage encoding *sak*) (Figure 3-1b). Rarely, in some strains, prophage appeared to undergo duplication and dual integration, generating populations with a Hlb⁻/sak² phenotype (cells with one prophage integrated in *hlb* and a duplicated prophage integrated in another chromosomal location, with both phages encoding *sak*) (Figure 3-1c) (Goerke et al., 2006). Such phage mobilization occurred to a significantly lesser degree however in nasal (colonization) isolates from healthy individuals, indicating selective pressure for Hlb-producing strains in the transition to invasive infection, with atypical prophage integration as a mechanism to allow for dual Hlb and SAK production. Previous work in the Fischetti Laboratory uncovered a plasmidial prophage, φBU01, with the phage DNA sequence highly homologous to known *hlb*-converting phages. Importantly, φBU01 did not appear to integrate within the *S. aureus* chromosome (Utter et al., 2014), suggesting that in addition to atypical chromosomal integration, maintenance of prophage in the extra-chromosomal compartment can result in a Hlb⁺/sak⁺ phenotype (Figure 3-1d) (Deutsch et al., 2016).

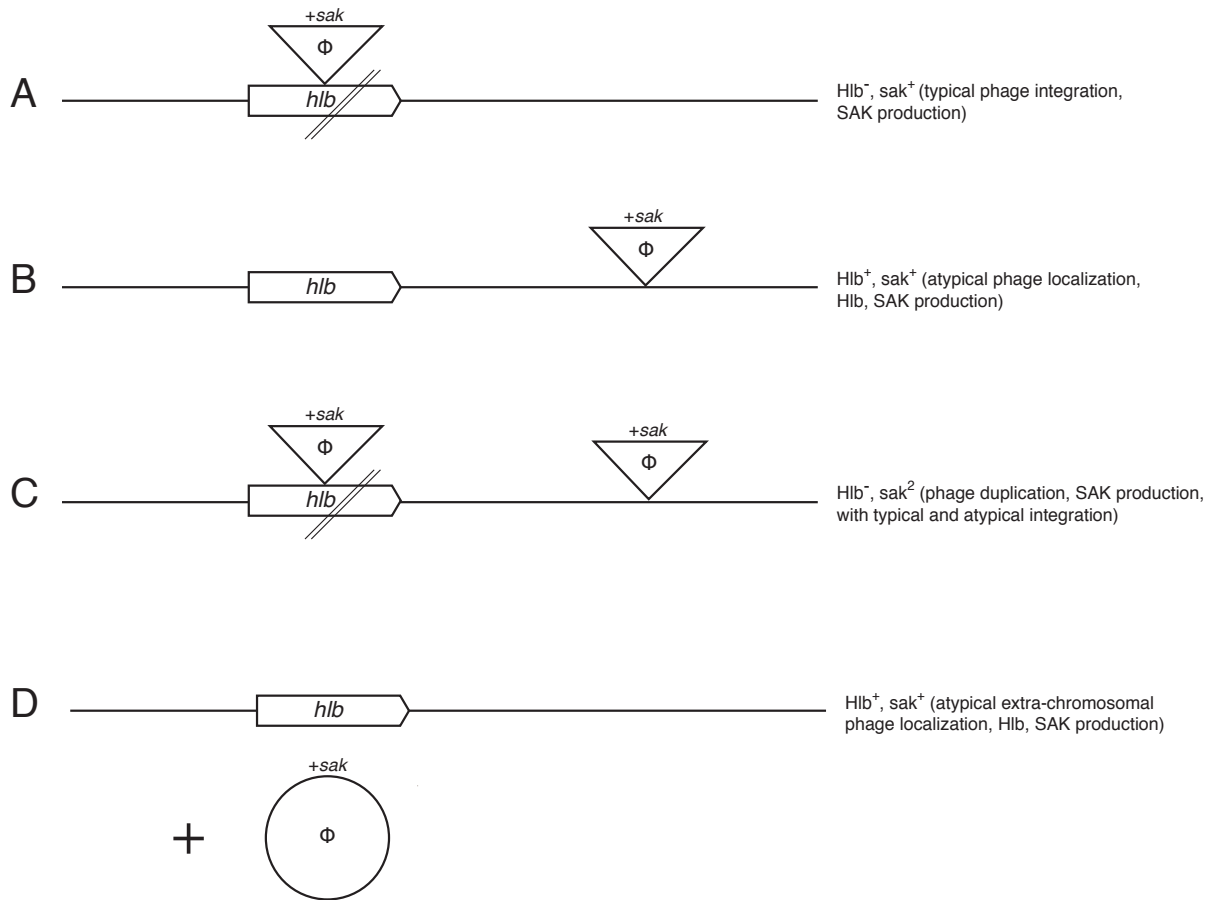


Figure 3-1. Illustration of phage localization in *S. aureus* cystic fibrosis and bacteremic isolates. Atypical *hlb*-converting phage localization is described in (Goerke et al., 2006). A) *hlb*-converting phage typically integrate in the chromosome and disrupt *hlb*, but positively convert cells for *sak*, *sea*, *scin*, and/or *chips*. Cells are Hlb^- , sak^+ . B) Atypical phage localization (off-target chromosomal integration) results in Hlb^+ , sak^+ phenotypes. C) Phage duplication and dual integration results in disrupted *hlb*, and 2 copies of *sak*. D) Alternatively, phage localization in the extra-chromosomal compartment could also result in the Hlb^+ , sak^+ phenotype.

3.2 The importance of phage-mobilization for bacterial pathogens

Excision/integration dynamics of lysogenic prophage also have important roles in other bacterial pathogens. *S. pyogenes* SF370 contains the episomal, phage-like chromosomal island, SpyCIM1, which integrates within the cell's DNA mismatch repair operon, disrupting transcription of the *mutS-mutL* genes and consequently increasing the mutation rate of the cell approximately 200-fold (Hendrickson et al., 2015; Scott et al., 2008). The phage-like element was found to be excised at low cell densities, allowing fidelitous genome replication, but would integrate and increase the cell's mutation rate at higher cell densities (Scott et al., 2008)—conditions where mutation might be beneficial (i.e. low nutrient availability) (Figure 3-2). Here, excision/integration is a dynamic, switch-like process; in *S. aureus* however, phage excision and re-integration (or extra-chromosomal localization) as previously described creates stable isolates with prophage not believed to continuously pop in and out of the chromosome. SpyCIM1's temporal dynamics suggest that *S. pyogenes* is using the phage-like element for its own benefit as a molecular switch at the DNA-level.

Phage acting as such DNA-switches have been found in a number of distantly related bacterial species, suggesting such a phage-role has existed over a long time scale. Feiner et al. review SpyCIM1's behavior and discuss a number of other species (*Listeria monocytogenes*, *Bacillus subtilis*, and *Escherichia coli*) where bacterial hosts have been found to employ similar beneficial strategies with their

lysogenic phages, allowing control of activities such as phagosomal escape (*L. monocytogenes*) (Rabinovich et al., 2012), sporulation (*B. subtilis*) (Kunkel et al., 1990; Takemaru et al., 1995), and biofilm formation (*E. coli*) (Wang et al., 2009). In all three cases, phage excision allows the transcription of key chromosomally-encoded genes, altering bacterial behavior (Feiner et al., 2015).

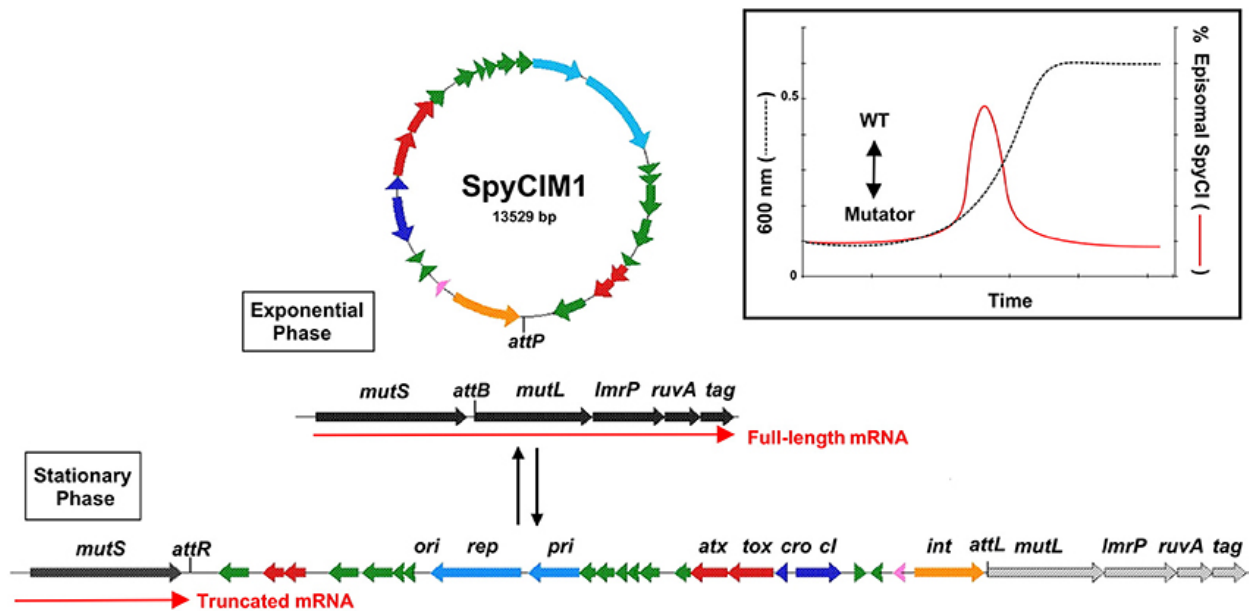


Figure 3-2. Illustration of SpyCIM1 genome and integration dynamics.

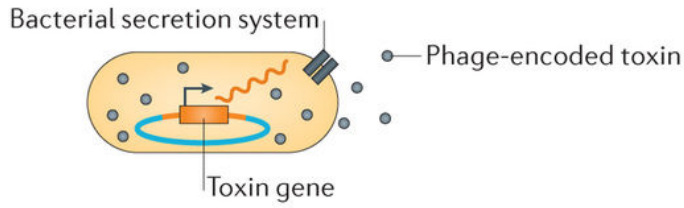
SpyCIM1 is a phage-like chromosomal island of *S. pyogenes*. In the exponential phase, SpyCIM1 excises from the chromosome and the mismatch-repair operon (MMR) is fully transcribed. At higher-cell densities, the episome integrates between *mutS* and *mutL*, disrupting transcription of the operon and increasing the cell's mutation rate. OD₆₀₀ and % episomal SpyCIM1 analysis reveals excision is a temporally controlled process, with the episome acting as a DNA-level switch.

Reprinted with permission from (Nguyen and McShan, 2014).

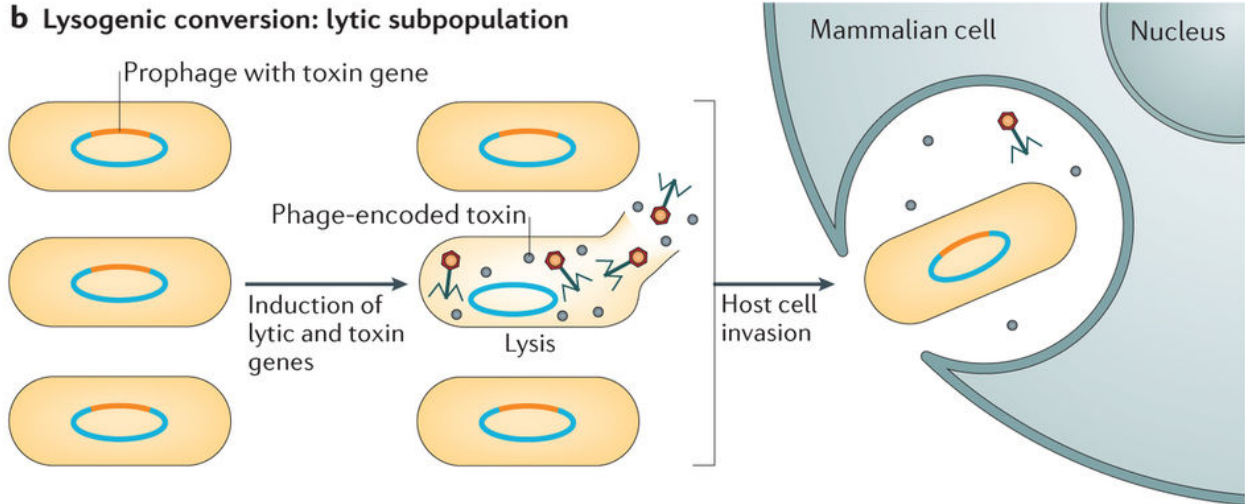
Importantly, for SpyCIM1 and the phages described in (Feiner et al., 2015), excision from the chromosome is not associated with lytic induction; if it were, the impacts of phage excision would be lost as phage induction leads to likely cell death. (Host benefits from phage induction into the lytic cycle are described in Section 1.3.4 (also well-reviewed in (Nanda et al., 2015).) While excision here is associated with a lysogenic state, in some cases it is irreversible, i.e., phages are cured or lost after excision. In *B. subtilis*, for example, excision of the phage-element *skin* allows reconstitution and transcription of a functional σ^k gene (*sigk*), promoting sporulation. In this case, *skin* and the bacterial cell die, however a copy of the phage genome remains in the new spore (Feiner et al., 2015; Kunkel et al., 1990; Takemaru et al., 1995). Regardless of reversible or irreversible excision, Feiner et al. describe phage capable of controlled excision/integration within the lysogenic cycle as “active lysogens” and termed the process “active lysogeny” (Figure 3-3c). Active lysogeny is distinguished from the more traditional effects of the lysogenic cycle, as phage excision allows the expression or regulation of chromosomally-encoded factors, in contrast to positive conversion (Figure 3-3a), or even the induction of a proportion of the population into the lytic cycle (Figure 3-3b).

Figure 3-3. Forms of lysogeny and mechanisms for expression of virulence or fitness factors. A) Lysogenic (positive) conversion involves the expression of phage-encoded factors in the bacterial cell. For *S. aureus*, phages carry an array of virulence factors (Table 3.1) and contribute to the pathogen's virulence potential. B) Induction of a subpopulation of cells into the lytic cycle can allow the increased production of phage-encoded virulence factors. For *S. aureus*, enterotoxin A and staphylokinase expression increases with induction (Sumbly and Waldor, 2003). For other species (e.g. *E. coli*) increased expression of toxins via induction allows for more successful host invasion and infection by the remainder of the population. C) Active lysogeny is a feature of temperate phage capable of controlled excision/integration within the lysogenic cycle. Phage integration can disrupt transcription of virulence or fitness factors, and excision (without lytic induction) allows the reconstitution and expression of genes. Excision can be reversible or non-reversible, leading to prophage reintegration or loss, respectively. Reprinted with permission from (Feiner et al., 2015).

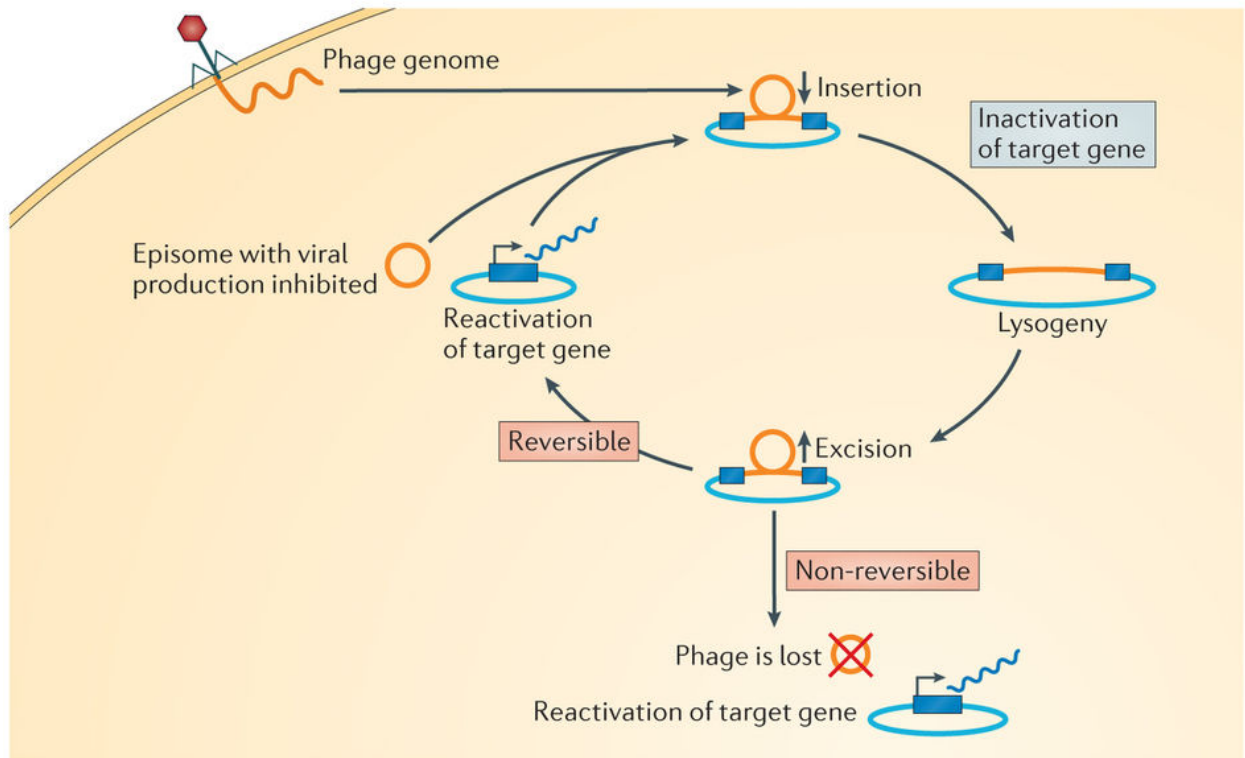
a Lysogenic conversion: expression during lysogeny



b Lysogenic conversion: lytic subpopulation



c Active lysogeny



3.3 Uncovering extra-chromosomally localized prophage in *S. aureus*

Given the importance of prophages in *S. aureus*, and the potential impacts of active lysogenic phage, research specifically targeted at uncovering extra-chromosomally localized phage can lend important insights into the virulence potential of *S. aureus* strains, either through the identification of novel phages, or the discovery of active lysogenic phage. Previous work in the Fischetti Laboratory screened clinical isolates of *S. aureus* for the presence of rare, cytoplasmically-localized prophage using an extra-chromosomal DNA enrichment and next-generation sequencing (NGS) approach. In this report (Utter et al., 2014), the plasmidial (non-integrating) prophage ϕ BU01 was identified and sequenced from the vancomycin-intermediate *S. aureus* (VISA) NRS19, and found to encode multiple virulence determinants including *sea*, *sak*, *scin*, and *chips*. In addition, an episomal prophage (found both chromosomally-integrated and extra-chromosomal in a population) was also uncovered in VISA NRS26 (Utter et al., 2014). Enrichment and screening of the cytoplasmic compartment in this previous report revealed that extra-chromosomally localized prophage were fairly widespread in *S. aureus*, and that such “hidden” elements could alter the virulence potential of a strain.

The following sections of this Chapter describe an expansion of this work, employing NGS to screen-by-sequencing 15 additional clinical isolates of *S. aureus*. Unlike the prior study however, the strains selected for this study had previously sequenced chromosomes, facilitating the classification of any extra-chromosomally

enriched prophage uncovered as either episomes or plasmids, and allowing the identification of potential active lysogenic phage. In this screening, we find extra-chromosomal prophage present in 5 of 15 strains, but surprisingly, these strains contain only episomal and not plasmidial prophage. Experimental work demonstrates that the enriched episomal prophages identified are circular DNA elements, and qPCR experiments reveal that enrichment and detection of such prophages by NGS would not occur if using conventional whole-genome DNA preparations. In addition, we find that in the *S. aureus* strain MSSA476, enrichment of its episomal phage (ϕ Sa4ms) is growth-phase dependent and that ϕ Sa4ms does not appear to replicate after its excision, suggesting its existence as a candidate “active lysogenic phage”. Follow-up experiments find that the excision of ϕ Sa4ms can alter the promoter sequence and transcription of the stress-response serine protease-encoding *htrA₂*, with promoter alterations affecting heat-stress survival in *S. aureus* COL. Here, the expanded and improved extra-chromosomal enrichment and sequencing of *S. aureus* clinical strains is shown to allow the detection of active lysogenic phage, giving greater insights into the genome dynamics and mechanisms by which phage generate diversity and enhance the virulence potential of the pathogen.

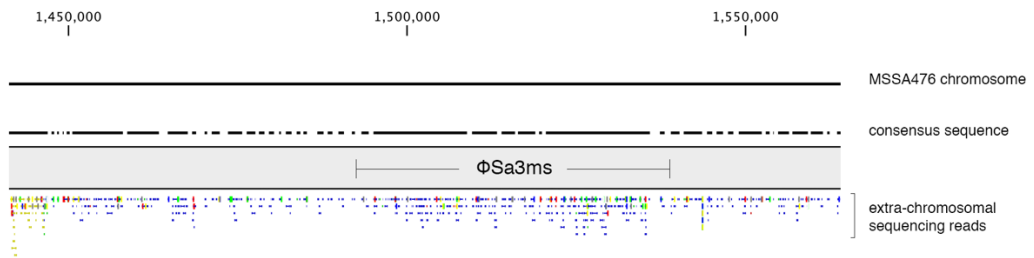
RESULTS

3.4 Extra-chromosomal sequencing reveals the presence of episomal prophage elements within *S. aureus* clinical isolates

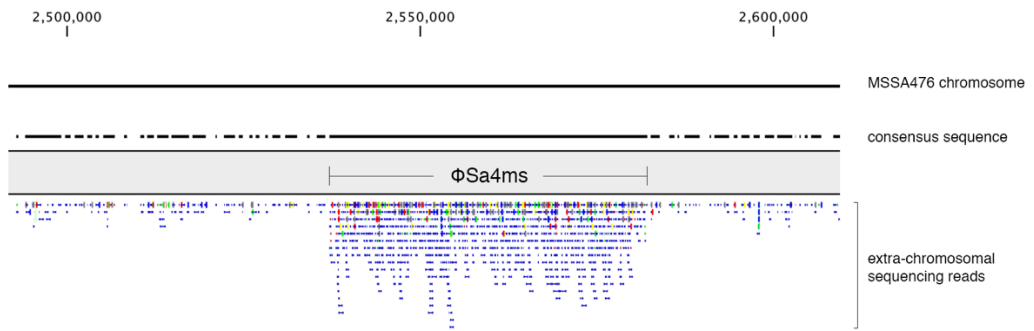
For this study, we expanded our previously developed extra-chromosomal DNA enrichment and sequencing approach to screen *S. aureus* clinical isolates for prophage elements in the extra-chromosomal compartment of the cell (Utter et al., 2014). We selected 15 clinical isolates sourced from different geographic regions, containing a diverse array of antibiotic resistances and virulence factors. In addition, these strains had fully sequenced chromosomes, facilitating the distinction of any detected prophage as integrated, episomal, or plasmidial. We enriched and prepared extra-chromosomal DNA (exDNA) as described in *Materials and Methods*, and sequenced samples with Illumina NGS. Extra-chromosomal DNA samples were analyzed by first mapping sequencing reads to their corresponding chromosomal sequences, followed by *de novo* assembly of unmapped reads. Visual examination of chromosomal read-mappings revealed areas of increased sequencing coverage, especially over prophage regions (Figures 3-4a, 3-4b). Coverage analysis of read-mappings highlighted regions of significantly increased read depth, indicating the presence of episomal elements (and potentially active lysogenic prophage) that were enriched in sequencing due to specifically targeting and isolating DNA elements from the extra-chromosomal compartment of the cell (Figure 3-1c). Read-mappings and coverage analysis are shown for strain MSSA476 as a representative example.

Figure 3-4. Read-mapping and coverage analysis of MSSA476 extra-chromosomal DNA sequencing. A) and B) Read-mappings of sequencing reads from MSSA476 exDNA. MSSA476 contains two integrated prophages: ϕ Sa3ms and ϕ Sa4ms. ϕ Sa4ms (B) has greater read coverage compared to ϕ Sa3ms (A) in exDNA sequencing. Selected portions of the read-mappings surrounding prophage integration regions for ϕ Sa3ms (A) and ϕ Sa4ms (B) are shown. Chromosomal positions are labeled at top, and consensus regions are shown below for MSSA476 chromosome sequence and MSSA476 exDNA reads. Locations of ϕ Sa3ms (A) and ϕ Sa4ms (B) integrated prophage genomes are shown. Extra-chromosomal reads are shown below for each. C) Coverage analysis of MSSA476 extra-chromosomal read-mapping. Portions of coverage analysis surrounding prophage regions shown for clarity. Chromosomal positions labeled at top of image, and approximate positions of ϕ Sa3ms and ϕ Sa4ms integrated genomes shown below. Histogram representation of higher read-coverage regions reveals enrichment of ϕ Sa4ms prophage due to exDNA isolation. Read-mapping across ϕ Sa3ms genome location does not contain any regions of higher coverage, indicating no or very low prophage enrichment by exDNA isolation.

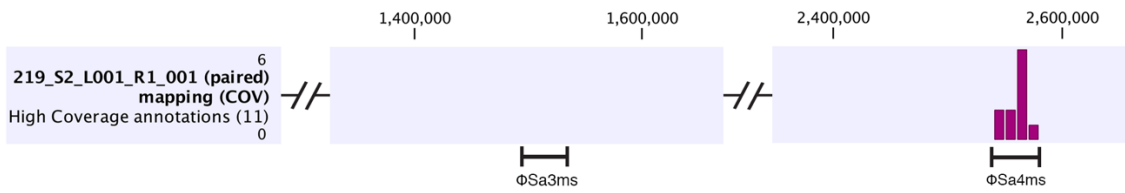
A



B



C



For each of the 15 strains, we documented whether prophage elements were enriched in sequencing due to exDNA isolation and classified strains as: 1) containing enriched prophage, 2) not containing enriched prophage, or 3) containing unclear prophage enrichment, when partial but not complete prophage regions had increased coverage detected (Table 3.2). Surprisingly, *de novo* assembly of unmapped reads did not reveal any prophage elements, suggesting no plasmidial prophage in the sequenced strains, and that all prophage uncovered in the extra-chromosomal compartment by our approach were episomal elements. Importantly, episomal prophage were identified in 1/3 (5 of 15) of the staphylococcal strains analyzed. These included: ϕ Sa4ms in MSSA476 (Sa4-like integrase), a *geh*-converting prophage in NRS143 (Sa6-like integrase), one typically intergenic prophage in BK2529 (Sa7-like integrase), as well as two strains each with three episomal phages. One of these strains, HPV107, contained episomal prophages with Sa2- and Sa3-like integrases, and in addition, one prophage with an unclear integrase type, however its sequence was homologous to the integrase of a prophage from *S. aureus* SA268 (Qu et al., 2014). The other strain, NRS22, contained episomal prophages with Sa2-, Sa5-, and Sa7-like integrase sequences. Interestingly, when integrated into the chromosome, the Sa2-like prophage of HPV107 disrupts a 6-phospho- β -galactosidase encoding gene, which to our knowledge is a novel integration site for a *S. aureus* prophage. The other phages we uncovered as episomes have previously described chromosomal integration sites (Bae et al., 2006; Goerke et al., 2006; 2009). Incidentally, known plasmids, such as

pSAS1 in MSSA476, were fully *de novo* assembled using the unmapped reads, and while they are not the focus of this current study, they do point to the sensitivity of this exDNA isolation and sequencing method.

Table 3-2. Detection of episomal prophage in *S. aureus* strains from extra-chromosomal DNA isolation and sequencing.

Strain	Resistance(s)	# Prophage Regions	Notes
Enriched prophage detected			
MSSA476	MSSA	2	<ul style="list-style-type: none"> • ΦSa4ms enriched, integrates immediately upstream of <i>htrA₂</i> • ΦSa3ms not enriched, <i>hly</i>-converting
NRS22	VISA/MRSA	4	3 enriched prophages: <ul style="list-style-type: none"> • Sa2-like integrase, intragenic in RK87_02365 (hypothetical protein) • Sa5-like integrase, intragenic in RK87_04825 (radical SAM) • Sa7-like integrase, intergenic between <i>rpmF</i> and <i>isdB</i>
NRS143	MSSA	4	<ul style="list-style-type: none"> • One enriched prophage: Sa6-like integrase, <i>geh</i>-converting
HPV107	MRSA	4	3 enriched prophages: <ul style="list-style-type: none"> • Sa2-like integrase, intragenic in RL05_04630 • Sa3-like integrase, <i>hly</i>-converting phage (ϕHPV107.1) • Unclear integrase type, intergenic between RL05_02285 (tRNA-Ser) and RL05_01940 (enterotoxin)

BK2529	MRSA	4	<ul style="list-style-type: none"> One enriched prophage: Sa7-like integrase, intergenic between <i>rpmF</i> and <i>isdB</i>)
Unclear enriched prophage			
NRS153	MSSA	4	<ul style="list-style-type: none"> Unclear enrichment of Sa1-like integrase prophage, intergenic between <i>sufB</i> and transposon-encoded integrase RK79_06750
NRS387	MRSA	1	<ul style="list-style-type: none"> Unclear enrichment of Sa3-like integrase prophage, <i>hly</i>-converting
NRS2	VISA/MRSA	2	<ul style="list-style-type: none"> Unclear enrichment of Sa7-like integrase prophage, intergenic between <i>rpmF</i> and <i>isdB</i>
No enriched prophage detected			
BAA-42	MRSA	4	
NRS156	MSSA	2	
NRS127	MRSA	5	
NRS158	MSSA	3	
NRS271	MRSA	3	<ul style="list-style-type: none"> Enriched ICE within RK77_00405 (membrane protein)
E2125	MRSA	5	
HDE288	MRSA	3	

Relevant resistances (MSSA, MRSA, VISA, VRSA) and total number of chromosomal prophage for each strain are listed.

3.5 QPCR characterization of MSSA476 validates extra-chromosomal sequencing data, but also reveals episomal prophage are detectable only in extra-chromosomal DNA samples

Our screening-by-sequencing approach did not reveal any non-integrating plasmidial prophage, however, a number of the clinical strains did contain episomal prophage elements that were enriched by exDNA isolation. Thus, we were curious what insights prophage enrichment, as uncovered by exDNA isolation and sequencing, revealed about an individual strain. To better understand the nature of enrichment, we chose to focus on the well-characterized *S. aureus* strain MSSA476 (Holden et al., 2004; Sumby and Waldor, 2003) and took a qPCR approach to determine the excision rates and copy numbers of its prophages. MSSA476 contains two prophages, ϕ Sa3ms and ϕ Sa4ms. ϕ Sa3ms is a *hly*-converting prophage, while ϕ Sa4ms integrates 30 bp upstream of the serine protease-encoding *htrA*₂. In our sequencing, ϕ Sa4ms was found enriched by exDNA isolation, while ϕ Sa3ms was not (Figure 3-4). Therefore, MSSA476 is ideal to understand the characteristics of both enriched and non-enriched phage in our screening.

We first wanted to validate our extra-chromosomal sequencing results by qPCR, measuring prophage copy number in exDNA samples by targeting excised prophage attachment sites (*attP*) normalized to DNA gyrase (*gyrA*). Sequencing data should have a direct correlation to prophage copy number, predicting that ϕ Sa4ms copy number would be greater than ϕ Sa3ms in exDNA samples. Indeed, we found the

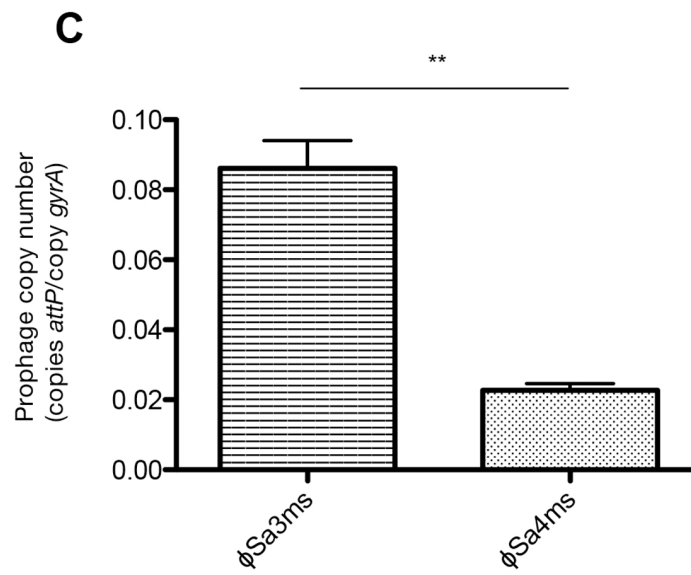
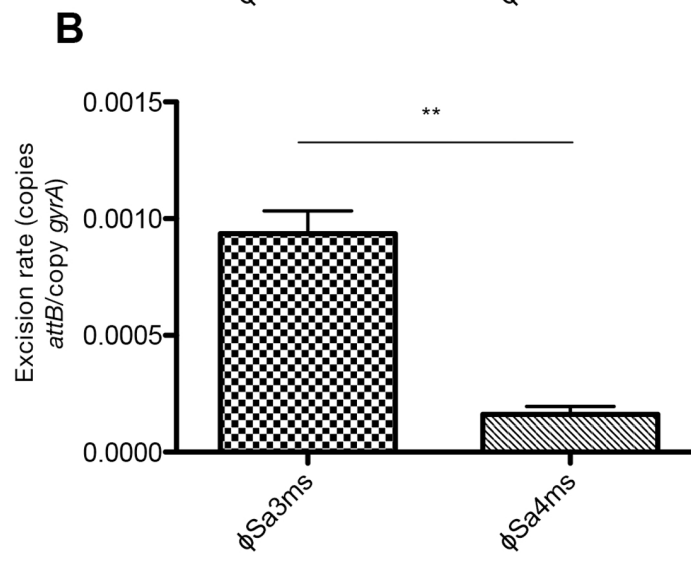
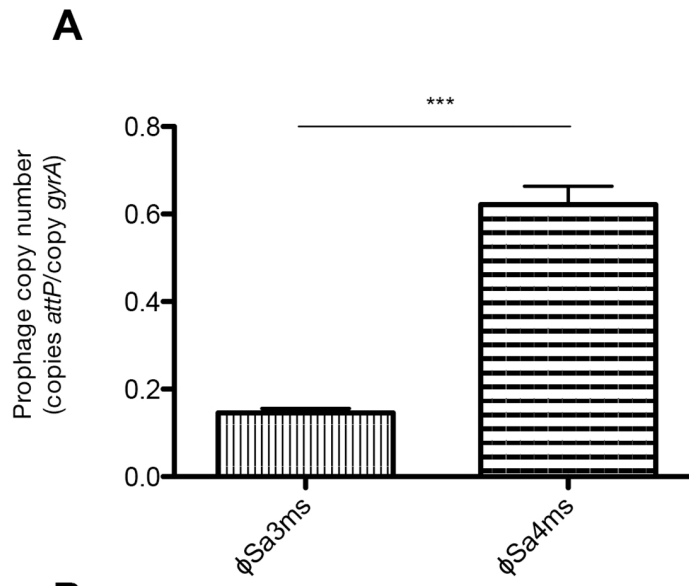
copy number of excised ϕ Sa4ms (copies *attP*/copy *gyrA*) was significantly higher than ϕ Sa3ms ($P = 0.0004$), supporting our exDNA sequencing data (Table 3-3, Figure 3-5a). Following this validation, we next measured the excision rates of ϕ Sa3ms and ϕ Sa4ms, since prophage enrichment in our exDNA samples suggested that the excision rate of ϕ Sa4ms would be higher than ϕ Sa3ms. We calculated the excision rates by targeting phage-less bacterial attachment sites (*attB*) normalized to *gyrA*. As *attB* sites are present on chromosomal DNA, we prepared the genomic DNA (gDNA) of MSSA476 using the same growth conditions as DNA prepared for extra-chromosomal sequencing and performed qPCR on gDNA. Surprisingly, we found the excision rate of ϕ Sa3ms (copies *attB*/copy *gyrA*) to be significantly higher than ϕ Sa4ms ($P = 0.0017$), despite ϕ Sa4ms enrichment in our exDNA sequencing and higher copy number by qPCR (Table 3-3, Figure 3-5b). This result was confounding, but suggested that if we also examined the gDNA preparations for prophage copy number by qPCR, ϕ Sa3ms copy number might be higher than ϕ Sa4ms. Copy number qPCR of MSSA476 gDNA indeed revealed that the excised prophage copy number of ϕ Sa3ms was significantly higher than ϕ Sa4ms ($P = 0.0015$) as suggested by ϕ Sa3ms's higher excision rate, but in contrast to the copy number results from qPCR of exDNA samples (Table 3-3, Figure 3-5c). The qPCR and sequencing data obtained thus far for MSSA476 appeared conflicting; exDNA samples showed enrichment of episomal ϕ Sa4ms compared to ϕ Sa3ms, however ϕ Sa3ms had a higher excision rate and higher copy number than ϕ Sa4ms when

gDNA was examined. We therefore performed additional experiments to uncover the basis of these apparent conflicting results.

Table 3-3. Copy numbers and excision rates of MSSA476 prophages from exDNA sequencing conditions.

Prophage	Prophage copy number (copies <i>attP</i> /copy <i>gyrA</i>)		Excision Rate (copies <i>attB</i> / copy <i>gyrA</i>)
	exDNA	gDNA	
ϕ Sa3ms	0.146 ± 0.010	0.086 ± 0.008	9.35 x 10 ⁻⁴ ± 9.75 x 10 ⁻⁵
ϕ Sa4ms	0.622 ± 0.042	0.023 ± 0.002	1.62 x 10 ⁻⁴ ± 3.37 x 10 ⁻⁵

Figure 3-5. QPCR characterization of MSSA476 excised prophage copy numbers and excision rates. A) Excised prophage copy number (copies *attP*/copy *gyrA*) from MSSA476 extra-chromosomally enriched DNA (exDNA) samples. Excised prophage copy number is significantly higher for ϕ Sa4ms than ϕ Sa3ms, in accordance with sequencing data. B) Excision rates of ϕ Sa3ms and ϕ Sa4ms (copies *attB*/copy *gyrA*). Excision rate of ϕ Sa3ms is significantly higher than ϕ Sa4ms. C) Excised prophage copy number from MSSA476 whole-genome DNA (gDNA) samples. Excised prophage copy number of ϕ Sa3ms is significantly higher than ϕ Sa4ms.



3.6 Extra-chromosomal DNA isolation enriches circular prophage elements

To uncover why ϕ Sa4ms was enriched by exDNA isolation but not in gDNA preparations, we first compared ϕ Sa3ms and ϕ Sa4ms prophage genomes for %GC content, which could alter DNA capture efficiency. However, %GC content does not appear to play a role in enrichment differences as ϕ Sa3ms and ϕ Sa4ms contain almost equivalent %GC content at 33.2% and 33.3%, respectively. Part of the extra-chromosomal enrichment protocol involves alkaline-lysis followed by centrifugation. We hypothesized that this step likely enriches for circular forms of prophage that would remain soluble after alkaline-lysis and not pellet during centrifugation (i.e., would be captured in the exDNA preparation). Linear prophage concatemers (contiguous copies of phage genome arising from prophage induced into the lytic cycle in a subpopulation of cells) would likely pellet with chromosomal DNA and other cellular debris and be removed from exDNA samples. The same linear concatemers however, would not be excluded in whole-genome preparations, potentially explaining the differences seen in qPCRs of gDNA and exDNA samples.

We designed and performed a selective depletion experiment of ϕ Sa4ms prophage in exDNA samples to test this hypothesis. Specifically, we examined if ϕ Sa4ms could be selectively removed from samples only by the combination of ϕ Sa4ms-specific restriction endonucleases (linearizing circular prophage) followed by linear DNA digestion, and not solely by the exonuclease treatment. ϕ Sa4ms depletion only by sequential endo- and exonuclease treatment would indicate the prophage exists as a

closed circular DNA element. A schematic of the digestion procedure is shown in Figure 3-6.

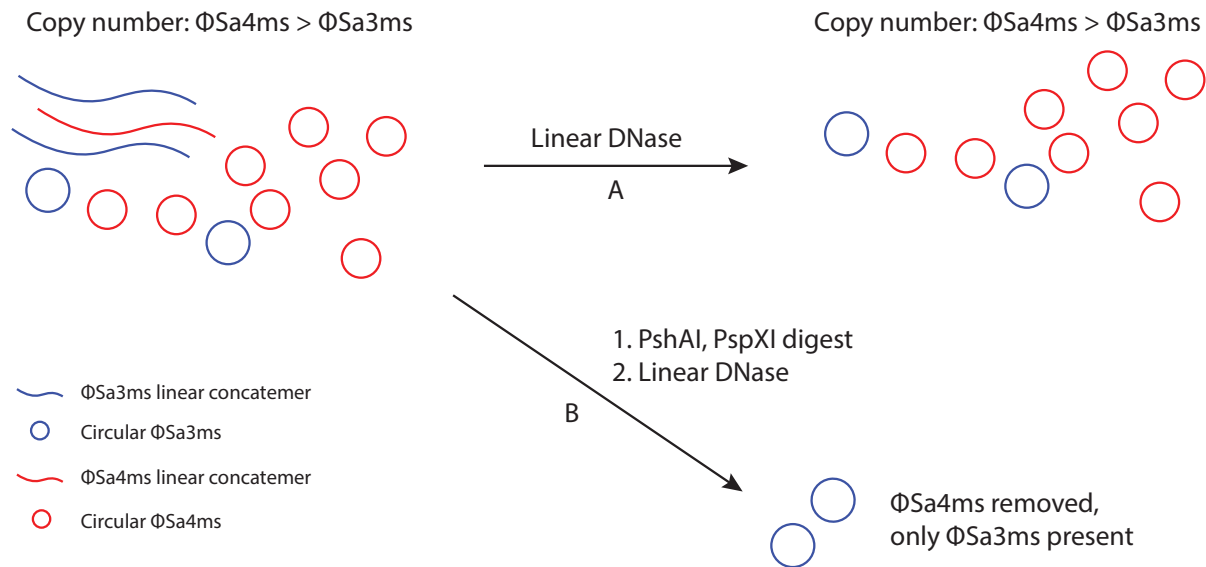
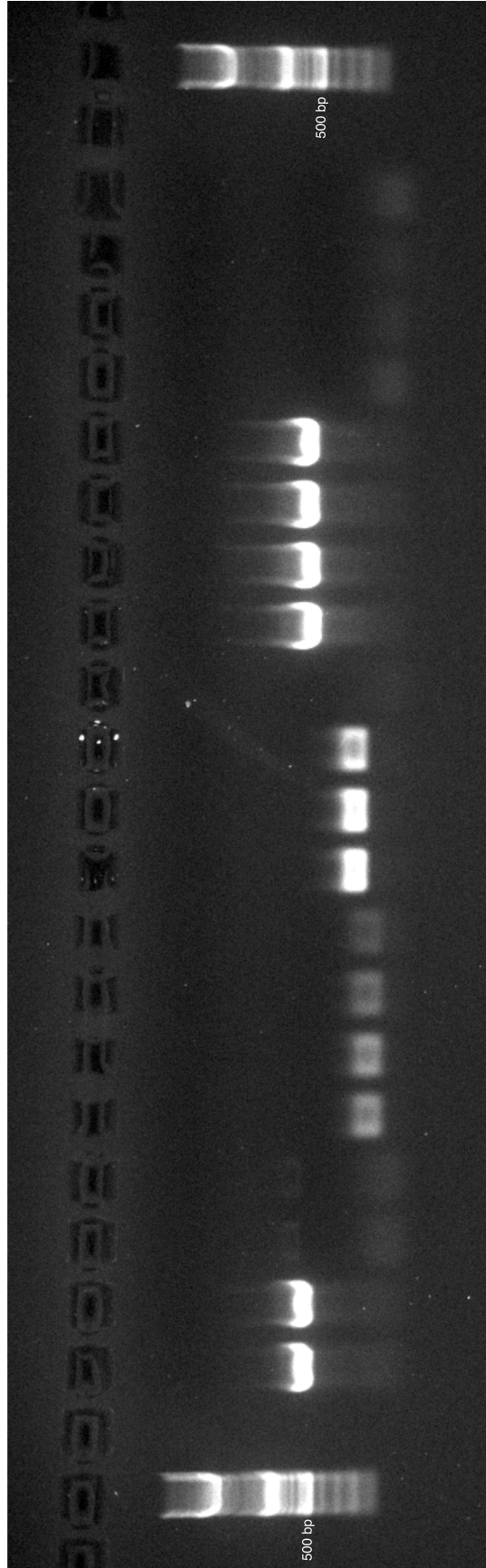


Figure 3-6. Schematic of endonuclease and/or exonuclease treatment of MSSA476 exDNA. ExDNA of MSSA476 (left) consists of both ϕSa3ms and ϕSa4ms genomes, in circular and linear (likely concatemer fragments) forms. Here, copy number of ϕSa4ms is higher than ϕSa3ms . Linear DNase (exonuclease) only treatment (A) removes linear concatemers of prophage DNA, leaving only closed circular prophage genomes (right). With exonuclease treatment, ϕSa4ms copy number should remain greater than ϕSa3ms . Sequential treatment (B) of MSSA476 exDNA with ϕSa4ms -specific endonucleases (PshAI, PspXI) linearizes ϕSa4ms circular genomes (and cuts ϕSa4ms linear concatemers) and treatment with linear DNase completely eliminates ϕSa4ms DNA. Following this treatment, only ϕSa3ms DNA should remain.

Thus, extra-chromosomal samples were treated as described in *Materials and Methods* and end-point PCR measurement was performed targeting *gapdh*, the *attP* sites of ϕ Sa3ms and ϕ Sa4ms, and the naturally occurring MSSA476 plasmid pSAS1. An agarose gel containing all PCR reactions is shown in Figure 3-7. *Gapdh* (a marker for linear DNA digestion) was depleted after linear DNase treatment but remained in high abundance after treatment with the ϕ Sa4ms-specific restriction endonucleases PspAH and PspXI. ϕ Sa3ms *attP* target was present in each condition tested, indicating that it does exist in the circular form in extra-chromosomally enriched DNA samples, however in low abundance. ϕ Sa4ms *attP* target is present and in greater abundance than ϕ Sa3ms in untreated, restriction endonuclease-only and linear DNase-only treated samples. Treatment with ϕ Sa4ms-specific endonucleases followed by linear DNase treatment results in the complete loss of ϕ Sa4ms target, verifying that ϕ Sa4ms is indeed abundant relative to ϕ Sa3ms in extra-chromosomally enriched DNA samples, and that this enrichment is due to circular forms of the prophage element. pSAS1, a circular plasmid in MSSA476, is not affected by any sample treatment (Figure 3-7).

Figure 3-7. Agarose gel of PCR reactions from ϕ Sa4ms selective-depletion experiment. 1% agarose gel stained with SYBR Safe DNA Gel Stain containing end-point PCR reactions from MSSA476 samples. MSSA476 exDNA was digested with Plasmid-safe exonuclease, PspAH/PspXI restriction endonucleases, both Plasmid-safe and restriction endonucleases, or left untreated with treatment indicated by (+) and (-). *Gapdh*, ϕ Sa3ms *attP*, ϕ Sa4ms *attP*, and pSAS1 target were amplified from treated and untreated samples. ϕ Sa4ms *attP* target is selectively-depleted from combination exonuclease and endonuclease treatment but not from solely exonuclease treatment, indicating its existence as a circular element in exDNA samples. Higher levels of ϕ Sa4ms target compared to ϕ Sa3ms target correlate with the phage enrichment detected by DNA sequencing. Negative controls for each primer set are shown. 500 bp ladder band is indicated.

	gapdh		ΦSa3ms		ΦSa4ms		pSAS1		(-) controls				
	-	+	-	+	-	+	-	+	gapdh	ΦSa3ms	ΦSa4ms	pSAS1	
Plasmid-Safe	-	+	-	+	-	+	-	+	+				
PspAH, PspXI	-	+	-	+	-	+	-	+	+				



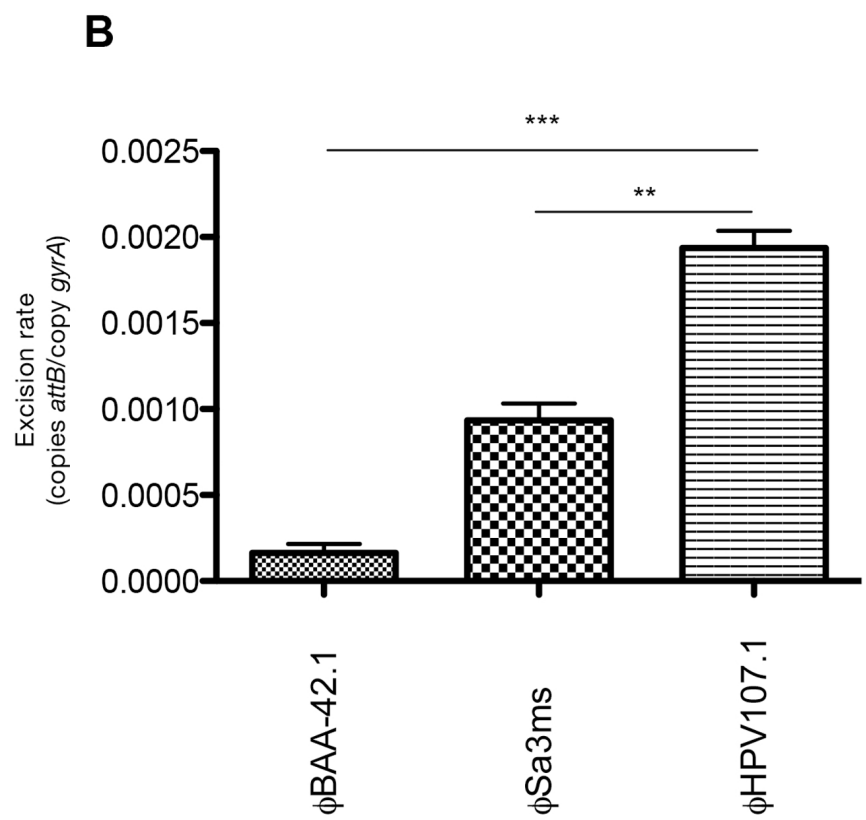
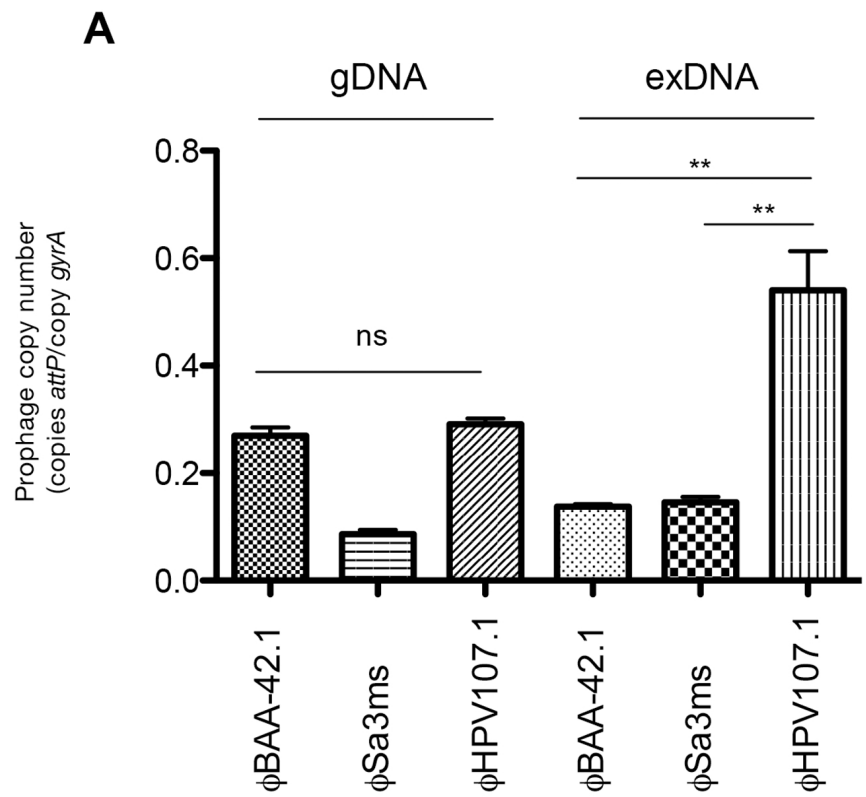
We were now curious if a similar pattern was present in other strains, which also contained episomal prophage enriched by exDNA isolation. To test this, we performed an inter-strain comparison, examining by qPCR the excision rates and excised prophage copy numbers of *hly*-converting phages in three strains: BAA-42 (containing ϕ BAA-42.1), MSSA476 (ϕ Sa3ms), and HPV107 (containing ϕ HPV107.1). Sequencing data revealed that only ϕ HPV107.1 was significantly enriched by exDNA isolation, and qPCR copy number examination of exDNA samples confirmed this result. ϕ HPV107.1 had higher copy number as compared to ϕ BAA-42.1 ($P = 0.0052$) and ϕ Sa3ms ($P = 0.0057$) in exDNA samples (Table 3-4, Figure 3-8a (right)). When we examined excision rates of the three phages, we found that in this comparison, ϕ HPV107.1 did indeed have the highest excision rate. The excision rate of ϕ HPV107.1 was significantly higher than ϕ BAA-42.1 ($P = 0.0009$) and ϕ Sa3ms ($P = 0.002$) (Table 3-4, Figure 3-8b). However as observed previously with MSSA476, prophage copy number data from gDNA samples did not correlate with exDNA data, verifying that the episomal prophage enrichment we uncover is only apparent in exDNA samples. Significant copy number differences in gDNA samples were not seen between ϕ HPV107.1 and ϕ BAA-42.1 ($P = 0.3205$), while ϕ Sa3ms had a lower copy number than either ϕ HPV107.1 or ϕ BAA-42.1 (Table 3-4, Figure 3-8a (left)). Similar to results for ϕ Sa4ms, qPCR of exDNA suggests that in a HPV107 population, ϕ HPV107.1 exists as a circular, episomal DNA element likely in a higher proportion of cells than that of ϕ BAA-42.1 or ϕ Sa3ms in their respective

populations. Induction of phage however, likely masks uncovering these events in qPCRs of gDNA samples.

Table 3-4. Copy numbers and excision rates of selected *hIb*-converting prophages.

Prophage	Prophage copy number (copies <i>attP</i> /copy <i>gyrA</i>)		Excision rate (copies <i>attB</i> /copy <i>gyrA</i>)
	exDNA	gDNA	
ϕ BAA-42.1	0.138 \pm 0.005	0.270 \pm 0.016	1.65 x 10 ⁻⁴ \pm 5.15 x 10 ⁻⁵
ϕ Sa3ms	0.146 \pm 0.010	0.086 \pm 0.008	9.35 x 10 ⁻⁴ \pm 9.75 x 10 ⁻⁵
ϕ HPV107.1	0.540 \pm 0.073	0.291 \pm 0.015	1.94 x 10 ⁻³ \pm 9.94 x 10 ⁻⁵

Figure 3-8. QPCR characterization of *hly*-converting prophages. A) Excised copy numbers of *hly*-converting prophages ϕ BAA-42.1, ϕ Sa3ms, and ϕ HPV107.1. Excised copy number experiments of prophage from gDNA (left) reveal no significant difference between ϕ BAA-42.1 and ϕ HPV107.1, however ϕ HPV107.1 has significantly higher excised copy number than ϕ BAA-42.1 or ϕ Sa3ms in exDNA samples (right). B) Excision rates of *hly*-converting prophages ϕ BAA-42.1, ϕ Sa3ms and ϕ HPV107.1. ϕ HPV107.1 has a significantly higher excision rate than ϕ BAA-42.1 and ϕ Sa3ms.



3.7 Extra-chromosomal localization of ϕ Sa4ms circular prophage is a temporal and rare event

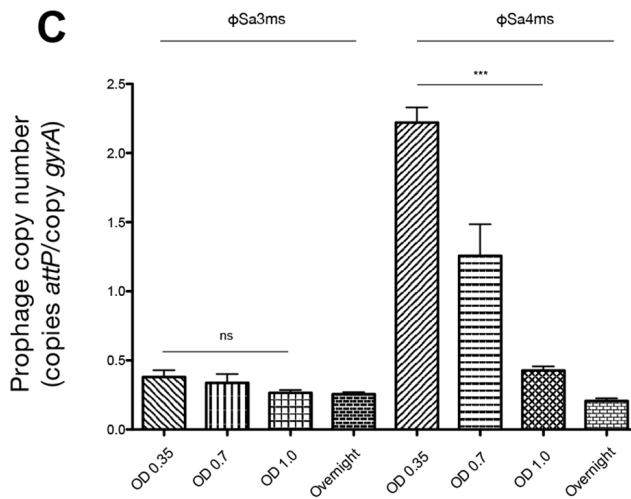
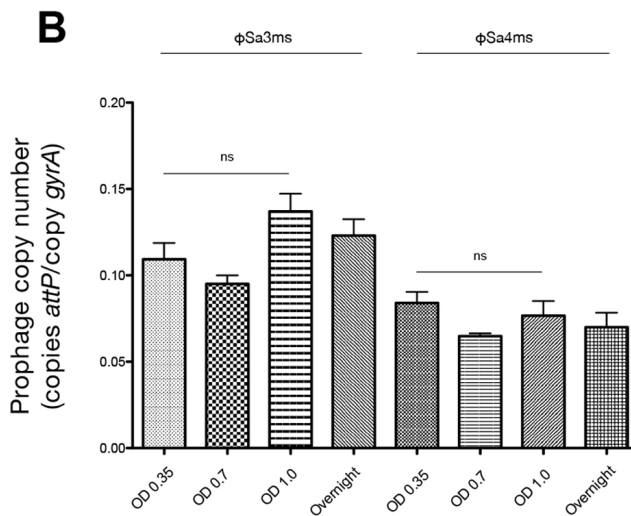
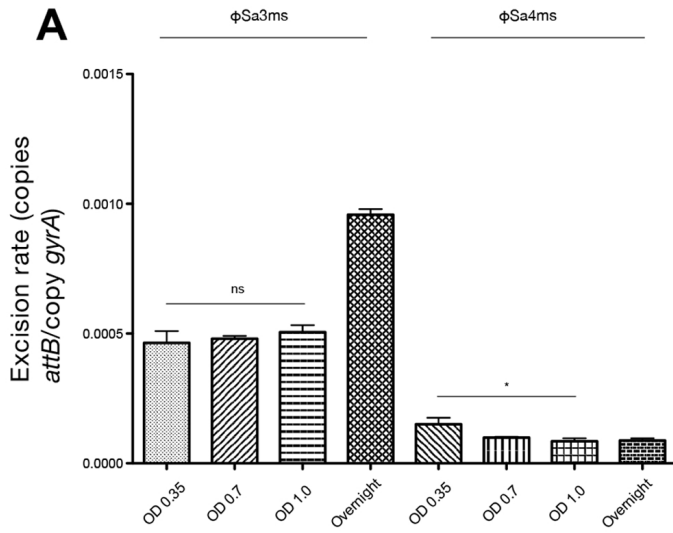
Since ϕ Sa4ms enrichment was due to episomal, circular copies of the prophage in the MSSA476 population, we were curious if such an event was merely a precursor to phage replication and the generation of linear concatemers or occurred without subsequent replication, suggesting that ϕ Sa4ms might exist in an “active lysogenic” cycle. To investigate this question, we repeated our qPCR approach, examining the excision rates and excised phage copy numbers of ϕ Sa3ms and ϕ Sa4ms at different time points of the growth cycle, to see if their values changed with different culture densities. We sampled cultures at $OD_{600} = 0.35, 0.7, 1.0$ and overnight, and prepared exDNA (to measure circular prophage copies) and gDNA (to examine excision rates and potential increases in overall excised prophage copy number). The excision rate of ϕ Sa3ms did not significantly change from $OD_{600} = 0.35$ to 1.0 ($P = 0.2403$) while that of ϕ Sa4ms did significantly decrease during this time ($P = 0.036$) (Table 3-5, Figure 3-9a). The ϕ Sa3ms excision rate does however, increase approximately two-fold from $OD_{600} = 0.35$ to overnight. Excised prophage copy number, as measured by *attP* target for whole-genome preparations did not change from $OD_{600} = 0.35$ to 1.0 for ϕ Sa3ms ($P = 0.118$) nor ϕ Sa4ms ($P = 0.527$) (Table 3-5, Figure 3-9b). Levels of excised prophage copy number over the same range for exDNA also did not change for ϕ Sa3ms ($P = 0.0982$) but did however significantly decrease for ϕ Sa4ms ($P < 0.0001$) (Table 3-5, Figure 3-9c).

Table 3-5. Copy numbers and excision rates of MSSA476 prophages at selected optical densities.

Prophage	OD ₆₀₀	Prophage copy number (copies <i>attP</i> /copy <i>gyrA</i>)		Excision rate (copies <i>attB</i> /copy <i>gyrA</i>)
		exDNA	gDNA	
φSa3ms	0.35	0.380 ± 0.049	0.109 ± 0.010	4.64 x 10 ⁻⁴ ± 4.52 x 10 ⁻⁵
	0.7	0.338 ± 0.064	0.095 ± 0.005	4.80 x 10 ⁻⁴ ± 1.10 x 10 ⁻⁵
	1	0.265 ± 0.021	0.137 ± 0.013	5.05 x 10 ⁻⁴ ± 2.73 x 10 ⁻⁵
	O/N	0.256 ± 0.014	0.123 ± 0.010	9.58 x 10 ⁻⁴ ± 2.14 x 10 ⁻⁵
φSa4ms	0.35	2.220 ± 0.110	0.084 ± 0.006	1.51 x 10 ⁻⁴ ± 2.47 x 10 ⁻⁵
	0.7	1.257 ± 0.229	0.065 ± 0.002	9.91 x 10 ⁻⁵ ± 3.13 x 10 ⁻⁶
	1	0.427 ± 0.030	0.077 ± 0.008	8.44 x 10 ⁻⁵ ± 1.14 x 10 ⁻⁵
	O/N	0.207 ± 0.019	0.070 ± 0.008	8.75 x 10 ⁻⁵ ± 8.15 x 10 ⁻⁶

O/N = overnight culture

Figure 3-9. QPCR characterization of MSSA476 prophage excision rates and copy numbers from logarithmic and overnight cultures. A) Excision rates of ϕ Sa3ms and ϕ Sa4ms samples at indicated optical densities. ϕ Sa3ms does not show a significant difference in excision rates comparing $OD_{600} = 0.35$ and 1.0 samples, whereas a significant decrease is found for ϕ Sa4ms. B) Excised prophage copy number from MSSA476 whole-genome DNA (gDNA) samples at indicated optical densities. Neither ϕ Sa3ms nor ϕ Sa4ms have significantly different excised prophage copy numbers comparing $OD_{600} = 0.35$ and 1.0 samples. C) Excised prophage copy numbers from MSSA476 extra-chromosomally enriched DNA (exDNA) samples at indicated optical densities. ϕ Sa3ms does not show a significant difference in phage copy number from $OD_{600} = 0.35$ to 1.0, whereas ϕ Sa4ms copy number significantly decreases in this interval.



The data above indicated ϕ Sa4ms was likely an active lysogenic phage, with the abundance of circular phage genomes not appearing to be a precursor to lytic cycle replication. The prevalence of ϕ Sa4ms's stable excision however was unclear (i.e., the percentage of cells with excised "active lysogenic" ϕ Sa4ms). We employed qPCR using the naturally occurring circular plasmid pSAS1 to understand the level of enrichment imparted by our exDNA preparation protocol. We found that pSAS1 existed on average at 1-2 copies per cell (copies pSAS1 target/copy *gyrA*) in gDNA preparations of MSSA476 at OD₆₀₀ = 0.35 and 0.7, but that the plasmid was enriched 1500-fold to an average of 2322 copies pSAS1/copy *gyrA* in exDNA. That ϕ Sa4ms copy number in our qPCR assay reaches, at a maximum, 2.22 copies *attP*/copy *gyrA* (Table 3-5), suggests that the ϕ Sa4ms excision we uncover is a rare event. The percentage of cells with stably excised ϕ Sa4ms, as well as its copy number per cell, is presently unclear.

3.8 Promoter alteration by ϕ Sa4ms excision/integration affects *htrA₂* transcription and heat-stress survival in *S. aureus*

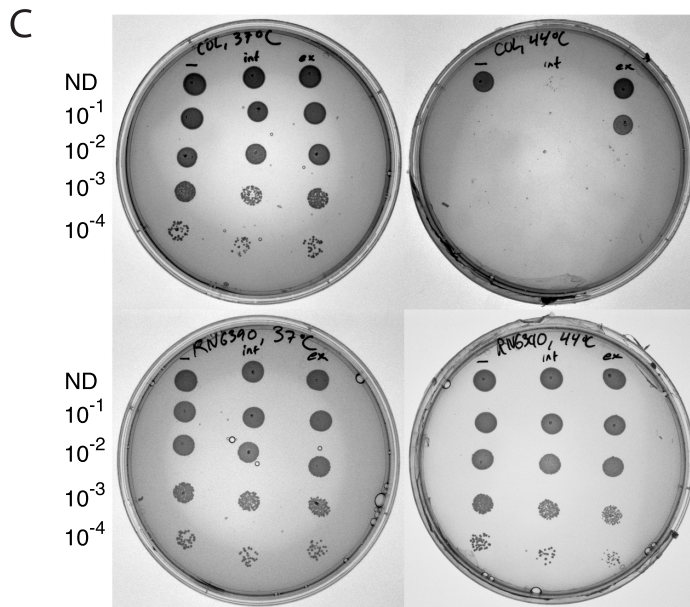
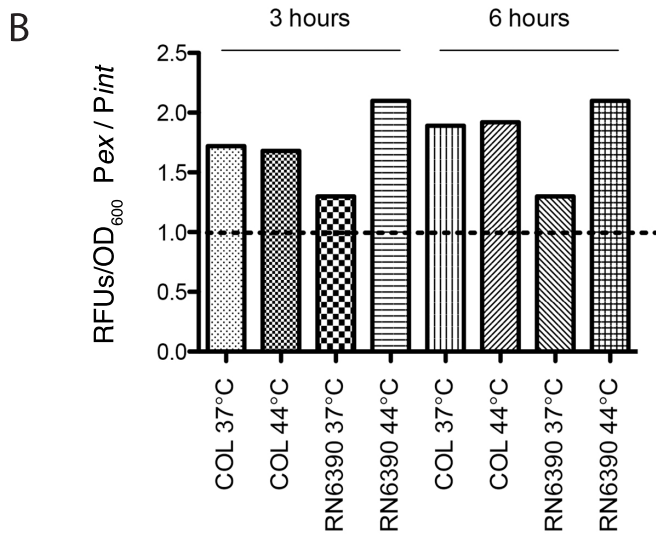
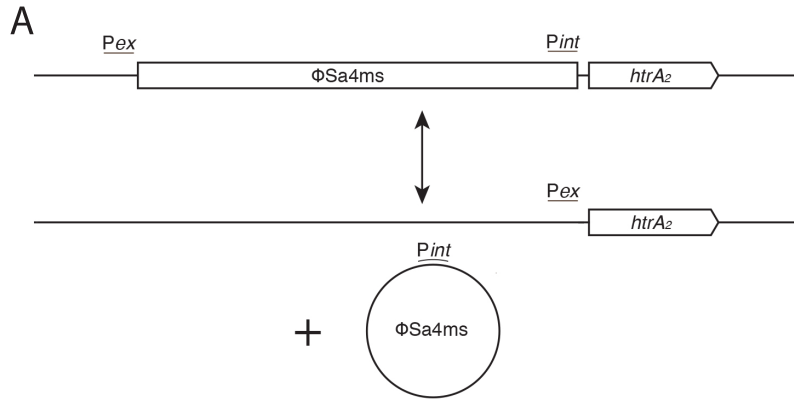
Since ϕ Sa4ms could act as an active lysogenic phage, a stable subpopulation of MSSA476 cells may exist with an altered important chromosomal sequence, since ϕ Sa4ms integrates 30 bp upstream of the stress response serine protease-encoding gene *htrA₂*. Sumbly and Waldor previously noted the possibility of altered *htrA₂* transcription by ϕ Sa4ms excision/integration (Sumbly and Waldor, 2003), and our data suggested that indeed a subpopulation of MSSA476 cells would harbor *htrA₂*

under an altered promoter (Figure 3-10a). We developed a *PhtrA₂-gfp* reporter system to examine whether GFP fluorescence would be altered when the GFP-encoding gene *gfpmut2* was under the control of the ϕ Sa4ms-integrated (*Pint*) or ϕ Sa4ms-excised (*Pex*) promoters. Experiments were performed in *S. aureus* RN6390 and COL *htrA₂* deletion knockouts, two well-characterized strains where *htrA₂* was shown to impact COL but not RN6390 survival in heat-stress (Rigoulay et al., 2005). Comparisons of GFP fluorescence at 37°C and 44°C showed that in both strains, fluorescence was greater when *gfpmut2* was promoted by *Pex* than by *Pint*, indicating that *Pex* is a stronger promoter of *htrA₂* than *Pint*. GFP fluorescence was greater in *Pex* constructs at both 37°C and 44°C at 3 and 6-hour time points (Figure 3-10b).

Due to its reported role in promoting heat-tolerance in COL, we examined if promoter alteration could affect survival of *htrA₂*-complemented *S. aureus* RN6390 and COL *htrA₂* knockouts. Complemented strains contained the full-length *htrA₂* gene under the control of the *Pint* or *Pex* promoter on the pCN35 plasmid or were left uncomplemented with empty pCN35 and grown in a dilution series at 37°C or 44°C on agar plates. COL constructs at 37°C did not display any survival differences among the three strains, however at 44°C, COL *Pex* displayed approximately 2-log increased survival over COL *Pint* (Figure 3-10c, top). Surprisingly, COL *Pint* survived 1-log worse than uncomplemented COL *htrA₂*, indicating that *htrA₂*-mediated heat-stress survival may depend upon specific

promoter sequences and not solely levels of transcription or promoter strength. RN6390 constructs showed no survival differences at 37°C or 44°C, in accordance with previous reports of HtrA₂ activity in the strain (Rigoulay et al., 2005) (Figure 3-10c, bottom). Environmental conditions may select for cells with one promoter versus another, and ϕ Sa4ms's excision/integration dynamics and active lysogeny could provide MSSA476 with a potential switching mechanism to create these advantageous subpopulations.

Figure 3-10. ϕ Sa4ms excision/integration alters the promoter and transcription of *htrA₂*. A) Diagram illustrating ϕ Sa4ms integrated and excised states in MSSA476 and the unique DNA regions of the *Pint* and *Pex* promoters. (Top) When ϕ Sa4ms is integrated in the chromosome, *htrA₂* is promoted by *Pint*. (Bottom) ϕ Sa4ms excision joins the *Pex* region immediately upstream to *htrA₂*, and the gene is promoted by *Pex*. *Pint* unique DNA sequence is carried on circular ϕ Sa4ms when the phage is excised. B) Ratio of GFP fluorescence from *Pex*- versus *Pint*-promoted *gfpmut2* constructs in COL and RN6390 *htrA₂* strains. Bars above the dashed line indicate samples where GFP fluorescence is greater with *Pex*-promoted *gfpmut2* than with *Pint*-promoted *gfpmut2*. C) Dilution series of COL and RN6390 *htrA₂* knockout strains complemented with *htrA₂* promoted by *Pint* (int) or *Pex* (ex). (-) indicates COL or RN6390 *htrA₂* knockout strains containing empty pCN35 plasmid. COL (top) or RN6390 (bottom) constructs are spotted in a log-dilution series and grown at 37°C or 44°C for 24 hrs. Dilution factor indicated on left of plates; (ND) = not diluted. COL constructs display equal survival at 37°C, but COL *Pex* displays 2-log survival above COL *Pint*. Unexpectedly, uncomplemented COL *htrA₂* shows 1-log survival above COL *Pint*. COL *Pint* shows few colonies at 44°C in the undiluted culture spot. RN6390 displays no survival difference among constructs at 37°C or 44°C.



DISCUSSION

This study described in this Chapter explores the prevalence of extra-chromosomal prophages in *S. aureus* as an extension of previous work uncovering the plasmidial phage ϕ BU01 in *S. aureus* NRS19 (Utter et al., 2014). We isolated and sequenced the exDNA of 15 clinically-relevant *S. aureus* strains with known chromosomal sequences, but unlike our previous study, we did not find any prophages existing as solely plasmidial elements. We did uncover however, several episomal prophages appearing to exist as active lysogenic phages. It therefore seems that the existence of plasmidial prophage in *S. aureus* is uncommon and ϕ BU01 may represent one of these rare prophages. Episomal prophages, on the other hand, appear to be fairly widespread and were identified in 33% of *S. aureus* strains (5 of 15) examined in this study.

3.9 Strains and phages possess different mobilization capacities

We distinguished strains that carried episomal prophage from those with no prophage detected in the extra-chromosomal compartment, but our study did not reveal why some strains have such a phage-mobilization capacity while others do not. Goerke et al. demonstrated a similar observation, finding that phages ϕ s80b and ϕ s84b (*hly*-converting phages) were integrated within the *hly* gene in *S. aureus* s64c, but were found to alternate between integrated and extra-chromosomal carriage in strain 8325-4 (Goerke et al., 2006). Both s64c and 8325-4 are phage-

cured strains, suggesting that a host-factor (or factors) is likely determining phage localization and mobilization capacity within the cell. In a separate manner, phage induction capacity into the lytic cycle has also been observed to depend upon host background, with ϕ Sa2mw induced by mitomycin C in strains MW2 and Newman, but not 8325-4, RN6390 or ISP479c (Wirtz et al., 2009). We believe that the phages we describe here are localized and harbored within the extra-chromosomal compartment in a manner distinct from lytic excision and replication (Deutsch et al., 2016; Utter et al., 2014), however it is possible similar host factors may govern both events. The *hIb*-converting phages we characterized from strains BAA-42, MSSA476 and HPV107 contained high sequence homology over their integration/excision modules, however they displayed different levels of enrichment in extra-chromosomal sequencing and qPCR characterization, with HPV107 carrying its *hIb*-converting phage extra-chromosomally in a greater proportion of the population. Host differences similar to those affecting ϕ s80b and ϕ s84b localization may account for the differences in *hIb*-converting phage localization among our three strains, however such factors have yet to be uncovered.

Within individual strains, we also noted differences in phage localization. In MSSA476, ϕ Sa4ms—but not ϕ Sa3ms—was enriched in sequencing, with the localization of circular prophage confirmed by qPCR and selective-depletion experiments. ϕ Sa3ms and ϕ Sa4ms share the same host background, indicating that a phage factor is responsible for localization differences, but it is currently unclear

which factor(s) may be responsible. Prophage excision requires recombination mediated by integrase; stochastic higher expression of a phage's integrase or excision-related genes may be one mechanism by which phage localize into the extra-chromosomal compartment. The process may also be controlled by as of yet uncharacterized factors in a more regulated process. If excision occurs without inducing conditions, then phages could be localized into the cytoplasm in a manner consistent with the lysogenic cycle. Feiner et al. reviewed such phage activity in a range of bacterial species, particularly those whose excision/integration dynamics can act as a molecular switch for the cell, terming the process "active lysogeny" (Feiner et al., 2015).

The mechanisms behind differences in mobilization capacity among strains and the phages themselves are presently unclear, however an approach using a transposon or gene-knockout screening, coupled with a reporter system, may be able to elucidate such factors. Screening candidates for increased phage mobilization by PCR is too exhaustive a task, but a reporter system in which a visual phenotype is apparent with phage excision could facilitate such a screening. For example, a reporter gene (*gfpmut2*, *xylE*) could be fused to *hly*, *geh* or another relevant phage integration site such that a phenotype is apparent when phages are excised, but absent with phage integration. Increases in fluorescence or pigmentation of colonies could indicate candidate genes that contribute to phage stabilization in the chromosome. In parallel, a screening in which potential factors are overexpressed

on a plasmid in the same reporter system could identify gene activity necessary for the phage excision detected. Outside of screening, candidate genes could also be identified between strains in which the same phage shows differential mobilization, e.g. *S. aureus* s64c and 8325-4. Such differences between the strains may be attributed to changes in gene expression rather than sequence however, and could complicate such an approach. Regardless, research focused on uncovering such factors will be important in understanding the behavior of various strains versus others and contribute to our understanding of the interplay between bacteria and phage. Their presence would suggest a mechanism by which bacteria use phage to increase their diversity and create new subpopulations, capable of altered gene expression, virulence, and/or fitness.

3.10 Episomal prophage are detected only in extra-chromosomally enriched DNA samples, and are circular DNA elements that appear to be active lysogenic prophages

qPCR characterization of prophage excision rates and copy numbers revealed, surprisingly, that episomal prophages are detected only in exDNA samples and that their presence is masked in gDNA preparations. In MSSA476 for example, overall excised prophage copy numbers as measured from qPCRs of gDNA is relatively low, with ϕ Sa3ms and ϕ Sa4ms at 0.086 and 0.023 copies *attP*/copy *gyrA*, respectively. This would correspond to very low increases in read-depth over the ϕ Sa3ms and ϕ Sa4ms prophage chromosomal locations if MSSA476 gDNA was sequenced and

read-mapped to a MSSA476 reference chromosome (likely 8.6 and 2.3% maximum increases, respectively). Using gDNA, coverage analysis tools would likely not find regions of significantly higher coverage spanning either prophage genome, so while ϕ Sa3ms copy number was greater than ϕ Sa4ms in gDNA samples, neither prophage would be found as enriched by this approach, and the episomal nature of ϕ Sa4ms would be overlooked. ϕ Sa4ms excised prophage copy number in exDNA samples however is much greater (0.622 copies *attP*/copy *gyrA*), and is sufficient for significantly high read-depth across the prophage location in the chromosome. The excised copy number of ϕ Sa3ms in exDNA samples, while elevated from that seen in gDNA samples (0.146 versus 0.086 copies *attP*/copy *gyrA*, respectively), was not high enough to have significantly higher read-depth or coverage over the ϕ Sa3ms genome in read-mappings. Thus, our exDNA isolation and sequencing approach allows the distinction of episomal elements, even when such elements would be masked in qPCR and sequencing of DNA prepared by other methods.

We showed that our extra-chromosomal DNA isolation procedure enriches circular DNA elements, allowing the identification of episomes and plasmids, and that whole-genome approaches do not impart such selectivity in sample preparations. Why ϕ Sa4ms copy number was lower than that of ϕ Sa3ms in gDNA despite the presence of ϕ Sa4ms episomes, we believe, is likely due to the presence of linear, lytic cycle prophage genome concatemers in the MSSA476 population. pSAS1 plasmid enrichment by our protocol was approximately 1500-fold, suggesting that in qPCRs

of gDNA, the percentage of total *attP* targets encoded by circular prophage is very low. The copy number of linear prophage concatemers in gDNA samples therefore likely masks the presence of circular phage elements, making it doubtful that the DNA elements we uncover would be detected by sequencing or qPCR in the absence of extra-chromosomal DNA enrichment. That the excised prophage copy number of ϕ Sa3ms and ϕ Sa4ms is so low in exDNA samples despite ~1500-fold enrichment for pSAS1 suggests that for MSSA476, both ϕ Sa3ms and ϕ Sa4ms excised prophage copy number is primarily composed of linear elements, likely from a small subset of cells whose phages are undergoing spontaneous lytic cycle replication. While both phages in MSSA476 are capable of such lytic events, only ϕ Sa4ms showed enrichment for circular prophage in its cytoplasm, suggesting ϕ Sa4ms's circular prophage is not participating in the lytic cycle, but is perhaps in a state akin to active lysogeny (Feiner et al., 2015). We also note that samples for sequencing were prepared in nutrient-rich conditions at mid-logarithmic phase, conditions unlikely to promote DNA damage and associated prophage lytic induction (Nanda et al., 2015). A model for how the MSSA476 population might exist in early logarithmic phase is presented in Figure 3-11.

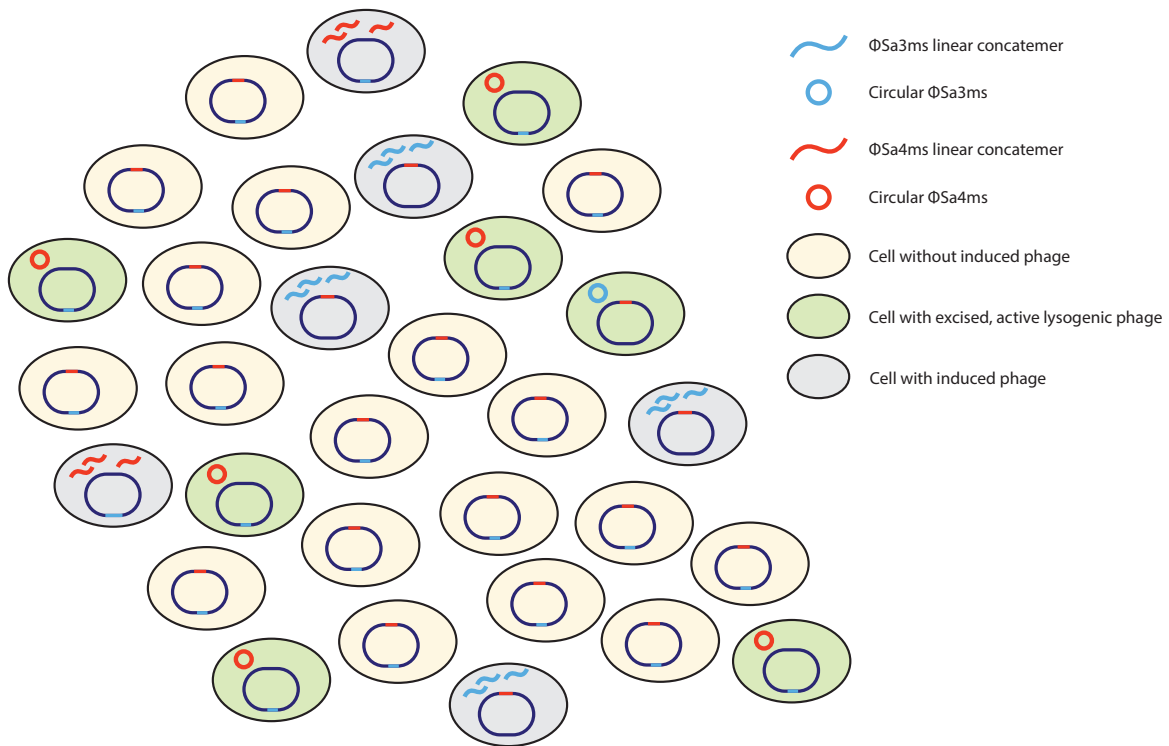


Figure 3-11. Qualitative model of MSSA476 early logarithmic culture. At early log phase, MSSA476 culture contains cells with prophage in both the lytic and lysogenic cycles. The vast majority of cells are stably lysogenized (tan) with ϕ Sa3ms (blue) and ϕ Sa4ms (orange). A subpopulation of cells contains excised prophage elements that appear to be in an active lysogenic cycle (green). Of these cells, those with ϕ Sa4ms excised outnumber those with ϕ Sa3ms excised. Cells with phage induced into the lytic cycle are pictured in gray. Here, ϕ Sa3ms-induced cells outnumber ϕ Sa4ms-induced cells. Subpopulations are shown at relative percentages for illustrative purposes, rather than the quantitative levels suggested by qPCR and other data.

However, to further rule out the presence of circular prophage as a precursor to lytic cycle replication, we examined MSSA476 samples by qPCR over a range of time points. Surprisingly, the results revealed that excision of circular prophage into the extra-chromosomal compartment is temporal, with the highest levels of circular ϕ Sa4ms in early logarithmic growth but rapidly decreasing with increased cell-density. This decrease occurred without any concurrent increase in overall ϕ Sa4ms copy number, showing that ϕ Sa4ms circular elements were not precursors to phage-replication and are likely not participating in the lytic cycle, but rather are in an active lysogenic state. The data also indicates potential control of this event by the bacterial cell, with some factors either promoting excision at early log growth, or perhaps increased re-integration at later growth points. In addition, these data show that phage enrichment would likely go undetected in MSSA476 if samples were prepared at $OD_{600} \geq 1.0$. Therefore, it may be beneficial to purify extra-chromosomal DNA at multiple time points in future studies, elucidating the entire mobilization dynamics of a bacterial genome over its growth cycle.

The time-course qPCR data also showed that the excision rate of ϕ Sa4ms decreased from early to later log phase, suggesting some circular ϕ Sa4ms may be re-integrating into the chromosome after excision. In addition, whether ϕ Sa4ms or related circular prophage elements undergo any replication or remain as single copy in this excised state is unclear. A previous study reported Hlb^-/sak^2 *S. aureus* strains with multiple *hIb*-converting phages integrated in the chromosome (Goerke

et al., 2006). Replication of excised lysogenic prophage could be the first step in generating such strains. Our qPCR approach examined bacterial populations as a whole, but cannot address these specific questions; further experiments on the single-cell level are necessary to uncover such exact excision/integration (and potentially replication) dynamics. One potential method to address this question is through fluorescence microscopy with fluorophores attaching specifically to modified phage genomes. Reporter systems have been previously developed to track P22 phage localization and replication in live cells (Cenens et al., 2015) and a similar approach could be used in *S. aureus* to look at phage replication and determine if it occurs in a lytic or lysogenic manner (i.e. the degree of replication and whether cells survive after phage genome replication). A complicating factor here is that it appears in MSSA476 and likely other strains of *S. aureus*, prophages can be in the lysogenic cycle in integrated and excised states and it is unclear if such systems can distinguish these cell types. Additional co-localizing labels specific to the bacterial chromosome may be necessary to help determine if for lysogenic cells, phage are integrated or excised. Nonetheless, such a system should be able to help uncover the dynamics and some of the questions about the phage we uncover by extra-chromosomal DNA isolation and sequencing.

3.11 What is the biological significance of episomal phage?

The phages we describe as enriched in our sequencing appear to be active lysogenic phage that have excised from the chromosome, and the distinction between phages in the lytic versus lysogenic or active lysogenic cycle is important when considering the roles of prophage as molecular switches or mechanisms to generate diversity in bacterial populations. Excision by phage induction leads likely to cell death, whereas excision of (active) lysogenic phage will generate stable diversity in the population that can be passed on to daughter cells. While under our conditions the percentage of excised phage is relatively low, other external environments could select for and expand certain prophage-excised subpopulations. For example, ϕ Sa4ms was shown to alter the *htrA₂* promoter, with the phage-excised (*P_{ex}*) promoter conferring increased heat-tolerance in COL. It is presently unclear if *HtrA₂* confers this tolerance in MSSA476, however if the protein plays a similar role as in COL, then qPCRs of phage excision rates and excised prophage copy number in cultures grown at elevated temperatures may show increased proportions of cells with excised (or lost) ϕ Sa4ms. Such growth could either select for survival of already ϕ Sa4ms-excised cells, or could drive ϕ Sa4ms lysogenic excision by an unknown mechanism. In either case, the overall percentage of cells with excised ϕ Sa4ms prophage would increase.

In other strains, the external environment could also drive the expansion of subpopulations with excised prophage. In HPV107 for example, a subpopulation

containing excised *hly*-converting prophage might expand in infection conditions (i.e., serum culture or low-iron environments). Goerke et al. found that *hly*-converting prophages moved to atypical chromosomal locations allowing Hly production in invasive disease isolates; localization of typically integrated lysogenic prophage into the cytoplasm (without induction) could precede generation of such unique *S. aureus* isolates (Goerke et al., 2006), or alternatively, prophage harbored in the cytoplasm without reintegration could achieve the same phenotype. The extra-chromosomal DNA enrichment and sequencing approach described here may allow characterization of strains for such a mobilization capacity or potential. Other phages such as those that negatively convert *geh* could excise under conditions selecting for lipase activity as well.

A clear question that follows from the research described in this Chapter is the biological role of phage mobilization. Two approaches may help drive at the answer for this question. One approach would be to grow cultures in a variety of conditions (e.g., BHI or serum culture, starvation or nutrient-rich conditions, or other relevant culture environments) and compare the extra-chromosomal DNA profiles of each sample. Comparison may show the favored excision of phage in one condition over another and suggest biological roles and help formulate better hypotheses of how specific phage may promote increased bacterial fitness. We did a “retroactive” extra-chromosomal sequencing of *S. pyogenes* SF370 at mid-logarithmic phase, which indeed showed the expected enrichment of episomal SpyCIM1, the phage-like

element acting as a switch in the strain's mismatch repair operon (Deutsch et al., 2016). Follow-up experiments examining exDNA of *S. pyogenes* SF370 in nutrient-rich versus nutrient-deficient conditions should show the enrichment of SpyCIM1 in rich rather than nutrient-poor conditions and could serve as a test case for extra-chromosomal DNA isolation and sequencing in a variety of environments. While the biological role of SpyCIM1 is already partially known (Hendrickson et al., 2015; Nguyen and McShan, 2014), without this information, extra-chromosomal DNA isolation and sequencing alone could offer promising potential avenues of research, i.e., exDNA sequencing of SF370 suggests SpyCIM1's biological role without knowledge of prior reports. While the same conclusions can be drawn from qPCR-based experiments, given the relative ease and low-cost of sequencing, profiling bacterial extra-chromosomal compartments in this manner will allow for multiple target identification and less bias in uncovering elements.

A more direct approach to uncover the biological role of such phage excision would be to prevent it outright by creation of phage integrase knockouts. As previously described, the movement of *hly*-converting prophage in *S. aureus* to atypical chromosomal loci has been shown to occur in isolates from cystic fibrosis and bacteremic patients, with phage mobilization thought to be important for infection (Goerke et al., 2006). An informative experiment could compare the virulence and dissemination of *S. aureus* harboring *hly*-converting phage that can freely excise/integrate (WT), versus those that are "locked into" the chromosome

(Δint), or are phage-cured. Here, the comparison of wild-type, Δint , and phage-cured strains should help elucidate both the role of the phage as a whole, as well as the specific benefits of phage excision/integration. Given that phage mobilization plays a key role in the transition from colonization to invasive infection, strains with locked-in phage may show a decreased virulence potential. However, negative conversion may allow for strains to better colonize in the first place, serving as a mechanism for the organism to “get a foot in the door”, or in this case, the nose. (Isolates harboring *hly*-converting phage are overwhelmingly represented in the nasal cavity, but have not been found essential for colonization (Verkaik et al., 2011).) If this is the case, then phage-cured strains should show decreased initial colonization and may be outcompeted by other strains or species. In addition, as the virulence factors typically carried on *hly*-converting phages were shown important for infection (Bae et al., 2006), phage-cured strains may have weaker virulence potential. Thus, the most virulent strain of *S. aureus* may be the one containing an *hly*-converting prophage capable of atypical localization, allowing colonization of the nose via phage gene products, and successful infection by concurrent production of Hly and phage-encoded virulence factors. An illustration of the potential benefits of harboring mobilizing phage is shown in Figure 3-12. Comparison of these three strain types (WT, Δint , and $\Delta \phi hly-c$) should illustrate some of the key biological roles of active lysogenic phage in the *S. aureus* lifecycle.

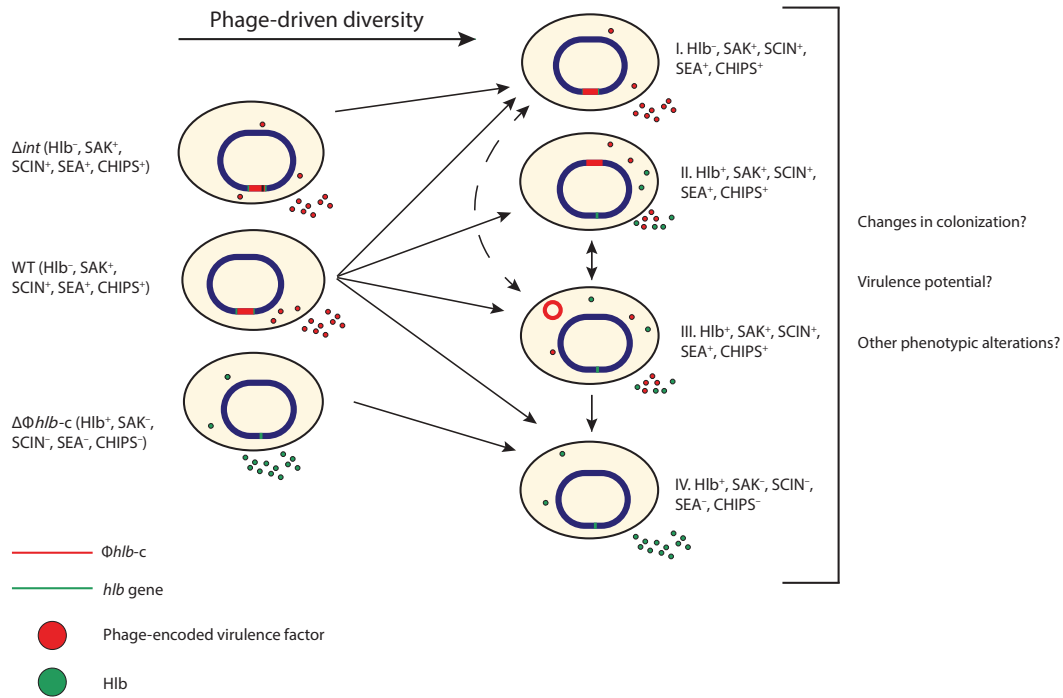


Figure 3-12. Mobilizing phage can generate diverse subpopulations of *S. aureus*. An illustration of a hypothetical experiment is shown above. Here, a *S. aureus* strain is lysogenized with a *hIb*-converting phage that can freely excise from and reintegrate into the chromosome (WT). Variants of the strain include an integrase knockout where the phage is “locked” in the chromosome (Δint), and a phage-cured derivative ($\Delta\phi hIb-c$). The WT strain can generate numerous phenotypically- and genotypically-altered subpopulations (I-IV) via phage mobilization. The external environment may select for the expansion of one or multiple subpopulations. For Δint and $\Delta\phi hIb-c$, the lack of phage mobilization and phage, respectively, prevents diversity in their populations. Δint can only exist as population I, and $\Delta\phi hIb-c$ as population IV. WT can reversibly switch between I, II and III, and irreversibly lose its phage, creating population IV. Comparison among the three strains for colonization, virulence, and other phenotypes (e.g. biofilm formation capacity) could illustrate the importance of phage mobilization in *S. aureus*, and phage as a potential switch allowing the bacteria to alter its phenotypes for success in multiple environments.

In a related but converse manner, one study found *S. aureus* colonization of mouse ears was actually enhanced with Hlb production. In this report, the *hlb*-converting phage of *S. aureus* MW2 (ϕ Sa3mw) was frequently lost upon murine ear colonization, and a bacterially-controlled phage-switch to alter the organism's infection program was suggested by the Authors (Katayama et al., 2013). Here, in contrast to typical observations in human isolates, ϕ Sa3mw was preferentially lost in mouse ear colonization. It is unclear why the loss of ϕ Sa3mw is preferred for mouse colonization while strains harboring *hlb*-converting phage are nearly always found in human nares, but it is known that the virulence factors encoded by ϕ Sa3mw are more human-specific (Katayama et al., 2013). Phage-loss in this case may be selected for due to the murine host, whereas in humans, the importance of such phage-encoded factors may select for strains harboring *hlb*-converting phage. In addition, this study did not examine the propensity of such strains to cause invasive infection; ϕ Sa3mw-cured strains may show weaker virulence potential and be selected against in such an experiment or environment. Regardless, for *S. aureus*, carrying lysogenic phage capable of excision without induction may allow the bacteria to successfully balance the needs of colonization and infection, which demand different sets of virulence factors.

The research detailed in this Chapter uncovered potential active lysogenic phage that could modulate the expression of *htrA₂* (ϕ Sa4ms), and allow the full-length transcription of *hlb* (ϕ HPV107.1) by excision from the chromosome. In addition to

these phage, this work also uncovered an intergenic prophage in HPV107 (unclear integrase type, intergenic between tRNA-Ser and enterotoxin), and 2 intergenic prophages in NRS22 and BK2529 (both with Sa7-like integrases, and intergenic between *rpmF* (50S ribosomal protein L32) and *isdB* (iron-regulated surface determinant)). The potential effects of their extra-chromosomal carriage on hosts are unclear, and phage integration in these loci has been previously reported (Bae et al., 2006; Goerke et al., 2006). Excluding ϕ HPV107.1, the typically-intragenic phages we found enriched in our screening included a *geh*-converting prophage in *S. aureus* NRS143, a 6-phospho- β -galactosidase-integrating prophage in HPV107, and 2 prophages in NRS22 (one prophage integrated within a hypothetical protein-encoding gene, and one prophage disrupting a radical SAM-encoding gene). In addition, we uncovered an enriched integrative and conjugative element (ICE) typically located within a predicted membrane protein encoding locus in NRS271. Lipase has been implicated in biofilm and abscess formation in *S. aureus* (Hu et al., 2012; Jabra-Rizk et al., 2006; Kuroda et al., 2007), however some clinical strains carry *geh*-converting phages without a clear mechanistic advantage. If some *geh*-converting phages are acting as switches to control the expression of lipase for the bacteria's benefit, then advantages to such prophage carriage would be apparent, and future work should investigate this possibility. The effects of the other intragenic phages are unclear, however their enrichment suggests that they could act as switches to also control underlying gene expression. Disruption of genes by the intragenic phages in NRS22 has been reported previously in other *S. aureus*

strains (Bae et al., 2006), however to our knowledge, disruption of a 6-phospho- β -galactosidase encoding gene (HPV107) has not been previously reported and represents a novel phage integration site in *S. aureus*. The role of the uncovered ICE is also unclear, but its potential as a DNA-level switch is intriguing. Overall, exDNA isolation and sequencing revealed the episomal nature of specific typically-integrated staphylococcal prophages. The reports of virulence program alteration by mobilizing *hly*-converting phages suggests that the DNA elements uncovered by our extra-chromosomal DNA isolation and sequencing approach may act as diversity promoting elements in *S. aureus*. The prevalence and number of prophage elements uncovered in this screening suggests their widespread use and importance to the pathogen. Follow-up experiments will have to elucidate their specific biological roles.

SUMMARY

This study screened the extra-chromosomal DNA of 15 clinical *S. aureus* isolates, uncovering the prevalence of episomal prophage with potential roles in virulence factor expression and regulation. QPCR characterization of one of these strains, MSSA476, verified that one of its phage, ϕ Sa4ms, exhibits episomal behavior, and may exist as an active lysogenic prophage. We show that episomal ϕ Sa4ms exists as a circular DNA element off the chromosome, and that it does not appear to be a precursor to lytic cycle replication. Importantly, the episomal prophage we uncover are only detectable in extra-chromosomally enriched DNA samples, and their presence would have been missed in sequencing or qPCRs of whole-genome DNA samples. Lastly, this work finds that ϕ Sa4ms appears to act as a phage-molecular switch, as its excision/integration alters the promoter sequence of *htrA₂*, changing its transcription levels and affecting heat-stress survival in *S. aureus* COL. ϕ Sa4ms behavior suggests it is an active lysogenic prophage, and the other episomal prophages identified may exhibit similar activity, given their integration sites. Episomal lysogenic prophage, or active lysogenic phage, promote the generation of stable, diverse subpopulations with impacts on bacterial infection; extra-chromosomal DNA isolation and sequencing should allow the increased discovery of such elements in *S. aureus* and other bacterial pathogens.

MATERIALS AND METHODS

3.12 Bacterial strains and growth conditions

Strains and constructs used in this study are listed in Table 3-6. For preparation of extra-chromosomal DNA, *S. aureus* strains were established from overnight cultures grown in Bacto Brain Heart Infusion Broth (BHI), and back-diluted 1:100 into 50 mL BHI without shaking at 37°C unless otherwise noted. Strains were grown to an OD₆₀₀ of 0.6 - 0.8. Cultures were centrifuged at 4000 RPM for 10 minutes at 4°C and used immediately or frozen overnight at -20°C. For qPCR studies, strains were back-diluted from overnight cultures and grown to specified optical densities. For *PhtrA2*-GFP reporter studies, overnight cultures were back-diluted 1:100 in 15 mL BHI and grown at 200 RPM at 37°C to an OD₆₀₀ = 0.2. *E. coli* was grown at 37°C, 200 RPM in LB media with selection as necessary.

Concentrations for antibiotics used are as follows, for *Escherichia coli*: ampicillin, 100 µg/mL; for *S. aureus*: erythromycin, 5 µg/mL, spectinomycin, 50 µg/mL. For heat shock studies, plates were grown at 44°C.

Table 3-6. Bacterial strains and constructs used in this study.

Strains	Notes	Source	
<i>E. coli</i>			
<i>E. coli</i> TOP10	Cloning host	Invitrogen	
<i>E. coli</i> DC10B	Cloning host	Lab strain	
<i>E. coli</i> DH5 α ::pCN35	Strain containing pCN35 plasmid	(Charpentier et al., 2004)	
<i>E. coli</i> DH5 α ::pCN56	Straining containing pCN56 plasmid	(Charpentier et al., 2004)	
<i>S. aureus</i>			
RN4220	Restriction deficient cloning host	(Kreiwirth et al., 1983)	
RN6390 <i>htrA2</i>	RN6390, <i>htrA2</i> :: <i>spc</i> Spc ^R	(Rigoulay et al., 2005)	
RN6390 <i>htrA2</i> DD01	RN6390, <i>htrA2</i> :: <i>spc</i> Spc ^R , harboring pCN35, Erm ^R	This work	
RN6390 <i>htrA2</i> DD02	RN6390, <i>htrA2</i> :: <i>spc</i> Spc ^R , harboring pCN35 with full length <i>htrA2</i> and 250 bp <i>int</i> -promoter, Erm ^R	This work	
RN6390 <i>htrA2</i> DD03	RN6390, <i>htrA2</i> :: <i>spc</i> Spc ^R , harboring pCN35 with full length <i>htrA2</i> and 250 bp <i>ex</i> -promoter, Erm ^R	This work	
RN6390 <i>htrA2</i> DD04	RN6390, <i>htrA2</i> :: <i>spc</i> Spc ^R , harboring pCN56, Erm ^R	This work	
RN6390 <i>htrA2</i> DD05	RN6390, <i>htrA2</i> :: <i>spc</i> Spc ^R , harboring pCN56 with <i>phtrA2-int</i> insert, Erm ^R	This work	
RN6390 <i>htrA2</i> DD06	RN6390, <i>htrA2</i> :: <i>spc</i> Spc ^R , harboring pCN56 with <i>phtrA2-ex</i> insert, Erm ^R	This work	
COL <i>htrA2</i>	COL, <i>htrA2</i> :: <i>spc</i> Spc ^R	(Rigoulay et al., 2005)	

COL <i>htrA2</i> DD11	COL, <i>htrA2::spc</i> Spc ^R , harboring pCN35, Erm ^R	This work	
COL <i>htrA2</i> DD12	COL, <i>htrA2::spc</i> Spc ^R , harboring pCN35 with full length <i>htrA2</i> and 250 bp <i>int</i> -promoter, Erm ^R	This work	
COL <i>htrA2</i> DD13	COL, <i>htrA2::spc</i> Spc ^R , harboring pCN35 with full length <i>htrA2</i> and 250 bp <i>ex</i> - promoter, Erm ^R	This work	
COL <i>htrA2</i> DD14	COL, <i>htrA2::spc</i> Spc ^R , harboring pCN56, Erm ^R	This work	
COL <i>htrA2</i> DD15	COL, <i>htrA2::spc</i> Spc ^R , harboring pCN56 with <i>phtrA2-int</i> insert, Erm ^R	This work	
COL <i>htrA2</i> DD16	COL, <i>htrA2::spc</i> Spc ^R , harboring pCN56 with <i>phtrA2-ex</i> insert, Erm ^R	This work	
			Genome/Chromosomal Accessions for read-mapping
BAA-42	MRSA	ATCC	JXZF00000000
MSSA476	MSSA; Hyper-virulent, community acquired	ATCC	JXZG00000000
NRS156	MSSA; vaginal tampon isolate	NARSA	JXZU00000000
NRS271	MRSA; Linezolid-resistant, wound isolate	NARSA	JXZW00000000
NRS153	MRSA	NARSA	JXZY00000000
NRS127	MRSA; sputum source from Tenn., oxacillin, penicillin, ciprofloxacin and erythromycin resistant	NARSA	JXZZ00000000
NRS387	MRSA; wound Washington State	NARSA	JYAD00000000
NRS22	VISA; MRSA; inpatient ICU, bloodstream	NARSA	JYAG00000000

NRS143	MSSA	NARSA	JYAH00000000
NRS158	MSSA; HT 2000 0319; Strain was isolated from skin infection in France	NARSA	JYAN00000000
NRS2	MRSA; Mu3; ATCC 700698; Purulent sputum, cardio thoracic surgery, Japan; Oxacillin and Tet resistant; VISA= MIC=4; white colonies, robust growth on BHI	NARSA	JYAO00000000
E2125	MRSA; Denmark; SCCmec1; 1964	VAF	JYAX00000000
HPV107	MRSA; Portugal; SCCmec1a, 1992	VAF	JYAY00000000
HDE288	MRSA; Portugal; SCCmecIVvar; MRSA; 1996	VAF	JYAZ00000000
BK2529	MRSA; USA; SCCmecIV; 1996	VAF	JYBA00000000

ATCC = American Type Culture Collection

NARSA = Network on Antimicrobial Resistance in *Staphylococcus Aureus*

VAF = Vincent A. Fischetti

3.13 Whole-genome and extra-chromosomal DNA isolation and manipulation

Whole genome DNA isolations (gDNA) were performed using the QIAGEN DNeasy Blood and Tissue Kit, including an added manufacturer-detailed pretreatment step for Gram-positive bacteria. Enzymatic lysis buffer was composed of lysostaphin (100 µg/mL) in 1X phosphate-buffered saline (PBS). Extra-chromosomal DNA isolation

was carried out as previously described (Utter et al., 2014). Extra-chromosomal DNA samples were visualized on 0.7% agarose 0.5X TAE gels stained with SYBR Safe DNA Gel Stain. Electrophoresis was carried out at 50 V for 1 hr in 0.5X TAE, and visualized with UV transillumination. Prior to DNA sequencing, extra-chromosomal DNA samples were concentrated as needed using Microcon DNA Fast Flow centrifugal filters, following manufacturer's directions (EMD Millipore).

3.14 DNA sequencing of extra-chromosomal *S. aureus* samples

DNA sequencing of extra-chromosomal DNA samples was performed using the Illumina MiSeq sequencer. Extra-chromosomal DNA was quality checked prior to library construction and sequencing using the Thermo Fisher Scientific Qubit Fluorometer High Sensitivity DNA kit to measure quantity of DNA and the Agilent Technologies High Sensitivity DNA assay to measure size and quality of DNA. DNA libraries were constructed as per manufacturer's instructions from 1 ng DNA per sample using the Illumina Nextera XT DNA Library Preparation kit. Each DNA library was barcoded to allow for multiplexing during sequencing using the Illumina Nextera XT Index kit. Libraries were quantitated and quality checked using Agilent Technologies High Sensitivity DNA kit. Libraries were sequenced using the Illumina MiSeq Reagent kit V2 (500 cycle). Prior to sequencing, libraries were normalized and pooled together to make a pooled amplicon library at 2 nM concentration. Sequencing generated FASTQ files to allow for off-instrument analysis.

3.15 Bioinformatic sequence analysis of extra-chromosomal DNA samples

Bioinformatic analysis was performed using CLC Genomics Workbench software unless otherwise described. Extra-chromosomal reads were mapped to respective chromosomal sequences (Table 3-6), and unmapped reads were saved as a separate file and *de novo* assembled for plasmidial elements. Read-mappings were visually examined for regions of increased read-depth corresponding to DNA element enrichment in extra-chromosomal DNA samples. Read-mappings were then subjected to coverage analysis to identify regions with significantly higher ($P < 0.05$) coverage. Prophage and other mobile DNA element regions with high coverage were noted for each sequenced sample.

3.16 QPCR analysis of *S. aureus* strains

For qPCR experiments, strains were grown as described for extra-chromosomal DNA sequenced samples, or to other desired optical densities. Cultures were divided, with one portion of the culture subjected to the QIAGEN DNeasy Blood and Tissue Kit for gDNA isolation, and the rest undergoing extra-chromosomal DNA isolation. gDNA samples were used to determine excision rates and phage or plasmid copy number per cell of the bacterial population, while exDNA samples were used only for phage and plasmid copy number measurements. Primer pairs and probe sequences for each target are listed on Table 3-7. All primers and probes were designed and purchased from Integrated DNA Technologies (Coralville, IA).

Amplification was carried out using the TaqMan Gene Expression Master Mix (Thermo Fisher) using the Life Technologies QuantStudio 12K-Flex Instrument following manufacturer's cycling protocol. Standard curves for each primer-probe set were generated for each experimental run, with amplification efficiencies and linear regression analyzed using QuantStudio Software. All primer-probe sets had efficiencies 90-110% and $R^2 > 0.98$. Excision rates, excised prophage copy numbers, and plasmid copy numbers were calculated by normalizing target (*attB*, *attP*, pSAS1, respectively) to *gyrA*. All targets were measured in biological triplicate and technical duplicate. Graphical and statistical analysis was performed using Prism GraphPad with significance testing done using two-tailed Student's t-tests. Values are reported as mean \pm standard error.

3.17 Linear DNase and restriction endonuclease treatment of extra-chromosomal DNA samples and end-point PCR of DNA targets

Prior to linear DNase and/or treatment with restriction endonucleases, extra-chromosomal DNA samples were treated with PreCR Repair Mix (NEB) to repair nicked DNA. PreCR-treated samples were then either 1) treated with PshAI and PspXI (NEB) following manufacturer's protocol, 2) treated with Plasmid-Safe-ATP-Dependent DNase (Epicentre), 3) treated with the ϕ Sa4ms-specific restriction endonucleases PshAI and PspXI, then the Plasmid-Safe-ATP-Dependent DNase, or 4) left solely PreCR-treated. Plasmid-Safe treated samples were treated over the course of 16 hours, where 2 μ L ATP solution and 2 μ L DNase were added at 2 and 4

hour time points, with the reaction incubated at 37°C. Samples were heated to inactivate enzyme prior to PCR. End-point PCR was carried out using target-specific primers (Table 3-7) and the KAPA2G Robust Hotstart Polymerase (KAPA Biosystems) with the following cycling protocol: 1) Initial denaturation 95°C, 3 min; 2) Denaturation 95°C, 15s; 3) Annealing 60°C, 15s; 4) Extension 72°C, 15s; 5) Repeat steps 2-4 33 times. Samples were normalized for total DNA prior to loading individual PCR reactions. PCR products were visualized using 1% agarose 0.5X TAE gels stained with SYBR Safe DNA Gel Stain. Electrophoresis was carried out at 100 V for 25 min in 0.5X TAE, and visualized with UV transillumination. Images were captured using Alpha Imager HP software.

Table 3-7. Primers and probes used in this study.

Primers	Sequence	Notes
qPCR/end-point PCR primers		
gyrA_F	CGTGAAGGTGACGAAGTTGT	For per cell normalization
gyrA_probe	TGTTTGCATGAGCTACATCAAGCCC	5' 6-FAM/ZEN/3' IBFQ
gyrA_R	CCTTTACCACCACGATTTGA	For per cell normalization
phihlb_attB_F	ACGTTTATATGTTATCGACCGT	for excision rates of <i>hly</i> -converting prophage
phihlb_attB_probe	ACGCGCTGATTTAATCGGACAATCTTCT	5' 6-FAM/ZEN/3' IBFQ

phiHlb_attB_R	TTGTCTGATGCACCATTATCA	for excision rates of <i>hlb</i> -converting prophage
phiSa4ms_attB_F	GACGCTTACGTCGGTACT	for phiSa4ms excision rates
phiSa4ms_attB_probe	ACCAATATCCACTAATGTCCACTCCATTCA	5' 6-FAM/ZEN/3' IBFQ
phiSa4ms_attB_R	TTGATGTGAAGCGGACAATC	for phiSa4ms excision rates
hlb_attP_F	AAAGTCTCCAGTTTGGATACATAGA	for <i>hlb</i> -converting prophage copy number/ end-point PCR measurement
hlb_attP_probe	CAACAGTATTTATTGGGTTTGGAGTCC	5' 6-FAM/ZEN/3' IBFQ
hlb_attP_R	GAAAGTATGTAATTTAGGGACCCATTAG	for <i>hlb</i> -converting prophage copy number/ end-point PCR measurement
phiSa4ms_attP_F	CCTTGCAACACATTCTGAACAC	for phiSa4ms copy number/ end-point PCR measurement
phiSa4ms_attP_probe	ACGGCCATTCTCAAACGTACACGA	5' 6-FAM/ZEN/3' IBFQ
phiSa4ms_attP_R	TAAGAGCAAACACGAGTGGAAA	for phiSa4ms copy number/ end-point PCR measurement
pSAS1_F	CCTCGGAACCCCTTAACAATCC	for pSAS1 copy number
pSAS1_probe	ATGGTCGGCTTAATAGCTCACGCT	5' 6-FAM/ZEN/3' IBFQ

pSAS1_R	GCGTTGAGAAGAACCCTTAACTA	for pSAS1 copy number
gapdh_PCR_F	GTCAACGAATATTGCAATTAATGGTATGG	for measuring <i>gapdh</i> target via end-point PCR
gapdh_PCR_R	CGCACCAGTAGAAGTAGGAATAATGC	for measuring <i>gapdh</i> target via end-point PCR
pSAS1_PCR_F	GAAGGTCGTCTATCTCTCAGATGTC	for measuring pSAS1 target via end-point PCR
pSAS1_PCR_R	AAGGATGGTCTCAAGAGGAATTAGCC	for measuring pSAS1 target via end-point PCR
<i>Pint</i>lex and <i>htrA</i>₂-related primers		
Pint_upstm	GCTTATGGATCCATAAATGATCAAACCACACCACCT	250bp upstream of <i>htrA</i> ₂ gene, phiSa4ms integrated primer, BamHI restriction site, for <i>Pint</i> construction
Pex_upstm	GCTTATGGATCCAAAAATCGCATAAATAATTGATGTGAAG	250bp upstream of <i>htrA</i> ₂ gene, phiSa4ms excised primer, BamHI restriction site, for <i>Pex</i> construction
P_dwnstm	GCTTATGGTACCCTAAGGAATTACATGTTTTTTACCAATATC	30bp within 5' end of <i>htrA</i> ₂ gene, Kpn1 restriction

		site, for <i>Pint/ex</i> construction
Pint_upstm_seq	ATAAATGATCAAACCACACCACCT	for Sanger sequencing of <i>Pint</i>
Pex_upstm_seq	AAAAATCGCATAAATAATTGATGTGAAG	for Sanger sequencing of <i>Pex</i>
P_dwnstm_seq	CCTAAGGAATTACATGTTTTTTACCAATATC	for Sanger sequencing of <i>Pint/Pex</i> constructs
full_htrA2_dwnstm	GCTTATGGTACCTTATTTTAGTTTAATATTAATTTCTTTC	3' end of <i>htrA2</i> , for complementation of <i>htrA2</i> , Kpn1 restriction site
full_htrA2_seq1	GTACTGACTTTTAGGAATTACATGT	For Sanger sequencing of <i>htrA2</i> constructs
full_htrA2_seq2	GTAATTACTGAATTAGATGGC	For Sanger sequencing of <i>htrA2</i> constructs
full_htrA2_seq3	GTCTGAAACGGTGGGATATC	For Sanger sequencing of <i>htrA2</i> constructs

3.18 Construction and testing of *PhtrA₂*-GFP reporter system and *htrA₂*-complemented knockouts

For construction of a *PhtrA₂*-GFP reporter system, 250 bp upstream of the *htrA₂* gene and 30 bp of *htrA₂* were amplified from MSSA476 gDNA template using Phusion High-Fidelity DNA Polymerase with two primer sets 1) Pint_upstm/P_dwnstm or 2) Pex_upstm/P_dwnstm (Table 3-7) to amplify two versions of the *htrA₂* promoter and 5' gene region (*Pint* or *Pex*). PCR products were gel purified, cut with restriction enzymes KpnI and BamHI (NEB), and further purified. pCN56 vector (Charpentier et al., 2004) was mini-prepped, digested with KpnI and BamHI, dephosphorylated with Antarctic Phosphatase (NEB), and gel purified before ligation with T4 ligase (NEB) to the purified PCR products. 2 μ L ligation mixture was transformed into One Shot TOP10 Chemically Competent *E. coli* (Thermo Fisher) and resulting colonies screened by PCR and Sanger sequenced (GENEWIZ; South Plainfield, NJ) using primers Pint_upstm_seq/P_dwnstm_seq or Pex_upstm_seq/P_dwnstm_seq for desired vector insert (Table 3-7). *E. coli* harboring pCN56 with *Pint* or *Pex* inserts were grown and miniprepped, and the vectors electroporated into electrocompetent *S. aureus* RN4220 using a Bio-Rad Gene Pulser with the following settings: 2.5 kV, 25 μ F, 100 Ω . Empty pCN56 vector was also introduced into RN4220. Vectors from RN4220 colonies were transduced using ϕ NM4 γ 4 (Heler et al., 2015) into *S. aureus* RN6390 *htrA₂* and *S. aureus* COL *htrA₂* (Rigoulay et al., 2005) following an established protocol (Olson, 2016). Colonies

were screened via PCR and inserts Sanger sequenced to ensure the correct DNA sequence.

To examine GFP fluorescence in each strain, overnight cultures of constructs were back-diluted 1:100 in 15 mL BHI supplemented with 5 µg/mL erythromycin and 50 µg/mL spectinomycin and grown at 37°C, 200 RPM to an OD₆₀₀ = 0.2. Cultures were then grown at 37°C or 44°C with shaking. At 3 and 6 hr time points, 1 mL culture was removed, an OD₆₀₀ value measured, and 200 µL culture pipetted in a quartz 96-well plate and RFUs measured on a Molecular Devices SpectraMax M5 instrument (485 nm excitation, 515 nm emission). Fluorescence of pCN56 (empty vector) cultures was subtracted as background, and OD₆₀₀ normalized RFUs for each sample were measured. Comparison of construct-GFP fluorescence was calculated as a ratio of *Pex/Pint*. The experiment was performed in triplicate.

For construction of *htrA2*-complement vectors, the *htrA2* gene and 250 bp upstream of the gene were amplified using the primer set 1) *Pint_upstm/full_htrA2_dwnstm* or 2) *Pex_upstm/full_htrA2_dwnstm* (Table 3-7) with Q5 DNA Polymerase (NEB) to generate two DNA fragments containing the full length *htrA2* sequence with different 250 bp promoter sequences. PCR products were treated as described above but ligated into pCN35 vector (Charpentier et al., 2004). The ligated vectors and pCN35 empty vector were transformed into electrocompetent *E. coli* DC10B prepared by standard techniques, shuttled into RN4220, transduced into *S. aureus*

RN6390 *htrA₂* and *S. aureus* COL *htrA₂*, then screened and sequenced as previously described using primers full_htrA2_seq1, full_htrA2_seq2, full_htrA3_seq3, full_htrA2_dwnstm, Pint_upstm_seq, and Pex_upstm_seq (Table 3-7).

To test viability and survival of complemented and mutant (empty vector-containing) *S. aureus htrA₂* strains, constructs were spotted in a log-dilution series onto BHI-spectinomycin-erythromycin agar plates and incubated at 37°C and 44°C for 24 hours following a protocol from (Rigoulay et al., 2005). Plates were examined visually for survival and photographed the following day using a Cell Biosciences AlphaImager HP instrument using AlphaImager HP software.

CHAPTER 4. CONCLUSIONS AND OUTLOOK

Despite a wealth of research over the past 100 years, we are still constantly surprised by the activities of the most abundant biological entity on earth: bacteriophage. While larger themes of phage biology and phage-bacteria interactions are clear, many of the details have yet to be filled in. Given the sheer number of bacteriophage in the biosphere, and the magnitude of their interactions with bacteria, there is clearly a long way to go.

Phages are the smallest “organism” on earth, and represent an evolutionary unit with an extraordinarily rapid turnover time. While their genome size suggests they are relatively simple, their dynamics allow nearly boundless opportunities for evolution, and thus are far more complex than we can presently appreciate—explaining our limited knowledge of them and their activities. The phage genome is on average 1% the size of a bacterial chromosome (Hatfull, 2008), and such a relatively small genome suggests that elucidating functional roles for phage genes should be a straightforward task. However, 80% of bacteriophage genes show no homology to known proteins; we simply do not know what the majority of phage genes do, how they affect the phage, and likely, how they affect the host (Hatfull and Hendrix, 2011).

From what we do know, phages have an enormous influence on the biosphere and their hosts, and play major roles in virulence and bacterial survival (Brussow et al.,

2004; Feiner et al., 2015; Gillis and Mahillon, 2014; Wilhelm and Suttle, 1999). The details of this which we can currently describe are likely just the tip of the iceberg, and as we learn more about the phage, we will no doubt uncover their invisible hand in many biological processes. One area where phage are likely to be found in increasingly important roles is bacterial genomic regulation. It is typically assumed that in comparison to eukaryotes, bacteria are relatively simple and do not encode the more advanced features of eukaryotic organisms. While true in some cases, many analogues of eukaryotic systems have been uncovered in bacteria, i.e. CRISPR systems (Marraffini, 2015). Bacteria are not thought to contain as many regulatory mechanisms as eukaryotes for transcriptional regulation, however we find examples where bacteria utilize phage to achieve the same end goal, either through disrupting transcripts (SpyCIM1, *hly*-converting phages (Feiner et al., 2015)) or promoter-sequence alteration (ϕ Sa4ms). It is likely that more eukaryotic system-analogues will be found in bacteria, and phage may turn out to be the tools to accomplish some of these tasks.

Even for known prophages, determining why they are maintained by bacteria in some cases has proven difficult. The *geh*-converting phages of *S. aureus* contain no obvious virulence or fitness factors, but are stably maintained in the chromosome. Prophage in this case may be kept around to prevent lipase expression or perhaps the phage encodes a virulence factor not yet uncovered. It is also a possibility that there is an effect beyond an obvious phenotype that we as researchers are currently

not measuring. It is hard to imagine that the effects of removing a 40 kb DNA element from a genome will be limited to simple on/off production of encoded virulence factors. Indeed, curing of SpyCIM1, a 13.5 kb DNA element of *S. pyogenes* SF370, was found to change global gene expression of the organism, affecting seemingly non-related portions of the genome (Hendrickson et al., 2015).

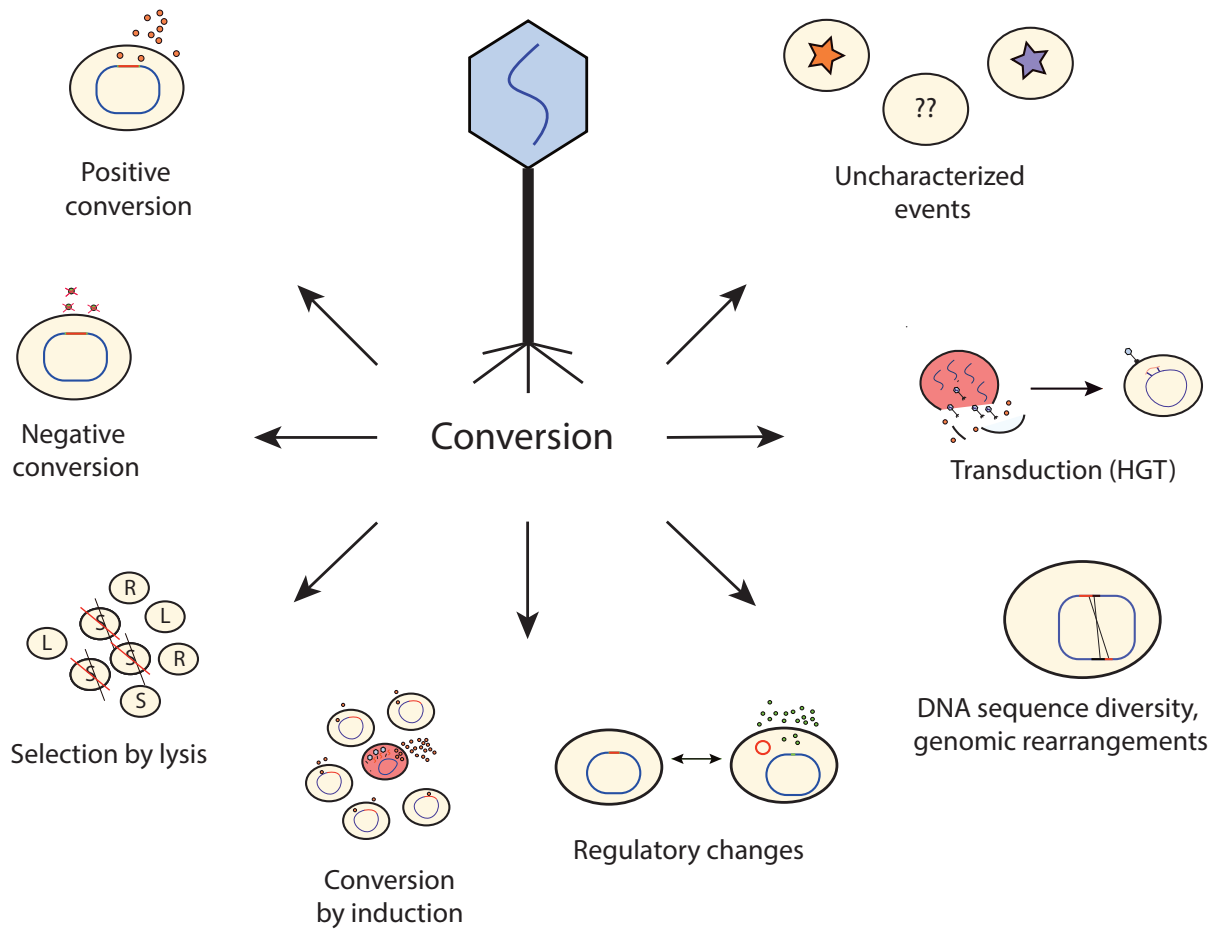
In light of the many ways phage affect their hosts, a new term with a “big tent” should be established to cover all the mechanisms of phage influence, including the more recently discovered phage-based switches, phage-driven gene expression changes and other novel host-modifying activities. “Conversion” could serve as such a term, with modifiers added (e.g., positive, negative, (active) lysogenic, lytic, regulatory, etc.) to label specific classes by which phage affect the host (Figure 4). It is likely that in almost every case of prophage carriage, there is always conversion, we just don’t have the tools or aren’t looking for phenotypes in the right way. Regardless of if we can observe conversion phenotypes, it is clear that phage-bacteria interactions generate diversity within bacterial populations, either contributing to altered genotypes and/or phenotypes. With the exception of successful bacterial defense against phage infection, almost all other bacteria-phage interactions are likely to alter the host and may generate distinct, biologically significant subpopulations. (Even successful defense can alter bacterial genome content, e.g., new phage spacer acquisition within a CRISPR array.) Whether or not

such subpopulations have increased fitness and success depends upon the external environment for selection.

Indeed the work presented in this Thesis for the Gram-positive pathogens *B. anthracis* and *S. aureus* show that phage do serve to create diverse subpopulations in each species. The research on *B. anthracis* illustrates a specific example of phage biology and a bacteria-phage relationship that we need to better understand: selection by lysis for phage-resistant bacterial populations. In *S. aureus*, a method to more easily get at unexplored phage biology is developed, and proves to uncover an example of a novel phage-switch: *htrA₂* promoter alteration driven by active lysogenic phage excision/integration. These are two examples in a likely near-limitless array of phage impacts on the host, and given the ubiquitous nature and importance of both phage and bacteria, advances in biology necessitate further study of their relationships.

In infectious disease for example, such research will allow us to 1) better understand mechanisms by which phage drive bacterial adaptations in infection environments (e.g., *htrA₂* regulation by phage excision/integration, superantigen and DNase upregulation by *S. pyogenes* via phage lytic induction in the throat (Broudy and Fischetti, 2003; Broudy et al., 2001; 2002)), and 2) better understand the biology of bacteria's natural enemy and aid in the development of new therapeutics.

Figure 4-1. Illustration of “conversion” and phage effects on bacterial hosts. Conversion is a broad-acting term, encompassing all of the ways phage affect their hosts. i) Positive conversion alters the phenotype of the host, where phage-encoded factors often contribute to virulence or fitness potential (e.g., conversion of *S. aureus* to SEA⁺, SAK⁺, SCIN⁺, CHIPS⁺, or promotion of vegetative survival in *B. anthracis* by phage-encoded sigma factors). ii) Negative conversion by phage integration can disrupt expression of host-encoded factors (*hly* in *S. aureus*). iii) Selection by lysis is the expansion of phage-resistant (R) or lysogenized (L) over-sensitive (S) cells in a population. In *B. anthracis*, selection by lysis expands a CsaB-deficient subpopulation harboring a markedly altered phenotype which may impart important survival advantages. iv) Conversion by induction refers to altruistic subpopulations of cells where phages induce into the lytic cycle for the benefit of the whole population. Phage induction can increase expression of phage-encoded factors and help promote infection (e.g., *stx* phage) or alternatively, cellular debris (eDNA) from phage-lysed cells can help increase biofilm formation (Nanda et al., 2015). v) Regulatory changes mediated by phage-excision or “active lysogeny” can alter gene expression in a number of species, including *S. aureus* (e.g., ϕ Sa4ms and *htrA*₂ expression). vi) Phage sequences can serve as anchor points for genomic rearrangements (*S. pyogenes* SSI-1); alternatively, phage excision and reintegration can alter bacterial genomes. vii) Phage transduction is one of the most important HGT mechanisms and can drive the dissemination of virulence and fitness determinants. viii) Novel mechanisms by which phage alter their hosts are likely to be discovered. In all cases i-viii, phage serve to increase the diversity of their hosts, creating subpopulations which may alter bacterial fitness.



For research focused on phage-based therapeutics, it is important to study phage-bacteria interactions not just for antibacterial development, but also to understand how resistant variants post-treatment may survive and cause further disease (i.e., how selection by lysis affects a bacterial population). For health and wellness in general, phage likely play roles in microbiome-associated bacterial species, and uncovering these interactions can potentially allow new strategies to improve human health. In addition, the more we learn about phage, the more tools we have at our disposal (e.g., CRISPR-based genome editing, endolysin and other phage-based therapies (Fischetti, 2005; Salmond and Fineran, 2015)).

Bordet suggested nearly a century ago that phage are the products of bacteria and not a distinct entity. Today his finding is obviously viewed as inaccurate, but in many ways, perhaps it is not far off from reality. Phage are selfish elements and the predators of bacteria—but their survival and propagation absolutely depends on the bacteria themselves, and clearly bacteria have in turn adapted their predators as tools integral to their own survival and success. Regardless of which lens the phage-bacteria/bacteria-phage relationship is viewed, it is clear we've only scratched the surface of its intricacies. Uncovering more of the story requires one thing from researchers: to look.

APPENDIX 1. RAW SEQUENCES OF ϕ BACA1 CONTIGS

Sequence file is available in FASTA format at:

<https://www.dropbox.com/sh/b3alrq7k5y7q6pq/AAbh2Usqstjt2MTzHXh2zJoSa?dl=0>

Password: bacillusphage

ϕ BACA1 Contig 1:

CTCCCTGGAGACCGCCGCTAGCTTTCCATGCAAAAAATTCGTTTTATTTTCATA
AAAGGGGGTTCAACTAAAGGAGGTGGTTCACATAGGACGAAAAGCGAAACCGA
TCCATTTGCAAATACTTGAAGGTAACAAAAATCGATTAACATAACAGGAAATAG
AACAACGTGTGAAGGCTGAACAAAATATTCAACCGAAAGCGAATAGAATCAAA
GCTCCAACCTTGGTTGAATGCTGTAGCTAAAAAGGAATTTAATCGTATTTCTAAA
GAATTAATGGAATTAGACCTTATTACAAATGTAGACATTAATGCTTTGGCGGCT
TATTGTGACGCCTACTCTGATTACGTTGAATGCACAAAGATTATCAGTGAAGAA
GGGTTAATGGTAGAGTATACGAATAAAGCAGCTGAAACCAATAAAGTCCCTCA
TCCCTTATTAACATAAAAAGAAACAATTGCATGAACAAATGAAGTCGTTGGCAAT
TGAATTTGGATTAACGCCGAGTTCTAGAGCATCTTTAGCAAAACCCAAGGGTGA
TGATAAACCAAAAACCAATGCTGAAAAGCGGTTTGGTGATAGGGTATGAGATT
AGAAGAAAGACTAATGCAATATGTTTATGACATTTTCGGATGGTAACATATTGGC
TTGTAAGAAACATAAATGGGCTTGTGAGCGTTTTTTAAGAGATTTAGAACGTAC
ACAAGAGGATGAGTGTCCATTCTATTTTGATATTGAACAGTTATATGATTTTTA
TGAATGGTGCAAGCAGTTTAAACATTTTAAAGGTGTATTAGCAGGGCAATATAT
TGAGTTAACCGATTTTCAGTTATTTGTAGCAGCTAATATATTTTGTTCCTTATC
AAAGCTACAAATAATAGACGTTTTCTACGTGCATTTATTGAACTTGCAAGAAAA
AATGCAAAATCGCAATTCTTGGCCCTTATTGCTTCTTATATAACCTTTTTATCTG
ATCAACAAGAAGAATGTTATATAGCTGGTTGGGATAGACAACAATCAAGCCTTG
TGTACAATGATATTTTAAAGCAACTAGGCGCATGTGATATGTTATCCAAAAAAT
ATAAGGATTCTTATGGGAAAATTACACATATAAAAAGTGGTTCAACAATAACAC

CACTTTCTAAAGAAGCAAAAAAGACCGGTGATGGTACAAACCCATCGCTTGGT
ATTGTCGATGAATATCATGCTCACGATACTAGTGAAATTTATGATGTAATCGAT
TCTGGAATGGGTGCACGTGAGAATACATTGATGTTTATTATCACCACAGCAGG
ATTTAACATCAATGGACCTTGTTACAAGGAGTATAAATATTGTTCAAGGATATT
AGATCCAAACGATGCAGGTGTGGAGAATGATGAGTATTTTGTGTTATTTGTGA
ACTTGATAAAGATGATGATATCAAGGATGAACTAATTGGATAAAAAGCCAATCC
AATCGTAGCAACTTATGAGGCTGGGATGAAGAAGCTACGTAGTGACTTGAAGG
TTGCTCTTGATAATCCTGAAAAAATGCGTTCCTTTCTAACGAAACGTATGAATA
TATGGGTTAACAGAAAAGAAAACGGTTATATGGATATGTCCAGATGGAATAAG
TGTGATGAAGTAATTGATCTATCTGAATTAAGGCATGGAATGCACAGTAGGT
GCTGATTTATCAGCGAAAATTGACTTGACTAGTGTAGATTTTGAATTCAAGAAA
GACGAGAAATACGTCGTGATTAGTCATAGTTTTATACCGGAAGACACTTTATTC
GAGAAAATGAAAACGGATAAGGTGCCATATGACATTTGGGCGCAGCAAGGTTG
GATTACTGTAACACCTGGTTCAGTAGTAGACTATAATTTTCGTGAAAGAGTATAT
AAAAACGATGGAATCAGATAATGAGTTTAAAATAAAAGAAATATGTGCTGATCC
ATGGAACGCAACTCAATTCATGCAGGATATGGAAGCGGAAGGGTATGTCGTTG
TAGAAATCCGGCAAGGTATGGCTACTTTATCAGGCCCAACAAAAGACTTTCGG
GAGCAAGTGTATCAAAAGAAAATTATTCATAATAACAATCCAGTACTGAATTGG
GCAATTGGAAATGCTGTTACTAAGCAAGATGCTAACGAAAATATTATGTTGGAT
AAGTCAAAAGCAACAGAAAGAATTGATCCGATTGCGGCTGTAATTAAGTTCGCAT
GTTAGATGCATGCTCAATTCTGGTGAAATGGATTTGAATTCATATATTTTAAGT
CAAAATTTCTCATTCTAGGAGGAATTACATGCGGTTTTTAAATGTTTTTTATCAGT
GTTTTAGATGATATTTTATTCGTTTCAGGGTTGTCCATTATTATAGGGACGACT
TTTTTTATTAACCCTATTTATGGATGGTATTTGTTGGGTATTATTCTCACAATGC
TGGGGGTGGTAATGATCAGAAGATAGAAAGGAGGTGAAATTTTTGATTTTTTCG
GCAGCTATTTAAGAATCAGGATACAACAACTTAAAAAATCCGACTCCTTGGTT
TAAAAGTTTATTTGGTTATCAAGCCGCAAGTGGTGAGAAGGTAACAGTTGAATC
ATCTTTAAGTGTTCCAACAGTTTACCGATGTATTAATATCCTTGCAAATAGTGTT
GCAATGCTTCCATTTCAAACATTTAAAGGGACAGCAAAGGGAAGGGAACGAGA
TAAGATGCATCAAGTGTCTTTTGTATTAGAAAGAAGACCAAACCCATTTCAAAG

TCCATTTAAATTCAAACATTTAATCGAAACACACCGTAATACATGGGGAAATGC
CTATATCAATATTCATTGGGGTGTGGATGGAAGACCGAAAGAATTGTGGGCAT
TAAATCCGGCTGTTACAACCCCAATCGTGGATCTGAAGACGAATAAATTATGGT
ATTTTACAAATTTACCAGATGGTACACCTATTAATAATATCTGATGATGACATTAT
TCATCTTACTACGTTGTCTACTGATGGATTGAAGGGAAAACCACCTATTCAGAT
TGCAAGGGAGTCTATAGGCAGCTCACAAGCGGCACAAAAATTTAAAGGTAAAT
TTTTTACAAATGGTGCAGCGCACAGTGGGCTATTA AAAACTCAACAAACATTGG
GTAAAGAGGCGAAAGAAATACTTCGTGACGCTTGGGAAGAAGCGAATACAGGA
TTAAATAACGCTCAAAGGATTGCCATTTTAGATGCTGGACTAGAATTTGAAAAG
GTTGGTATGCCTTTAAAAGATGCTCAATTTATTGAAGGTATGAAATTTGATAAA
GGTGAGATTGCAAATATTTTAAACATTCCTTTGCACATGATTAATGAGTTGGAT
CGTGCTACTTTCTCCAATATTGAGCAACAGGCGTTGGACTTTATTCAA AATACA
TTGAGTCCAATTCTTATACAGTATGAAGAAGAGTTTTCTACAAAGCCTTTTCA
TTAATGAGCAAAAACGTTATTATTTAAAGTTTAATCTGACAAGTTTATTGCGC
GCTGATTCTAAATCACGAGCAGAATTTTACAAAATCATGCTAGATGCCGGTGCT
TTCTCAATTAATAAAGTACTAGAACTAGAGGATATGGATGGAATTGGAGAATAT
GGTGATAAACATCGTGTGATTTAAACCATGTATCCATTGAAATTGCGGATGAA
TACCAATTAGCAAAAGCTAGTGGAGGTTTCGTCTCTGAAAGGAGGTGAGGACAA
TTAAAGACGTGTTTACTATTA AAAACCAAACAGATTCGTCAGCCGATCTATTCA
TTTATGGCGACATCATAACAATTCCGGATGGAAATGGGATGATTCAGATGTTA
TGCCTGATGATGTAAAAACATTTTAGGGCAATTGGATGATAAAAGTAACTTAA
ATATCTATGTAAATAGTGGTGGCGGCTCTGTATTTGCTGGTTTAGCCATTTATA
ACATGTTAAAGCGCAATAAGGCTCAAAAAACTGTTTATGTGGATGGTGTTCAG
CTTCTATTGCTTCTGTAATTGCTTTGGCTGGTGATCGTGTTGTTGTCCCTTCTAA
TGCTTTCTTAATGATTCATAAACCTTGGACCTATGCAGCAGGAAATGCAATTGA
TTTCCGAAAAGCGGCAGAGGATCTTGATAACATTGAGTCAGGAATCATGAATG
TATACAAAGAGAACTTAAAAGAAGGCATTGAAATTGAAGAAATTCACAATTAG
TAGATGCCGAGACCTGGTTAAGTGGTGAAGAAGCTGAAAAATACTTCAACATC
GAGGTTGTGGAAGCAAAGATGTTGCAGCATGTATGAGTGATTA CTTTGATAA
ATATCAAAAAACACCTAATAAGGTAGTAGCAAAAGCTCCTTCCATTCAAAGAA

GGATACTAATGAACAATTAAAAATTTAAAAATGCACTAGACCTGTTAGAACTATA
GGTCTATTTTTGGTGCCAAAACAAGGAGGAAATACCGAATGGATAAACATGAA
CAAGAGTTACGTCAAAAAGTTGCTGATTTAAAAGCGAAAGCAGAAGAGTTTAAT
AATAGCGGTAAATATGAAGATGCTAAGGCGAAGATTGAGGAAGCAAAAAACGC
GAAAAATGAACTAGATAATTATCTAGCCATGAAGCAAATCCAAGTTCCCGATCC
TGTAATTCACAAGCAGGAGTATTACCTCCAGCATCAGTAAAAAACGAAGACCC
ATCATATAAAGAAGTGTTTATGAAAGCTATCCGTGGTCAAATTTAACTCATGA
AGAAGCAAGTGTTATGCAGGAATATAAAGCAGCATTATCTGAGAATGCAGGTA
AAGATGGCGGTTTTATTGTACCGGAAGATATTACTACAACCTATTAATCAGTTAA
AACAAACGGTTGATAACTTAGAACAATATGTAAATGTACAACCTGTTTCAACAA
ACAAAGGAGCTCGTACATTAGAAAAACGTGCGGCATCTACACCTTTTGCACCAT
TATCTGAGTATGGTAAGCCAAATGCAATGCAAGAAATCGCTTCTCCTGAATTTG
ATCGTTTATCTTATGCTATTGAAGATTACGCAGGATTCTTACCAGTACCAAATG
ATCTATTAGATGATACAGATCAAGCTTTAGAAGAATATTTACGCCAATGGATCG
CGAAGAAATCTATTGCCACTCGTAACTACCTAATTTTACAAGAACTCAACAAAT
TGACAAAGGTTGATTTTAAGGATTATAAAGGCATTAAAACAGCATTAAATGTTA
CATTGGACCCAGCTTTTGCAGCCGGAGCTAATATTTTCACTAACCAAGATGGAT
TCAATTACTTAGATCAATTAGAAGATAAGGATGGTCGTCCGCTTCTTCAACCAG
ATCCAACAAATCCAACCTCGTAAATTATTGTCAGGAAAGCCAGTTATTGTTTTAT
CCAATAAGACAATCGCTACAGATAAAGATGGGAAAGCACCTTTCATTGTTGGTA
ATTTAAAAGAAGCTATTATTCTTTGGGATAGAAAACAATTATCTATCGATATGA
CTACAGAGGGTGAAAACGCTTGGAGAACAATACTTCTGAGTTCCGAGCGATT
GAGCGTGAGGATGTTACACCATGGGATACAGAAGCGGTTGTATATGGGCAAAT
TAATATCACACCGAAAGCTGGAGTTTAATAAAAATAGGGGGTGTCTTCTTGGTA
CTGAAATTAGAAGAAGCGAAAGAGTATCTTCGTGTGGATGGTGATGAGGAGGA
CACACTCATTTCTCCTTGATAATAGCAGCTGAACAATATATTTAAAACTCAAC
AAGTAAAGATGTAAATTTGAATGACGAGCTTGCTAAATTAGCAGCTCGTATTTT
AATTGCTCATTGGTATGAAAATCGTGAGCCAGTTGGGAAAACCTGGAAAACCTATC
ATTTAGTTTGCAGTCAATATTAATTCAATTGCAATATTGTGTAGGTGATTCCAC
ATGAACCCAGGGAAATTAGATAAACGTCTTACATTCCAAGTAATAGACGAGGAT

GCAAAGGGCCCAGATGGTGATCCAATAGAAGGATATAAAGATTCTTTTACTGTA
TGGGGCTCTTTTATTTTTTTAAAAGGAAGAAAATACTTTGAAGCAGCCGCAGCG
AATAGCGAAGTCCAAGGTGAAACAGAAATCAGATATCGTGCTGATGTGAATGC
CGATATGAAAATTAAGTATAAGAATACGATTTATGACATTGTTTCGGTTATTCC
AACTGAAAAACACACGTTGTCAATCATGTGGAAGCGTGGTGGAAATGAATGGCT
GATGGTTTAGATTTATTAGGTTTTGATCGTTTAATCACTGAATTAGACCAGATG
GGACTACGTGGGGAAAAAATTGAAGATAGAGCTCTTGCAGCAGGTGGAGAACC
TATTCGAAAAGCTATTTCTGAAATAGCCCCAAGAAGTGATAACCCTAAAACAGC
AACAAAAAGTGAACCATGGCGTACAGGACAACATTTAGCTGATAATATCCGTGT
TACAAAGGCTAAAATGGAGGGCGGCATAAAAACTATCAAATCGGTATAGATA
AAGCAGATCGTTCCTCATATTTTTACGGGAAGTTCGTGGAATGGGGGACATCTA
AAATGCCAGCCCAACCTTTTATAGAACCTGGATTTAATTCTTCGAAAGAAGCGG
CAATTCGTGCTATGACAGATATTTTGAAGAATGAAATGAGGCTGAATCTATGAT
AAATTTGCGCCCTGAAATTGTACAAGCTCTTGAAAATAATCAGGAGCTGGTTTC
TTTATTAGGTGGAAAACGCGTTTATTATCGTAAAGCCAAAAATGCTGAAGAGTT
TCCACGTATTACATTTTTTGAATTAGACAATAGGCCAGATGGATTCGCAGATAA
TAATGAAAGCGAAAGTGAAATAACATTCCAAATCGATATTTGGTCAAAGGCAG
TACAACAGCAATCCACCAAAAAGTGAATGAGGTCATGAAAAGTATTGGTTTCTC
ACGTTATAAGGTTGCTGATTTATATGAAGAGGATACGAAAATCTTTCATTACGC
GATGCGATTCGCGAAAGGAGTGGAATTATAGATGGCTGGAGAAATTATTACAA
TTAGTTCGACTGTCGGTGTAGATAGTCTTGTTTATTCGAAATTATTGAAAGATG
ATACAACAGGCGTCAACTACGACACAGTAAAGAAATTGGAAGGTGCTGTAAAG
GTTAAAACATCTAAAAAAGTAGCTTCTGAAATTATGTGGAGCGATAACAAGAAA
TCGGAAATTGCTGAATCTGACGGTGAAGTTGAAGTTGAAATTGAAGTTAGGGG
ACTTTCACTATCCACGAAAGCAGATATTGAAGGATATCCAGAAGTTAAAGATGG
CGTATTAGATGAAAAACGTGTGGGAGAAAAACCATATTTAGCAATTGGATATCG
CTTTTTAAAAGCTAACGGTAAATATCGTTATGTTTGGTTACTTAAAGGAAAGCT
TTCGCAAGAGGAAGAAGAAGCCGAAACTAAGAAGGATAAACCAAACCTTCCAAA
CAACTAACTTAAAGGTTTCATTCATTGAACGCGATTTTCGATGATAGACCAAAT
TTACAGCTGATGCAGATGAACCGACATTTACAAAAACGGTAGGAGATACTTGG

TTTAGTAAGGTGTATGAAAAACCAGTAGGTAAGTAAGAGGGGGGAGCAAAAG
CTCTCTCTTTCTTTATTAATTTAGGAGGAATAAACTATGAACTAACATTA
ATCGATAAGGAAAATAAACTTTTAATTTACCGGAGTTCATTCCAGCTCGTTTA
ATCCGTCAAGCACCTGAGCTTGCTGAAATCCCAAACAATCCTGGTCCAGAAGAT
ATGGATAAAATGGTTAAATTTGTGGTGAAAGTGTATGATGGTCAATTTACATTA
GACCAGTATTGGGATGGTGTGATGCTCGTAAATTCTTATCGACAACCTTCAGAT
GTAATTAATGCAATTATAAATGAACTGTGGAAGCAGCTGGTGGTAATCCTGTA
TCTGGAGAAGAAAACCCAAACGCGTAGAGGGGGGAGGGCTAACGTTTCAGTGA
GTTTATGGACGAGCTTTACCTCTCTTTATTACGTCAGGGATATAAACACCATCA
CATCGATAACGAAATGGATATTTGGCATTATTTAAGGTTAAATCAGAAACATCG
TGAACAAGGTAATTCAAATGGCGGGAGCCAAAATTCAAACGAGATTGAAGTAC
CAGCAGAAAATATTATCTAGCAAGGGGGTGAGACATTGGCGAATGAAATGAAT
AATTTAGTAGTTAGACTTTCGCTTGATAATGTTAATTTCCGTCAAGGTATTGCA
AATTCAGGCCGTGCAGTAAGGACATTACAGAATGAATTGAAATCTGTAAGTACA
GGTATGGGCGGTTTCGCTAGTGCTAGCCAACAAACACAAGCAAAAATGGATAC
TCTAAGCAGGCTCATTGACGCGCAAAAAGAGAAAGTTAAAGCGTTAAGGCAAG
CTTATGATCAAAAATAAGGCTAAATTAGGTGAAAATGATGCAGCAACTCAAAGAT
ACGCTTCACAAGTTAATAAGGCTGTTGCAGATTTAAATAGATTTGAAAATGAAT
TAAAGCAAGTAAATAAGCAAGCTGAACAAAAGGGAATCGATAAGTTAAACAAT
TCTTTAAAGTCTCTACAAGCTGAATTCCAGTCTATTACATCCGGTATGGGCGGT
TTTTCTAATGCAACTGAACAAACACGCGCTAAAGTAGATGTTTTAACTAGAATG
GTAGATAAGCAAAAAGAGAAGATTAGAGAACTTCAACAAGCTTATAATCGTGCT
AAAACAGAAGAAGGCGAAGCAAGTCAGTCAGCACACGATATGCTGAACAACCT
TCATCGGGCAACAGCTGAACTTCATCAATTTGAAACTGGATTGCAACAGGCAAA
TCGTGAATTGGAACAGCAAGGCAATCGTCTATTGAACTTCGGTAATCGTATGGA
GACATTAGGTAATCATTTGCAAAATGCTGGAATGCAGATTGGCATGGTATTTGG
TGGTATGACTTATGCAATTGGTCGAGGATTGAAATCAGCTGTGGAAGAATCCAT
GAACTTTGAACAACAGATGGCTAATATAAAAAGCAGTATCTGGTGCAACAGGAG
ATGAAATGAGAAAACCTCTCTGAATTAGCTGTAAATATGGGGGAAGACACAAAAT
ATTCTTCTGTAGAAGCTGGAAAAGGAATTGAAGAACTAATAAAAAGCTGGTGTG

GTTTAACCGACATCATCAATGGTGGATTAGAAGGAGCTTTAAACTTAGCAGCCG
CAGGTGAATTGGAAGTAGGAGAAGCAGCAGAAATTGCGTCAACCGCTTTAAAT
GCATTTAAAAGGGATGGTTAAGTGTTACAGATGCCGCTAACTTACTTGCAGGA
GCCGCTAACGCTTCAGCCACTGATGTACATGAACTGAAATACGGTCTATCAGCT
TCTGCAGCTGTTGCAGCCGGAGCAGGTATGACATTTAGGGATACATCCACAGC
TTTAGCAGTATTTGCACAAAATGGTTTAAAAGGATCTGATGCAGGGACGTCCTT
AAAAACGATGCTTATGAGGTTGAACCCCTCTACTAAAGAAGCATATAACAAAAT
GAAAGATTTAGGTCTAATCACATACAACGCTCAAGCTGGATTTGATTTCTTAGT
ACAAAATGGGATTACACCAGCATCTAGAAGTGTGGGAGACATCGAAGTCGCAT
TAGAAAAATATGTAATGAAAACCTGAAGGAGTTAAGAAATGGAATGATAAATGC
GAACTACATTCCGTGAATTAGCAACTAGTTCAGCTTTCTTATCATCAAAATTC
TACGATCAACAAGGGAAAATCCAAAGTTTAGAAAATATATCTGGAATTCTTCAT
GAATCCATGAAAGGTTTAAACAGACCAACAACGAAGTATGGCTTTAGAAACATTG
TTTGGTTCTGATGCAGTTCGTGGCGCAACAATTTTATTTAATGAAGGCGCGCAG
GGTGTGAATAAAATGTATGGTGAGATGTCTAAAGTAACTGCTTTAGAGACAGC
CAATACAAAATGAACACTTTGAAAGGTCGAATTGAACAATTGAGTGGAGCATT
CGATACAATGAAAAGACAATTGGTGATGCGCTTGCCCCTGTGGTTAGTGCTTT
TGTTGCTGGGCTACAGAACTTGTGGATGGGTTCAATGCATTACCTGGTCCAGT
ACAAAAGCGATTGCGATTACAGGTGGAATTGTTCTTGCTTTAACGGCTATTGC
AACAGTTATTGGCGTAGTTCTAGCAGCGGTTGGAATGGTGGTTTTCGGGAATTG
GTTCTTTAGGAGTTGCACTCGCAGCAGTTGGTGGTGTGCTGGAATCACAGCA
GGAGTAGTAGGATTTTTAGGCGGTGCAATAAGTTTATTATTGGGACCAGTAGG
ATTGATAGCGGCGGCGCTTATCGGAACTGGAGTCGTAGCGTATAAAGCGTATC
AGAAAGCAACTGAGGACAGTATCGCGTCAGTGGATCGCTTTGCTACTAATACA
GAAGGGAAAGTGAGTTCCTCCACAAAGAAAGTTCTTAGTGAGTATTTCAAATTA
TCGGATGGCATTAGACAAAAGTTAACTGAAATTAGACTAAATCATGAAGTAATT
ACAGAAGAACAATCGCAGAAATTAATTGGTCAATATGACAAATTAGCTAATACC
ATCATTGAAAAAACAATGCAAGACAACAAAAAGAAATTGAAGGACTTAAAAA
GTTTTTTGCTGATTCATATGTTTTAACAGCTGAAGAAGAAGCAAAGCGAATAGA
ACAAATGAATCAGCACTATGAACAGGAAAAATTTAAAAACGCAAGAAAAGGAAA

ATAAAATTAAAGAAATCTTACAAACAGCAGCTAGAGAAAACAGAGAATTAACAA
CATCTGAGCGCATCTCTTTACAAGCATTACAAGATGAAATGGACAGAGTTGCAG
TTGAACATATGTCTAAAAATCAAATGGAGCAAAGGTTATTCTTGAAAATATGC
GTGTGCAGGCTAGTGAAATTCAGCTAGACAAGCAGCAGAAGTTGTTAAGAAT
AGTGCTGATACTAGAGACAAGGTTATAGCAGATGCAAAGAAAACCTCGTGATGA
TAAAATTGCAGAAGCTATTCGTCAAAGAGACGAAAATAAAACCATTACAGCAGA
AGAAGCAAATGCAATTATAGCCGAAGCAAACGTCAGTATGATAGCACTGTTTC
TACAGCAAGAGATAAACATCAAGAAATTGTAAGCGAAGCTAAGGCGCAAGCTG
GTGAACATGCTAATCAGGTAGATTGGGAGACTGGTCAAGTAAAATCTAAATTTG
AAGTTATGAAAGATGATGTTGTTAGAAAAATGAAAGAAATGGGTTCCGATGTTT
CTAATAAATATGACGAAATGAAAAATGCAGCCAGCAATAAAGTAGAAGAAATA
AAAAATACAGTTTCAAGAAAATTTGAAGAAAAGAAAAAAGCTGCTTTAGATAAA
ATGTCAGAAATAAAAAGTGGTATTGAAGATAAGTGGAATGCAGTTGAAAAGTT
CTTCAGTACAATCAATCTTTATTCCATAGGTAAGAGTATTCTAGAGGGACTTGG
AAGAGGTATCGATGATGCATCTGGTGGTTTATTTAGTAAAGCGGCCGGAATTG
CAAGCGAGATAAAAAAACCATTTTCAGGAGCTCTTGAAATAAACAGTCCATCGA
AAGTAATGATACCCGTTGGTAGTGCGGTTCCAGAAGGTGTTGGTGTGGGATG
GATAAAGGGAAACGTTTTGTTGTGGATGCAGCAAAGAATGTAGTCGGAACCTGT
TAAGAAGCAGATGGGTAATATGCCATCTGTATTTGATTTTGGATTCCAAACCTC
TCATTATAGTGTTCCAAATGATTTAGTGAGTGGTTTTACAGATTATACGCAGCC
TAATACTTCTCATAGTAGCTCATCTACTTCTAAAAAATATTCCCGAATAGACA
AGCTGAAGAAAAAGAATTAAATCTCACATTGAATATGACTAATGTTTTAGACGG
GAAAGAATTAGCGGGTGGAACCTTATATGTATACGACAGATTTTCAAGATCGTGA
TAAAAACGTAAATCTCAATTTTAAAGGTGGTGGCAATGTGGGGAAACTAAGCT
TTACATTTAATAATGTTTCGAAAAGATTATGTGCAAATGCTTGCAGGAAGAAAAC
GTCCAACATGGGCTCCAATTAACGAAAACCTCTTAAAAGTCCCCCATCGTCCAG
GGGCTTATTTTATTAATACAGAACTGAGGAACGTCATATCGATGTTCCCTATTT
TTATTAGTGCAAAAAAAGACATTGCTGATTTGCAAAAAGTTAAAAGAAGACTTAG
CGAACTGGTTGTATACTGAAACGCCGGTTGAGTTAATATTTGATGATGAACTAG
ATCGAACGTACTTAGCTTTTATTGATGGAGCCTTAGATTTGGATGAGTTAGTTA

ACAAAGGAAGAGGTATTATTAGCTTTCTTTGCCCAATGCCATACAAATTAGGCG
CTACTAAAACAAGTGAGTTCGTTCAAGGTTGGACTACAGAAACCACAGCGTATT
TTACAAATGAAGGTAGCGTTGAAACATCGCCGATAATCGAAATTGAGGTTAAAA
AGCCAAGTACCTTTTTAGATGTCTGGTTTGGTGAATATCCCAATGAACGTGATT
ATTTTCGCCTTGGTTATCCCCGAACGTGGAGGAAACACCAGTGCAAGCGCGT
GAACGCGTGATGTGGGATGAAATGGGTTCGCCTATAGGTTGGACTCCTGTTAC
AGGTCAATTTGAGGACATGAAAGGGACAGGTAGTTTTAAATCAAGGGATGGTC
ATGCACTGTATTGTGAAAATTACGGACAAGATAAAGGGTTCTATGGTGCAATAG
CTAAGAAAAACATTCCAGGCGGACCATTACAAGATTTTCGAAATAGAGGCATGG
ATGACTTTTCAGTCTAAAAGCATCGAAGAAATGGGGCGTTGTGAAGTTCTCTTA
CTGGATGACACAAGCAATCTGGTAGCTCGCATTAAACATGAATGATTTATACGTC
ACTGCAGAAATCACAAAAGCGCATATGAAAATGGGGAATAGTGGAACGCCTAA
TAGCATTCGTAAATTGGTCGATACCAGCGGATTTTATTCAAATACATTCAACAA
ATTTTCGGGGGCGCTTGCATCGCTAGAAGAGGGAAACAATGGTCTGTTTTATG
TAGCTAAATTTAAAGATGGTACAGAGATAGACGGAGCATCACTAGTTGAACAAT
GGAACGATGTTGACAACAGTAATCCAATGACAAATCGGAAAATCGCACAAGTA
ATGATTGCAATGTGCAGATGGGACAATCACCCCGCAGTTGATATCATGCAAATT
GATGACTTGAAAATTTGGAAAGTGAATAAAGTTGATGAGAACGCAAGACCATA
TATCTATGATGTTGGCGACAAAATTATCATTGATACCGAAAAAAGCCTCGTCAC
AATCAATGGTAAGAATGCTATAAATTTTAAGGATATCTTCAGTAACTTTCCAAC
GGTCATACAAGGATATAACCGTATGGATATTTCTCCTCCTGACGTTAAGGCGAA
AGTATCGTTTAGAGAGAGATACCGATGAGGAAACCTAGTGGAACATTTTCATATT
GTTGATTTTAAGAGCGATCAAATCATAGCGGCTATTCAACCACAAGATTATTGG
GGTGATAAGCGACATTGGGAAATTAATAAACATTGATATGCTTGATTTCACT
GTATTTGATGGAACAGAACAAGCAACTACATTAATGCAACAAAATTTAGTTTTA
AAGGAAGTAAGAGACGGTTCGTATAGTTCGGTATGTCATCGATGATACGGAAAA
AAAATCCGATGGTTCGTTCCATGACGGTGTATGCTTCAGGTGAATGGGTGTTGTT
GAAAAAGGCAGGAATTATCAAACCACAACGGATTGAGAGCAAGACAGTGAATG
AATTTATTGATATGGCGCTTGTAGGAACCAAATGGCAGCGTGGAATTACAGAAT
ATGCTGGTTTTTCATACAATGACAATCGAAGAATTTATTGATCCACTCAAATTC

TAAAAGATATCGCCTCACTTTTTGGTTTTGGAAATTGTTTATCGAGCAGAAGTTG
TTGGTTCTCGTATTGTTAGCCGTTATGTAGACATGGTGCAAAAAGAGGTAGAG
ATACTGGGAAAGAGGTTACTTTAGGTAAAGATCTAAATGGAATTACTAGGAGA
GAAAACCTCTCAAAATGTTTGTACAGCACTTGTGGGATTTGTAAGGGGAGAAAA
CGAAAAATAATAACTGTAGAGAGTATTAATAATGGTCTCCCTTATATTGTCTGA
TAGTTCAGCTTTTCAGCGTTGGAACGAAGACGGTCAACATAAATTTGGTTTTTA
CACGCCAGAACTGAAGAACAAAATATGACACCTGAACGTTTAATGGCACTTAT
GAAGATTGAATTTAAAAACGGATGAATTCTACTGTTCAATATGAAGTGGATGC
AATTGCACTTGATAAGATATTTGGATTGTCACACGAGGAACTGTAGAAGGTGA
CATTATAAGGATTAAGATACAGGGTTTACCCCTGAATTATATCTAATTGCTCG
TGCTATCGCTGGCGATGAATCATTTACAAATCCATCTGAAAATAAATATGTGTT
TGGTGATTATATAGAAGTAATCGATACGAGAGAAGAAATGCAAAAGTTATACAA
TAAGATTCGAAATTCCTGTGGGATAAAGCAAGTAACGAGGCATTAAAGCTGC
TAGAAAAGCAATTAGAAGACACGTCTAGTGGTTTTAATGAAAGATTAATTGCTA
TGAAGACAAGTATTGAAAAACGGACGAATCTATTATTTTAAATGCCCAAGCTG
TTAATCAAAAATTAGAAAAGCTAATAGCTGACTTGAAAGTTACTGCTCAACAAA
TAAGTGCAAAAGTCGGAAAAGGTGATATCGCTTCTGAGCTAAATATTAATCCAC
AAAGTGTACTIONATAAAGTCAGAACTTATCGACCTAGTTGGTAAAGTAAAGGCAG
AATGGTTAATTGCGGGATTACTCGAAGGTATGACCATAAAAACTAGTAACTCTA
AAGAGCATATCCATATGCAGAATCAAGTGGTTAAGTTCGTTAATCAAGGTATCC
CTAAAATGATAATGGGGTTTGAGAATGAGTACAACAGTAGCACTTCAAATCCAT
ATATTACCTTAGGACAGGGGGATGGATCAGGACGAAATGTTGGTACCATTTAT
AAAGATGGTGGTGGACTTTACTTACGTTTTATAGATTTAAATGGTGCTGAAAAT
AATATTCGCTTAACAGCACAAGGGAATATAGGTGTTACAGCTCAAGATGGTATT
TGGGTAAATTCCAAAAGAACAAATTTTACATCTCTAATAGAAGTCCCAGCCATT
AGGTTTAATTCGTTAGGTACTACTCCAGGTTTCGCAGCAGGGTAATTTTTGGATT
GGCAATGGATATAAAGGATTTGGAATATATTACTACGATAATTATTGGAAGTTT
GTACAAGGTTCATAATAAATAAATGAAGGAGAAATAAAATGAATAAATTTTTAG
GGGTTTTAACAGTAGTTGGGGAAGATGGAACGATAAAAAGTACCATTAGACAAG
TTACAAACCGCAGGTATTAAGCCTAATTCAAAAGTGGAATATTCAGCGACAAT

TCTAACTTATTCATTAGAACCGCAGAGAAATTTTGTGATATTTGTGGCACTAAT
ACTAATACTACGAGTGTTGGTAATCAAGAAATTTGCAAAGACTGTTTAGATAAA
ATTACAAAAGCGTCACAAGAGAAACAACAGACGGTCTCAGAATAGAAAATTTA
ATTAGTTAAAACAGATGGAGCAGCAAACGCTGGTCTTTTTTATTTTGCATAAAG
GAGTGATTTTATGACATTCAAGACCTATGAAATTAACGTAGATTTAGTAAATGA
TACATCCACAACACTAGTTCCAATCGCTTTTCGCAAATGATAGAAACTCCGCTAA
ATTTGTATTAAATATAACAAATGAAGGACGGGAATTAGATTTAAGCCAAGCGAA
ATCGGTGCGGATGTCATTTAAGAAGCCAGATGGAACCTCGTGTTTTCCAAAACG
ATTGCCAACCGATTAATGCAATGAAGGGTAAATATCAAATTGTATTAAAGACCC
AAACTCTGACTTCAGTTGGTAATGTTATCGCGCAGATCCACATTGAGGAAGAG
GACAGAATCCTTGATACACAAAAGTTCTTTTTTGTAGTAAATGATTCGTTGGCA
AGTGATGAAGCGATTGAGAGTACAAATGAATTCACAATTATTCAAAAAGCAATT
GAAGCAGGGAAGAACTTGAAGGTGTAGATATCAACGGGATTATTGACGCTGG
CGTGAAAGCGGAGGGGGCCGTAAAGAAAACAGGGGATACGATGACGGGGCAC
CTTGATTTAGATGTGACTATTACAACAAAAAGCATTAGAAGCACCTCAAGTGGA
AATAGACAATCTGGAATATTTTTTGTATCCAAACGGGGACTTAGGTGCCTATGAT
TGGGGGAATCCTGATGGCGGGACAGCTCTTTTTAGATACACTAGAGCTAGTAA
ATCATTCGATATAACCGCCCCACTACTAATCTCGTAAGGAAGGCAGAGGTATT
TACAGATATAGCTAAACCTAATGGTGACGCAGCTATTTTCGATACAAACAGGACA
AGACATGCTTGCAGAAGTAATAAACTAGGGAGAGGTATCCGTA CTATATACG
CTCCAGGTAGCGCGCTTAATAGCCCTTCAGATAAAGTGTTCCGTGGTATTGCAA
ACCTTCAAGGTACTTCTTATGGGTACATAATTGGAGTTAGTTCTGATAATAAAG
TTTGGTCTAATTTTATCAATGGTTCTACCTGGTCTGGGTTGGGTTTGTGCTAATG
GGAATATAAAAGATGGACAAGCTACTCTTACTTTAACAGATAACGCCGCTCAGT
ATGGCACAACATATACGCCTATAGCTATTAGAAGAGGTAATACTGTA ACTATTC
GAATGGCAATTACTCGAAACAGTAATGCAAGTGGAATTTTAACTACTTTACCAT
CCGATATGCGACCTAAAAATGGATGGATCTCTACGATTATTTGACTGACGGAA
TGCCAAGTGATTTAACTATTAGAGTAAATGGTGAGGTTGAAGTTCTCACTAAAA
GTAAAACATTCTACATCACGCTTACTTACGTAGTAGATTAAAAGGAGGATATCA
CATGGCTAAATATTACGGTTATTGTTATGACGAAAACGGTAAATTC ACTGAAAT

GATTCCTTTAGAAAGAAAAGGAAATTACTGAAAAACAACTTTTTACCGAGAAGA
AATGAAAGAGATTGTTACAGAAGAGAACTATGTAAGCTTCATCAATCGATTGT
GGAGGGAGCTTACAAGCCGTCTGAAGGTGAGGAAGAACCAATCAGTAAATACG
ATTGTCCTGATTGTGTAATGGCAAATGTAGAGTATGAACTTTTTAAAGTACCAT
ACGAGGAAGATGTTGTTATAGGTTATGAGCCTGACATCCCTGAAAACTGTACCT
TAGAGGTTTGTCTCTGATGGAATTTATTATCCAATATTCAAGGATGGTAAATGGA
TAAAAACAGTTGAACCGAAGCCTGAAGAACCACAACCACAAGAACCATCTGAA
TTAGAAAAAGTAAAAAAGCAACAGGAATTAATGCAACAAGCAATGGATGAAAT
GATTATACAAAATCCAACCCCGGATGAATTAGTAGAGTTAAAGAAACGTTTGAT
ACTTATGCAATCAGCAATTGATGATCTCATTATTTCCGCTACTCCAGCAACACT
GGAAGGAGGTAGTAACTAATGGCTGAATATATGGCGCAACGAATTATTGATGA
AGCTTTTACCTATACGTTTATCATTATAAAAAATGAAGGCGTACAAGGAGCGAAT
TGATAAATACCTAACTGATAATGGTAGAGCAGATTTAATTACAGATAACGTAGT
AGCGGCTTATTTAGTATAAAAATACGGCTTTGAGTAAAAATTCAATTCATAGATC
AAGAGAGGCATATACATGCTTCTCTTTTTATTTTGAGGAGATGATCAGTGTGAA
ACGAATAGTAGACCAAGCAATTTATGAAAAGCATGTTAGCCATGAAAATAAAAA
CCTAGTCAAAGATTTTCTAATTGAAAAGAAAGCACAAAGGGAAAGCGGCAAGCA
CTTTACAGCAATATCATTGGGACTTACGAATTATTTTGTTTCTAATACATCAACA
CTTCGAAAATAAAAAATCTTATTGAATTAACACGAAAAGACATTCGCAATTTATC
TATTATTTTTCAAGAGCTGGGAATGTCTAATGCACGTGTGAATGGATTAATGAG
TGCATTAAGATCCGCATTAGAATTTTGTGCGGATGACGACGACTATGCTTATGA
ATTTAATGTAGGTTCCAGAGTTCGAGGATTACCTAAAAATCCAGTTAGAGAAAT
TACTTTTATAACTGAAGAACAAATTGAGTGGTTAATCGATGAATTACTTAAACA
AGAGAAATATATGTTAGCAACTTATTTAGCGCTTTCTTACTACAGTGCAGCAAG
AAAGAATGAGGTTTATCAGGTTCAAAGGAAGAGCTAACAGAGCGATATTATA
CAAATATCGTTCGAGGGAAACGCGGTAAAAAGTTTAGGTTATATTACAATCCCC
GAGTACAAGAATGTATTCGTTTATATATAAATCAACGAGGTAAGGATACTGTTC
CAGATTTGTTTGTAAGAGTTTATAAGAATGGTGAACGAAGAGTGTTAAATAAGA
GTGTATTCAACTACTGGTGCAAGATATTCGCTAAGATGCTGTATGAAAAAGAAG
GAAAGGAATATAAAATCAATCCTCATTGTTTCCGTCATAGCAGATTAGATAATT

TGAAAGTACAAGGCGTACCATTAGAAAAGTTAAAATCGCTTGCAAATCATTTCAG
ATATTTCAACAACACAATCCTATTTAAAAGATAGAAGTGAAGAGGATATTGCAG
ACATCTTTGAAATGGATCCAAGTTGTTTTGCAGCGTAAAAGGAGATGAGGAGA
TTGCCAGAACATGAAAATCATGATGATTTTACAAAAGTAATTATTGGATTAACG
AGGGTAGAAACAAAGATTGATGGTCTTGGTAATGTAAGGGAGCTTGCGATTGA
AGCGCAACAATCAGCGAAAAGTGCTCATTACGCGTTGATCGATTGGATAGGC
TTGTATTTTGGATGGGAACAACAGTTATCGGTTTCGCTTATCGCCGGTGCGATAG
CGTTACTTTTTAAATTTGCAGGAAAGTGATCGTATATACGGTCACTTTTTTTATT
GAAGGGAGGTGAAAATATGAAAAATTTTGATACGGCTTCAATTAGTCGATATGT
CGTATTAGTAATCGCTGTGATTAATAGTGTCTTAAATCTTGTGGGATACCAAAC
GATTGATGACAAAATCACGAACGATTTAGTCGCGGTAATTACAGGGGCATTCA
CTTTGTATGTAGCTTGGA AAAACA ACTATTTAAGTAATAAAGGCTTACAGCAA
AAGATGTATTAGAAAAAATAACTTACACTAAGAGGAGATGTTGAATAATGGCT
AAATATAGTTTACATGGTGGTCACAATAATATTGTACAAGGTGCTAATTATGGT
GGCCGTAAAGAACATATTATGGATCGACTTGTTAAGGATGCAGTTGCAGCTAA
ACTTCGAGCATTAGGGCACACGGTATATGACGATACAGATGAAACGGGTTCTA
CACAAGCACAAA ACTTATCAAATATTGTTTCGTA ACTGTAATTCTCATGATGTTG
ATTTAGTTATCTCATTCCATTTAAACGCTTATAATGGAACAGCTAATGGGGTAG
AGGTTTGTATTATGACCAACAATCTTTAGCAGCAAAGTGTCGGCTCAACTTG
CAAAGATATCGGTTGGTCTAACCGTGGCGCTAAAGAGCGAAAAGAACTTTAC
GTATTGGCAAACACTAAAGCACCAGCAATCTTAATTGAACTTGGGTTTCATTGAT
AATGATGCGGATATGGCCAAGTGGCATGTAGATAATATCGCAA ACTCAATTGTA
TATGCTTTAACTGGACAAACTGTCCGGTGGTAATGGGAACACAACA ACTCCACC
GTCTAAACAAAATATCATTCAATCAGGAGCGTTTTTCACCGTATGAAGCTCCTGA
TGCTATGGGCGCGCTAACGTCCTTAAAAATGACAGCTAAATTCATTTTACAATC
TGATGGATTAACATATTTTGTCTGACCCAACATCGGACGCTCAATTAAAAGC
AATGAAAGAATACCTTGACCGTAAAGGTTGGTGGTATGAAGTTAAATAATACAA
AAGAATAGTTTTATGAACAAAAAAGCCGTCATTAGACGGCTTTTTTAATTTTT
CCATTCAACGAGAGTACGTTTATTACATCTACGACAGATAAACCCCTCAGCTTT
ATGTACAATAGGCTGTTTTTTGTTACAATTTGGGCATTTTACAAGTTGCTTACCT

AAAGCGGAATATATAAAAAGTGCAGAAAAGAATGCTAAACCTAAACCTGGTAA
TATTCCAATTATGGTAAAGCATAGCACTACTGAAATTAATAAACCGAACGATCC
GATTA AAAAGTATATAACTCTTTTCAACTGATTAGCTGTAGA ACTTTTCTTTTCT
TCTAATTCAATAATGAATGTTTCTCCATCAGCTGTTTTTTCGTAGCTCCATAAAAC
CTCCCCCTTATATTAAGTAAATCATACCAATTAATTGTATATTTTAAAAGTGTGA
TTTTATTCAATATCCACCCATATATCCTCAACCCGCATATTGAGTGCCTGGGCT
ATACGCATTGCAACTCGTAGTGTTGGTTCGCTCTTCCCCCGTACTATCATACTT
AATGTTTGATCTGTTATGCCAGCTCGTTTTTGCTAATGCAGATTGTTTAATCATTT
TATCAGCTAAAATTACTTTCAATTTGCACTGCATAAAATCCCTCCTTTTAAAATA
CTCAATCATATTTTTGAAAAA ACTTTTGATTTTTTTTATTGTTGGACAAACAAGTT
TTTAGTAGTGAAGTCATATACCTATATCAAAGTAACTACAAAGGTAAGGAAACA
GGCGTTATTACCATGAAAAGGAGACGGTCTACAAAGGTAGCTGAAATTGTAGA
TGTTTCAA AATTAACAAAGTAATTACCAATGTATATATCAAGGTTTCGATTACCA
TGGTTTTGAGTCCTGCAACATAATGAGAATGGGATTTTAAATTTTGTTTATAAG
GGAGCGAGGAAGATGGGAAGCGGAGGAGCTACGAGATTAGAAAATGGATATG
AGGTTATTGGAAACAAAATAAAGTTCTTTTTTAAATCAAGATCCAACAAAAGGGT
GGAACCAAATTCGAAACCTAAATTTAGAAACATTCAAGAAATAAATGAGTGGT
GTGGAAGTTCTGCTAATGAGATAGTTTGTCAATGGGATGCACTAAATCAAATG
CAATGAGTACATCGGAAACCACAGATTTTTTATATAGGTGGATGAGTTGGTATG
TAACCAAACCTTTAGATAGCACAGCAGTCGAAATAAGGAAATTGCCGGATGAG
TTAGCGATATTCATTACGAATGTTCCATTTCGATGCAATTGATTTATTGAAGCGT
ACTTCTCAGATGGTTTTAGAGTGCGTGTGTTTGATGTTTAAAATGTTTCATGTGA
AGGAGTGGTCTTATGTTTAAACGAAAAGAAATCATACCATTTTCGTGACTTTATG
GATGGATCATTTAAGAAGCAAAGCAAACAAAGATACTAAGCGTTGAACCAAT
AAGTCCAATAGCATTTTTTTCATATGGCTCAACCGCTTGTACACACATATGTAGC
GCTAGGGATATTAGGGGGACTTACAATTGGAGCCGTGTTATTGGAAAGATACT
TAGTTCAAAATGATCATATTACAGCGGGTAAAATGGTATCCGATGGGTTGTATC
ATGGACTCCGGATAGGTAGTATTGGCTTCATTGTATATGTGTTTCATTTCGTATCG
TAAGGATGTTTTAAAGGGGAGTGTATGAACTTGATGAAGGAATGGTTTCATAAA
AGAGCTGTCAAGAATCTGTTAATTGAGGTATTCAAAAAAAGTGGTATCTATTAT

GAACATCAAACAAGGGGCGGTAAATTACCCGTTTTCCCTAAAATCCATAATGTT
TTAGAAACAAAAGATTCTATTCGATATACATTTACTTTACCGAATGGAGTAGAT
CCACAAACGATTGAAAAGAAATGGTTTTGCTTTCAGCAAATCTTAGGAAAGGAA
CTGGCGATCGAAGGGGATATCAAGCGCTTTGTACTTCACTCGTTCAAACATAAT
AAAAGTTTACAAGCATACTCGTATAACTATTCAGATTGGTTACCACATCTAAAA
GGACATAGCATCCCTGTAGTGGTAGGAAAGGACCAATTTGGGAAATGGATTGT
ATATGATATGACGGATTCCAATAGCCCACACCTATTAATAGCAGGAGAAACCG
GATCAGGAAAAAGTAGTATGGTTCGAGTTATATTGTCTACATGGATTCAATATT
TGCCACCAGAATCATTGCAGCTGTATTTAGGTGATCTGAAGAACTCAGAATTC
ATTTTTTAAGAAGAGTGCAGCATGTAAAGAAAGTGTGCATGGAAGAAGCAGAA
ATGGAGTTAATGTTAAATCAGTTGTGGATGGAAATTATTAAGACGTAAGTGC
ATGGAGAAATATGAAGTGGACCATGTTAACGAATACAACAAAGTAACCAGAGA
AGAAAAATTACCTTATATTGTAATTTGTATTGATGAAGTGGCTATGTTGGAAGA
TGAAACCGATAGTATGAAGATTGTTAGAAAAATATCAGCTGTTGGACGATCGCT
AGGCGTGTTTTTACTGTTATCGATGCAACGTCCGGATGCAACAGTTATAGATGG
TAAATTGAAAGTGAATATGACAGTTCGAATGGGTTTTCCAGTGTGATTCATCACT
AAACGCAGGGATTATTGGTACACCCGGATCAGAACTGTTAGAACAATCAGGAC
AAATGATTTTTCAAATTAAGGATTAAAGAAAGTGCAAGCTCCAGAGCTAAAGT
TAGAAAAAGCAAAAAAATAGTGGCTCCTTTCAGAATGAAAAAAGAAATAGAA
GTAAGTACTGAAGTGAAAGAGGAGCCTTTATTTGGGGTGTTAGATGATGAGGA
ATAGAGATATGGCTATTTTGAAGGATTTGACTAAATTTTCGTTGTATGTCACGGG
ACGACATTATGGAATTACACTTCGGCCATTTGAAAAATCCAATCACATCATGCA
ATACAGTATTAAGATTACGTAGAGATGGACATATAGAAGTGAATACTACAT
TTCAGCCATATGTATATTTTCCGCAACCAAGTACAATTAGGAAAACAAGTCAAA
AAATACCACACTTTTTAGGCATAGTAGACGCGTATAAACAGTTAATTCACATG
AGAAACCTAAGATTTTTAAAGTAGAACCTAAGTATGGAAAAGAATATATGGAAC
CTGACATATTTACGATTTGGCGAAAAGCTCCATTTTTTTATTGAAGTACAAAAAT
CAATATACAGTAAAGCCGTAATGCAAGAAAAAATTAAGATATGAAGTGTATT
TTTGTAGTATGAAATGGCAAGAAGAATCATGGCAACCATCCAATAAAAAAATAT
TCCCCGCCATTTAATTCTTACTGATAGAAAGTATGATGTCTCCAGCACAAATT

TCCGTATTTTTCAAGCGAATTCAATTAAAGATTTCTCAATCAAATAACACCTAA
ACAACCTAAAAAAGATATTTCTATTCAAGTTGGATCAAGAAAAAATTAATTTAA
AAGGAGCGATTTATTATGAGTGAAGCAACAAAAGAGTTAAATGAAATTTTTTGT
AAGTATGATGTGAGTGCTGAAGAAATAATCGAAATGATGTCACAATGGTTAGA
AAGAAAAGTTTGTGATAATCATGAAGAACTTTAGAGGAATATGGAGAAAACG
ACTTTATACGTTTAGATAACCTTCATGCTGATATAAATAAATTAGATTGGAAGT
ATAATTTCCCGTATTAATAAATAATCACAAAAAATAATGGGCATATATATAA
GAAGAGAGTGTCACTCAAATGACCACTCTCTTTTGACCACACAGACCACATTG
ACCACAACCTGGTACCACATTTATTATTTACTTTTATGTCCATTTTGTCTAAAATAG
AAAATATAGCTAGACAAGAAGGTACGTTTTAACACATAATGGACACAATGCTTC
TTTAGAGGTGTAAAGAAAAA ACTTACACTATAAAAGCATTATATCACTTATACC
GCAGGGTTTAACCTTCTTGTTTTTCTTCACCGACCACTTTTTGACCACTTCGAC
CACTTTTTAGTACATTTCCAAGCATTTCAGTTACTTCAATTTGACGTTCTTCATA
AACATCAGTATAAATATTTAAAGTTGTAGAAACATTTGTATGACCAAGTAATTT
CGAAACAACCTTTGCATTTGCACCAGAATCGATTAAAATAGTTGTAAACGTTCT
TCGGATATCGTGGAATCTAATATACGGTACGTCAATTGCTTCGCACAAAGCTTT
CATTTGATAGCGTATCGTATATGGATGCACGATTTTTTTTATTTCTTGTACAAATT
AATAGGTCGAAAGAATTTTCCTTCTTGTGATTTTGATATTTTAAACAATTCTCCCA
TTAATTCTTCTGTCATTGGGATTATACGATTAGATGCTTCGGTTTTTGTCTCACC
TAATTCATACTTACCATCCACAAGTGTTAACGTCCTTTGAACATGGATAGTCTT
GTTTTCGAAATTAATATCATTCCACTTTAGAGCCAATACTTCTCCGATACGCAT
GCCTGTATGCAATGCTAAAACAAATGTAATATAGTAACTTCCTTGTATTTTTGC
ATACTCCATAAATTTCAATTGCTTCTTCAATTGTCCAACCTAGCTTGCGCTTTCTTT
TTAACTTTTTGGTCGTTTTGCTTTCTTAGCTGGATTAGAGTTAATCATTTCTAGCT
CTACACCTTTATCAAGTATTTGTTTTAACATAACATCAACAGATGAAATGTATTT
CGTAGTTAGACCCTCTTTAAGTAGTTTCTGGTGAAAATTATGAACAGTTAGGGG
TTTTATATCTGATAACCTCTTCTCGCCAAATTCAGGCATAACACGAGAGCGTAG
AATGCGTTTGTATTGATACAATGTTGATGGTCTACATGATGATTCTTTTTCTTGC
ATCCAGATTTCTACGAGCTGAGAAAAGCGAATATCACTATTCTCATAATCCCCA
TTTGCTAAATCATTTGTTACCCTAGCCACTTCTTCTTGAGCAGCTTTCTTTGTTT

TAAAACCACCTTTAGTGATTTGTTTCCGTTTACCTGTGAGAGGGTCTTTGCCGA
TATCCATAGTAAAAGACCACCTCTCACCACGTTTACGAAAGTATGCCATGATTT
TTCACCTCGTCATAGTCGTTTTCTAGATACAAGCTGTGATATGTGGTAGTGGTA
TAAGAAATGATAGCATGTAAGCCTAATTTCTGTAAAAGGAAATTTACAGATATA
AAAGAAGTGAGCTACAATATTTGTATATTAATAAAGGAGGGGAAAATATGTG
GGAATTTACAAAGGACCCTGGTGGTCACAGAGGAACCGATCCTGGTGTAGGGT
GGCATAACGATCCAGGCGGTGGTGGCTGGAATACAATGAAGATCCAGGAACA
GGATGGAAACCAATTTATGGTCCGGGGACAGGTGTATAAAAAGGGGGAGAGTG
AGATTATGAAAATCTACATAAAAGACCCAGGAGGCTCAAAGGTAATTTCTGATC
CAGGAGGAGCAGGTGGAAGTCCGTTAGTACTTGATCCAGGTAATGGGGGCACA
GGATTAATAAATAGAACCAGGTGGACATAGAATGAACGAGCCAGGTGGTGGAGG
TTTAAAAATAATACTGATCCAGGAGGATGGTAATTTATGTTATTACACTCTAAA
GAATCACAGGAACCTGGTACAGGATGGAATTTATACGATCCGGGTACAGGAAT
GGGTATTTTCGATCCAGGTGGCGGAATGGGTATGTATGATCCTGGGGCAGGTG
GAGGATACATAAAAGATCCAGGCACAGGAATATAAAAAAGAGAGCTATATGCT
CTCTTTTTTATCGGTAAAAATTTGTTAATTTTTACCGTTGCGATTGGAAATCATT
TCTTCTAAAATCAAATCATAACAACCTCGTTATGATTTTTTAAGAACTTTGCATAC
AAAACGAGTTGCTTGCAGAATTGCTCTCGATGAGACTCATCCAGGCCTGCGAA
AACCGTTTGAATCTCATTGAGAGTATTTGCTATATTCTTCTCGTTTAGTGTAGTT
GTTCTTCCCATTAAGCATCAACCGATACACCTAGATATGATGCAATGCGATCC
AATGTGTCGAGATCAGGCTGATTATAGTTGATTTCTAAATTACCAACCTGGCTA
CGACTTAATTGTACTTTTTTCACCGAACTCTGATTGAGTCAGGGAACGACTTGCT
CTAAACTTTTTTAAATTTTCTCCAAATGTATTCATAATTTTCAGTATAAATACATG
AGAATTTTTTAGACTATACATGTCATGAAATTTGTCTATATAATATTAATTATCAC
GTAAATTGACAATGAATTTGAAAACGTATAGAACAAATGTTCTTTTGGTGGTAA
AATATTCTTAATGAAAAAATTGATTTTTTTGAAAAAACTTTCTCAACATGATTTG
ACCATAATCGGAACGAACATTCTAAATCTTATGATAAACTGAAATTAATAAAAA
AAGGAATGAAAAAAGACCCACGGTGTATAGATGTGAGGCCACACATCTATA
ACATTTACCCCTAGCCTAGATAGGGAAAAGTTTCCATGAGTCAGTACATAGTAT
ATCATACTTCGTAAGCATAAAGAGAATTATGGTTCGTTTTCTATTGAGAAATA

AGGGATGTGTTTTGGGTTCTGATTTAGGAGGAATTTTATAATGAAGAGCTTTAT
CAAGAACTTACAAGAACATATCAATTATGTTAAGTTGGACGTTGGCACATTAGC
TAAAAAAGCAGAAATTGATAGAACTAATCTTAATAGGGTATTAAATGGGAAAAT
TAAAGAAATGAAGTTAGATTCATTTTTATTAATGGCTCCTGATCTGTATCCGAA
CTGGGCAGAACGTAGAAAGAAAATTAGAGAGTTTATATTAGTTTGCGAGAGTG
ATTTAAACATAAAAAAGGGGCTGTCTTATTGTCAAACAGTCGGTGAGTATCAAT
TAATGAGAAAGTTAATAAAGAAACATATTAGCAGTGATAAGAAAGGGAAAATA
AACAAATATTTACATTTGTATGATTTATACAATCAAAGGAATCTCAGTAAGTTG
GAAGGAGAAGGATTACAACGAAAACATAATGAATTACCTTTCTCTAAAAATGTT
GACTATCAAATAATAGTAGACATGCTGCATGGATTCTCTCTATATGACAGTAGT
AATTTTCATGGCTATGGTCCCGTATTCTAAAAAAATTGATCTAAACTTACCTCTA
GTAGAAAATGCATTTATAAAAAAACATTTGGATTTGCAACACGATGATCGAAAA
GCTCATATTAATTTGTTTAGCAATAAATTAAGAATGCAGAGACATTTGTAAT
AGTATTATAAAATCGGCTCCGGAAGATTCAGTTATAAAGGCCAAAGCATTAAGT
TGCTTAGGGGAGTCTTTTATATTTGAAAACCTTTGCAGGCGGAAATGTACTTT
TTGGAAAGTTTAAAGTTAATAAAAAAATTAGGTATTACTGATTATAGTAAATTG
TATCGTGCAGTACATGGCACATTAGCCTTTTTACGAATTGAATATGGAATAAAC
TTAGATGAAATAGATTGGAATTTTGTAGGTGAAGCAGAAAAAGCATTCTTTGAT
GCTAAATTTGGGTCTGGGGATAAAGCTAAAGTTTATTTTGAAGACTTAAAAAGA
CAAGGAAAAACTTTGTCTGCATTTAAATTATATTATTTATTTTTTTGTAGATGGAA
ATGATATAATGGTTCTTAAAGATGCGTTAGAAAAAATTGCGAATAATGGAAATG
TATTCATTTCAAATTTAATTACACGTGTATTAATTAAGAGGGAGTGAAGTAGG
TTGAAAAAAATTATTATTACAATGGTATGTGTCTTAGGATTACTAGGAGTATTT
GAACAAAATAAAGATACTTCACAAGTGCATTCGATTAAGGCAGAAACAACATAT
TTCATGGTTGATCCAGGAACTCATTAAAAAAATAAAAGTTATTTTTTTCAAGACG
CTACTAAAAGTAGCGTCTTGAGTGCTTTTTAGGGGATATGCATTTTTTGAAATG
CGTAACAAAAATGCACAGTTTGTAAAGAATCACATAGTTATTGGGATGGAGG
AGTTCGTATTGTTAATAAGTGGCGAAGATAAAATAAAATCCATGATTAATATT
TATTGGGGGATAAAGTCTCAGAAAATGATACTCTTCATGCTTTAGAAGAAATAC
ATAAACAAGGATTCATTACTIONGATAATGAATTAAGTGAAGTCATACAGCTAATGG

AACCAAAAAAAGGACTAGCCTCATGCTAATCCTTTTTTCTTGTTTTAACATTCTT
TGGATAGCTACTTCTAAAAGTGCTTTGACACTTTTCGATCTCGTCAGGAGACAGT
TTTCTTCCATCCCAATGTAATTCGTCACTTTCAAATATTTCTTTTATATTATTGC
TGATTTTAATGGTGCTATCACTTTTCCCTAACAAAAAGTCAGTGGGTACATTGA
AGAAATCAGCTAATTTTTCAATGTTCTCACGAGAAGGGATTTTCGTCCCTTTTT
CATATTTAGAAACAGTTTGCTTGCTAACACCAATGTTTTCGCCTATTTTTTTCTTG
AGTTAGCTTCTTTTCTTTTCTTAACTCAAATATTCTCTCCCCTATGATATTCATC
TATAACATCCTTTCCCGCTACTTGTAATAAAAGTATCTAGTTTAAATGTATCAATC
AGTAGCTCTATTGGCAACGCAAAAATAAAAAATAAATTTTTTAAAAATAAAATGT
TGCCTTGAGGGCTACTTTTGGTTATACTAAGTTTAGAAGTTGAAGGTGGTGACT
TAAAATGCTAAATACACAAAGAATTAAATCTTTACGACAAGAGAATGGGACTC
TTTAGACTATGTTTCAAAGCTTTAGGTCTAAAATTTAAACGTTTCATATCATAAT
GTTGAAAAAGGCGAATCAGGTTTATCAGTAGAGAACTAAAAAACTTTCAGA
GCTTTACGGTGTACCAATTAGTGATTTAATAAAGTGAGTGAGTTTTTTTTTACA
ATTAAAGTCGCCCTGAAGACTACAAGTTAAGGGCGACTACATGATAGTGTAT
CCATATTTATATTTCTAAAAAATGATTGGAGTGAAAAGAATGTATCAAATAAAG
CAACTACCATTCTCGATGAAAGCGGAGGATGTACAAGAATTCTTAAATATTTCT
CGTTCATCTGCATATGCACTTATGAAGAGAAAAGATTTTCCACAATCGTAATC
GGAAAAAGCAAACGTGTTAAAGCGGAAGATTTTCTTAAATGGGTGGAAGCACA
AAAGGTGGGAGCAAATGCTAGTTAAAATTAATTTTCGGATTTTCGATAAAATTA
CCGTTTGATAAATAAGGGGGTGATTTAGTGGAAGATTTAACAGCATTAGCTATA
TTCGGATTTTCAACCACAGGTGGTTTATGGCTGCTTTATATCACTTATGAGCCG
ATAAGAAAATGGGCTTGGAGTGATGTAGAACAAAATAAAAAGACCCATGGCAG
TGGGTCCATTAGAAAAAACAAATTTTTATAAGTATACCACGGAAAGTAGGGAAA
TGGTACATGGATTTAATCGAATATCAAGTGCTATTACCTAATAAGTTTTTGAAT
TTAGCAAAAAGCCAAGATGAATTA AAAAGAATGATTGAACAGTATCTCAGTATC
GGTTATCCGCATTATGAAATTCACAAATTATTA AAAAGTGGACAAGCGCATATA
GCAATTTGCACGAGGAGGTAAGGGCTATGTCTGAAGTAAAAGTGAAATGGATA
AAACTCTCAACAACGATGTTTGAGGATGAAAAAATACGCCTAATTGAGAGCATG
CCTGAAGCTGATACATTATTAATCATATGGATTAAGTTATTAGCTCAAGCTGGT

AAAACAAATGCAAGTGGTTATATTTTTTTTAAACGAGAATATCCCATATACGGAA
GATATGCTAGCGACGCTATTTAATCGACCTCTAAATACAGTTCGGATGGCACTA
GGTGTATTTAAAAATTTTCGGAATGATTGATATTGACGATAACCATTACATCAAC
GTCGTTAATTGGGGAAATCATCAGAATCTAGACCGTTTAGAAAAGATAAAGGA
AGACACTAGAAAACGCGTAGCGGCACACCGAGAAAGAAAAAACAACAAACAC
TTAGTTGTAACGTTACAGGTAACGATGACGTAACGGACATAGATAAAGATTTAG
ATAAAGATATAGATAAAGAAATAAAAAAGAATTATAGTCCTGAAAAACCTCAGG
ACATCGTTCAATCTATTCCATATCAAGAAATTGTTGATTATCTCAATATGAAAG
CAAAAACCAATTACAAATATACATCTAAAAAACACAAGATCTAATTAGGACAA
GATGGAAAGAGGGTTTCAGATTAAATCATTTTCAACAGGTAATTGATATCAAGG
TTTCACAATGGATCGATAATACGGAAATGAGTGGCTATTTGAGACCTATCACTT
TATTTGGAECTAAATTCGAAAGTTATTTAAATGAAAAACCTGTACGACGAAAAG
GAGTCTATAAAGGAGGTTCAACTAATGCAAGCGATCAAAAAGATAGTAGCTTC
ATCAACAAATACGACTTCAAGAAACGTTAATCAAAGATATGTATTGTGCGCTAA
TAGATGTACGAATGTATTTTTAGTAGGAAAAGAAAATTTTAAGGATGTTTGCAG
TAAACGCATGTTGATAGATACAGAAACATGCGAGGAATTTTGTCCGCAATGCA
GATCGGTAGAAAAGGAAGATCAGAAATTAGCTATAGAGACACTATCTATAAAA
AAGAAAAATGAAATCATTCATTTATATGATTCATTTGCTGATAACAGTTTAATAA
ATGACAAACTCAAAAAAGCTACATTTGAAAATTATGTACCTACCAAAGGGACT
TAGCTGATGCAAAGAAACAATAATGAATTTTGTGCTTCATTCAATAAAGAAG
AACCAACAAGCATGATAATAACGGGTGATTATGGAGTAGGAAAAGTCATTTG
TGTGTGGCAGCCACTAAAGGACTTATGAAAAAGGGTCACAGTGCAATGTTTATT
CAAATGAATAAGCTATTTACCAAATCAAATCAACTTGGAATAAAAATAGCGAA
ATGACAGAGGACAAGCTTATGTCCCTTATAGCAAAGTTGATGTCTTGATTATC
GATGACTTTGGAGCGGAATTCACAGAGAAAGATAAAGAAGGCGTCACTTGAA
ACAAACGAAAACAAATGAAATTGTAGATAGCCGTATAGGTAAAAGTACATTATT
TACTACTAATTTTACGGTCGATGAATTAGCAGGAATGTATGGAGAACGTGATTT
CAGTCGGATGATGGAAAACGCTGAAATGTTAGAAATGTATGGGGATAATTATA
GATTACGTAATTTCAAAAAGGAGGAATAAGTATGTGTGTATTATGCCGTAATAC
AGGAATTATTCGTAAAGAACTTATCCAGGTGTGATTGAAACGAGCGGTTGTAA

TTGTGAAGTAGCAAAGAAACAGCAAGCAGAAAATGATAAGCGTTGGCAAGCAT
GGTTAATAAAAATTCGAATCAATGAAACAAGAGTTACAGCGTAATAAACAACAAA
AAGTTAGTTAACAAGGGGGAGAAAGCTATGAAAAATACAGGTGTTGCAAGAAA
AGTGGACGAGCTAGGGCGTGTGGTAATTCAGTTGAGCTACGCAGAACTTTGG
GGAGTGCTGAAGGAACGGCACTGGGATTTTCATGTTGAGGGTGAAAATATTGTT
TTAAGAAAACAAGAAAAGTCATGCTTTGTAACAGGTGAAGTTTCTGAATCAAAC
ATGGAATTATTGGGCGTTCGAATGTTTTTTGAGTAAGACGGGAGCAAGTGAGTT
ACTTGATGCTCTTGAAAAGAGTGTGAAGGTACATGCCTAAGCAACTAAATATTT
TCGATGTAGAGCCAGCAATTTGTGAGTTCGATGTAATGAAAGCCAATATTAAGA
AAGGAACTGGACGCAATACATACGCTGATGTACGCGTCCAAGTTCCAAATAAT
GCAAAGTGTACGGATGAGTTGCCACGCACAACCTAAACAAGATGATCGCTATGA
CATCTTTGAACAATATGTAATAGCAATTTGGAGATTCCAACGTGCTGTAGATAA
GCTTTTTAGTTGGGATACAGCGGAAGAGTTATGTAAGGCAGCAAGGGATAAGA
AAGAAATTATCACGATAAGGATTTATTTAGGGAGTGGCTTTAAACCTGATGTTG
TCGAGTACATGCGGTAGTAAAGGGGAGTGGGACATATGAAAAAATAGAAATT
GATGTTAGCAGCAACAAGCTGTTAATAGTGAAGGACGGAAATGTAACAGCAGT
AAATCCACCAATGAGTGGATTTGGTGAACAAGTCGCGGTTTTGGATAAACGGTA
AAGTTGATCGTGTGGATACTAAGTTTACTGAAAAGATAAAAATAATTTTTTTGGAA
AGTAGGTTTCGCTTATGAGTGTAGCAAGAAATCATGAAGCGATGAAAGAATCAC
GTTTAAAAATATACATCGCTTTAGAAGAAGCTAACTTCATTTGGGATGAAAGAG
ATGTAATTCGTTTTTCGTGAAATGTGGAGTCAAGGTATGAGTTTGCCAGAAATGG
CAGAATCACTAAGGAGACACCATGCTGAGGTTGCGCTCCTTGTAATAGATCAG
GCTGATAAGTATTTAATTGAAAATCGTCCGATAGGATTAGGCATTTTCTAAATA
GGAAGTGGGAAAAAGAAATGGCAAAAGAAAGTCAACGTAAATTTAAACAGATG
TATGAAAATTTAGAACGGTATGGAATGGCGTTAAATGGTGCTGTATATGGTCG
GGATACGTTTTGGTGGTGTAGACAAAAGAAATCGAAAGATTATCGTGGCAAAC
AAAGAAGTGC GGATATGAAGGCGAGACAAAATTAACAGGGGTTAGCATGGACA
AGAAACAAATCTACATCGATGTATTACTACATAAAGGGATTTACAAGGAAAAAG
ATACAGGACGGCAGCTTTATGAAATGGATGAAATAGAGTTATGGAAACTATTAA
AGGGAGATGAAAAGAATGGAAGTAATAGAAAACAGTGTTTATGAAATCACTAA

ATTATTAGCTGGATCTAAAGGTGGTAAGTAATGAAAAAAGAAACCGTGGTGCA
GGTGCAAAGTGAACCTTGAGGTAGTAAAGAGTGAGATTCGTAAGATGGAATATC
ACCTGATTGGATTGAATAACGAAAAGCGTAAGACAAATATGGCTTTGGAAGAG
CTGAAGAATCGGAAAGAGAAGTTGAAAAGTTACTTATAAGGAGCGGGTTGAAT
ATGGAACTAACTAAATTATTCGTAGTACAAGCTGGGTAAAAAAGCACATTGGG
TACAAAGGGAAAGATAAATTCAGCAAGATGATGTTAGCGATGTTAGTTGAATTT
ATGGAGTGTGCGAATGATTGGCGTGGTTTTAAATATTGGAGCGAGAACCCTAA
GGCAAAGAAACGTTGTTAGAGGAATATGTGGATGGATTTCACTTTGTATTAGA
AACAGGACTGGATTTAAAAGAACACACTATAATCATGACGCTTCCAAATGAAGT
TGAATTACCAGAAGAAATTCATGACATGTCGGAACAACGTATCATAAAACAATA
CAAGATATTGACAGGTAAAGTGCTTGAGTTAGAAATTGAGGTTCCATAACGGTAT
AGATTATATGGATGGATCATATGGGAGACTTTATTTATCGATATTTACTGTTAGG
TAAATTATTAGGATTCACTGAAGAACAAATTGAAAAGGCGTATATGGATAAGAA
TGCGGTGAACCATCAGCGTCAGGAAAACGGATATTAAGACCGAATTTGAATTTT
GTTAAGAAATGAGGGTGATTGAAATAAGTTGGTGGGCAATAGCGATCGGTTTA
TATCTATTGATTGGAGTTGCATTACTTATATGGATAATCGCAACGGATAGTTGG
GGTTCGTTATTCTTATATCCTGTTTTTTCGCGTAGTCATTGTTTTGGGATGGCTT
CCATTAATGATAAGAAGCATTGTACAAGAGATATCTAAAGCGATTCATAAGTGG
AAAAGAAAGCAGAAAACCTGAATAGAAGTATTATTTTCAGGGAGGGAGAATAAAT
GATTTATGAAGTTACAGATTATTGCAGTCAGTGTGATAGAAAAATAGAGAATTG
CGATTGCTGTTGTAATAAGTGTGATGAGTGGTTGCACGATTGTAAATGTAAAGA
TAAATAAGCAAAAAAGGGGAATGAAAGATATGAAATGGATGTACAACCTTGAT
AGCAATAATGAGATTTGGACAAGCGATAAATTTGAAATGAAAGAAGAAGCTATT
CAAGCAGCTTTAAAAGATTGGACAGATAAAATGGTAGCGGATAGAGCGGCAGT
CGATAATGAATTCCAAATTGGACAATTCAAACAGTATTCTCCATGGATCAATGC
AGATGTATTGTTGGATGAATTGTATGAACGAGCAACCGATGAATGTGGAGAGG
TTGCGGAATATTGGCTTTCAGGTGTGCCGATGGACGAAGGGGAAAAGCTTCAA
GAACAAATTAATAAGGTAGTTACAGAATGGCTAAAAGGAATAAATGAGCATCCT
AGCTTTGGTTCAATTGAAAATATTGAAACGATAGATGCTAGCAAAATTGAATAT
AAAGAAAACCTAAACAAAAGCGTTATTT

φBACA1 Contig 2:

AACAAAAGCGTTATTTTGCAGAAAAGTGAGGGAGTAGAATGGCTAAAACAGAA
AAGTTTAGTGTCGTCCTTGAGTTACCAAGGGATATAGAAGTAGGTTCAACTGTA
AAGCAAAAAGGAAAAGTGTTAACTATCACCAGTATTAGAAAGATTGAGTGTATA
TCAAGCAGATTAATTTTAGTTAGTGGAATGCTACAGTCCAGAAATGAGGTGAA
AGCAACATGAAGCGTATTGGGATAAATGAAAAGTGCATTGGGTGTGGTGC
TGTC AACGATCCAGAATGCGAATGTGAATGGAGAACATGCTCGTGTGTGGTT
ATCCAGACTGTTTCGTTTATGAAGAAGGTCGCTATTATCATTGTAAAACTGTG
ATCATTCAACTGATCCAGGACATTATACGTAATCAAAAACTAAACAAAATAGT
TATTTTAATCGAAAAGTGAGGGAACAAAATGGCTAAAACAGAAAAATTCAGTGT
AGTTCTTGAGTTGCCAAGGGATATAGAAGTAGGTTCAACTGTAAGGCAAAAAG
GAAAGATATTA ACTATTACGAGTATTAGAAAAATCGAGTGTATATCAAGCAGGT
TAATTTTAGTTAGCGGGAATGCTACAGTTCAGAAATGAGGTAAGGGCGACATG
AAGCGTATTGGTATAAATGATAAGTGTATTGGCTGTGGTGC GGAGGTTGATGA
TCCAGAGTGCGAGTGCGAATGGAGAACATGCTCGTGTGTGGTTATCCAGATT
GTTTCGTTTATGAAGAAGGTCGCTATTACCATTGTAAAAATTGCGACCATTCAA
CTGATCCAGGACATTATATGTAAGTAAAAAATAAGGGGATGGAAATCATGAG
AGAACGTGAAAATTGGGATGTATTGTGTGAAGAATGCGATAAAGTAATCATCAT
TGGTGTA AAAACGGAATCCGGGGATCATTATTGTGAAGCATGTTATGACAAGTT
AGCGTACGGAAACAAAGATAAGTAATTTAATAAAAATCGTTATTTTATTAGAAAG
TGAGGAAGATAGCCATGAAAACATATGAAGAGTTGGTTGAAAAGTGTAAAGGAA
CTGGTTGAAAAGGATGGACTCCAGAATCAGTGCGTGAATGTTTCGAAGCATA
TTCTGAATTCGGCATTGATGCTATTCAATCCGCAATGAATGAAGCGCTACTTAA
TAATGGGTGTT CAGATAATGTATTAGATTATCGGCCGAATCTAGAAAATTTAAA
AGCGTTGGGATTGGAAGAGGATTATGTTTTCCAAGCTTTAGCTTATATGGGGAA
TGCTTCTCAATTTATGAGTTGGGCAAATACGGTACTGGCACTCGTGGACGATGT
TCCAGAACAGTTAAAACAAGATATCAAAAAAGTACATTCTGGTATTTATGAAAT
GCAAGAAAAATTAAGAGAATATAAGAAAGAGGATGATGAGTAATGGAAGAAAT
CTTAGTGCAGGGAAACATAACTGAAGATTTAAAAGATTAGGTGTTAAGGCAA

ATAGAACATATGGTGATGAACTACTTTCGTACCAAGTATATGAAGTTTTCGGAGG
AAGATTTTTCGAAAGTTAAGTGATGATGCGGAGAATATGGATACAGATGATAGT
CATTGGAAAAATGGCGGATGGCGCTGGGATACAGGAAGTAATCAACCGATACC
TACCGACAAAGCTGAAGTCAACAACCAAGAATTAGTATGCTGGGTAGAAACAA
TAAACGATGACGAAGAAACATATCGAAATGATTGGTATGTGGATCTACTAGAAT
ACCTCGATGTTGGAGTTGGCTGCACAGCTTTCCGTAATGTGTGTGCCGTAACG
AAGGACTTGGCGAAATACAACAATATGTCAATGGCCGAGTTATTCAAAAAGTAT
CAAGGGTAATTCAAATAAAAACTTTATTTAATAGAAAAGGAGAATGAATATGGG
AACATTAGTTGTTAATTGTGGAGAATATGAATTTACTAGATTTGAAAGTGCTGT
CCGAAC TTTGGAACAAGAATATGGTTATGAAGGCGAAGCTTGGGAAATGGTTG
TGGCAAGTGGTGATTTAGAGATATTAAGTGACTTCTTAAATTCTGATGGTTTGA
ATGCAGAAATCGAATAAAAAATTTCA TTTTGTGCGAAAAGGGGAATGGATATGACC
GTAGTAAGCAGATCACATAGAGCATTAAAAAGAAAATACAGACCAATAAGAAA
AGAGTTTAAGAAAGATATTTTAGAAGCGACAAAGAATAATCGCGCTTTTGCAAT
GATGATTATTGAGACATATACAGCAAGTCAACATAGAACGCACATTATGAAAGT
TTGGGAGCTACTAGGAATTCATCATAGAGAAGCTTATAAAGATTATTGCGATAA
ATTGATGGGTAAGCATTTAACGGGACGTGATGAAATAATGAGGTCGATATATTT
TGCGGATAAAGTATTATACGACAAGTACCATCGCAAGTTACCAGAATGCTATGC
AATGGGTGATGCACTAGGTATTGCTTATAAGGTATTAACAATAAAAAGAGCAG
CTAGCAAAAGCTAACTGCTCGGGTAATGGAATATGGTTCGAAATGGGTGTCT
ACAGTATTGACGGAATATTGAGTTTTATTTCAGGGGAGGAAGAGAATGAGTAAA
GTAATTGAAGGACAAGAAGTTTATGTAAGCACAAGTGGTGGATGGGTAGGTAA
GTCAGAACCTAATTTAAGAAAATACATCGTTGTCAGAGCTAATAAAAACAAGTTT
TTACGCTAATCCTGAAGGGGTAGAAGATAAATCACCATATAGATTCAACCAAAA
GGATTTATCGCATAACACTGGATGGGGATATCATTATCAAGCTTATCGGACCGA
AAAGGAATATTGGGACATGATTGAGAGAGGTAAAGAAAAAGCTCAATTAAGAA
AAGAATTAAGGATACGGTTGATAAGATGTCACTTATAGAATTACGGAAGTTAA
AAGAAGTACTGTTTGTAAACAAAATAATCCTTTAATAGAAAGTGAGGTGAATACA
TGGATAAGATATATGCATTTTCAGATTGCCACAACAGCGGGCTTGTTAGCCATGA
TTGTACTCAATATTATAACCGGTCAAGAAGTAAGATCATCCTCAATAGTTGTAG

CAGCAGTTTGTTCGCTAGGAATGTTAAAGTTTAATCCGTTGTTTAGAGAAATGA
TTGATAAATATAGAAAGCGAGGTTAAGAGAATGAAACCTTTGAAGAAAAGAAA
GGTAAGAAAAGCTATTGCTCGCCGTGCTAAGGCAGTTGAGAAACATCAAGTTG
ATAAAGCTTGGAGAAACATTTTTGTACGAAATGGCTATTTAAAATAAATGAAAA
CCGAATACAGTCCGGCTAGAAAAGTAGAGGACACCAATTCATTAACCGGCGA
TTAAGGCTGTTTTAGGAATAGGTGTCCTTTTTATTTTGAAAAGGGAGATGGGGA
AATGAAGGTGTTAAAAGATCAATTACGTGAATGAAAAAGCAATCTAATCAAAT
GAAAAAGAAACCTAAGAAGAAACGAAAAGAGAAGTTAAGCACACGTGACATTG
AAGGTTTAATGGGAATTCATGGGCCGCGTTATGAACGTAGACGTGGAGCATT
AGACAAAAGTAATTTAAAATAAAAAGGAGTGGTCTTACATGACTAAACAATTA
TCTTTCTTACCAAAAATTGATAGAACAGCGACACAGGAGGAATTAGAAGGTGT
GTTGGAAAGTGTACGTATACATAGACAATTTGGGATGATGCGTAAAGAAATGA
AAGTCACTCCTTCTTATGAAATACGTGAGCACGGTCCTACACATACAGTTGGTA
AGCCGTTAGAAGATGTTGCTATAGCAAATATTCAGCAAAGCAAACGAGAAGAG
TGGCTTGAAAGAATGTCAGTACGTATTGATCAGTTTTTAAATCGATTAGGAAAC
GGACGTGCTGGAAGCATCCAAAGAGATATTATTTATAAACGTTATTTAGAAGAA
GAGGACGTATGTGATTACATGGTTTATAACGAAATAGGAATGTCAGAGCGTAC
TTATCGACGTTGGAAGTCTAAAGCATTTTACAAACTTGCTTTTTCGCTTGGATT
AGAAGTTTACGAGACAGAAGAAACGGGAGGTAATGAATAATGAATTTTCGTTCA
ACCGATACGTGATCCAGAACAATAACAGCAGCTAAAAGATTATTTTAAGGAGAA
GAGCTTACGTAATTACATTCTTTTCATTATGGGAATCAATACAGGCCTTAGAAT
CTCGGATATTTTGAAATTAAGGTAGGAGACGTCAGAGGCAGTCATATATCTAT
GAGGGAAAAGAAGACAGGGAAGCAGAAACGCATACAAATTAAGTGCAGCACTGA
AAAGAGAACTTAAATGGTTCATTGAAGAAAGAGAAGATAATGAGTACCTATTGC
AAAGTAGACAAGGGAGGAATCGTCCTATTGGGCGCAGCATGGCCTATAAGATA
TTAAGTGGTGCAGCGGAAGAGTTCGGATTAGATGAAATAGGTACACATACATT
GAGAAAGACATACGGGTATCATATGTACATGCAAACGAAAAACATAGCATTACT
CATGGAGATATTCATCACTCGTCAGAGAAGGTCACATTACGTTATATAGGGGT
AAACCAAGATGCAATGGATAAAGCAATGACTAGGTTTAAAATCTAATCATTGCT
TTTTTCTTTTTTAAACACATACAGTTACTCATAAATTTTCGTACTGTGTAACCTCAA

AGGAAAAGTATTATAAAGTTAATGATACCAAGGGATTTGGCGAAGGGGTCAGT
TACACACAATATAAGATATGGGTAAGTCATTGATATAAAATACATATGAGTGAA
GAATAAAAATAAGTGGCAGAGTCATGACCGCTTTTTGGCAGGAAATGTGCCGG
TTGTTTTGGGATTTACGTGATATATTTGTATTGTGAGAAGTGGCGGAAAACACA
ACTCACTATGTTGATTCTAAAATTCTAAACGGCTTCATAATGACGGCGCATAAA
ATCCGAAACCAGCAGATGGTACTGATTGAATGTTACCGTTAATAAGGAGAGCTT
TTGCTCTTCTTTGAGCTAACAACATCCTAGGTAGACAGAATTAGGAGAACCTGA
TAAGTTTTCCGATGGTGTCTGTCGTGGTTGTTAGTTCAAAGAAGATTAAAACCT
CACATACCATAATTA AAAAGTAAATAAGAAAATGATGAAAAAAGCATCCATTCG
GGTGCTTTTTATTTTGAAGGAGGATGAAGGATGGAATTAACATTTGAGGGATTA
GAACAGTGTTTTAATGAAGCTAAAGATGTAGAGGCTAATTATGTAGCCGTACAG
ATCGAAATGGAAGAATTCCCTAGTGATGAGTTGATTATTAATGACAAACACAAT
ATCTCTTTAAAACCTAGAGTACTATAAGAAAACCTTATAACGAAGACTTAGAACAC
AGATATGCTCCAGGTATTCGTATTGTAGGTTATGCATACGGACATACGTTATCT
GGTATTCAACGTGAGTTAAAGTTACTCAATGATTAAGGAGGATGAATGATGAGT
GAACAGAAGAGCGCATTGTCAGTAAAGGTAGAAGTTGATACAAAAGAAGCGAA
TGAAAACATTAAGAATTA ACTGCTGCAGTTAATGAATGCGCGGAAGCATTGTA
TAATTTAGAAAAGGTTATAAGTAATTTTACAGGTCAGCATAGGAAGGTTAGATT
CTTTAATGATTGTGGCGAATTGATTGTTTCAAAGAAGGAGTGAGGATAGATGCA
AGTCTATTGTTCTAGCTGTAATAAAGATTACCATATGCAACCAAAGTAGCACA
GCTTCCTAATCGTATTGAGAAGTGTTACTTCACTTGTCTCATTGTGGCCATGA
ACATGTTGCGGCATATGTGAACGATAAGATTCGTAAACATCAAGCTGACATTGC
AAAGTGTCATGATCGTATTAACAAGAGGAACCTAGACATCGAGAATGAAATGA
AACGGTTGAGGAAGAGGATGGAGGGAAGTAAATGATGATGATATTAGGATATC
TTATTATTGGTTTACTTTATAGTTCCATTACAATGTATCCAGTTGCGAGAGACG
TTGGACAACGAAAGAAACATGACGGTGTATATATAGTAAGTACATTTATTATTT
CTATTGCATTTGCCATTTGTCTCGCTCCTTTCTGGATTATTCTTCTTGGGTTTAA
TATAGCTAAGTGGTTTTATAAATGGAAGAATAGAAACCAAATGAAGTGTGAATG
TTTTAATTGTGGTTATGAATCAACGATAGATATAGTAACAGGTGCTGGTAAACG
TTGCTCACAATGTAATGGTATAACAATACCTAAAGCGTCAGGTGGTACACATGC

CAAGTAAACCATTCAAGCCATGTAAGTCGTTAGGTTGCAACGAACTAACAAGG
GATAAGTATTGCACTAAACATTTAGAAAAGGAAAACGAAACCGTAAAATATTAT
GACAAACATATCCGAAACAAAAGCTCACGTTTATTCTACAACCTCAAGATTGTGG
AAGGATATGCGTGAGTTTATTTATCGTAGAGATCATGGTCTATGTGTTCAATGT
AGAAGCAATGACATCATTAAGATAGGTGATGTAGTCGATCACATCATACCCATT
CGAGTGGATTGGTCTAAACGATTAGAACCATCTAATTTACAAACGCTCTGTCAT
GCTTGCCATAATAAGAAAACAAAAGAAGACGAGAAGAAAAACAGAAAATAATT
CGAAAGAAAAAAATCATAAACAACCCCCACCATGAAAAAGCAAAGGACGACT
CCCTGGAG

APPENDIX 2. PRELIMINARY DATA AND SUGGESTED FUTURE EXPERIMENTS

A2.1 Determination of fetal bovine serum (FBS) component(s) responsible for *dcsaB*'s phenotypic switch

To determine the FBS component(s) involved in *dcsaB*'s phenotypic switch, we fractionated FBS into >10 kD and <10 kD fractions. Briefly, FBS was filtered in 10,000 MWCO Amicon Ultra-15 Centrifugal Filter Units (EMD Millipore). Flow-through was collected and sterile filtered through 0.22 μ m filters and labelled "FBS flow-through". The >10 kD fraction was washed 3X in 1X PBS and resuspended to 10% of its original volume (i.e., 1.5 mL from 15 mL starting material) and labelled "FBS proteins". BHI broth was also subjected to this fractionation procedure and split into <10 kD "BHI flow-through" and >10 kD "BHI proteins" fractions.

Sterne *dcsaB* from an overnight culture grown in BHI at 30°C, 150 RPM was back-diluted 1:100 and grown in the same conditions, however in four different combinations of each fraction component: 1) reconstituted BHI (BHI flow-through + BHI proteins); 2) BHI-FBS (BHI proteins + FBS flow-through); 3) FBS-BHI (FBS proteins + BHI flow-through); and 4) reconstituted FBS (FBS proteins + FBS flow-through). The 4 cultures were formulated as 90:10 mixtures, with 90% culture volume as flow-through and 10% culture volume as 10X concentrated >10 kD

fractions. Cultures were grown for 24-36 hours, the time until reconstituted FBS cultures were dispersed and resembled those grown in unfractionated FBS.

Examination of cultures revealed that the two different fractions of FBS appear to play different roles in the *dcsaB* phenotypic switch (Figure A2-1). Reconstituted BHI and reconstituted FBS were used as controls for the *dcsaB* phenotype and to ensure that the fractionation procedure did not alter serum activity. *dcsaB* grown in reconstituted BHI resembled that of *dcsaB* grown in unfractionated BHI. The culture was connected as one bacterial mass that fell to the bottom of culture tubes, with the rest of the supernatant clear (Figures A2-1, A2-2a). Reconstituted FBS cultures were dispersed with *dcsaB* in shorter chains and possessing a Sterne-like phenotype (Figures A2-1, A2-2b).

BHI-FBS (BHI proteins, FBS flow-through) cultures were of an intermediate phenotype between that of BHI and FBS alone. In BHI-FBS, the bacterial clump associated with *dcsaB* was less compact and its rope-like structures appeared unraveled, however *dcsaB* chains were still of longer length and cells did not disperse into the surrounding media (i.e., the culture was not turbid) nor did they show any apparent division septa (Figures A2-1, A2-3a). FBS-BHI (FBS proteins, BHI flow-through) cultures had a distinct phenotype where a compact bacterial pellet was present at the bottom of culture tubes, however, cultures were also turbid with dispersed cells harboring clear division septa (Figures A2-1, A2-3b-d).

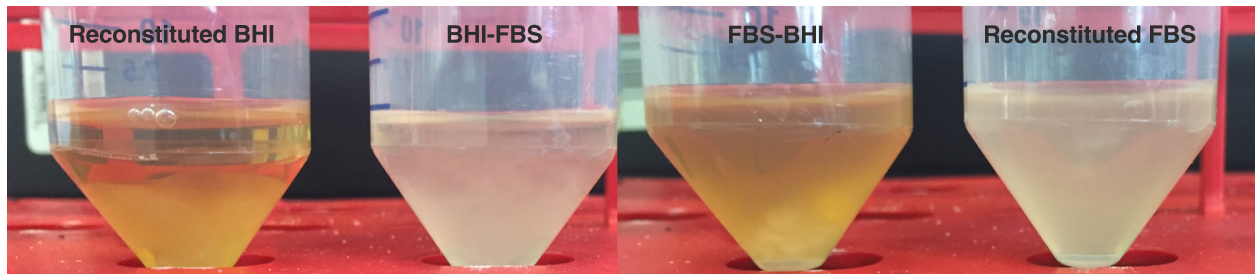


Figure A2-1. *dcsaB* displays different phenotypes in fractionated FBS.

Sterne *dcsaB* was grown in combinations of BHI and FBS previously split into >10 kD and <10 kD fractions. Left) *dcsaB* grown in reconstituted BHI (BHI >10 kD and BHI <10 kD fractions) displays a bacterial clump at the bottom of the culture tube with non-turbid growth. Middle-left) Growth in BHI-FBS (BHI >10 kD and FBS <10 kD fractions) results in a more loosely-bound bacterial clump, however still connected as one mass. Supernatant surrounding the mass is not turbid. Middle-right) FBS-BHI (FBS >10 kD and BHI <10 kD fractions) culture displays turbid growth. Media contains bacteria with clear division septa and a tightly wound bacterial mass at the bottom of the culture tube. Right) Reconstituted FBS (FBS >10 kD and FBS <10 kD fractions) culture displays turbid growth typical of *dcsaB* in unfractionated FBS. No bacterial mass is present in the culture tube.

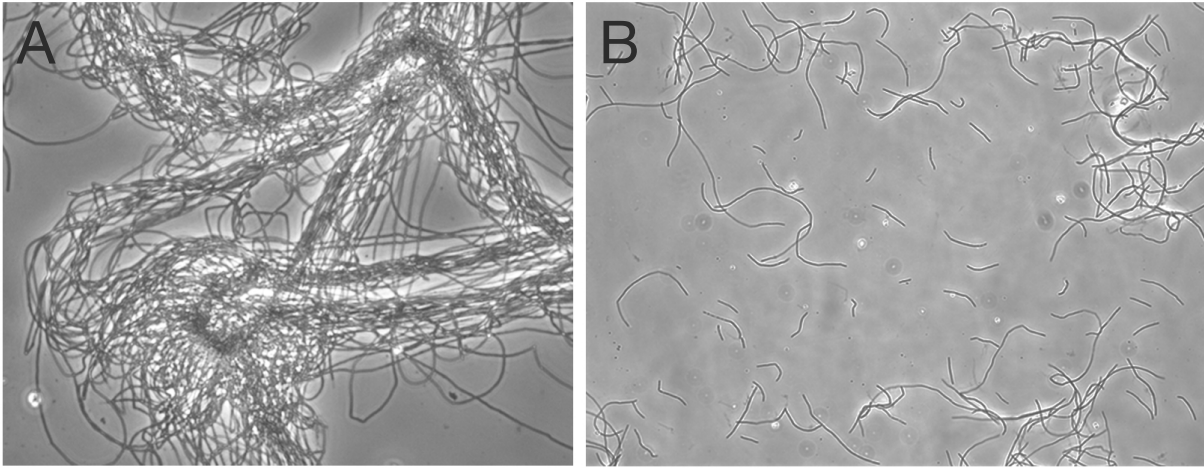
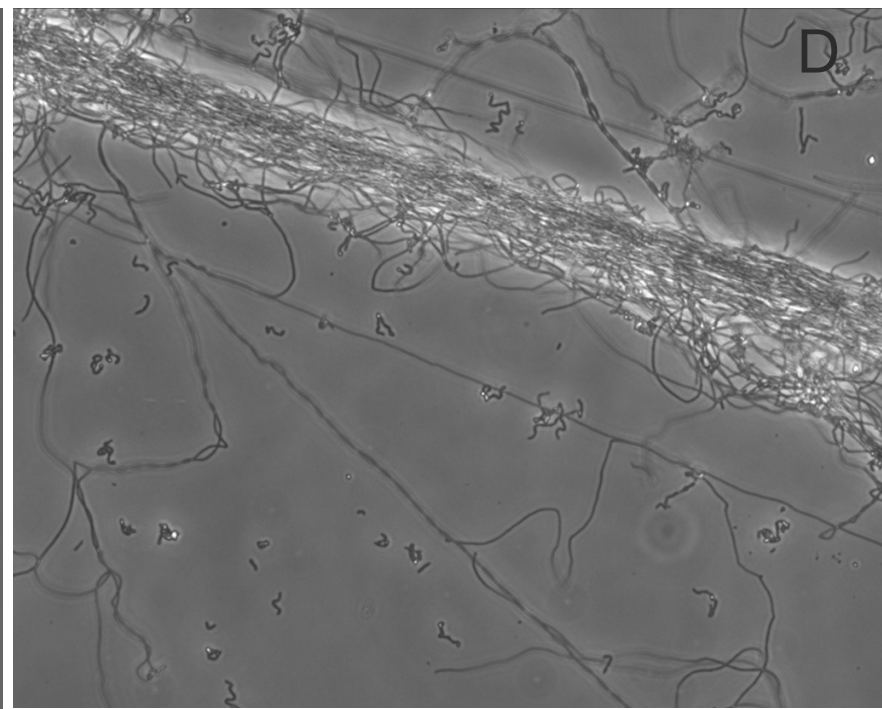
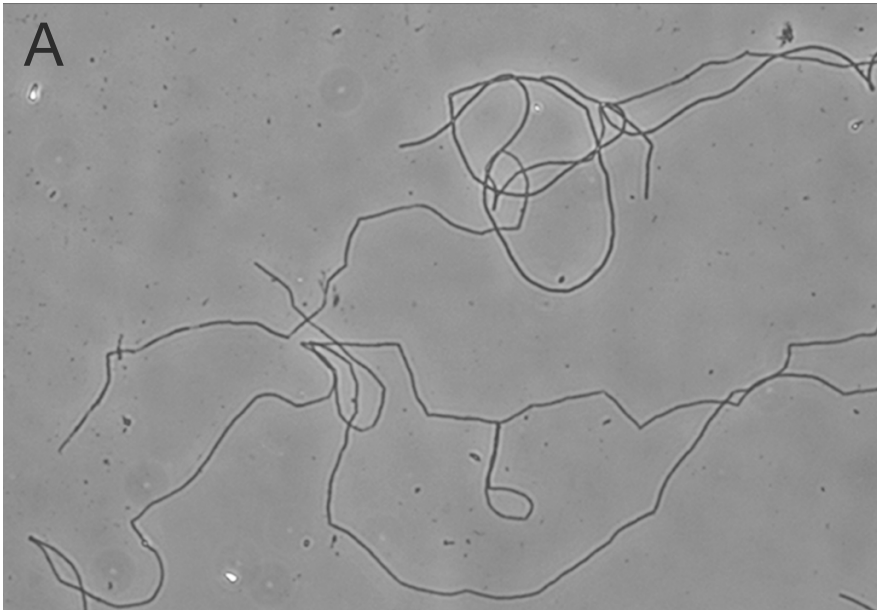


Figure A2-2. Sterne *dcsaB* growth in reconstituted BHI and reconstituted FBS. A) *dcsaB* grown in reconstituted BHI possesses long chains with multi-chain, rope-like structures, resembling growth in unfractionated BHI media. Image captured at 100X magnification. B) *dcsaB* grown in reconstituted FBS has shorter chains and clear division septa, resembling growth in unfractionated FBS. Image captured at 100X magnification.

Figure A2-3. *Sterne dcsaB* growth in BHI-FBS and FBS-BHI mixed fraction cultures. A) *dcsaB* in BHI-FBS (BHI proteins, FBS flow-through) grows in long chains, however tight, rope-like multi-chain structures are less apparent. Image captured at 100X magnification. B) and C) *dcsaB* grown in FBS-BHI (FBS proteins, BHI flow-through) displays compact, twisted chains with an aberrant morphology (B), however cells contain clear division septa (C). D) *dcsaB* grown in FBS-BHI shows a mix of chain morphologies: 1) rope-like, multi-chain structures without clear division septa, 2) long chains without apparent division septa, but not associated with rope-like forms, and 3) shorter chains with clear division septa. Images in B), C), and D) captured at 1000X, 400X, and 100X magnifications, respectively.



These results suggested that multiple components of FBS likely promote different aspects of *dcsaB*'s phenotypic switch. Components <10 kD (likely small molecules or peptide fragments) appear to play a role in breaking-up/unravelling the multi-chain structures associated with *dcsaB* growth in BHI, however, cell separation was not observed in these cultures containing BHI proteins and FBS flow-through. The formation of multi-chain structures may be due, in part, to increased levels of SCWP on the *dcsaB* cell surface (contributing to *dcsaB*'s "stickiness" and the propensity of chains to bind together). We find in our RNA-seq data that a number of the genes associated with SCWP synthesis are upregulated 4-16-fold in *dcsaB* grown in BHI vs. FBS, and 4-8-fold in *dcsaB* BHI as compared to Sterne BHI. Sterne does not show differential expression of SCWP synthesis genes between BHI and FBS culture. *B. anthracis* may therefore respond to components in the FBS <10 kD fraction and downregulate its SCWP synthesis genes to allow for multi-chain unravelling and in part, cellular dispersion associated with FBS and animal-host environments. Complementary to the <10 kD FBS fraction, the ability of the FBS-BHI cultures (FBS proteins, BHI flow-through) to grow with turbidity while still containing a dense cellular pellet, suggests that a larger molecular-weight component of FBS plays a role in cell separation, however likely indirectly as heat-killed FBS cultures were capable of turbid growth. When added together, these fractions of FBS appear to both unravel the bacterial mass associated with *dcsaB* growth in BHI and allow for cell separation and dispersion, critical events in *B. anthracis*'s pathogenesis.

Since multiple components of FBS appear to play different roles in the *dcsaB* phenotypic switch, experiments to specifically uncover these compounds will highlight molecular signals that the pathogen uses to sense its external environment and precipitate an infectious or non-infectious response. Such work will allow for a better understanding *B. anthracis*'s biology, and in addition, may allow avenues for development of novel approaches to treat infection. Interference of signaling pathways in *B. anthracis* may prevent the organism from sensing its external environment and executing its infection program (i.e., production of anthrax toxins and PDGA capsule in mammalian environments) and allow better treatment outcomes.

Follow-up experiments could elucidate the FBS active principles by a variety of approaches. The approach described above could be expanded to fine-tune molecular weight cutoffs and find a range in which the active components are found (e.g., the “rope-unravelling” compound is <3 kD or <1 kD, or the “cell-separation” compound is >30 kD and <50 kD). Getting a better defined molecular weight range followed by mass-spectrometry could allow identification of switch signals. In addition, treatment of the lower molecular weight fractions could remove non-polar (e.g., charcoal stripped FBS) or other serum compounds. The absence or presence of fraction activity could help elucidate the nature of the components integral to *dcsaB*'s phenotypic switch.

A2.2 Uncovering ϕ BACA1-pXO1 crosstalk in *B. anthracis*

During the course of research conducted for this Thesis, it was discovered that ϕ BACA1 presents different plaquing efficiency on *B. anthracis* Sterne compared to Δ Sterne indicator strains (Figure A2-4). A similar observation was noted with other *B. anthracis*-infecting phages but not further explored in (Schuch and Fischetti, 2009). Our result suggests potential ϕ BACA1-pXO1 (and more broadly phage-pXO1) crosstalk that could allow for successful phage infection. We have observed Δ Sterne lysis by ϕ BACA1 previously, although at a much lower efficiency.

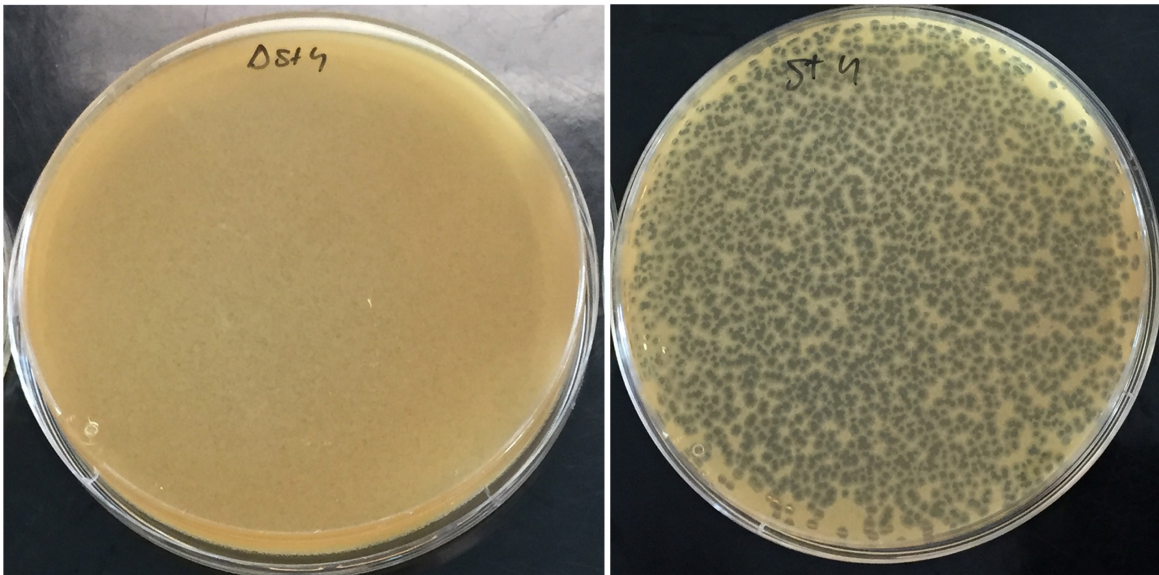


Figure A2-4. ϕ BACA1 plaquing efficiency on *B. anthracis* Δ Sterne versus Sterne strains. ϕ BACA1 stock at 10^{-4} dilution was added to either Δ Sterne (left) or Sterne (right) in a BHI soft-agar overlay. Δ Sterne does not display any PFUs, whereas plaques are apparent on the Sterne plate. Δ Sterne and Sterne displayed equivalent growth in BHI-only negative controls (not pictured).

Experimental work to uncover potential phage-plasmid crosstalk and the genes involved in this event should be a relatively straightforward task. Sterne could be cured of its pXO1 plasmid to generate a Δ Sterne strain with a similar chromosomal background to Sterne. Following plasmid curing, pXO1 DNA could be purified and digested to make a library of ~2-3 kbp fragments hosted in Δ Sterne. This library could then be tested for clones harboring increased ϕ BACA1 susceptibility and candidates Sanger sequenced to uncover the gene(s) important for increased phage sensitivity. Uncovering such phage-plasmid crosstalk would, to our knowledge, be a rare finding, however it would be of critical importance in understanding the environmental interactions between *B. anthracis* and its bacteriophages.

In addition to characterizing this pXO1-driven crosstalk, it is also possible that the *dcsaB* phenotypic switch is partially (or fully) precipitated by a pXO1-encoded factor as well, as a number of pXO1 genes are differentially expressed with elevated temperature and/or CO₂/bicarbonate conditions—some of the same conditions which appear to cause the *dcsaB* phenotypic switch. Generating a *dcsaB* mutant in Δ Sterne and testing its ability to execute a phenotypic switch could identify pXO1 as an integral part of *dcsaB*'s ability to overcome the limitations associated with CsaB-deficiency. If Δ Sterne *dcsaB* cannot execute the phenotypic switch associated with Sterne *dcsaB* (or perhaps does so less efficiently), then the same library screening approach as described above could be undertaken, except in a *dcsaB* chromosomal background, and would uncover the pXO1 gene(s) associated with

dispersion and differential expression in FBS and likely in animal-host environments. Genes highlighted by this approach would give researchers more insights into the mechanisms by which *B. anthracis* executes its multifaceted lifestyle and deals with the threat and consequences of bacteriophage infection.

APPENDIX 3. RNA-SEQUENCING DIFFERENTIAL EXPRESSION DATA

Representative pXO1 differential expression (DE) data comparing *dcsaB* and Sterne in FBS culture are shown. The full DE dataset is available at: <https://www.dropbox.com/sh/b3alrq7k5y7q6pq/AABh2Usqstjt2MTzHXh2zJoSa?dl=0>

Password: bacillusphage

Table A3-1. Differential expression (DE) of pXO1-encoded genes comparing *dcsaB* and Sterne in FBS

Gene Name	Base Mean	Log ₂ Fold Change (relative to <i>dcsaB</i>)	Log ₂ Fold Change Standard Error	Wald Statistic	P-value	Adjusted P-value	Gene Product
AW20_RS00005	40.28794778	-0.490798703	0.38062251	-1.289463156	0.197237117	0.346059833	hypothetical protein
AW20_RS00010	95.3907458	-0.099657705	0.29940662	-0.332850705	0.739246981	0.838469831	hypothetical protein
AW20_RS00015	141.841706	-0.586029343	0.311808046	-1.879455486	0.060182326	0.147014984	disulfide formation protein

AW20_RS 00020	229.2474758	-0.725721958	0.283674816	-2.558288282	0.0105 18885	0.039266833	ArsR family transcription al regulator
AW20_RS 00025	1245.398124	-1.194286171	0.236542347	-5.048931774	4.44E- 07	9.90E-06	RNA chaperone Hfq
AW20_RS 00030	98947.27241	-0.863221596	0.249173039	-3.464345896	0.0005 31523	0.003679375	hisitidine kinase
AW20_RS 00035	319.4364786	0.145773982	0.241252511	0.604238196	0.5456 8529	0.68695407	hypothetical protein
AW20_RS 00040	199.28654	0.469822078	0.279286127	1.682224902	0.0925 25237	0.201549057	transposase
AW20_RS 00045	215.9477031	0.20666064	0.255799138	0.807902019	0.4191 46989	0.579591376	hypothetical protein
AW20_RS 00050	1453.391531	-0.547510834	0.219591421	-2.493316143	0.0126 55611	0.044947659	hypothetical protein
AW20_RS 00055	6715.447841	-0.500661095	0.229506752	-2.181465648	0.0291 48993	0.085439802	recombinase XerS
AW20_RS 00060	8512.976489	-0.220167255	0.173325781	-1.270251053	0.2039 95218	0.354104906	hypothetical protein
AW20_RS	1442.322615	-0.47248248	0.268809962	-1.757682177	0.0788	0.179528642	metal-

00065					01602		binding protein
AW20_RS 00070	163.2857252	-1.044700058	0.320002774	-3.264659383	0.0010 95958	0.006573442	transposase;p pseudo=true
AW20_RS 00075	39.80538607	-1.163014458	0.591522954	-1.966135802	0.0492 82926	0.126797388	transposase
AW20_RS 00080	263.8019101	-0.336857234	0.247516363	-1.360949356	0.1735 29694	0.317247877	transposase
AW20_RS 00085	1077.399961	-0.197305634	0.172224852	-1.145628129	0.2519 49053	0.410487689	transposase
AW20_RS 00090	6922.346539	0.027366035	0.239721538	0.114157596	0.9091 12865	0.946964898	hypothetical protein
AW20_RS 00095	7802.140801	0.124144625	0.216353865	0.573803593	0.5661 00717	0.702329306	type VII secretion protein
AW20_RS 00100	880.0068621	-0.051460847	0.261908783	-0.196483853	0.8442 3147	0.906698924	membrane protein
AW20_RS 00105	505.0798772	-0.514809968	0.32901197	-1.56471501	0.1176 49747	0.240528372	membrane protein
AW20_RS 00110	492.6544954	-0.700258148	0.3102765	-2.256884255	0.0240 15308	0.07356784	membrane protein

AW20_RS 00115	3056.12698	-1.462902866	0.367911604	-3.976234643	7.00E- 05	0.00072877	hypothetical protein
AW20_RS 00120	657.5803757	-1.405356179	0.440697768	-3.188934185	0.0014 27984	0.008137083	transposase
AW20_RS 00125	2474.705448	-0.713182998	0.283225111	-2.518078274	0.0117 9971	0.042733678	integrase
AW20_RS 00130	81.53620979	-0.320648495	0.390043762	-0.822083381	0.4110 29443	0.571692744	DNA-binding protein
AW20_RS 00135	319.4700036	-0.684821911	0.245562875	-2.788784381	0.0052 90628	0.022672982	transition state regulator
AW20_RS 00140	145.0826688	-0.736757473	0.298723257	-2.466354578	0.0136 49614	0.047531989	hypothetical protein
AW20_RS 00145	434.7144813	-0.489971204	0.267041331	-1.834814116	0.0665 33236	0.159121837	ArsR family transcription al regulator
AW20_RS 00150	2210.238201	-0.693300265	0.213213075	-3.251678003	0.0011 47259	0.006809538	ATPase;pseu do=true
AW20_RS 00155	20194.88175	-0.875852984	0.196343904	-4.460810672	8.17E- 06	0.000121285	Lethal factor
AW20_RS	3900.263686	-0.89332468	0.23216851	-3.847742664	0.0001	0.00110746	ribonuclease

00160					19211		
AW20_RS 00165	356.9205462	-1.071375415	0.278585925	-3.8457629	0.0001 20178	0.001112816	hypothetical protein
AW20_RS 00170	151.4991323	-1.124093446	0.3718195	-3.023223492	0.0025 00975	0.012737107	hypothetical protein
AW20_RS 00175	12627.33504	-0.521245605	0.282880681	-1.842634159	0.0653 82443	0.157226583	transcription al regulator
AW20_RS 00180	177591.0628	0.216513963	0.272647886	0.794115688	0.4271 28085	0.586786753	protective antigen
AW20_RS 00185	616.3591551	-0.820528024	0.278724518	-2.943867405	0.0032 41388	0.015695144	hypothetical protein
AW20_RS 00190	493.2485061	-0.784489061	0.218001338	-3.598551591	0.0003 19994	0.002485308	germination protein XC
AW20_RS 00195	1020.204571	-0.825115797	0.18572247	-4.442735418	8.88E- 06	0.000127916	germination protein XA
AW20_RS 00200	1045.859044	-0.931241648	0.231182458	-4.028167429	5.62E- 05	0.00061308	germination protein
AW20_RS 00205	1157.078063	-0.819698305	0.2377903	-3.447147786	0.0005 66539	0.003851652	resolvase
AW20_RS 00210	8665.18771	-0.842555367	0.220960437	-3.813150341	0.0001 37207	0.001240295	transposase

AW20_RS 00215	518.5022341	-1.125746745	0.193555455	-5.816145804	6.02E- 09	2.48E-07	hypothetical protein
AW20_RS 00220	3438.27036	-0.423457505	0.302835547	-1.398308455	0.1620 2046	0.304001547	hypothetical protein
AW20_RS 00225	20261.22109	-0.450309252	0.22707776	-1.983061887	0.0473 60517	0.12312871	anthrax toxin expression trans-acting positive regulator
AW20_RS 00230	176.7775063	-0.844698404	0.293542272	-2.877603958	0.0040 07079	0.018552253	transposase
AW20_RS 00235	595.4803311	-0.541470943	0.200855493	-2.69582342	0.0070 21488	0.028465221	transposase
AW20_RS 00240	2622.129431	-0.37688982	0.212521935	-1.773416098	0.0761 59783	0.175379655	adenine phosphoribos yltransferase
AW20_RS 00245	1113.809566	-0.2635663	0.258193916	-1.020807555	0.3073 45624	0.471770571	adenine phosphoribos yltransferase
AW20_RS 00250	8757.074351	-0.002289827	0.254770638	-0.008987798	0.9928 28871	0.997902358	calmodulin- sensitive

							adenylate cyclase
AW20_RS00255	1518.156802	-0.391075267	0.176797609	-2.211994102	0.026967072	0.080576313	hypothetical protein
AW20_RS00260	310.7777827	-1.133370892	0.242183205	-4.679807963	2.87E-06	5.06E-05	hypothetical protein
AW20_RS00265	13635.594	-0.791363913	0.316270476	-2.502174474	0.012343308	0.044206248	hypothetical protein
AW20_RS00270	9574.538594	-0.66304155	0.303788351	-2.182577272	0.029066955	0.085328024	hypothetical protein
AW20_RS00275	7284.619741	-0.518508924	0.254467483	-2.037623503	0.0415876	0.112211764	hypothetical protein
AW20_RS00280	812.2553554	-0.819040841	0.221784207	-3.692962869	0.000221656	0.001821798	transposase
AW20_RS00285	1637.819277	-0.300280391	0.181912164	-1.650688909	0.098802114	0.21186739	transposase
AW20_RS00290	307.3928467	0.30109773	0.219273018	1.373163616	0.169701488	0.312755182	transposase
AW20_RS00295	215.4565265	-0.873579346	0.330026485	-2.646997697	0.008120991	0.032168146	hypothetical protein
AW20_RS	1770.796188	-0.48359844	0.157348034	-3.073431729	0.0021	0.011186612	UDP-glucose

00300					16121		6-dehydrogenase
AW20_RS00305	454.088118	-0.622686332	0.269381354	-2.311542068	0.020802932	0.066105808	UTP--glucose-1-phosphate uridylyltransferase
AW20_RS00310	497.3734375	-0.627760585	0.247675252	-2.534611675	0.011257204	0.041187358	hyaluronan synthase
AW20_RS00315	100.3814544	-0.350703856	0.431943747	-0.811920205	0.41683742	0.577097243	hyaluronate synthase
AW20_RS00320	199.0323073	0.198536822	0.279565505	0.710162084	0.47760363	0.631099917	hypothetical protein
AW20_RS00325	6632.227967	-1.011115458	0.214830698	-4.706568792	2.52E-06	4.49E-05	phosphatidic acid phosphatase
AW20_RS00330	132813.8708	-1.149459047	0.243426884	-4.721988921	2.34E-06	4.23E-05	S-layer protein
AW20_RS00335	1130.043522	-1.281553467	0.243992371	-5.252432528	1.50E-07	4.00E-06	hypothetical protein

AW20_RS 00340	784.5682394	-1.145897466	0.263625121	-4.346692987	1.38E- 05	0.000187222	hypothetical protein
AW20_RS 00345	3519.146471	-0.915642326	0.245058324	-3.736426135	0.0001 86654	0.001595352	cell surface protein
AW20_RS 00350	2186.763531	-0.275258126	0.197267037	-1.395357939	0.1629 07928	0.304964497	hypothetical protein
AW20_RS 00355	814.7299149	-0.955540275	0.286402291	-3.336356955	0.0008 48841	0.005361893	membrane protein
AW20_RS 00360	743.2068529	0.223189599	0.223560905	0.998339129	0.3181 1494	0.481946246	CAAX amino protease
AW20_RS 00365	206.1556122	1.693143599	0.365591983	4.631238315	3.63E- 06	6.15E-05	hypothetical protein
AW20_RS 00370	524.7986827	1.46946708	0.386466028	3.802318899	0.0001 43348	0.001281594	hypothetical protein
AW20_RS 00375	960.7375923	1.734194226	0.38203669	4.539339465	5.64E- 06	8.92E-05	membrane protein
AW20_RS 00380	84.4683098	-0.361137408	0.352321291	-1.025022947	0.3053 5236	0.470169342	hypothetical protein
AW20_RS 00385	168.3689169	-0.162313041	0.274766394	-0.590731049	0.5547 0064	0.694014576	lytic transglycosyl ase;pseudo=t

							rue
AW20_RS 00390	64.08590631	-0.475284684	0.367571226	-1.293041047	0.1959 96863	0.344307393	membrane protein
AW20_RS 00395	488.6030874	-0.340623306	0.251091718	-1.356569259	0.1749 18115	0.318662704	hypothetical protein
AW20_RS 00400	124.5689047	0.092932182	0.281361717	0.330294337	0.7411 77571	0.840101031	hypothetical protein
AW20_RS 00405	32.40852174	-1.639068861	0.545081378	-3.007016799	0.0026 38252	0.013352785	hypothetical protein
AW20_RS 00410	36.71061686	-0.466949632	0.447278384	-1.043979877	0.2964 947	0.46119601	hypothetical protein
AW20_RS 00415	112.3076433	-0.538997506	0.282058888	-1.910939631	0.0560 12339	0.139700211	hypothetical protein
AW20_RS 00420	115.9115024	-0.829081134	0.397967888	-2.083286511	0.0372 25115	0.102923926	hypothetical protein
AW20_RS 00425	432.8726726	0.650966577	0.206497592	3.152417276	0.0016 19247	0.009037363	hypothetical protein
AW20_RS 00430	7295.531763	0.478733618	0.192512917	2.486761025	0.0128 91196	0.045550212	ATPase
AW20_RS 00435	440.0056256	0.199374582	0.199300081	1.000373814	0.3171 29637	0.481058177	hypothetical protein

AW20_RS 00440	492.6717989	-0.82802337	0.325809355	-2.541435224	0.0110 3984	0.040631221	hypothetical protein
AW20_RS 00445	3658.777802	-0.89960411	0.321713439	-2.796290114	0.0051 69297	0.022286979	hypothetical protein
AW20_RS 00450	921.6523179	-1.597642487	0.378006765	-4.226491787	2.37E- 05	0.000293056	hypothetical protein
AW20_RS 00455	826.1922088	-1.49084136	0.385479522	-3.867498203	0.0001 09958	0.001048382	DNA-binding protein
AW20_RS 00460	176.779715	-0.669301931	0.27807877	-2.406878928	0.0160 89503	0.054307157	hypothetical protein
AW20_RS 00465	201.7778963	-0.368506836	0.284311679	-1.296136821	0.1949 28351	0.342852703	membrane protein
AW20_RS 00470	50.66702448	-1.145931596	0.385036853	-2.97616082	0.0029 18818	0.014502557	hypothetical protein
AW20_RS 00475	45.07721675	-0.02827616	0.421852199	-0.067028594	0.9465 5894	0.96846138	hypothetical protein
AW20_RS 00480	79.59185248	-0.611176864	0.334516404	-1.827046016	0.0676 92851	0.160852346	hypothetical protein
AW20_RS 00485	101.6345659	-0.026152655	0.285740261	-0.091525971	0.9270 74671	0.956812233	membrane protein
AW20_RS	162.4220842	-0.002027731	0.233443662	-0.008686169	0.9930	0.99796839	hypothetical

00490					69527		protein
AW20_RS 00495	70.99709979	-0.602435248	0.371383233	-1.62213906	0.1047 73576	0.220088784	chromosome partitioning protein ParA
AW20_RS 00500	94.94883553	-0.710453775	0.341511803	-2.080319829	0.0374 96207	0.103522926	pilus assembly protein CpaB
AW20_RS 00505	189162.8175	0.458609249	0.1952193	2.34920036	0.0188 1378	0.061147465	hypothetical protein
AW20_RS 00510	2876.116883	-1.402875308	0.309396142	-4.534236593	5.78E- 06	9.11E-05	hypothetical protein
AW20_RS 00515	1468.567299	-0.473997878	0.223241437	-2.123252223	0.0337 32722	0.095058521	hypothetical protein
AW20_RS 00520	1132.287783	0.393416163	0.242568552	1.621876206	0.1048 29857	0.220088784	surface layer protein
AW20_RS 00525	68.61730551	-0.320398333	0.335741966	-0.954299328	0.3399 32148	0.503760191	hypothetical protein
AW20_RS 00530	62.55730685	-0.219726934	0.360343917	-0.609770067	0.5420 14132	0.683851915	hypothetical protein
AW20_RS 00535	128.7867504	-0.344388355	0.303602171	-1.134340883	0.2566 51586	0.415420162	hypothetical protein

AW20_RS 00540	131.6222278	-0.305642313	0.32900264	-0.928996538	0.3528 9088	0.515993228	hypothetical protein
AW20_RS 00545	597.1041683	-0.277423122	0.270284961	-1.026409761	0.3046 98479	0.469983808	hypothetical protein
AW20_RS 00550	284.451115	-0.469900958	0.280925518	-1.672688764	0.0943 88582	0.20463416	hypothetical protein
AW20_RS 00555	7488.697885	0.374444318	0.198997519	1.8816532	0.0598 83118	0.14648017	hypothetical protein
AW20_RS 00560	3528.430114	-0.882808217	0.389671492	-2.265519125	0.0234 80842	0.07224095	cell division protein FtsZ
AW20_RS 00565	25524.10619	-0.754429607	0.276207834	-2.731383815	0.0063 06897	0.026277197	plasmid replication protein RepX
AW20_RS 00570	1646.116972	-0.105217502	0.216224636	-0.486612	0.6265 33318	0.753906088	hypothetical protein
AW20_RS 00575	92.52409772	-1.679239447	0.348879697	-4.813233509	1.49E- 06	2.80E-05	hypothetical protein
AW20_RS 00580	1328.829374	-0.796633748	0.206964786	-3.849127007	0.0001 1854	0.001103017	conjugal transfer protein TraG
AW20_RS	3238.038611	-0.078864518	0.184602292	-0.427213103	0.6692	0.786194293	hypothetical

00585					24119		protein
AW20_RS 00590	1316.019332	-0.219272398	0.264930039	-0.827661518	0.4078 62218	0.56909151	hypothetical protein
AW20_RS 00595	457.7892578	-0.12501907	0.276714332	-0.451798318	0.6514 14282	0.773613796	Cro/C1 family transcription al regulator
AW20_RS 00600	4360.692625	-0.89089181	0.284410154	-3.13241914	0.0017 33722	0.009554733	hypothetical protein
AW20_RS 00605	2126.12283	-0.825788255	0.162850117	-5.070848393	3.96E- 07	8.93E-06	transposase
AW20_RS 00610	431.8119866	-1.104354443	0.269210592	-4.102195359	4.09E- 05	0.000468746	transposase
AW20_RS 00615	745.8985858	0.362313561	0.22034256	1.644319466	0.1001 1023	0.213657165	GNAT family acetyltransfe rase
AW20_RS 00620	1849.896387	-0.489937105	0.190640452	-2.56995354	0.0101 71215	0.038421598	CAAX amino protease
AW20_RS 00625	523.884729	-0.212958596	0.234794573	-0.906999652	0.3644 06981	0.526488708	hypothetical protein
AW20_RS 00630	13806.08837	-0.630448414	0.182436468	-3.455714865	0.0005 48836	0.00376269	hypothetical protein

AW20_RS 00635	1725.722958	-1.038416902	0.203547818	-5.101586992	3.37E- 07	8.04E-06	transposase;p pseudo=true
AW20_RS 00640	351.2926219	-1.206385028	0.262534762	-4.595143972	4.32E- 06	7.19E-05	TetR family transcription al regulator
AW20_RS 00645	540.4027878	-1.108320579	0.221201082	-5.010466348	5.43E- 07	1.17E-05	nucleotidyltr ansferase
AW20_RS 00650	285.264997	-0.79133082	0.323717018	-2.444514118	0.0145 0474	0.049870427	S1 RNA- binding domain protein
AW20_RS 00655	766.9210729	-0.949623087	0.232967914	-4.076196888	4.58E- 05	0.000514014	hypothetical protein
AW20_RS 00660	1312.69454	-0.924274539	0.170998259	-5.405169283	6.47E- 08	1.92E-06	ATPase AAA
AW20_RS 00665	1635.161057	-0.957246181	0.28974627	-3.303739449	0.0009 54045	0.00588947	hypothetical protein
AW20_RS 00670	2200.986624	-0.758230712	0.209356778	-3.621715622	0.0002 92656	0.002318484	membrane protein
AW20_RS 00675	1033.050265	-1.378027053	0.24758817	-5.565803309	2.61E- 08	8.60E-07	membrane protein

AW20_RS 00680	20.2856091	-1.730175319	0.615633431	-2.810398576	0.0049 48018	0.021623412	hypothetical protein
AW20_RS 00685	7263.086719	-0.729172523	0.157136053	-4.6403897	3.48E- 06	5.96E-05	nucleotidyltr ansferase
AW20_RS 00690	3786.939213	-0.961171431	0.163093283	-5.893384547	3.78E- 09	1.66E-07	hypothetical protein
AW20_RS 00695	52483.152	-0.837348194	0.149038178	-5.618346967	1.93E- 08	6.62E-07	group II intron reverse transcriptase /maturase
AW20_RS 00700	8736.876998	-0.881426782	0.166023351	-5.309053086	1.10E- 07	3.05E-06	DNA-binding protein
AW20_RS 00705	45.88027229	-0.048259142	0.449672991	-0.107320526	0.9145 34701	0.949837206	phosphoaden osine phosphosulfa te reductase
AW20_RS 00710	1116.189197	0.171158803	0.173263979	0.987849892	0.3232 26169	0.486976442	hypothetical protein
AW20_RS 00715	3566.035883	1.211678168	0.245553032	4.934486689	8.04E- 07	1.65E-05	hypothetical protein

AW20_RS 00720	353.7389678	-0.335889521	0.260766611	-1.288084851	0.1977 16428	0.346474502	hypothetical protein
AW20_RS 00725	2105.35779	-0.661692619	0.168105209	-3.936181537	8.28E- 05	0.000831118	integrase
AW20_RS 00730	882.1353058	-0.091515005	0.18383418	-0.497812785	0.6186 16004	0.746001202	hypothetical protein
AW20_RS 00735	3834.727678	-2.529140712	0.365261283	-6.924195994	4.38E- 12	4.10E-10	hypothetical protein
AW20_RS 00740	10497.36941	-0.395136412	0.227163696	-1.739434688	0.0819 58331	0.184612754	XRE family transcription al regulator
AW20_RS 00745	8200.559172	-0.479011147	0.153314977	-3.124359778	0.0017 81924	0.009782576	hypothetical protein
AW20_RS 00750	2158.346426	-1.052783397	0.300234798	-3.506533562	0.0004 53984	0.003230299	hypothetical protein
AW20_RS 00755	59.48491693	-0.309445864	0.358076787	-0.864188565	0.3874 84313	0.54958796	hypothetical protein
AW20_RS 00760	111.7125042	-0.348566649	0.323972567	-1.075914087	0.2819 65681	0.444905186	SAM- dependent methyltransf erase

AW20_RS 00765	29.24870795	-0.93937892	0.476151928	-1.972855435	0.0485 12035	0.125175222	hypothetical protein
AW20_RS 00770	398.8254697	-0.533092785	0.206360894	-2.583303327	0.0097 85924	0.037287183	hypothetical protein
AW20_RS 00775	361.4242563	-0.305846043	0.254507291	-1.201718196	0.2294 72729	0.384768475	group II intron reverse transcriptase /maturase
AW20_RS 00780	103.4797797	-0.323014547	0.321680746	-1.00414635	0.3153 08077	0.479604606	hypothetical protein
AW20_RS 00785	239.9134389	-0.383269169	0.256113657	-1.496480792	0.1345 2841	0.265702925	transposase
AW20_RS 00790	59.72288321	-0.411173885	0.387997123	-1.059734366	0.2892 65464	0.452915236	hypothetical protein
AW20_RS 00795	104.6837238	-0.47100818	0.344429156	-1.367503801	0.1714 67447	0.315398361	hypothetical protein
AW20_RS 00800	2011.023637	-0.534865805	0.205734255	-2.599789737	0.0093 2809	0.035757677	hypothetical protein
AW20_RS 00805	2383.688051	-0.465111377	0.17767383	-2.617782137	0.0088 50329	0.034341685	hypothetical protein

AW20_RS 00810	23.61520445	-0.859429859	0.587438463	-1.463012576	0.1434 63938	0.278244917	hypothetical protein
AW20_RS 00815	1154.062111	-0.563658263	0.272288882	-2.070074473	0.0384 45371	0.105683082	hypothetical protein
AW20_RS 00820	155.482404	-1.100883673	0.290238987	-3.793024793	0.0001 48823	0.001326388	hypothetical protein
AW20_RS 00825	96.89868454	-0.456198971	0.327106294	-1.394650545	0.1631 21245	0.305163523	transposase
AW20_RS 00830	366.4712863	-0.704037473	0.253854256	-2.773392431	0.0055 47518	0.023526425	DNA topoisomeras e I
AW20_RS 00835	14.18670735	-2.905992942	0.782115575	-3.715554368	0.0002 02759	0.001709388	hypothetical protein
AW20_RS 00840	81.22748452	-0.171368971	0.334344603	-0.512551929	0.6082 64787	0.736320531	hypothetical protein

REFERENCES

- Abeles, A. L., Snyder, K. M., and Chatteraj, D. K. (1984). P1 plasmid replication: replicon structure. *J. Mol. Biol.* 173, 307–324.
- Ahn, J.-S., Chandramohan, L., Liou, L. E., and Bayles, K. W. (2006). Characterization of CidR-mediated regulation in *Bacillus anthracis* reveals a previously undetected role of S-layer proteins as murein hydrolases. *Mol Microbiol* 62, 1158–1169. doi:10.1111/j.1365-2958.2006.05433.x.
- Anderson, V. J., Kern, J. W., McCool, J. W., Schneewind, O., and Missiakas, D. (2011). The SLH-domain protein BslO is a determinant of *Bacillus anthracis* chain length. *Mol Microbiol* 81, 192–205. doi:10.1111/j.1365-2958.2011.07688.x.
- Antonation, K. S., Grützmacher, K., Dupke, S., Mabon, P., Zimmermann, F., Lankester, F., et al. (2016). *Bacillus cereus* Biovar *anthracis* Causing Anthrax in Sub-Saharan Africa-Chromosomal Monophyly and Broad Geographic Distribution. *PLoS Negl Trop Dis* 10, e0004923. doi:10.1371/journal.pntd.0004923.
- Arndt, D., Grant, J. R., Marcu, A., Sajed, T., Pon, A., Liang, Y., et al. (2016). PHASTER: a better, faster version of the PHAST phage search tool. *Nucleic Acids Res.* 44, W16–21. doi:10.1093/nar/gkw387.
- Aziz, R. K., Bartels, D., Best, A. A., DeJongh, M., Disz, T., Edwards, R. A., et al. (2008). The RAST Server: rapid annotations using subsystems technology. *BMC Genomics* 9, 75. doi:10.1186/1471-2164-9-75.
- Bae, T., Baba, T., Hiramatsu, K., and Schneewind, O. (2006). Prophages of *Staphylococcus aureus* Newman and their contribution to virulence. *Mol Microbiol* 62, 1035–1047. doi:10.1111/j.1365-2958.2006.05441.x.
- Beres, S. B., and Musser, J. M. (2007). Contribution of exogenous genetic elements to the group A Streptococcus metagenome. *PLoS ONE* 2, e800. doi:10.1371/journal.pone.0000800.
- Beres, S. B., Sylva, G. L., Barbian, K. D., Lei, B., Hoff, J. S., Mammarella, N. D., et al. (2002). Genome sequence of a serotype M3 strain of group A Streptococcus: phage-encoded toxins, the high-virulence phenotype, and clone emergence. *Proc. Natl. Acad. Sci. U.S.A.* 99, 10078–10083. doi:10.1073/pnas.152298499.
- Bertozi Silva, J., Storms, Z., and Sauvageau, D. (2016). Host receptors for bacteriophage adsorption. *FEMS Microbiol. Lett.* 363, fnw002. doi:10.1093/femsle/fnw002.

- Binetti, A. G., Bailo, N. B., and Reinheimer, J. A. (2007). Spontaneous phage-resistant mutants of *Streptococcus thermophilus*: Isolation and technological characteristics. *International Dairy Journal* 17, 343–349.
- Bishop-Lilly, K. A., Bishop-Lilly, K. A., Plaut, R. D., Plaut, R. D., Chen, P. E., Chen, P. E., et al. (2012). Whole genome sequencing of phage resistant *Bacillus anthracis* mutants reveals an essential role for cell surface anchoring protein CsaB in phage AP50c adsorption. *Viol. J.* 9, 246. doi:10.1186/1743-422X-9-246.
- Blackburn, N. T., and Clarke, A. J. (2002). Characterization of Soluble and Membrane-Bound Family 3 Lytic Transglycosylases from *Pseudomonas aeruginosa*†. *Biochemistry* 41, 1001–1013. doi:10.1021/bi011833k.
- Boyd, E. F., and Brüssow, H. (2002). Common themes among bacteriophage-encoded virulence factors and diversity among the bacteriophages involved. *Trends in Microbiology* 10, 521–529.
- Brézillon, C., Haustant, M., Dupke, S., Corre, J.-P., Lander, A., Franz, T., et al. (2015). Capsules, toxins and AtxA as virulence factors of emerging *Bacillus cereus* biovar *anthracis*. *PLoS Negl Trop Dis* 9, e0003455. doi:10.1371/journal.pntd.0003455.
- Broudy, T. B., and Fischetti, V. A. (2003). In vivo lysogenic conversion of Tox(-) *Streptococcus pyogenes* to Tox(+) with Lysogenic Streptococci or free phage. *Infect. Immun.* 71, 3782–3786. doi:10.1128/IAI.71.7.3782-3786.2003.
- Broudy, T. B., Pancholi, V., and Fischetti, V. A. (2001). Induction of lysogenic bacteriophage and phage-associated toxin from group a streptococci during coculture with human pharyngeal cells. *Infect. Immun.* 69, 1440–1443. doi:10.1128/IAI.69.3.1440-1443.2001.
- Broudy, T. B., Pancholi, V., and Fischetti, V. A. (2002). The in vitro interaction of *Streptococcus pyogenes* with human pharyngeal cells induces a phage-encoded extracellular DNase. *Infect. Immun.* 70, 2805–2811. doi:10.1128/IAI.70.6.2805-2811.2002.
- Brussow, H., Canchaya, C., and Hardt, W. D. (2004). Phages and the Evolution of Bacterial Pathogens: from Genomic Rearrangements to Lysogenic Conversion. *Microbiology and Molecular Biology Reviews* 68, 560–602. doi:10.1128/MMBR.68.3.560-602.2004.
- BUCK, C. A., ANACKER, R. L., NEWMAN, F. S., et al. (1963). PHAGE ISOLATED FROM LYSOGENIC *BACILLUS ANTHRACIS*. *Journal of Bacteriology* 85, 1423–1430.
- Calendar, R., and Inman, R. (2005). “Phage Biology,” in *Phages*, eds. M. K. Waldor,

- D. I. Friedman, and S. L. Adhya (Amer Society for Microbiology).
- Canchaya, C., Fournous, G., and Brüssow, H. (2004). The impact of prophages on bacterial chromosomes. *Mol Microbiol* 53, 9–18. doi:10.1111/j.1365-2958.2004.04113.x.
- Capparelli, R., Nocerino, N., Lanzetta, R., Silipo, A., Amoresano, A., Giangrande, C., et al. (2010). Bacteriophage-resistant *Staphylococcus aureus* mutant confers broad immunity against staphylococcal infection in mice. *PLoS ONE* 5, e11720. doi:10.1371/journal.pone.0011720.
- Carlson, P. E., Bourgis, A. E. T., Hagan, A. K., and Hanna, P. C. (2015). Global gene expression by *Bacillus anthracis* during growth in mammalian blood. *Pathog Dis* 73, ftv061. doi:10.1093/femspd/ftv061.
- Casjens, S. R., and Hendrix, R. W. (2015). Bacteriophage lambda: Early pioneer and still relevant. *Virology* 479-480, 310–330. doi:10.1016/j.virol.2015.02.010.
- Cenens, W., Makumi, A., Govers, S. K., Lavigne, R., and Aertsen, A. (2015). Viral Transmission Dynamics at Single-Cell Resolution Reveal Transiently Immune Subpopulations Caused by a Carrier State Association. *PLoS Genet.* 11, e1005770. doi:10.1371/journal.pgen.1005770.
- Charpentier, E., Anton, A. I., Barry, P., Alfonso, B., Fang, Y., and Novick, R. P. (2004). Novel cassette-based shuttle vector system for gram-positive bacteria. *Applied and Environmental Microbiology* 70, 6076–6085. doi:10.1128/AEM.70.10.6076-6085.2004.
- Chlebowicz, M. A., Mašlaňová, I., Kuntová, L., Grundmann, H., Pantůček, R., Doškař, J., et al. (2014). The Staphylococcal Cassette Chromosome mec type V from *Staphylococcus aureus* ST398 is packaged into bacteriophage capsids. *Int. J. Med. Microbiol.* 304, 764–774. doi:10.1016/j.ijmm.2014.05.010.
- Cho, I., and Blaser, M. J. (2012). The human microbiome: at the interface of health and disease. *Nat. Rev. Genet.* 13, 260–270. doi:10.1038/nrg3182.
- Choudhury, B., Leoff, C., Saile, E., Wilkins, P., Quinn, C. P., Kannenberg, E. L., et al. (2006). The structure of the major cell wall polysaccharide of *Bacillus anthracis* is species-specific. *J. Biol. Chem.* 281, 27932–27941. doi:10.1074/jbc.M605768200.
- Coleman, D. C., Sullivan, D. J., Russell, R. J., Arbuthnott, J. P., Carey, B. F., and Pomeroy, H. M. (1989). *Staphylococcus aureus* bacteriophages mediating the simultaneous lysogenic conversion of beta-lysin, staphylokinase and enterotoxin A: molecular mechanism of triple conversion. *J. Gen. Microbiol.* 135, 1679–1697. doi:10.1099/00221287-135-6-1679.

- Coleman, D., Knights, J., Russell, R., Shanley, D., Birkbeck, T. H., Dougan, G., et al. (1991). Insertional inactivation of the *Staphylococcus aureus* beta-toxin by bacteriophage phi 13 occurs by site- and orientation-specific integration of the phi 13 genome. *Mol Microbiol* 5, 933–939.
- D'Herelle, F. (2007). *On an invisible microbe antagonistic toward dysenteric bacilli: brief note by Mr. F. D'Herelle, presented by Mr. Roux. 1917.* doi:10.1016/j.resmic.2007.07.005.
- Day, W. A., Rasmussen, S. L., Carpenter, B. M., Peterson, S. N., and Friedlander, A. M. (2007). Microarray analysis of transposon insertion mutations in *Bacillus anthracis*: global identification of genes required for sporulation and germination. *Journal of Bacteriology* 189, 3296–3301. doi:10.1128/JB.01860-06.
- Deutsch, D. R., Utter, B., and Fischetti, V. A. (2016). Uncovering novel mobile genetic elements and their dynamics through an extra-chromosomal sequencing approach. *Mob Genet Elements* 6, e1189987. doi:10.1080/2159256X.2016.1189987.
- Echols, H. (1986). Bacteriophage λ development: temporal switches and the choice of lysis or lysogeny. *Trends in Genetics* 2, 26–30.
- Enquist, L. W., and Skalka, A. M. (1978). Replication of bacteriophage lambda DNA. *Trends in Biochemical Sciences* 3, 279–283.
- Etienne-Toumelin, I., Sirard, J. C., Duflot, E., Mock, M., and Fouet, A. (1995). Characterization of the *Bacillus anthracis* S-layer: cloning and sequencing of the structural gene. *Journal of Bacteriology* 177, 614–620.
- Fagan, R. P., and Fairweather, N. F. (2014). Biogenesis and functions of bacterial S-layers. *Nat Rev Micro* 12, 211–222. doi:10.1038/nrmicro3213.
- Feiner, R., Argov, T., Rabinovich, L., Sigal, N., Borovok, I., and Herskovits, A. A. (2015). A new perspective on lysogeny: prophages as active regulatory switches of bacteria. *Nature Publishing Group* 13, 641–650. doi:10.1038/nrmicro3527.
- Filippov, A. A., Sergueev, K. V., He, Y., Huang, X.-Z., Gnade, B. T., Mueller, A. J., et al. (2011). Bacteriophage-resistant mutants in *Yersinia pestis*: identification of phage receptors and attenuation for mice. *PLoS ONE* 6, e25486. doi:10.1371/journal.pone.0025486.
- Fischetti, V. A. (2005). Bacteriophage lytic enzymes: novel anti-infectives. *Trends in Microbiology* 13, 491–496. doi:10.1016/j.tim.2005.08.007.
- Fischetti, V. A. (2006). *Gram-positive Pathogens*. ASM Press.

- Fitzgerald, J. R., Sturdevant, D. E., Mackie, S. M., Gill, S. R., and Musser, J. M. (2001). Evolutionary genomics of *Staphylococcus aureus*: insights into the origin of methicillin-resistant strains and the toxic shock syndrome epidemic. *Proc. Natl. Acad. Sci. U.S.A.* 98, 8821–8826. doi:10.1073/pnas.161098098.
- Gamaleya, N. F. (1898). Bacteriolysins—ferments destroying bacteria. *Russ Arch Pathol Clin Med Bacteriol* 6, 607–613.
- Gillis, A., and Mahillon, J. (2014). Phages preying on *Bacillus anthracis*, *Bacillus cereus*, and *Bacillus thuringiensis*: past, present and future. *Viruses* 6, 2623–2672. doi:10.3390/v6072623.
- Goerke, C., Pantucek, R., Holtfreter, S., et al. (2009). Diversity of Prophages in Dominant *Staphylococcus aureus* Clonal Lineages. *Journal of Bacteriology* 191, 3462–3468. doi:10.1128/JB.01804-08.
- Goerke, C., Matias y Papenberg, S., Dasbach, S., Dietz, K., Ziebach, R., Kahl, B. C., et al. (2004). Increased frequency of genomic alterations in *Staphylococcus aureus* during chronic infection is in part due to phage mobilization. *J. Infect. Dis.* 189, 724–734. doi:10.1086/381502.
- Goerke, C., Wirtz, C., Flückiger, U., and Wolz, C. (2006). Extensive phage dynamics in *Staphylococcus aureus* contributes to adaptation to the human host during infection. *Mol Microbiol* 61, 1673–1685. doi:10.1111/j.1365-2958.2006.05354.x.
- Guichard, A., Nizet, V., and Bier, E. (2012). New insights into the biological effects of anthrax toxins: linking cellular to organismal responses. *Microbes Infect.* 14, 97–118. doi:10.1016/j.micinf.2011.08.016.
- Hatfull, G. F. (2008). Bacteriophage genomics. *Current opinion in microbiology* 11, 447–453. doi:10.1016/j.mib.2008.09.004.
- Hatfull, G. F., and Hendrix, R. W. (2011). Bacteriophages and their genomes. *Curr Opin Virol* 1, 298–303. doi:10.1016/j.coviro.2011.06.009.
- Heler, R., Samai, P., Modell, J. W., Weiner, C., Goldberg, G. W., Bikard, D., et al. (2015). Cas9 specifies functional viral targets during CRISPR-Cas adaptation. *Nature* 519, 199–202. doi:10.1038/nature14245.
- Hendrickson, C., Euler, C. W., Nguyen, S. V., Rahman, M., McCullor, K. A., King, C. J., et al. (2015). Elimination of Chromosomal Island SpycIM1 from *Streptococcus pyogenes* Strain SF370 Reverses the Mutator Phenotype and Alters Global Transcription. *PLoS ONE* 10, e0145884. doi:10.1371/journal.pone.0145884.
- Hendrix, R. W. (2005). “Bacteriophage Evolution and the Role of Phages in Host

Evolution,” in *Phages*, eds. M. K. Waldor, D. I. Friedman, and S. L. Adhya (American Society for Microbiology).

Hoffmaster, A. R., Hill, K. K., Gee, J. E., Marston, C. K., De, B. K., Popovic, T., et al. (2006). Characterization of *Bacillus cereus* isolates associated with fatal pneumonias: strains are closely related to *Bacillus anthracis* and harbor *B. anthracis* virulence genes. *J. Clin. Microbiol.* 44, 3352–3360. doi:10.1128/JCM.00561-06.

Hoffmaster, A. R., Ravel, J., Rasko, D. A., Chapman, G. D., Chute, M. D., Marston, C. K., et al. (2004). Identification of anthrax toxin genes in a *Bacillus cereus* associated with an illness resembling inhalation anthrax. *Proc. Natl. Acad. Sci. U.S.A.* 101, 8449–8454. doi:10.1073/pnas.0402414101.

Holden, M. T. G., Feil, E. J., Lindsay, J. A., Peacock, S. J., Day, N. P. J., Enright, M. C., et al. (2004). Complete genomes of two clinical *Staphylococcus aureus* strains: evidence for the rapid evolution of virulence and drug resistance. *Proc. Natl. Acad. Sci. U.S.A.* 101, 9786–9791. doi:10.1073/pnas.0402521101.

Hu, C., Xiong, N., Zhang, Y., et al. (2012). Functional characterization of lipase in the pathogenesis of *Staphylococcus aureus*. *Biochem. Biophys. Res. Commun.* 419, 617–620. doi:10.1016/j.bbrc.2012.02.057.

Inal, J. M., and Karunakaran, K. V. (1996). phi 20, a temperate bacteriophage isolated from *Bacillus anthracis* exists as a plasmidial prophage. *Curr Microbiol* 32, 171–175.

Iyanovics, G. (1962). The Pathogenicity of *Bacillus anthracis* Lysogenic with Mutants of Phage W. *Microbiology (Reading, Engl.)* 28, 87–101. doi:10.1099/00221287-28-1-87.

Jabra-Rizk, M. A., Meiller, T. F., James, C. E., and Shirliff, M. E. (2006). Effect of farnesol on *Staphylococcus aureus* biofilm formation and antimicrobial susceptibility. *Antimicrob. Agents Chemother.* 50, 1463–1469. doi:10.1128/AAC.50.4.1463-1469.2006.

Kamal, N., Ganguly, J., Saile, E., Klee, S. R., Hoffmaster, A., Carlson, R. W., et al. (2017). Structural and immunochemical relatedness suggests a conserved pathogenicity motif for secondary cell wall polysaccharides in *Bacillus anthracis* and infection-associated *Bacillus cereus*. *PLoS ONE* 12, e0183115. doi:10.1371/journal.pone.0183115.

Kaneko, J., Kimura, T., Narita, S., Tomita, T., and Kamio, Y. (1998). Complete nucleotide sequence and molecular characterization of the temperate staphylococcal bacteriophage phiPVL carrying Panton-Valentine leukocidin genes. *Gene* 215, 57–67.

- Katayama, Y., Baba, T., Sekine, M., Fukuda, M., and Hiramatsu, K. (2013). Beta-hemolysin promotes skin colonization by *Staphylococcus aureus*. *Journal of Bacteriology* 195, 1194–1203. doi:10.1128/JB.01786-12.
- Kern, J. W., and Schneewind, O. (2008). BslA, a pXO1-encoded adhesin of *Bacillus anthracis*. *Mol Microbiol* 68, 504–515. doi:10.1111/j.1365-2958.2008.06169.x.
- Kern, J., Ryan, C., Faull, K., and Schneewind, O. (2010). *Bacillus anthracis* surface-layer proteins assemble by binding to the secondary cell wall polysaccharide in a manner that requires csaB and tagO. *J. Mol. Biol.* 401, 757–775. doi:10.1016/j.jmb.2010.06.059.
- Kiel, J. L., Parker, J. E., Holwitt, E. A., McCreary, R. P., Andrews, C. J., De Los Santos, A., et al. (2008). Geographical distribution of genotypic and phenotypic markers among *Bacillus anthracis* isolates and related species by historical movement and horizontal transfer. *Folia Microbiol. (Praha)* 53, 472–478. doi:10.1007/s12223-008-0074-2.
- Klee, S. R., Brzuszkiewicz, E. B., Nattermann, H., Brüggemann, H., Dupke, S., Wollherr, A., et al. (2010). The genome of a *Bacillus* isolate causing anthrax in chimpanzees combines chromosomal properties of *B. cereus* with *B. anthracis* virulence plasmids. *PLoS ONE* 5, e10986. doi:10.1371/journal.pone.0010986.
- Klee, S. R., Ozel, M., Appel, B., et al. (2006). Characterization of *Bacillus anthracis*-like bacteria isolated from wild great apes from Cote d'Ivoire and Cameroon. *Journal of Bacteriology* 188, 5333–5344. doi:10.1128/JB.00303-06.
- Koehler, T. M., Dai, Z., and Kaufman-Yarbray, M. (1994). Regulation of the *Bacillus anthracis* protective antigen gene: CO2 and a trans-acting element activate transcription from one of two promoters. *Journal of Bacteriology* 176, 586–595.
- Kolstø, A.-B., Tourasse, N. J., and Økstad, O. A. (2009). What sets *Bacillus anthracis* apart from other *Bacillus* species? *Annu. Rev. Microbiol.* 63, 451–476. doi:10.1146/annurev.micro.091208.073255.
- Kreiswirth, B. N., Löfdahl, S., Betley, M. J., O'Reilly, M., Schlievert, P. M., Bergdoll, M. S., et al. (1983). The toxic shock syndrome exotoxin structural gene is not detectably transmitted by a prophage. *Nature* 305, 709–712.
- Kunkel, B., Losick, R., and Stragier, P. (1990). The *Bacillus subtilis* gene for the development transcription factor sigma K is generated by excision of a dispensable DNA element containing a sporulation recombinase gene. *Genes & Development* 4, 525–535.
- Kuroda, M., Nagasaki, S., Ito, R., and Ohta, T. (2007). Sesquiterpene farnesol as a competitive inhibitor of lipase activity of *Staphylococcus aureus*. *FEMS*

- Microbiol. Lett.* 273, 28–34. doi:10.1111/j.1574-6968.2007.00772.x.
- Laaberki, M.-H., Pfeffer, J., Clarke, A. J., and Dworkin, J. (2011). O-Acetylation of peptidoglycan is required for proper cell separation and S-layer anchoring in *Bacillus anthracis*. *J. Biol. Chem.* 286, 5278–5288. doi:10.1074/jbc.M110.183236.
- Langmead, B., and Salzberg, S. L. (2012). Fast gapped-read alignment with Bowtie 2. *Nat. Methods* 9, 357–359. doi:10.1038/nmeth.1923.
- Lawrence, M., Huber, W., HHervé, P., Aboyoun, P., Carlson, M., Gentleman, R., et al. (2013). Software for computing and annotating genomic ranges. *PLoS Comput. Biol.* 9, e1003118. doi:10.1371/journal.pcbi.1003118.
- Lederberg, E. M., and Lederberg, J. (1953). Genetic Studies of Lysogenicity in *Escherichia Coli*. *Genetics* 38, 51–64.
- Lee, C. Y., and Iandolo, J. J. (1986). Lysogenic conversion of staphylococcal lipase is caused by insertion of the bacteriophage L54a genome into the lipase structural gene. *Journal of Bacteriology* 166, 385–391.
- Lee, C. Y., and Iandolo, J. J. (1985). Mechanism of bacteriophage conversion of lipase activity in *Staphylococcus aureus*. *Journal of Bacteriology*.
- Leendertz, F. H., Yumlu, S., Pauli, G., Boesch, C., Couacy-Hymann, E., Vigilant, L., et al. (2006). A new *Bacillus anthracis* found in wild chimpanzees and a gorilla from West and Central Africa. *PLoS Pathog* 2, e8. doi:10.1371/journal.ppat.0020008.
- León, M., and Bastías, R. (2015). Virulence reduction in bacteriophage resistant bacteria. *Front Microbiol* 6, 343. doi:10.3389/fmicb.2015.00343.
- Li, H., Handsaker, B., Wysoker, A., Fennell, T., Ruan, J., Homer, N., et al. (2009). The Sequence Alignment/Map format and SAMtools. *Bioinformatics* 25, 2078–2079. doi:10.1093/bioinformatics/btp352.
- Lindsay, J. A., Ruzin, A., Ross, H. F., Kurepina, N., and Novick, R. P. (1998). The gene for toxic shock toxin is carried by a family of mobile pathogenicity islands in *Staphylococcus aureus*. *Mol Microbiol* 29, 527–543.
- Love, M. I., Anders, S., Kim, V., and Huber, W. (2016). RNA-Seq workflow: gene-level exploratory analysis and differential expression. *F1000Research* 4, 1070. doi:10.12688/f1000research.7035.2.
- Love, M. I., Huber, W., and Anders, S. (2014). Moderated estimation of fold change and dispersion for RNA-seq data with DESeq2. *Genome Biol.* 15, 550. doi:10.1186/s13059-014-0550-8.

- Lunderberg, J. M., Nguyen-Mau, S.-M., Richter, G. S., Wang, Y.-T., Dworkin, J., Missiakas, D. M., et al. (2013). *Bacillus anthracis* acetyltransferases PatA1 and PatA2 modify the secondary cell wall polysaccharide and affect the assembly of S-layer proteins. *Journal of Bacteriology* 195, 977–989. doi:10.1128/JB.01274-12.
- Marraffini, L. A. (2015). CRISPR-Cas immunity in prokaryotes. *Nature* 526, 55–61. doi:10.1038/nature15386.
- McKenzie, A. T., Pomerantsev, A. P., Sastalla, I., Martens, C., Ricklefs, S. M., Virtaneva, K., et al. (2014). Transcriptome analysis identifies *Bacillus anthracis* genes that respond to CO₂ through an AtxA-dependent mechanism. *BMC Genomics* 15, 229. doi:10.1186/1471-2164-15-229.
- Mesnage, S., Fontaine, T., Mignot, T., Delepierre, M., Mock, M., and Fouet, A. (2000). Bacterial SLH domain proteins are non-covalently anchored to the cell surface via a conserved mechanism involving wall polysaccharide pyruvylation. *EMBO J.* 19, 4473–4484. doi:10.1093/emboj/19.17.4473.
- Mesnage, S., Couture-Tosi, E., Mock, M., Gounon, P., and Fouet, A. (1997). Molecular characterization of the *Bacillus anthracis* main S-layer component: evidence that it is the major cell-associated antigen. *Mol Microbiol* 23, 1147–1155.
- Mignot, T., Couture-Tosi, E., Mesnage, S., Mock, M., and Fouet, A. (2004). In vivo *Bacillus anthracis* gene expression requires PagR as an intermediate effector of the AtxA signalling cascade. *Int. J. Med. Microbiol.* 293, 619–624. doi:10.1078/1438-4221-00306.
- Mignot, T., Mesnage, S., Couture-Tosi, E., Mock, M., and Fouet, A. (2002). Developmental switch of S-layer protein synthesis in *Bacillus anthracis*. *Mol Microbiol* 43, 1615–1627.
- Mirzaei, M. K., and Maurice, C. F. (2017). Ménage à trois in the human gut: interactions between host, bacteria and phages. *Nat Rev Micro* 15, 397–408. doi:10.1038/nrmicro.2017.30.
- Missiakas, D., and Schneewind, O. (2017). Assembly and Function of the *Bacillus anthracis* S-Layer. *Annu. Rev. Microbiol.* doi:10.1146/annurev-micro-090816-093512.
- Moayeri, M., Leppla, S. H., Vrentas, C., Pomerantsev, A. P., and Liu, S. (2015). Anthrax Pathogenesis. *Annu. Rev. Microbiol.* 69, 185–208. doi:10.1146/annurev-micro-091014-104523.
- Mock, M., and Fouet, A. (2001). Anthrax. *Annu. Rev. Microbiol.* 55, 647–671. doi:10.1146/annurev.micro.55.1.647.

- Morgan, M., Obenchain, V, Hester, J., and Pagès, H. *SummarizedExperiment: SummarizedExperiment container*. R package version 1.6.5.
- Nakagawa, I., Kurokawa, K., Yamashita, A., Nakata, M., Tomiyasu, Y., Okahashi, N., et al. (2003). Genome sequence of an M3 strain of *Streptococcus pyogenes* reveals a large-scale genomic rearrangement in invasive strains and new insights into phage evolution. *Genome Res.* 13, 1042–1055. doi:10.1101/gr.1096703.
- Nanda, A. M., Thormann, K., and Frunzke, J. (2015). Impact of spontaneous prophage induction on the fitness of bacterial populations and host-microbe interactions. *Journal of Bacteriology* 197, 410–419. doi:10.1128/JB.02230-14.
- Nguyen, S. V., and McShan, W. M. (2014). Chromosomal islands of *Streptococcus pyogenes* and related streptococci: molecular switches for survival and virulence. *Front Cell Infect Microbiol* 4, 109. doi:10.3389/fcimb.2014.00109.
- Nguyen-Mau, S.-M., Oh, S.-Y., Kern, V. J., Missiakas, D. M., and Schneewind, O. (2012). Secretion genes as determinants of *Bacillus anthracis* chain length. *Journal of Bacteriology* 194, 3841–3850. doi:10.1128/JB.00384-12.
- Novick, R. P., and Matthews, A. M. (2005). “Staphylococcal Phages,” in *Phages* (American Society of Microbiology), 297–318. doi:10.1128/9781555816506.ch15.
- Novick, R. P., Christie, G. E., and Penadés, J. R. (2010). The phage-related chromosomal islands of Gram-positive bacteria. *Nature Publishing Group* 8, 541–551. doi:10.1038/nrmicro2393.
- O’Flaherty, S., Ross, R. P., and Coffey, A. (2009). Bacteriophage and their lysins for elimination of infectious bacteria. *FEMS Microbiol. Rev.* 33, 801–819. doi:10.1111/j.1574-6976.2009.00176.x.
- Oh, S.-Y., Budzik, J. M., Garufi, G., and Schneewind, O. (2011). Two capsular polysaccharides enable *Bacillus cereus* G9241 to cause anthrax-like disease. *Mol Microbiol* 80, 455–470. doi:10.1111/j.1365-2958.2011.07582.x.
- Oh, S.-Y., Lunderberg, J. M., Chateau, A., Schneewind, O., and Missiakas, D. (2017). Genes Required for *Bacillus anthracis* Secondary Cell Wall Polysaccharide Synthesis. *Journal of Bacteriology* 199, e00613–16. doi:10.1128/JB.00613-16.
- Olson, M. E. (2016). Bacteriophage Transduction in *Staphylococcus aureus*. *Methods Mol. Biol.* 1373, 69–74. doi:10.1007/7651_2014_186.
- Passalacqua, K. D., Varadarajan, A., Byrd, B., and Bergman, N. H. (2009a). Comparative transcriptional profiling of *Bacillus cereus* sensu lato strains

- during growth in CO₂-bicarbonate and aerobic atmospheres. *PLoS ONE* 4, e4904. doi:10.1371/journal.pone.0004904.
- Passalacqua, K. D., Varadarajan, A., Ondov, B. D., Okou, D. T., Zwick, M. E., and Bergman, N. H. (2009b). Structure and complexity of a bacterial transcriptome. *Journal of Bacteriology* 191, 3203–3211. doi:10.1128/JB.00122-09.
- Perry, L. L., SanMiguel, P., Minocha, U., Terekhov, A. I., Shroyer, M. L., Farris, L. A., et al. (2009). Sequence analysis of *Escherichia coli* O157:H7 bacteriophage PhiV10 and identification of a phage-encoded immunity protein that modifies the O157 antigen. *FEMS Microbiol. Lett.* 292, 182–186. doi:10.1111/j.1574-6968.2009.01511.x.
- Plaut, R. D., Beaber, J. W., Zemansky, J., Kaur, A. P., George, M., Biswas, B., et al. (2014). Genetic evidence for the involvement of the S-layer protein gene sap and the sporulation genes spo0A, spo0B, and spo0F in Phage AP50c infection of *Bacillus anthracis*. *Journal of Bacteriology* 196, 1143–1154. doi:10.1128/JB.00739-13.
- Ptashne, M. (2004). *A Genetic Switch*. CSHL Press.
- Qu, T., Feng, Y., Jiang, Y., Zhu, P., Wei, Z., Chen, Y., et al. (2014). Whole genome analysis of a community-associated methicillin-resistant *Staphylococcus aureus* ST59 isolate from a case of human sepsis and severe pneumonia in China. *PLoS ONE* 9, e89235. doi:10.1371/journal.pone.0089235.
- Rabinovich, L., Sigal, N., Borovok, I., Nir-Paz, R., and Herskovits, A. A. (2012). Prophage excision activates *Listeria* competence genes that promote phagosomal escape and virulence. *Cell* 150, 792–802. doi:10.1016/j.cell.2012.06.036.
- Radnedge, L., Agron, P. G., Hill, K. K., Jackson, P. J., Ticknor, L. O., Keim, P., et al. (2003). Genome differences that distinguish *Bacillus anthracis* from *Bacillus cereus* and *Bacillus thuringiensis*. *Applied and Environmental Microbiology* 69, 2755–2764. doi:10.1128/AEM.69.5.2755-2764.2003.
- Rakonjac, J., Bennett, N. J., Spagnuolo, J., Gagic, D., and Russel, M. (2011). Filamentous bacteriophage: biology, phage display and nanotechnology applications. *Curr Issues Mol Biol* 13, 51–76.
- Raz, A., Serrano, A., Lawson, C., Thaker, M., Alston, T., Bournazos, S., et al. (2017). Lysibodies are IgG Fc fusions with lysin binding domains targeting *Staphylococcus aureus* wall carbohydrates for effective phagocytosis. *Proc. Natl. Acad. Sci. U.S.A.* 114, 4781–4786. doi:10.1073/pnas.1619249114.
- Rigoulay, C., Entenza, J. M., Halpern, D., Widmer, E., Moreillon, P., Poquet, I., et al. (2005). Comparative analysis of the roles of HtrA-like surface proteases in

- two virulent *Staphylococcus aureus* strains. *Infect. Immun.* 73, 563–572. doi:10.1128/IAI.73.1.563-572.2005.
- Rollins, S. M., Peppercorn, A., Young, J. S., Drysdale, M., Baresch, A., Bikowski, M. V., et al. (2008). Application of In Vivo Induced Antigen Technology (IVIAT) to *Bacillus anthracis*. *PLoS ONE* 3, e1824. doi:10.1371/journal.pone.0001824.
- Salmond, G. P. C., and Fineran, P. C. (2015). A century of the phage: past, present and future. *Nat Rev Micro* 13, 777–786. doi:10.1038/nrmicro3564.
- Samson, J. E., Magadán, A. H., Sabri, M., and Moineau, S. (2013). Revenge of the phages: defeating bacterial defences. *Nat Rev Micro* 11, 675–687. doi:10.1038/nrmicro3096.
- Schneewind, O., and Missiakas, D. M. (2012). Protein secretion and surface display in Gram-positive bacteria. *Philos. Trans. R. Soc. Lond., B, Biol. Sci.* 367, 1123–1139. doi:10.1098/rstb.2011.0210.
- Schuch, R., and Fischetti, V. A. (2006). Detailed genomic analysis of the Wbeta and gamma phages infecting *Bacillus anthracis*: implications for evolution of environmental fitness and antibiotic resistance. *Journal of Bacteriology* 188, 3037–3051. doi:10.1128/JB.188.8.3037-3051.2006.
- Schuch, R., and Fischetti, V. A. (2009). The secret life of the anthrax agent *Bacillus anthracis*: bacteriophage-mediated ecological adaptations. *PLoS ONE* 4, e6532. doi:10.1371/journal.pone.0006532.
- Schuch, R., Nelson, D., and Fischetti, V. A. (2002). A bacteriolytic agent that detects and kills *Bacillus anthracis*. *Nature* 418, 884–889. doi:10.1038/nature01026.
- Scott, J., Nguyen, S. V., King, C. J., Hendrickson, C., and McShan, W. M. (2012). Phage-Like *Streptococcus pyogenes* Chromosomal Islands (SpyCI) and Mutator Phenotypes: Control by Growth State and Rescue by a SpyCI-Encoded Promoter. *Front Microbiol* 3, 317. doi:10.3389/fmicb.2012.00317.
- Scott, J., Thompson-Mayberry, P., Lahmamsi, S., King, C. J., and McShan, W. M. (2008). Phage-Associated Mutator Phenotype in Group A Streptococcus. *Journal of Bacteriology* 190, 6290–6301. doi:10.1128/JB.01569-07.
- Smoot, J. C., Barbian, K. D., Van Gompel, J. J., Smoot, L. M., Chaussee, M. S., Sylva, G. L., et al. (2002). Genome sequence and comparative microarray analysis of serotype M18 group A Streptococcus strains associated with acute rheumatic fever outbreaks. *Proc. Natl. Acad. Sci. U.S.A.* 99, 4668–4673. doi:10.1073/pnas.062526099.
- Soufiane, B., Sirois, M., and Côté, J.-C. (2011). Mutually exclusive distribution of

- the sap and eag S-layer genes and the lytB/lytA cell wall hydrolase genes in *Bacillus thuringiensis*. *Antonie Van Leeuwenhoek* 100, 349–364. doi:10.1007/s10482-011-9590-1.
- Sozhamannan, S., Chute, M. D., Chute, M. D., McAfee, F. D., McAfee, F. D., Fouts, D. E., et al. (2006). The *Bacillus anthracis* chromosome contains four conserved, excision-proficient, putative prophages. *BMC Microbiol.* 6, 34. doi:10.1186/1471-2180-6-34.
- Sozhamannan, S., McKinstry, M., Lentz, S. M., Jalasvuori, M., McAfee, F., Smith, A., et al. (2008). Molecular characterization of a variant of *Bacillus anthracis*-specific phage AP50 with improved bacteriolytic activity. *Applied and Environmental Microbiology* 74, 6792–6796. doi:10.1128/AEM.01124-08.
- Stirm, S. (1968). *Escherichia coli* K bacteriophages. I. Isolation and introductory characterization of five *Escherichia coli* K bacteriophages. *J. Virol.* 2, 1107–1114.
- Sumby, P., and Waldor, M. K. (2003). Transcription of the toxin genes present within the Staphylococcal phage phiSa3ms is intimately linked with the phage's life cycle. *Journal of Bacteriology* 185, 6841–6851.
- Summers, W. C. (2005). “History of Phage Research and Phage Therapy,” in *Phages Their Role in Bacterial Pathogenesis and Biotechnology*. eds.M. K. Waldor, D. I. Friedman, and S. L. Adhya (Amer Society for Microbiology), 450.
- Swanson, M. M., Reavy, B., Makarova, K. S., Cock, P. J., Hopkins, D. W., Torrance, L., et al. (2012). Novel bacteriophages containing a genome of another bacteriophage within their genomes. *PLoS ONE* 7, e40683. doi:10.1371/journal.pone.0040683.
- Takemaru, K., Mizuno, M., Sato, T., Takeuchi, M., and Kobayashi, Y. (1995). Complete nucleotide sequence of a skin element excised by DNA rearrangement during sporulation in *Bacillus subtilis*. *Microbiology (Reading, Engl.)* 141 (Pt 2), 323–327. doi:10.1099/13500872-141-2-323.
- Tarlovsky, Y., Fabian, M., Solomaha, E., Honsa, E., Olson, J. S., and Maresso, A. W. (2010). A *Bacillus anthracis* S-layer homology protein that binds heme and mediates heme delivery to IsdC. *Journal of Bacteriology* 192, 3503–3511. doi:10.1128/JB.00054-10.
- Thammavongsa, V., Kim, H. K., Missiakas, D., and Schneewind, O. (2015). Staphylococcal manipulation of host immune responses. *Nat Rev Micro* 13, 529–543. doi:10.1038/nrmicro3521.
- Thomer, L., Schneewind, O., and Missiakas, D. (2016). Pathogenesis of

Staphylococcus aureus Bloodstream Infections. *Annu Rev Pathol* 11, 343–364. doi:10.1146/annurev-pathol-012615-044351.

- Twort, F. W. (1915). AN INVESTIGATION ON THE NATURE OF ULTRA-MICROSCOPIC VIRUSES. *The Lancet* 186, 1241–1243. doi:10.1016/S0140-6736(01)20383-3.
- Utter, B., Deutsch, D. R., Schuch, R., Winer, B. Y., Verratti, K., Bishop-Lilly, K., et al. (2014). Beyond the chromosome: the prevalence of unique extra-chromosomal bacteriophages with integrated virulence genes in pathogenic *Staphylococcus aureus*. *PLoS ONE* 9, e100502. doi:10.1371/journal.pone.0100502.
- van Zyl, L. J., Taylor, M. P., and Trindade, M. (2015). Engineering resistance to phage GVE3 in *Geobacillus thermoglucosidasius*. *Applied Microbiology and Biotechnology* 100, 1833–1841. doi:10.1007/s00253-015-7109-9.
- Verkaik, N. J., Benard, M., Boelens, H. A., de Vogel, C. P., Nouwen, J. L., Verbrugh, H. A., et al. (2011). Immune evasion cluster-positive bacteriophages are highly prevalent among human *Staphylococcus aureus* strains, but they are not essential in the first stages of nasal colonization. *Clin. Microbiol. Infect.* 17, 343–348. doi:10.1111/j.1469-0691.2010.03227.x.
- Wang, X., Kim, Y., and Wood, T. K. (2009). Control and benefits of CP4-57 prophage excision in *Escherichia coli* biofilms. *ISME J* 3, 1164–1179. doi:10.1038/ismej.2009.59.
- Wang, Y.-T., Oh, S.-Y., Hendrickx, A. P. A., Lunderberg, J. M., and Schneewind, O. (2013). *Bacillus cereus* G9241 S-layer assembly contributes to the pathogenesis of anthrax-like disease in mice. *Journal of Bacteriology* 195, 596–605. doi:10.1128/JB.02005-12.
- Webb, J. S., Thompson, L. S., James, S., Charlton, T., Tolker-Nielsen, T., Koch, B., et al. (2003). Cell death in *Pseudomonas aeruginosa* biofilm development. *Journal of Bacteriology* 185, 4585–4592.
- Wilhelm, S. W., and Suttle, C. A. (1999). Viruses and Nutrient Cycles in the Sea - Viruses play critical roles in the structure and function of aquatic food webs. *Bioscience* 49, 781–788.
- Wirtz, C., Witte, W., Wolz, C., and Goerke, C. (2009). Transcription of the phage-encoded Panton-Valentine leukocidin of *Staphylococcus aureus* is dependent on the phage life-cycle and on the host background. *Microbiology (Reading, Engl.)* 155, 3491–3499. doi:10.1099/mic.0.032466-0.
- Wommack, K. E., and Colwell, R. R. (2000). Virioplankton: viruses in aquatic ecosystems. *Microbiology and molecular biology reviews : MMBR* 64, 69–114.

- World Health Organization (2003). *Manual for Laboratory Diagnosis of Anthrax*. Geneva.
- Yamaguchi, T., Hayashi, T., Takami, H., Nakasone, K., Ohnishi, M., Nakayama, K., et al. (2000). Phage conversion of exfoliative toxin A production in *Staphylococcus aureus*. *Mol Microbiol* 38, 694–705.
- Yano, J. M., Yu, K., Donaldson, G. P., Shastri, G. G., Ann, P., Ma, L., et al. (2015). Indigenous bacteria from the gut microbiota regulate host serotonin biosynthesis. *Cell* 161, 264–276. doi:10.1016/j.cell.2015.02.047.
- Young, J. A. T., and Collier, R. J. (2007). Anthrax toxin: receptor binding, internalization, pore formation, and translocation. *Annu. Rev. Biochem.* 76, 243–265. doi:10.1146/annurev.biochem.75.103004.142728.
- Zheng, J., Peng, D., Song, X., Ruan, L., Mahillon, J., and Sun, M. (2013). Differentiation of *Bacillus anthracis*, *B. cereus*, and *B. thuringiensis* on the basis of the *csaB* gene reflects host source. *Applied and Environmental Microbiology* 79, 3860–3863. doi:10.1128/AEM.00591-13.
- Zitvogel, L., Daillère, R., Roberti, M. P., Routy, B., and Kroemer, G. (2017). Anticancer effects of the microbiome and its products. *Nat Rev Micro* 15, 465–478. doi:10.1038/nrmicro.2017.44.
- Zwick, M. E., Joseph, S. J., Didelot, X., Chen, P. E., Bishop-Lilly, K. A., Stewart, A. C., et al. (2012). Genomic characterization of the *Bacillus cereus* sensu lato species: backdrop to the evolution of *Bacillus anthracis*. *Genome Res.* 22, 1512–1524. doi:10.1101/gr.134437.111.
- Łobocka, M. B., Rose, D. J., Plunkett, G., Rusin, M., Samojedny, A., Lehnerr, H., et al. (2004). Genome of bacteriophage P1. *Journal of Bacteriology* 186, 7032–7068. doi:10.1128/JB.186.21.7032-7068.2004.